IDENTIFICATION, ISOLATION, AND CHARACTERISATION OF HIV-1 NEUTRALISING ANTIBODIES

Constantinos Kurt Wibmer

A thesis submitted to the Faculty of Health Sciences, University of the Witwatersrand, Johannesburg, in fulfilment of the requirements for the degree of Doctor of Philosophy.

8th August 2016

DECLARATION

I declare that this Thesis is my own, unaided work. It is being submitted for the Degree of Doctor of Philosophy at the University of the Witwatersrand, Johannesburg. It has not been submitted before for any degree or examination at any other University.

Constantinos Kurt Wibmer

8th August 2016 in Johannesburg, South Africa

ABSTRACT

A preventative HIV-1 vaccine would contribute substantially to ending the AIDS epidemic. While the correlates of protection are unknown, broadly neutralizing HIV-1 antibodies (bNAbs) can prevent infection in animal models. However these antibodies are rare even in natural infection, their epitopes are still being characterized, and all the factors underlying their development have yet to be elucidated. Characterising bNAb targets, and defining how bNAbs develop in HIV-1 infected people, might therefore provide blueprints for the rational design of an HIV-1 vaccine. Here, we characterized the broadly neutralizing plasma specificities of two individuals in the CAPRISA cohort, CAP248 and CAP257. This paved the way for the isolation of a monoclonal antibody (mAb) from each donor, targeting two recently described sites of vulnerability on the HIV-1 envelope trimer.

The CAP248-2B mAb targets a glycan-independent epitope in the gp120-gp41 interface, distinct from previously described epitopes. Using mutagenesis, protein crystallography, and electron microscopy, we identified key components of this epitope in the gp120 C terminus, and in gp41 upstream of the membrane proximal external region (MPER). Mutations that escaped CAP248-2B made heterologous strains up to 100-fold more sensitive to MPER bNAbs. For CAP257, we described the sequential development of three distinct bNAb specificities, and analogous to CAP248 we showed that escape from the earliest bNAbs exposed the epitopes for later bNAbs. Immunotype toggling during early CAP257 escape pathways resulted in viral diversification that immediately preceded the development of neutralization breadth. Lastly, we isolated a strain-specific CD4 binding site (CD4bs) antibody called CAP257-RH1, which recognises an N276 glycan-dependent epitope that overlapped with one of the CAP257 plasma bNAb specificities. CAP257-RH1 represents an early member of the CAP257 CD4bs response, and its strain-specificity could be attributed to a preference for unglycosylated V5 loops, found in an early minority population of autologous viral envelope sequences. This rare feature may be important for the induction of N276 glycan-dependent CD4bs antibodies.

Thus, in this thesis we describe new targets for HIV-1 neutralizing antibodies, delineate the viral pathways that drove neutralization breadth, and identify unique viral variants that may potentially enhance the immunogenicity of the CD4bs and MPER. These data may serve as a roadmap for the induction of HIV-1 bNAbs by vaccination.

PUBLICATIONS FROM THIS THESIS

Wibmer C.K., Bhiman J.N., Gray E.S., Tumba N., Abdool Karim S.S., Williamson C., Morris L., Moore P.L. 2013. Viral escape from HIV-1 Neutralizing Antibodies Drives Increased Plasma Neutralization Breadth through Sequential Recognition of Multiple Epitopes and Immunotypes. PLoS Pathogens 9(10), e1003738.

Wibmer C.K., Gorman J., Ozorowski G., Bhiman J.N., Sheward D.J, Elliott D.H., Rouelle J., Smira A., Joyce M.G., Ndabambi N., Druz A., Burton D.R., Connors M., Abdool Karim S.S., Robinson J.E., Ward A.B., Williamson C., Kwong P.D., Morris L., and Moore P.L. 2016. Structure and Recognition of a Novel HIV-1 gp120-g41 Interface Antibody that Caused MPER Exposure through Viral Escape. *Submitted.*

Wibmer C.K., Gorman J., Anthony C.S., Mkhize N.N., Druz A., Schmidt S., Louder M., Abdool Karim S.S., Mascola J., Williamson C., Moore P.L., Kwong P.D., and Morris L. 2016. Structure and recognition of a strain-specific glycan-dependent CD4 binding site HIV-1 neutralizing antibody. *In preparation.*

REVIEW FROM THIS THESIS

Wibmer C.K., Moore P.L., Morris L. 2015. HIV broadly neutralizing antibody targets. Curr Opin HIV AIDS 10(3), 135-143.

CO-AUTHORSHIP AS PHD CANDIDATE

Mufhandu H.T., Gray E.S., Madiga M.C., Tumba N., Alexandre K.B., Khoza T., **Wibmer C.K.**, Moore P.L., Morris L., Khati M. 2012. UCLA1, a synthetic derivative of a gp120 RNA aptamer, inhibits entry of human immunodeficiency virus type 1 subtype C. Journal of Virology 86, 4989-4999.

Moore P.L., Gray E.S., **Wibmer C.K.**, Bhiman J.N., Nonyane M., Sheward D.J., Hermanus T., Bajimaya S., Tumba N.L., Abrahams M.R., Lambson B.E., Ranchobe N., Ping L., Ngandu N., Abdool Karim Q., Abdool Karim S.S., Swanstrom R.I., Seaman M.S., Williamson C., Morris L. 2012. Evolution of an HIV glycan-dependent broadly neutralizing antibody epitope through immune escape. Nature Medicine 18, 1688-1692.

Lacerda M., Moore P.L., Ngandu N.K., Seaman M., Gray E.S., Murrell B., Krishnamoorthy M., Nonyane M., Madiga M., **Wibmer C.K.**, Sheward D., Bailer R.T., Gao H., Greene K.M., Karim S.S., Macola J.R., Korber B.T., Montefiori D.C., Morris L., Williamson C., Seoighe C. 2013. Identification of broadly neutralizing antibody epitopes in the HIV-1 envelope glycoprotein using evolutionary models. Virology 10(347).

Doria-Rose N.A., Schramm C.A., Gorman J., Moore P.L., Bhiman J.N., DeKosky B.J., Ernandes M.J., Georgiev I.S., Kim H.J., Pancera M., Staupe R.P., Altae-Tran H.R., Bailer R.T., Crooks E.T., Cupo A., Druz A., Garrett N.J., Hoi K.H., Kong R., Louder M.K., Longo N.S., McKee K., Nonyane M., O'Dell S., Roark R., Rudicell R.S., Schmidt S.D., Sheward D.J., Soto C., **Wibmer C.K.**, Yang Y., Zhang Z., NISC Comparative Sequencing Program, Mulkin J.C., Binley J.M., Sanders R.W., Wilson I.A., Moore J.P., Ward A.B., Georgiou G., Williamson C., Adbool-Karim S.S., Morris L., Kwong P.D., Shapiro L., Mascola J.R. 2014. Developmental pathway for potent V1V2-directed HIV-neutralizing antibodies. Nature 509(7498), 55-62.

Richardson S.I., Gray E.S., Mkhize N.N., Sheward D.J., Lambson B.E., **Wibmer C.K.**, Masson L., Werner L., Garrett N., Passmore J.A., Karim Q.A., Karim S.S., Williamson C., Moore P.L., Morris L. 2015. South African HIV-1 subtype C transmitted variants with a specific V2 motif show higher dependence on α4β7 for replication. Retrovirology 12:54.

Doria-Rose N.A., Bhiman J.N., Roark R.S., Schramm C.A., Gorman J., Chuang G.Y., Pancera M., Cale E.M., Ernandes M.J., Louder M.K., Asokan M., Bailer R.T., Druz A., Fraschilla I.R., Garrett N.J., Jarosinski M., Lynch R.M., McKee K., O'Dell S., Pegu A., Schmidt S.D., Staupe R.P., Sutton M.S., Wang K., **Wibmer C.K.**, Haynes B.F., Abdool-Karim S., Shapiro L., Kwong P.D., Moore P.L., Morris L., Mascola J.R. 2016. New Member of the V1V2-Directed CAP256-VRC26 Lineage That Shows Increased Breadth and Exceptional Potency. J Virol 90:76-91.

ADDITIONAL PRIOR CO-AUTHORSHIP

Gray E.S., Taylor N., Wycuff D., Moore P.L., Tomaras G.D., **Wibmer C.K.**, Puren A., DeCamp A., Gilbert P.B., Wood B., Montefiori D.C., Binley J.M., Shaw G.M., Haynes B.F., Mascola J.R., Morris L. 2009. Antibody specificities associated with neutralization breadth in plasma from human immunodeficiency virus type 1 subtype C-infected blood donors. Journal of Virology 83, 8925-8937.

Gray E.S., Madiga M.C., Hermanus T., Moore P.L., **Wibmer C.K.**, Tumba N.L., Werner L., Mlisana K., Sibeko S., Williamson C., Abdool Karim S.S., Morris L. 2011a. The neutralization breadth of HIV-1 develops incrementally over four years and is associated with CD4+ T cell decline and high viral load during acute infection. Journal of Virology 85, 4828-4840.

Gray E.S., Moody M.A., **Wibmer C.K.**, Chen X., Marshall D., Amos J., Moore P.L., Foulger A., Yu J.S., Lambson B., Abdool Karim S., Whitesides J., Tomaras G.D., Haynes B.F., Morris L., Liao H.X. 2011b. Isolation of a monoclonal antibody that targets the alpha-2 helix of gp120 and represents the initial autologous neutralizing-antibody response in an HIV-1 subtype C-infected individual. Journal of Virology 85, 7719-7729.

Tomaras G.D., Binley J.M., Gray E.S., Crooks E.T., Osawa K., Moore P.L., Tumba N., Tong T., Shen X., Yates N.L., Decker J., **Wibmer C.K.**, Gao F., Alam S.M., Easterbrook P., Abdool Karim S., Kamanga G., Crump J.A., Cohen M., Shaw G.M., Mascola J.R., Haynes B.F., Montefiori D.C., Morris L. 2011. Polyclonal B cell responses to conserved neutralization epitopes in a subset of HIV-1-infected individuals. Journal of Virology 85, 11502-11519.

CONFERENCE OUTPUTS FROM THIS THESIS

Wibmer C.K., Gorman J., Mkhize N.N., Druz A., Schmidt S.D., Louder M.K., Abdool Karim S.S., Mascola J.R., Moore P.L., Kwong P.D., Morris L. Structure and Recognition of a Strain-specific Heterologous HIV-1 Neutralizing Antibody Resembling Broadly Neutralizing CD4-binding Site Antibodies. Keystone Symposium X8: HIV Vaccines. Olympic Valley, California, USA, March 2016. (Poster Presentation)

Wibmer C.K., Gorman J., Ozorowski G., Bhiman J.N., Sheward D.J., Joyce M.G., Elliot D.H., Rouelle J., Smira A., Ndabambi N., Druz A., Abdool Karim S.S., Robinson J., Ward A.B., Williamson C., Kwong P.D., Morris L. Moore P.L. Structural Characterisation of an HIV-1 Broadly Neutralising Antibody Epitope in the gp120-gp41 Interface. Biophysics in the Understanding, Diagnosis, and Treatment of Infectious Diseases, Stellenbosch, South Africa 2015. (Oral Presentation)

Wibmer C.K., Sheward D., Bhiman J.N., Ndabambi N., Elliot D.H., Rouelle J., Smira A., Abdool Karim S.S., Robinson J., Morris L., Williamson C., Moore P.L. Viral escape pathways from broadly neutralising antibodies targeting the HIV envelope cleavage site enhance MPER mediated neutralisation. HIV R4P Conference in Cape Town, South Africa, October 2014. (Oral Presentation)

Wibmer C.K., Sheward D., Bhiman J.N., Ndabambi N., Elliot D.H., Rouelle J., Smira A., Abdool Karim S.S., Robinson J., Morris L., Williamson C., Moore P.L. Viral escape pathways from broadly neutralising antibodies targeting the HIV envelope cleavage site enhance MPER mediated neutralisation. Health Sciences Research Day and Postgraduate Expo, University of the Witwatersrand, Johannesburg, South Africa, September 2014. (Oral Presentation)

Wibmer C.K., Bhiman J.N., Gray E.S., Tumba, N., Abdool Karim S.S., Morris L., and Moore P.L. Escape from HIV-1 neutralising antibodies drives an increase in plasma neutralisation breadth through the recognition of multiple epitopes and immunotypes. AIDS Vaccine Conference in Barcelona, Spain, October 2013. (Poster Presentation)

Wibmer C.K., Gray E.S., Bhiman J.N., Abrahams M.R., Abdool Karim S.S., Williamson C., Moore P.L., Morris L., Neutralisation breadth in an HIV-1 subtype C infected individual is conferred by three distinct antibody specificities. Health Sciences Research Day and Postgraduate Expo, University of the Witwatersrand, Johannesburg, South Africa, September 2012. (Oral Presentation)

For Costa, because it was always for us.

For Jin, who had to suffer through it all to get us to this point.

For mom and dad, who sacrificed so much to make sure I had an education.

For Elin, who laid the foundations for the scientist I have become.

And Chapter 5, for Mike, to whom I wish I had the chance to be a better mentor.

ACKNOWLEDGEMENTS

I would like to acknowledge the contribution of both past and present NICD AIDS researchers, including but not limited to those listed as co-authors on the papers contained within this thesis, as well as to the members of the various administrative teams that have kept it all ticking. In particular, I would like to thank Dr. Elin Gray for laying the best foundations on which to build a scientist, as well as Prof. Penny Moore and Prof. Lynn Morris for doing their best to lay the bricks - despite the swirling tempest.

I am grateful for the mentorship I received directly from both Dr. Jason Gorman and Dr. Peter Kwong at the Vaccine Research Center (NIH), as well as to the rest of team in building 40 with whom I collaborated and socialised. I would also like to extend my gratitude to the Columbia University-Southern African Fogarty AIDS International Training and Research Program for providing the opportunity to receive this training in protein x-ray crystallography.

In addition, this work would not have been possible without input from all of our collaborators at the Vaccine Research Center, the University of Cape Town, the Scripps Research Institute, Tulane University, and CAPRISA (including the participants themselves). I would also like to thank the various funders that supported my PhD studies, including the National Research Foundation and the Poliomyelitis Research Foundation, as well as the conference organisers of the many meetings for which I received scholarships to travel abroad and present these data.

Lastly, I am forever indebted to all of those people who over the years have supported and encouraged me despite my overwhelming innate ability to frustrate their efforts.

To my high school matric biology and science teachers.
To my parents.
And of course to my wife, Jinal.
I could not have done this without you.

Thank you

TABLE OF CONTENTS

LIST OF FIGURES

CHAPTER ONE

CHAPTER TWO

CHAPTER THREE

CHAPTER FOUR

CHAPTER FIVE

ABBREVIATIONS

Ad5	Adenovirus type-5
AIDS	Acquired Immunodeficiency Syndrome
APOBEC3G	Apolipoprotein B mRNA editing enzyme catalytic polypeptide-like 3G
bNAb	Broadly neutralizing antibody
CA	Capsid protein
CAPRISA	Centre for the AIDS Program of Research in South Africa
C1, C2, C3, C4, C5	Conserved gp120 regions 1 to 5
CCR1, 2b, 3, 5, 8, 9	Chemokine (C-C motif) receptor 1, 2b, 3, 5, 8, 9
CD4	Cluster of differentiation 4
CD4bs	CD4 binding site
CDR	Complementarity determining region
CoR	Coreceptor
CoRbs	Coreceptor binding site
CRF01	Circulating Recombinant Form 01
CT	Cytoplasmic tail of gp41
CXCR1, 4, 6	chemokine (C-X-C motif) receptor 1, 4, 6
D gene	Diversity gene
DC-SIGN	Dendritic cell-specific intracellular adhesion molecule-3-grabbing non-integrin
dUTPase	Deoxyuridine triphosphatase
ESCRT	Endosomal sorting complexes required for transport
Env	Envelope glycoprotein
Fab	Antigen binding antibody fragment
Fc	Crystallisable antibody fragment
FP	Fusion peptide
FPPR	Fusion peptide proximal region
FWR	Framework region
Gag	Group-specific antigen
gp160, gp120, gp41	glycoprotein 160 kDa, 120 kDa, 41 kDa
HIV-1, HIV-2	Human Immunodeficiency Virus type-1, -2
HPV	Human Papillomavirus
HR-1, HR-2	Heptad repeat helix 1, 2
IC_{50}	50% inhibitory concentration

ID_{50}	50% inhibitory dilution
ID	Inner Domain
IgG	Immunoglobulin
IN	Integrase
J gene	Joining gene
MA	Matrix protein
mAb	Monoclonal antibody
MPER	Membrane proximal external region
Nef	Negative factor
NC	Nucleocapsid protein
OD	Outer Domain
OPV	Oral Polio Vaccine
PBMCs	Peripheral blood mononuclear cells
Pol	Polymerase
PR	Protease
Rev	Regulator of expression of viral proteins
RT	Reverse Transcriptase
RNA	Ribonucleic acid
SHIV	Chimeric Simian/Human Immunodeficiency Virus
SIV	Simian Immunodeficiency Virus
SP1 / SP2	Spacer peptides 1 and 2
SU	Surface Unit
TAD	Trimer Association Domain
Tat	Trans-activator
TCLA	Tissue culture laboratory adapted
TM	Transmembrane Region of gp41
$tRNA^{Lys3}$	Transfer RNA molecule for Lysine codon 3
UNAIDS	United Nations programme on HIV/AIDS
V1, V2, V3, V4, V5	Variable loop regions 1 to 5
VH gene	Heavy chain variable gene
Vif	Viral infectivity factor
Vκ gene	Kappa light chain variable gene
Vλ gene	Lambda light chain variable gene
Vpr	Viral proteinR
Vpu	Viral protein unique

AMINO ACIDS

Amino Acid	Three-Letter code	One-Letter code
Alanine	Ala	A
Arginine	Arg	R
Asparagine	Asn	N
Aspartic acid	Asp	D
Cysteine	Cys	C
Glutamic acid	Glu	E
Glutamine	Gln	Q
Glycine	Gly	G
Histidine	His	H
Isoleucine	Ile	I
Leucine	Leu	L
Lysine	Lys	K
Methionine	Met	M
Phenylalanine	Phe	F
Proline	Pro	P
Serine	Ser	S
Threonine	Thr	T
Tryptophan	Trp	W
Tyrosine	Tyr	Y
Valine	Val	V

CHAPTER ONE: INTEGRATED NARRATIVE

The purpose of this integrated narrative is to provide a full literature review, and then discuss how the results contained within this thesis contribute to the field as a whole. To assist the reader, first author publications that contribute to the chapters of this thesis are marked with an asterisk symbol (*****), while co-author contributions made during the synthesis of this thesis are marked with a double asterisk (******).

VACCINES: WEAPONS OF MASS PROTECTION

A vaccine is a biological preparation administered to an individual to improve immunity to a particular disease, and is usually derived from the causative agent itself. The earliest forms of vaccination (known as variolation) were performed by exposing healthy individuals to low doses of infectious material, such as the dried powdered scabs of someone who had recently recovered from an infection with *Variola major* (the causative agent for smallpox) (1, 2). The first accepted report of vaccination was a self-published treatise by Edward Jenner in 1798, describing the use of *Variolae vaccinae* (the causative agent for cow pox) inoculation as a means to protect against smallpox infection (3). A hundred years later, Louis Pasteur showed that when chickens were inoculated with live, attenuated cultures of the causative agent for fowl cholera (later identified as *Pasteurella multocida*) they became resistant to infection with unattenuated, virulent inoculums, thus providing the first example of a vaccine developed in the laboratory (4). In the ~135 years since then, vaccines have been developed for roughly two dozen human diseases, saving millions of lives each year.

Many of the early vaccines were developed through attenuation of live pathogens, or the use of whole, killed pathogens (5) While these attenuated pathogens closely mimic natural infection, and probably best stimulate all arms of the immune system, they still have the potential to revert back to more virulent forms and cause fatal infection (1). This is epitomized by the Oral Polio Vaccine (OPV) (6), which is frequently used in the developing world because it is easier and cheaper to administer than the inactivated alternatives. Attenuation of poliovirus results from only a few mutations, which revert back to more neurovirulent forms after extended transmission in under-vaccinated communities, or replication in the gut of immunocompromised individuals (7, 8). The advent of genetic engineering provided a new alternative to vaccine design: the batch production of pure, recombinant antigens from a pathogen of interest, in a surrogate expression system. The hepatitis B virus surface antigen, expressed in yeast, was the first recombinant vaccine and conferred complete protection against hepatitis B infection (9, 10). Subsequently, recombinant sub-unit vaccines have been developed for Lyme disease, cholera, Human Papillomavirus (HPV), and meningitis, with several more in development. Despite these successes some diseases have evaded vaccine discovery, notably Acquired Immunodeficiency Syndrome (AIDS), which is caused by the Human Immunodeficiency Virus (HIV) - the subject pathogen of this thesis.

RAPID EMERGENCE OF A GLOBAL PANDEMIC

HIV is a zoonotic lentivirus, having crossed the species barrier to humans from other old world simian primate species, probably somewhere around the turn of the 19th century (11, 12). Simian Immunodeficiency Viruses (SIVs) are endemic in over 40 primate species, some of which have been infected for at least tens of thousands of years (12, 13). While these mostly represent established monophyletic infections, there is evidence for more recent zoonotic transmission between chimpanzee and gorilla simian species (14). The even more recent transmission of various SIV strains to humans has occurred at least twelve times, but the majority of these events were dead-end infections with limited secondary spread within human populations (12). Twice, transmission from sooty mangabeys has led to the established transmission of HIV-2 in west Africa (Groups A and B), however HIV-2 is largely non-pathogenic, and is being increasingly replaced by HIV-1 infection (15). HIV-1 can be divided into four known transmission events (Groups M, N, O, and P) of which only M and O show considerable secondary spread amongst humans. Group M and N are most closely related to SIV infecting chimpanzee sub-species found only in Cameroon, Gabon, and the Republic of Congo (Figure 1A) (16). Similarly, Group O and P share high homology with SIV from a gorilla sub-species that lives in the same region of Africa (Figure 1B) (17, 18). The transmission of group M and O likely occurred in southern Cameroon, and subsequently diversified throughout the Congo River Basin.

Group M viruses have rapidly spread throughout the world, and as of 2014 there are 34.3 million – 41.4 million people are living with HIV-1, with ~2 million new infections each year (http://www.unaids.org). The dissemination of group M relative to the other non-pandemic groups N, O, and P appears to have been driven largely by successful adaptations of the SIV virulence factor Vpu (described below) to the human viral restriction factor, tetherin (19). The oldest HIV-1 group M sequence fragments were recovered from the stored infected tissues of two individuals originally sampled in 1959 and 1960, and potentially coincide with the spatiotemporal origins of the HIV-1 group M pandemic in Kinshasa (11, 20, 21). Today Kinshasa is home to such HIV-1 diversity that, unlike viruses from other parts of the world, those cannot be easily categorized into individual clades (Figure 1C) (22). The most globally prominent group M clades: A, B, C, and circulating recombinant form 01 (CRF01), cluster geographically, and therefore probably represent individual founder events that expanded in isolation.

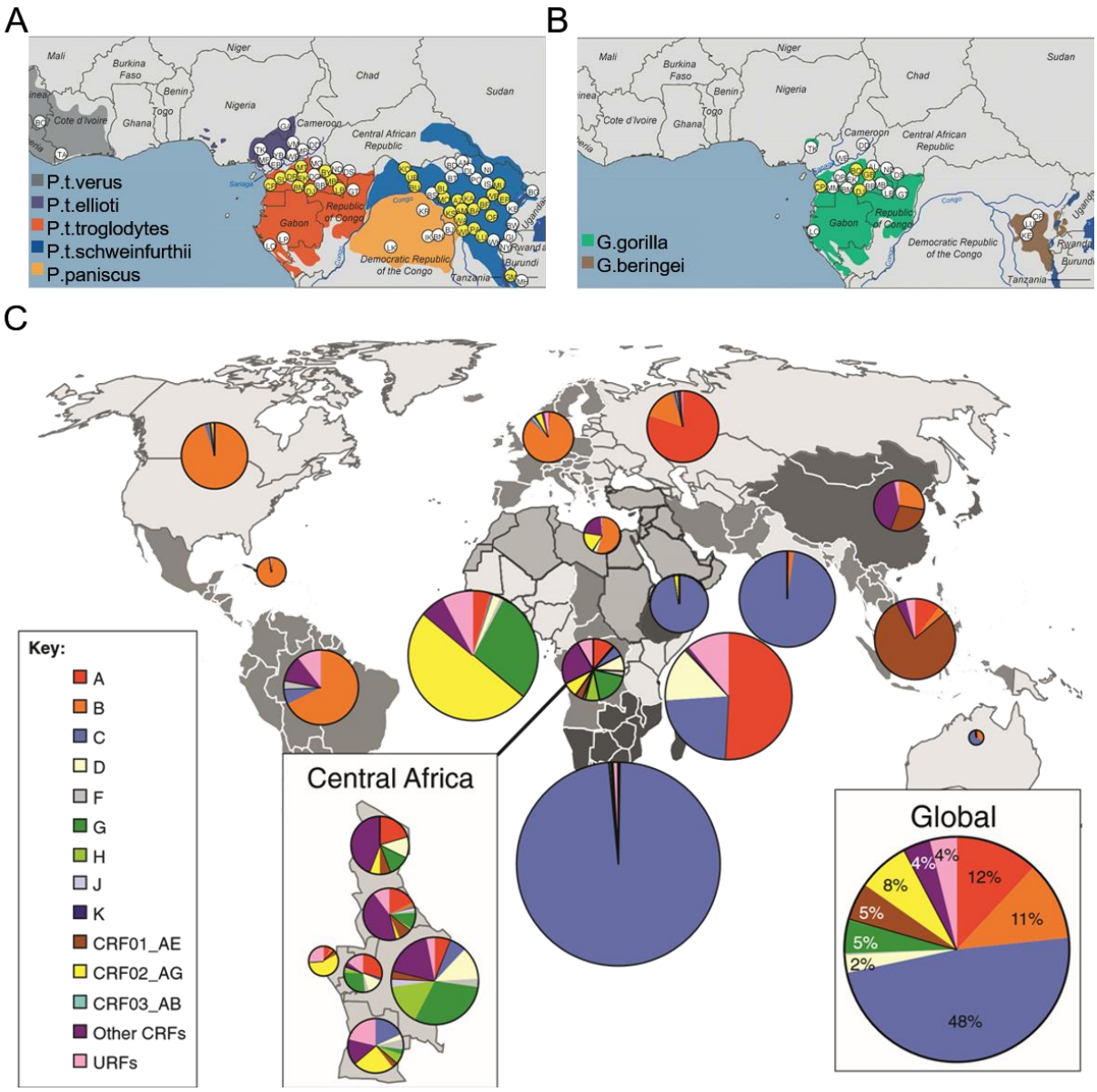

Figure 1: Geographical distribution of SIV_{cpz} and SIV_{gor}, relative to the global diversity of HIV-1 group M

A) A map of central and western Africa, showing the distribution of various common chimpanzee species, *Pan troglodytes verus* (gray), *P. t. ellioti* (purple), *P. t. troglodytes* (orange), *P. t. schweinfurthii* (blue), and of the bonobo *P. paniscus* (yellow). Yellow spheres mark regions where SIV-infected chimpanzees were found, and white spheres where they were not. B) Geographical distribution of western and eastern gorilla species, *G. gorilla* (green) and *G. beringei* (brown), with SIV infections indicated and in A. C) Geographic clustering of the most prominent HIV-1 group M clades. An inset of central Africa shows the high level of clade diversity found within the region, indicative of the age of the local epidemic there. The pie charts have been sized relative to the number of people living with HIV-1 in each region, with regional clade-bias probably representing individual founder events. Figure 1A and 1B were taken from (12), while Figure 1C was taken from (23).

Clade B represents the oldest and most globally dispersed pandemic clade, having first spread to Haiti (possibly in the 1960s), where it circulated for some years before distinct emigration events into North or Central America, and then the rest of the world (24), including South Africa (25). The South African clade B epidemic spread almost exclusively in males, but by the late 1980s clade C had begun to emerge, and coincided with increased infection rates in women (26). At this time, clade C epidemics were already established in many other countries of southern Africa, and have since evolved in India, Ethiopia, and more recently in select regions of Brazil, West Asia, and Oceania. Collectively clade C viruses now contribute to roughly half of all new infections each year (Figure 1C). This rapid expansion of a single founder event into an epidemic-associated clade is linked to the stable transmission of HIV within specific populations at high-risk for infection. These include people who share needles (predominantly for intravenous drug use), people who regularly engage in anal sex, and people who have frequent unprotected sex with multiple partners.

In South Africa, the clade C epidemic disproportionately affects young women, particularly those from impoverished backgrounds, who are at high risk for infection from older, wealthier men (27). This is particularly significant because South Africa has more than 6 million HIV infections, more than any other country worldwide. HIV-1 prevalence rates in the south eastern province of KwaZulu-Natal can be as high as 40% (28), and the HIV-1 prevalence amongst South African women aged 15-24 is 3.5 times than men of the same age, an imbalance that is partially driven by poverty, gender inequality, early sexual debut, and poor retention in the education system (29). To better understand the risk factors that predispose this ‘key population’ of women to HIV-1 infection, and develop effective intervention strategies, the Centre for the AIDS Programme of Research in South Africa established an acute infection study cohort (CAPRISA 002) in 2004 comprised of approximately 250 high-risk women from both metropolitan and rural areas of KwaZulu-Natal (30). In this thesis, we study two CAPRISA 002 participants, CAP248 and CAP257, who developed HIV-1 broadly neutralizing antibodies. The information gained from these studies will hopefully inform the development of an HIV-1 vaccine designed to mimic these protective responses in healthy people. Vaccination provides a discreet long-term intervention strategy for women who, for various reasons, are unable to negotiate first-line HIV prevention strategies such as condom use or monogamous sexual relationships.

THE HIV-1 PROTEOME

Mammalian lentiviruses have a gene structure that is millions of years old (Figure 2A), and encodes the three essential polyproteins called group-specific antigen (Gag), polymerase (Pol), and envelope (Env), as well as two essential transcription regulating elements trans-activator (Tat) and regulator of expression of viral proteins (Rev) (31). Several additional accessory proteins with host-specific functions have also arisen over the course of lentiviral evolution, and primate lentiviruses can be distinguished by having viral protein R (Vpr), negative factor (Nef), and often viral protein unique (Vpu)-like genes, as well as the absence of deoxyuridine triphosphatase (dUTPase) (32). The known HIV-1 proteome is briefly described in Figure 2B. Gag and GagPol polyproteins are expressed on cytoplasmic polysomes, and co-localize at the host cell plasma membrane with the *env* gene products that are expressed and processed in endoplasmic reticulum polysomes and the golgi apparatus respectively (33, 34). The assembled virions bud from the cell, and are then processed by HIV protease into the functional, infectious viral particle in a process termed viral maturation (33).

The Gag polyprotein is sub-divided into the matrix protein (p17, MA), capsid protein (p24, CA), nucleocapsid protein (NC), p6 protein, and two short spacer peptides (SP1, p2 and SP2, p1). The complex is directed towards cholesterol-rich lipid rafts, where it inserts into the membrane via post-translational myristoylation of the MA N terminus (35). The myristic acid (MYR), normally sequestered in a hydrophobic pocket, is released allosterically following interactions between the cationic MA N terminus and negatively charged fatty acids in the plasma membrane (36). MA proteins assemble into a trimer, and are also involved in recruiting the trimeric surface antigens encoded by Env (37). The viral capsid is made up of ~12 pentameric and ~200 hexameric forms of CA, which are cleaved from MA and then from SP1 by maturation to condense the capsid around the viral genomic RNA (38). The capsid proteins are also cleaved from NC which are zinc finger proteins, responsible for the specific condensing and packaging of two copies of viral RNA into the complete virion, as well as protecting and shuttling these into the host cell nucleus after infection and subsequent uncoating of the capsid (39, 40). The last of the Gag proteins, p6, is a recruitment factor for both viral proteins (like Vpr) as well as the host cell ESCRT (endosomal sorting complexes required for transport) machinery that are necessary for viral budding (33).

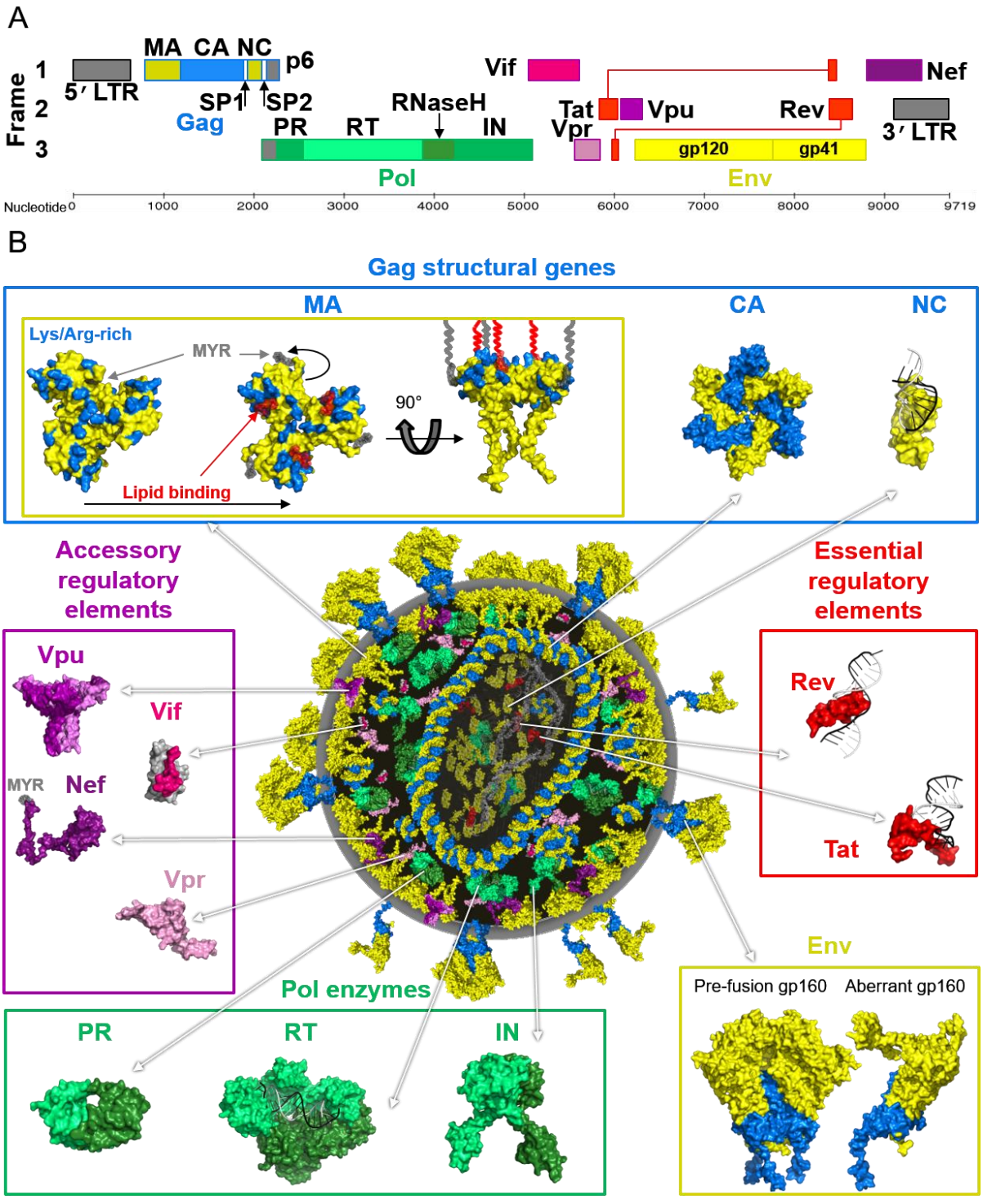

Figure 2: The HIV-1 Proteome
A) A linear schematic of the ~10 kb HIV-1 genome is shown, with each of the various HIV-1 genes encoding the viral proteome indicated in their respective reading frames. Gag or Env structural genes are boxed in blue or yellow respectively, Pol enzyme genes are boxed in green, and the essential or accessory regulatory factors are boxed in red or purple respectively. B) The entire HIV- proteome as it is packaged into infectious virions is shown, coloured as in A. Some crystal structures (such as Vif) are of partial protein fragments, as the complete structure still needs to be elucidated.

Pol is expressed as part of the GagPol polyprotein at ~5% total Gag expression, directing the incorporation of viral enzymes protease (PR), reverse transcriptase (RT), and integrase (IN) into the mature virions. These Pol proteins are all highly conserved and constitute the main targets for anti-retroviral drugs (41). The viral RNA itself also folds into key secondary structures that regulate its interactions with other molecules (42), and is packaged into virions with a host cell transfer RNA molecule for the amino acid lysine ($tRNA^{Lys3}$) which serves as a primer for reverse transcription after infection of a new target cell (43). HIV-1 RT exists as a heterodimer of one polymerase domain that synthesizes the viral complementary DNA, and a second ribonuclease H domain that degrades the original RNA strand (44). The newly synthesized double stranded viral DNA is then inserted into the host genome by IN (45). The accessory protein Vpr, which is associated with p6 in the virus, plays a key role in nuclear import of the pre-integration complex, and arrests the cell cycle in G2 facilitating HIV-1 integration through the action of cellular DNA repair enzymes (46).

The other accessory proteins Vif, Vpu, and Nef all contribute towards evading the host immune response and disease progression. Vif is present in almost all lentiviruses, and functions to bring the host apolipoprotein B mRNA editing enzyme, catalytic polypeptide-like 3G (APOBEC3G) and E3 ubiquitin-protein isopeptide ligase complex together (47). Subsequent polyubiquitination of APOBEC3G is a proteasome targeting signal that results in its degradation. APOBEC3G that is not destroyed is packaged into the viral core, where it deaminates cytidine causing hypermutation of the viral genome (48). As alluded to above, HIV-1 Vpu functions to block the action of host tetherin, which would normally colocalise with Env in lipid rafts where it cross-links viral particles to the plasma membrane (49). In monkeys, SIV Nef performs this function but cannot bind to human tetherin (50). Vpu also assembles into ion-channels (which may be linked to anti-tetherin activity), and together with Nef and Env function to downregulate CD4 expression in the host cells (51, 52). Nef is an even more complex adapter protein than Vpu, affecting a multitude of cellular interactions (53, 54).

Lastly, Env is the sole protein expressed on virion surfaces, where it is responsible for mediating viral entry (discussed below). As such, it is relatively immunogenic and the sole target for neutralizing antibodies, thus forming one of the principle components for the rational design of a recombinant HIV vaccine.

THE HIV-1 ENVELOPE TRIMER

The *env* gene is transcribed in the rough endoplasmic reticulum as a single glycoprotein (gp160) that oligomerizes into a trimer, and is then cleaved by furin-like host cellular proteases in the Golgi apparatus into the surface unit gp120, and the transmembrane protein gp41 (34). Concomitantly with translation, the gp160 protomers are stabilized through several disulphide bonds, and extensively glycosylated with both N- and O- linked glycans that altogether make up almost half its molecular weight (55). Unlike other HIV-1 proteins that are packaged in abundance, the Env trimer is sparsely incorporated into viral membranes which appear to have ~14 functional trimeric spikes per virion (56). In addition, gp160 is also aberrantly processed into forms that are not entry competent, such as gp160 monomers and dimers, uncleaved Env, or prematurely triggered post-fusion conformations of gp41 (57). These aberrant forms of gp160 expose decoy epitopes for non-neutralizing antibodies that do not bind to native, pre-fusion envelope trimers. Together with the extremely sequence variable nature of the *env* gene, these unusual features all make HIV-1 Env trimers difficult to neutralize by the human humoral immune system.

The three gp120 sub-units include all of the binding sites that engage with various host cell receptors. Historically, gp120 is divided into five conserved (C1 – C5) and five hypervariable (V1 – V5) regions which are sequentially interspersed with each other in a linear sequence (Figure 3A). In the tertiary structure of native unliganded Env, gp120 can also be divided into the inner domain (ID), outer domain (OD), and trimer association domain (TAD) (Figure 3B) (58, 59). The three IDs exist at the trimer axis where they interact with gp41, and are not accessible to neutralizing antibodies, whereas the OD and TAD are more antigenically exposed (58, 60). In accordance C1 – C5 comprise the core of the trimer, while V1 – V5 extend out from the TAD and OD, forming the most solvent exposed and distal regions from the trimer axis (Figure 3C) (58, 61). The TAD at the trimer apex is comprised of V1, V2, and V3 (59). While V1 is extremely diverse in both sequence and length, V2 is generally conserved in both sequence and structure, and its variable loop region is confined to a relatively short sequence structurally adjacent to V1 (62). Similarly V3 is relatively conserved as an important component of the co-receptor binding site (63), though it is more variable clade B strains (where it was identified) and is associated with coreceptor switching.

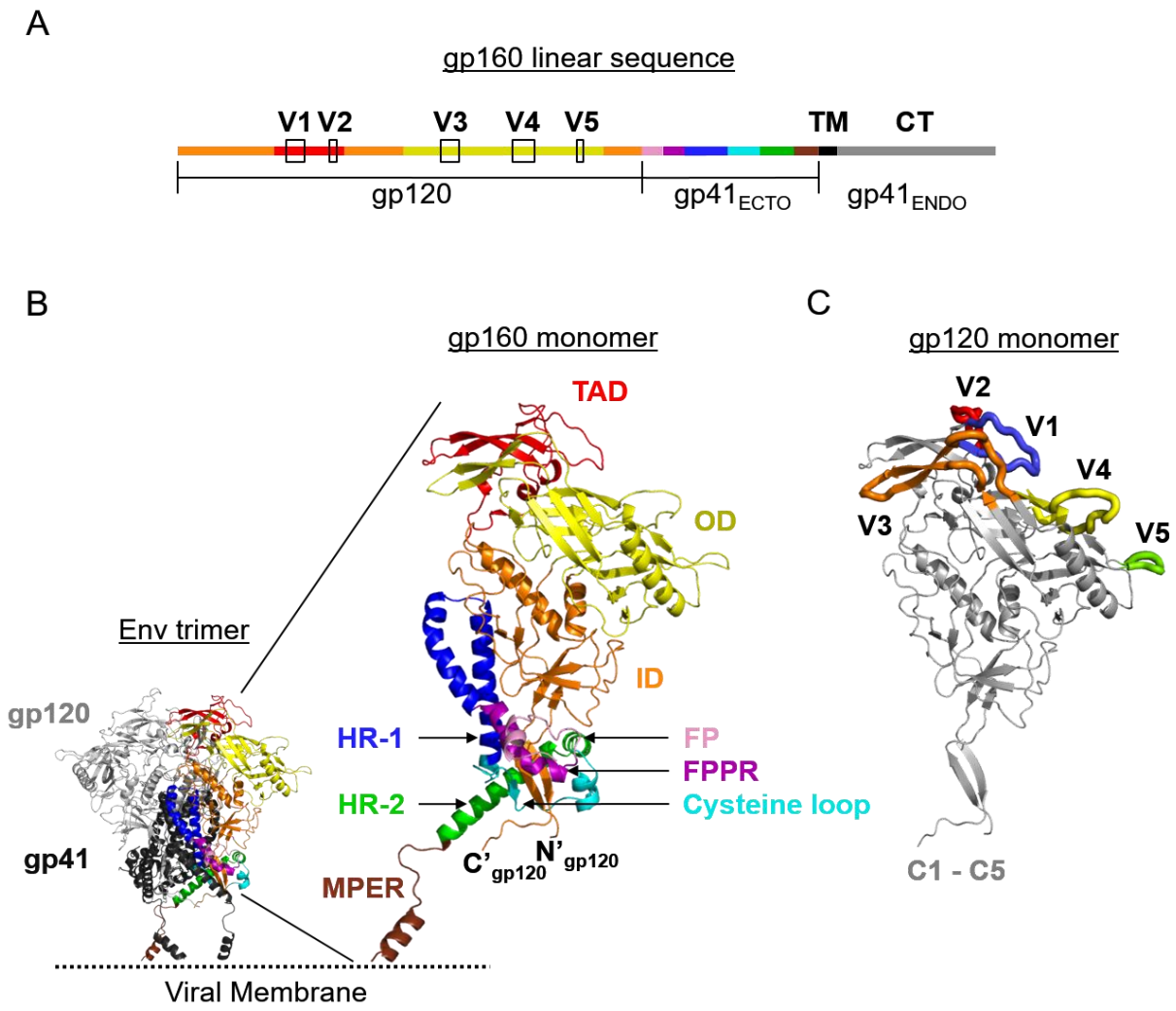

Figure 3: Structure of the HIV-1 Envelope
A) A linear schematic of the gp160 sequence is shown. For gp120, the trimer association domain is shown in red, the inner domain in orange, and the outer domain in yellow. Key regions of the gp41 ectodomain are coloured as follows: fusion peptide (FP) in pink, fusion peptide proximal region in purple (FPPR), heptad repeat helix 1 (HR-1) in blue, immunodominant cysteine loop region in cyan, heptad repeat helix 2 (HR-2) in green, and the membrane proximal external region (MPER) in brown. The transmembrane region and cytoplasmic tail of gp41 is coloured black and grey respectively. B) The Env trimer is shown in cartoon, with two gp120 and two gp41 protomers coloured dark and light grey respectively. The remaining gp120-gp41 heterodimer is coloured as in A, and labelled in a zoomed inset. In addition the N and C termini of gp120 and the relative position of the viral membrane are indicated. C) A single gp120 monomer is shown in cartoon and the conserved regions C1 – C5 are coloured in grey. The hypervariable loops V1 (blue), V2 (red), V3 (orange), V4 (yellow), and V5 (green) are indicated. The standard amino acid numbering system for Env is based on a reference sequence of the tissue culture laboratory adapted (TCLA) clade B strain HXB2, as it is defined on the LANL HIV Sequence Database. This numbering system is used throughout this integrated narrative, as well as in the publications below. An explanation can be found at the following link: (http://www.hiv.lanl.gov/content/sequence/HIV/REVIEWS/HXB2.html)

The three gp41 proteins form the hydrophobic core of the Env ectodomain, and contain all of the viral machinery necessary to fuse with the host cell (64). In the linear sequence, gp41 ectodomain is divided into the fusion peptide (FP), the fusion peptide proximal region (FPPR), heptad repeat helix-1 (HR-1), the immunodominant cysteine loop region, heptad repeat helix-2 (HR-2), and the membrane proximal external region (MPER) (Figure 3A and 3B). A short transmembrane region separates the gp41 ectodomain from the ~150 amino acid long cytoplasmic tail, which regulates Env incorporation, intracellular trafficking, and surface expression, as well as a number of cellular functions that influence infectivity and disease progression (65, 66).

The critical components for CD4 binding are all located in the OD of gp120, which has a stable β barrel structure (61, 67). The primary host receptor, CD4, initially engages with the OD, causing subtle rearrangements in the ID, and facilitating the dissolution of the TAD (Figure 4A) (68). In this CD4 bound form, the base of V1V2 rearranges to form part of the bridging sheet, providing additional stabilizing interactions with CD4 to complete the CD4 binding site (CD4bs), while the released V3 loop extends towards the host cell membrane and forms an important component of the coreceptor binding site (CoRbs) (60, 69). The coreceptor CCR5 is critical for the binding and entry of all but a few anomalous HIV-1 strains (70, 71). CXCR4 using strains (synonymous with the onset of AIDS) sometimes emerge late in infection (rarely in clade C), and this switch in coreceptor tropism is largely determined by the sequence of V3 (70). Strains that have become CD4 independent, or are able to use alternate coreceptors such as CCR1, CCR2b, CCR3, CCR8, CCR9, CX3CR1, CXCR4, and CXCR6 are even rarer, and probably evolve in the presence of unusual selection pressures, or are tissue-culture adapted strains (72-75). The CoRbs in its entirety is shielded by V1V2 in the TAD, and only properly exposed on entry-mediating Env after CD4 engagement. This CD4 bound conformation of Env is often referred to as the “open conformation”, because these rearrangements expose a number of highly immunogenic epitopes for non-neutralizing antibodies. One of these epitopes overlaps with a region of V2 that is able to bind the host cell integrin α4β7 (76). While this receptor binding site is not exposed on entry-competent trimers, it is accessible on many forms of incorrectly processed, aberrant forms of Env, and might serve to traffic virions toward the gut-associated lymphoid tissues which are rapidly depleted during acute HIV-1 infection (77). In addition, there is evidence for the clustering of Env on the virion surface, and

the co-localization of α4β7 and CD4 suggests a role for α4β7 in stabilizing the interaction between Env and CD4 (56, 78). We have identified viral strains with specific V2 sequences (P/SDI/V) that bind better to α4β7 than strains with the global consensus for this site (LDI/L/V) (79)**. These α4β7 high-binding strains clustered geographically, forming a distinct phylogeny that probably expanded from one or two founder populations in South Africa. Similarly to α4β7, non-critical interactions between Env and a host dendritic cell specific C-type lectin (DC-SIGN) have also been described (80). DC-SIGN is highly expressed in mucosal tissues, and like α4β7, may facilitate the capture and dissemination of free virions (81).

The FP is cleaved from the gp120 C terminus during viral maturation, and retracts from the solvent into a pocket at the protomer interface, but surprisingly remains relatively solvent exposed (82). The FP, FPPR, and N-terminal portions of HR-1 together form a relatively dynamic unit that sits between two adjacent gp120 protomers. This is held in place through interactions between the FPPR and a tryptophan clasp formed by a region between the cysteine loop and HR-2 that wraps around the N and C termini of gp120, near the viral membrane (58, 82-84). When CD4 binds to gp120, the movements responsible for shifting Env into the open conformation translate down the gp120 termini, facilitating the release of the FPPR which subsequently results in shedding of monomeric gp120 (85). In tandem with gp120 release the HR-1 helix uncoils, driving the FP into the host cell membrane, and the fully formed HR-1 and HR-2 helices collapse into a stable 6-helix bundle, bringing the host and viral membranes closer together (Figure 4B) (86-88). The MPER of gp41 is also relatively hydrophobic and associates with the viral membrane. CD4 binding is associated with exposure of MPER epitopes (89-91), and it is thought that through this process the MPER pulls the viral membrane towards the host cell. This collapsed gp41 stabilizes the formation of pores in the viral and host cell membranes, facilitating viral entry (92).

THE CHALLENGE OF AN HIV-1 VACCINE

Live attenuated viruses closely mimic natural infection, and thus elicit highly effective immune responses that efficiently stimulate all arms of the immune system. Early studies suggested that macaques inoculated with attenuated SIV were protected against infection by more pathogenic strains (93). In support of these data, six individuals of the Sydney Blood Bank Cohort who had all been infected with an

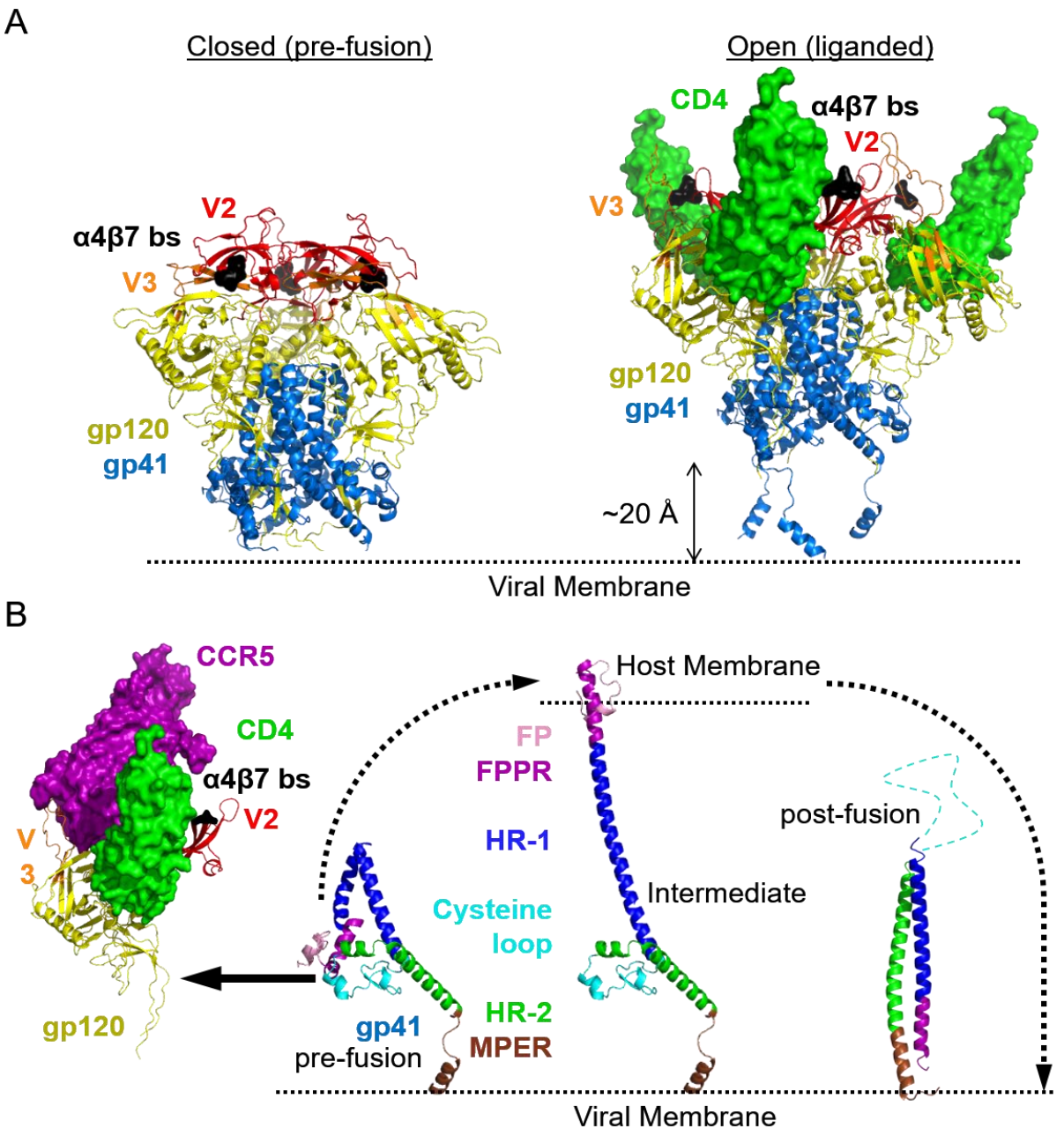

Figure 4: HIV-1 Membrane Fusion
A) A cartoon representation of Env in the closed pre-fusion (left) and open CD4-liganded conformations (right). V1V2 is coloured red and V3 is colured orange. The rest of gp120 is shown in yellow and gp41 in blue. The V2 and V3 loops are labelled in both conformations to illustrate the structural rearrangements that occur after CD4 (shown in green) binding. The α4β7 binding site, which is occluded in the pre-fusion conformation but exposed on more open conformations of Env, is indicated in black. The possible 20 Å translocation of Env and subsequent exposure of the MPER after CD4 engagement is shown relative to the location of the viral membrane. B) A cartoon representation of the gp41-mediated fusion events. Each gp120 is stably bound in the open conformation by CD4 and CCR5. This promotes gp120 dissociation from gp41, and the concomitant release of the fusion peptide which is driven into the host cell membrane by HR-1 helix formation. Finally the entire gp41 complex collapses into a highly stable 6-helix bundle that fuses the host and viral membranes.

attenuated HIV-1 strain lacking nef/LTR, derived from the contaminated blood products of a single individual, all showed delayed disease progression (94). However, in both the macaque and human examples of infection with attenuated SIV or HIV, this eventually led to AIDS-related immunological damage (95-97). In the most extreme of circumstances, the high mutability of HIV can even facilitate partial rebuilding of the attenuated virulence factors (98). These data strongly attest to the dangers of a live attenuated HIV-1 vaccine, and as such various recombinant HIV-1 antigens are being tested as HIV-1 vaccine candidates for the prevention of infection.

More than 200 HIV vaccine trials have been conducted since 1988, culminating in the three different approaches that have now been tested in large-scale phase III vaccine efficacy trials (99). The first two of these, the AIDSVAX trials, focused on the past successes of using surface antigen proteins to induce neutralizing antibody responses to the pathogen. Unfortunately, immunization with the recombinant surface antigen of HIV-1 failed to protect or delay disease progression in both vaccine trials, casting doubt as to the relevance of antibody-based vaccines for preventing HIV-1 infection (100, 101). The second approach was to use non-replicative adenovirus type-5 (Ad5) vectors engineered to express various internal HIV proteins (not subject to antibody-mediated neutralization) that might stimulate a protective cell-mediated immune response. However, these Ad5 vectors also failed to induce protective immunity, and unexpectedly there was a suggestion from the STEP trial that individuals who were already Ad5-seropositive pre-vaccination had enhanced acquisition of HIV-1 (102-104). These data might suggest that stimulating either the humoral or cellular arms of the immune system independently fails to induce protective immunity. One theory is that an effective HIV-1 vaccine might need to elicit both infection limiting antibodies to prevent initial viral dissemination, as well as a cellular capability to rapidly kill those cells that do get infected, and thus prevent the establishment of a viral reservoir.

This hypothesis was tested in the third approach to a phase III HIV-1 vaccine efficacy trial, RV144. This trial was designed to elicit both antibody and cellular immune functions by combining the initial AIDSVAX recombinant monomeric gp120 vaccine antigens with a canarypox vector based prime (ALVAC vCP1521), that like the Ad5 vector was designed to present various HIV-1 gene products (Env, Gag, and PR) to the cellular immune system. Remarkably, results from the RV144 trial showed a

modest 31.2% efficacy for the prevention of HIV-1 infection in some statistical analyses (105). These results were not without controversy though, since they were interpreted from very limited data with only 51 infections in the vaccine arm (8197 enrolled) and 74 infections in the placebo arm (8198 enrolled). Even more surprising was the finding that this modest vaccine efficacy did not correlate with neutralizing antibodies or cellular immunity, but rather with binding antibodies that targeted the V2 region of gp120 at a site that overlaps with both known neutralizing antibody epitopes, as well as a binding site for the α4β7 integrin (106, 107). Each of these are described in more detail below. Confounding the correlates results even further was the suggestion that IgA binding antibodies to a different epitope commonly associated with non-neutralizing antibody effector functions actually correlated inversely with protection (106). While the mechanisms of protection from HIV-1 are clearly not yet fully understood, these data have greatly rejuvenated hopes of developing an HIV vaccine. Efforts are currently underway to both repeat and understand the results of RV144, as well as to design better vaccine immunogens that might also be able to elicit the types of immune responses expected to protect against HIV-1 infection.

Historically, most vaccines have worked through the action of neutralizing antibodies (108). Further rationale for pursuing neutralizing antibodies for HIV-1 vaccination comes from passive immunization studies in animal models, showing that infusions with neutralizing antibodies provided superior protection from infection with chimeric simian / human immunodeficiency viruses (SHIVs) when compared to non-neutralizing antibodies (109-111). This large difference between the protective effects of neutralizing and non-neutralizing antibodies could explain why the RV144 trial or previous HIV-1 vaccine trials have failed to provide sufficient protection (Since no vaccine immunogen to date has been able to elicit cross-reactive neutralizing antibodies). A large number of both neutralizing and non-neutralizing antibodies have been isolated from HIV-1 infected individuals (see below), including the isolation of several highly potent, and broadly cross-clade reactive neutralizing antibodies since 2009 (112)*****. These latter antibodies all bind with higher affinities to native, pre-fusion Env than to the monomeric gp120 proteins used in most vaccine trials, and most are able to prevent infection through passive immunization studies (113, 114). This has opened up the possibility of using these antibodies in passive immunotherapy in humans. To date, two of these antibodies have been tested in separate phase I clinical

trials where they were shown to be both safe, and able to reduce viral load (115-117). However, reminiscent of HIV-1 anti-retroviral monotherapy, escaped viral variants emerged as antibody levels tapered, and in some individuals resistant viruses were already present pre-vaccination. Therefore, it is likely that combinations of three / four antibodies will be needed for HIV-1 immunotherapeutic applications (118).

In addition to their therapeutic benefits, these broad and potent antibodies have facilitated an unparalleled characterization of the HIV-1 Env in its native, pre-fusion state, culminating in the rational design of next-generation stabilized Env immunogens with reduced exposure of non-neutralizable epitopes (119, 120). Early immunogenicity studies with Env trimers showed a promising induction of neutralizing antibodies, although these were still strain-specific for the vaccine strain (121). It is hoped that a greater understanding of how broad and potent antibodies normally develop *in vivo*, coupled with the design of stable, trimeric, pre-fusion Env immunogens will greatly expedite the rational design of an effective HIV-1 vaccine.

THE BASIC STRUCTURE OF AN ANTIBODY

Antibodies are large 150 kDa molecules comprised of two 50 kDa heavy chain and two 25 kDa light chain proteins. Each heavy chain is formed by the recombination of variable heavy (VH), diversity (D), and joining (J) genes, that are then fused to the constant gene segments (122). Similarly, the two light chains of the antibody are formed from the recombination of variable lambda (Vλ) or variable kappa (Vκ) genes and the light chain J gene, which is also joined to constant regions. The recombined V(D)J regions of both heavy and light chains, together with the first constant domain, form the two antigen binding fragments (Fab) of the antibody (123). The remaining constant domains assemble into the single glycosylated antibody crystallizable fragment (Fc) which interacts with various cellular receptors to mediate a plethora of effector functions. The Fab domains can be further subdivided into the framework regions (FWRs), which fold into a stable β barrel structure, and the conformationally diverse complementarity determining regions (CDRs) which determine antibody specificity (124). Both heavy and light chain CDR-1 and CDR-2 loops are encoded for by the variable genes alone, while the CDR-3 loops are formed directly from V(D)J recombination events and are thus the most diverse in both sequence, length, and structure.

The stochastic nature of V(D)J recombination results in an extremely diverse pool of naïve B cells that migrate to the germinal centres, where they may encounter antigens to which they are able to bind (usually with relatively low affinities) (125). Some of these B cells are autoreactive and almost always deleted, but those that bind to a compatible antigen then begin to undergo successive rounds of affinity maturation through somatic hypermutation (126). B cells expressing mutated antibodies with higher affinity for the antigen than their predecessors are selected for additional clonal expansion and further maturation. Specific DNA sequence motifs guide this process towards the CDRs, but as B cells become highly mutated through constant stimulation, maturation can also occur in the FWRs, particularly in FWR-H3 (125, 127). The numbering of antibody sequences, as well as the way CDRs are classified, is done using several different systems that give slightly different loop locations and lengths. For the purposes of this narrative, the Kabat numbering system will be used throughout.

THE HUMORAL RESPONSE TO HIV-1 NATURAL INFECTION

Antibody responses to HIV-1 can be divided into three categories: binding (also called non-neutralizing) antibodies, strain-specific neutralizing antibodies, and broadly neutralizing antibodies (bNAbs) (128). Non-neutralizing antibodies are the first to appear within days of infection, and target epitopes on a variety of HIV-1 gene products such as aberrant Env and monomeric gp120. These include post-fusion gp41 epitopes, followed by epitopes in the CD4bs, CoRbs, V2 (RV144-like antibodies), and V3 that are only exposed in the open conformation (129). These are also the types of antibodies most frequently elicited by current vaccination strategies. The rapid development of anti-gp41 responses appears to be driven by a population of established antibodies that are cross-reactive with commensal gut bacteria (130, 131). HIV-1 tissue culture laboratory adapted (TCLA) strains are neutralized by some of these non-neutralizing antibodies, particularly those that bind epitopes in the CD4bs or V3. These TCLA viruses have evolved a more open Env conformation in the absence of *in vivo* immune pressures, and are classified as tier-1 “easy-to-neutralize” strains (132). Tier-1 viruses sporadically emerge in blood, but are rapidly neutralized and do not represent transmitted/founder strains (133).

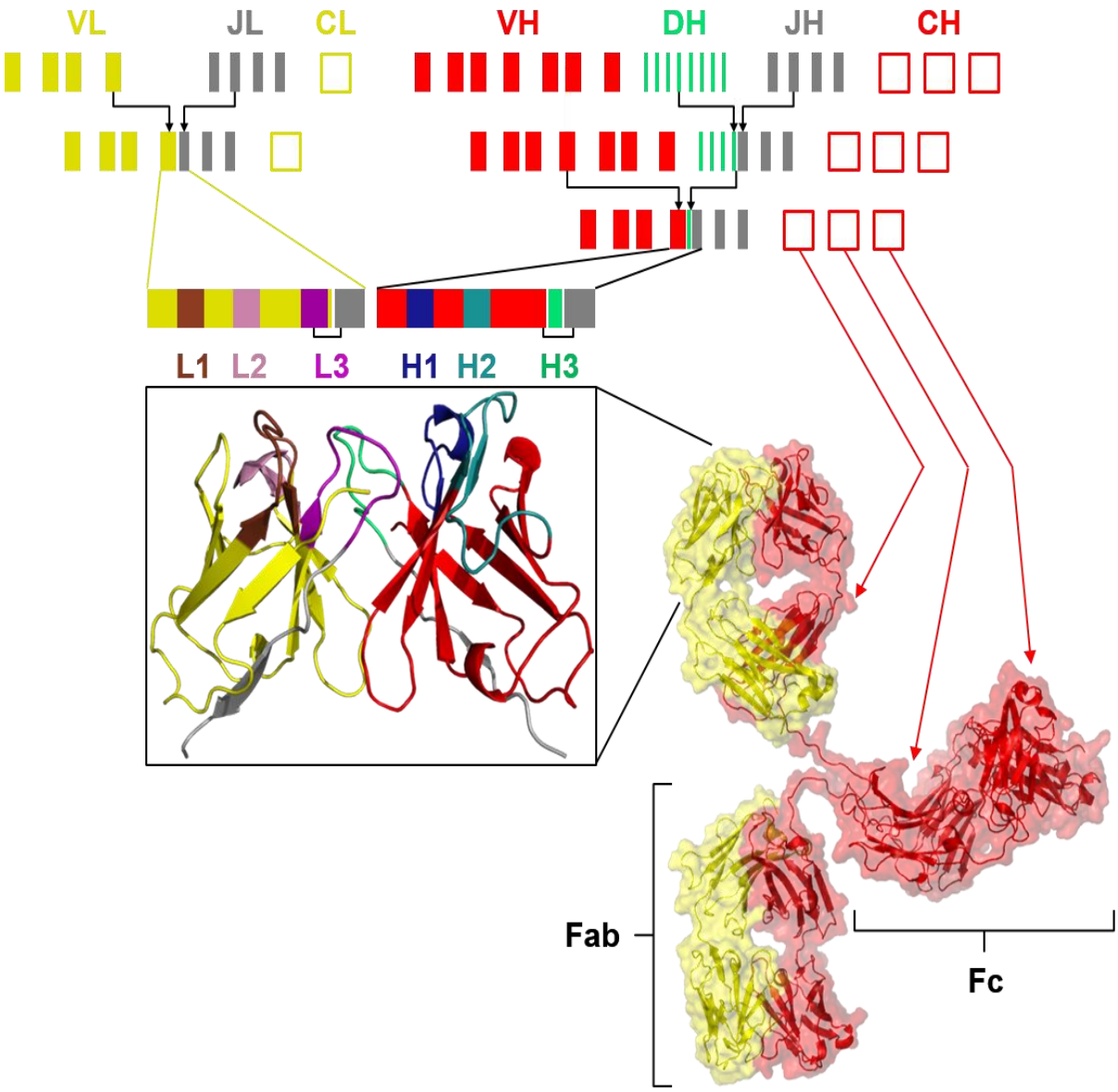

Figure 5: The basic structure of an antibody
A schematic showing an example of the initial recombination and gene rearrangement events that lead to the production of an antibody. The variable light (VL) and variable heavy (VH) chain genes are drawn as closed yellow and red blocks respectively, while the D genes, J genes, and constant genes are each shown as green, grey, and open boxes. The CDR loops regions for the heavy and light chains are indicated on both the schematic of the final recombined gene segment, as well as on the variable domain region of a model antibody shown in cartoon view. The light chain CDR loop regions L1, L2, and L3 are shown in brown, pink, and purple respectively, while the heavy chain CDR loop regions are shown in dark blue, light blue, and green respectively. The full length antibody is also shown on the right, the heavy and light chains coloured red and yellow as above, and the domains that make up the Fab and Fc fragments are indicated.

Therefore, while tier-1 strains are frequently used to assess the effectiveness of HIV-1 vaccine responses, a successful vaccine will likely need to elicit antibodies that are able to neutralize tier-2 strains, which comprise the majority of transmitted / founder viral variants, and have a harder to neutralize phenotype due to a more closed Env conformation.

The first tier-2 neutralizing antibodies develop after months of infection, but are almost always strain-specific. This strain-specificity is largely determined by the targeting of hypervariable regions, and autologous neutralizing antibody responses have been mapped to V1, V2, V4, V5, as well as the α2 helix in gp120 (134-137). Conversely, bNAbs usually take years to develop but target highly conserved regions of the Env trimer (138, 139). While all individuals eventually develop some level of cross-reactive neutralization, only ~20% of infected individuals develop truly broad neutralizing antibody activity that is capable of neutralizing 40% - 99% of the globally circulating HIV-1 strains (139-143). Monoclonal antibodies have been isolated from a large number of individuals with broad serum neutralizing activity, and their epitopes have been extensively characterized using structural biology and phenotypic mutagenesis studies. The strategies used to isolate bNAbs, the unusual features that enable broad neutralization, and the targets for these bNAbs are discussed in Chapter 2 of this thesis, which is a review published in Current Opinions in HIV and AIDS (112)*****, but bNAb targets will also be briefly discussed below for the purposes of this narrative.

HIV-1 Broadly Neutralizing Antibody Targets

The targets for bNAbs on HIV-1 Env trimers are often divided into five epitope clusters that were roughly defined by the first antibody isolated for each site: the V2 site, the N332 supersite, the CD4bs, the gp120-gp41 interface, and the MPER. The first HIV-1 bNAbs were isolated in the 1990's, and target epitopes on monomeric gp120 (b12 targets the CD4bs while 2G12 targets the N332 supersite) or linear peptides of gp41 (2F5 and 4E10 target the MPER) (144-147). Of these, only 4E10 was truly broad, but lacked the neutralization potency exhibited by other the bNAbs, and together with 2F5 was unfavorably autoreactive (148). It was not until two decades later that the first broad and potent neutralizing antibodies were isolated (PG9 and PG16 which target the V2 site), identifying novel quaternary structure specific epitopes only present on native pre-fusion trimers (149). The V2 site is comprised of a short, mostly cationic

peptide in V2 (between position 165 and 171), and two highly conserved glycans at position N156 and N160 (62). This epitope overlaps considerably with the antibodies isolated from RV144 vaccinees, but the vaccine-induced antibodies do not bind glycan, and recognize a different conformation of V2 from that which is bound by the V2 bNAbs and other conformation dependent V2 non-neutralizing antibodies (150, 151). Furthermore, the V2 bNAb epitopes do not overlap with the α4β7 binding site.

Almost all of the subsequently identified V2 bNAbs share a common epitope with PG9, and therefore often possess similar mechanisms of neutralization that involve unusually long, anionic (often tyrosine sulphated) CDR-H3 loops of between 24 and 37 amino acids long (152-156). The average CDR-H3 length is 11 to 14 amino acids, and CDR-H3 lengths required by V2 bNAbs are extremely rare in the naïve B-cell pool and often autoreactive (157). As part of a large collaborative effort, we isolated a family of V2 bNAbs from CAP256 (a participant of the CAPRISA 002 cohort) with the longest CDR-H3 loops described to date. CAP256 antibodies were particularly broad against clade C strains, and differed from other V2 bNAbs in the extent to which they were dependent on the glycans at positions N156 or N160 (156)**. We later showed that members of the CAP256-VRC26 antibody lineage were sensitive to N160 mutations in a potency-dependent manner, with the least potent antibodies being the most heavily glycan dependent (158)**. Thus, the breadth of a bNAb response is enhanced by its ability to bind glycans where the peptide contacts may be suboptimal, however the most potent bNAb interactions still rely almost entirely on peptide-peptide contacts. This is probably because a high affinity for the host-derived glycans would increase the autoreactivity of the antibody.

The isolation of PG9 and PG16 was possible after significant advancements in the ability to culture B cells, and screen their activity in high-throughput neutralization assays. Soon after this, additional broad and potent antibodies with N332 glycan dependent epitopes were isolated by the same method (154). Like the V2 antibodies, these new N332 dependent bNAbs use long CDR-H3 loops of between 18 and 24 amino acids to extend between multiple glycans and make a limited number of peptide-peptide contacts (159, 160). This is in contrast to the first N332-dependent bNAb isolated, 2G12 (CDR-H3 length of 14), which binds exclusively to glycans through a unique mechanism of variable heavy (VH) chain domain exchange between

the two Fab arms, creating a third antigen binding site at the VH-VH interface (161). The new N332 glycan dependent bNAbs could be divided into two groups, those that also dependent on the glycan at N301 and/or amino acids of V3 (PGT121-PGT134 and 10-1074), and those that are substantially reliant on glycans at N386 and N392, and contact amino acids at the base of V4 (PGT135-PGT137) (154, 162, 163). Together with 2G12, these bNAbs define a glycan supersite of at least three distinct sites of vulnerability that overlap the glycan at N332 (160). Of these, the PGT121 lineage is the most well described, where various members evolved to recognize the glycans at positions N137, N156, N301, and N332 with varying affinities (83, 162, 163).

The CD4bs is currently the most extensively characterized of the bNAb targets, and at least 20 different bNAbs lineages have been isolated. The majority of these are derived from the VH1-2 or VH1-46 germline genes, and despite developing in different donors display a structurally convergent mechanism of neutralization, even in cases where the sequences differed by >50% (164, 165). These antibodies mimic CD4 in the way their VH domains interact with gp120, and the two complexes bear remarkable overall structural likeness (166). This is key to the breadth of this bNAb class, because even slight deviations in the angle of approach to the CD4bs can result in extensive clashes with the TAD or ID of gp120 in the native pre-fusion trimer (167). This binding angle allows for a diverse repertoire of CDR-H3 lengths, which can range between 12 and 23 amino acids within a single VH-gene-restricted CD4bs bNAb lineage (168).

An important component of the interaction that orients all of the VH-gene-restricted antibodies with respect to the CD4bs is a salt bridge between a VH1-2/46 germline encoded R71 in the CDR-H2 and D368 in gp120, which mimics the interactions between R59 of CD4 (in the equivalent C'' sheet) and D368 (164-166, 169). In the case of bNAbs that are derived from the VH1-2 germline, the light chain CDR-L3 is always five amino acids long to prevent clashes with loop D in gp120, and the associated N276 glycan (170). This is less of a restriction for VH1-46 germline-derived antibodies because the light chain is oriented a further ~6 Å out of the CD4 binding site (171).

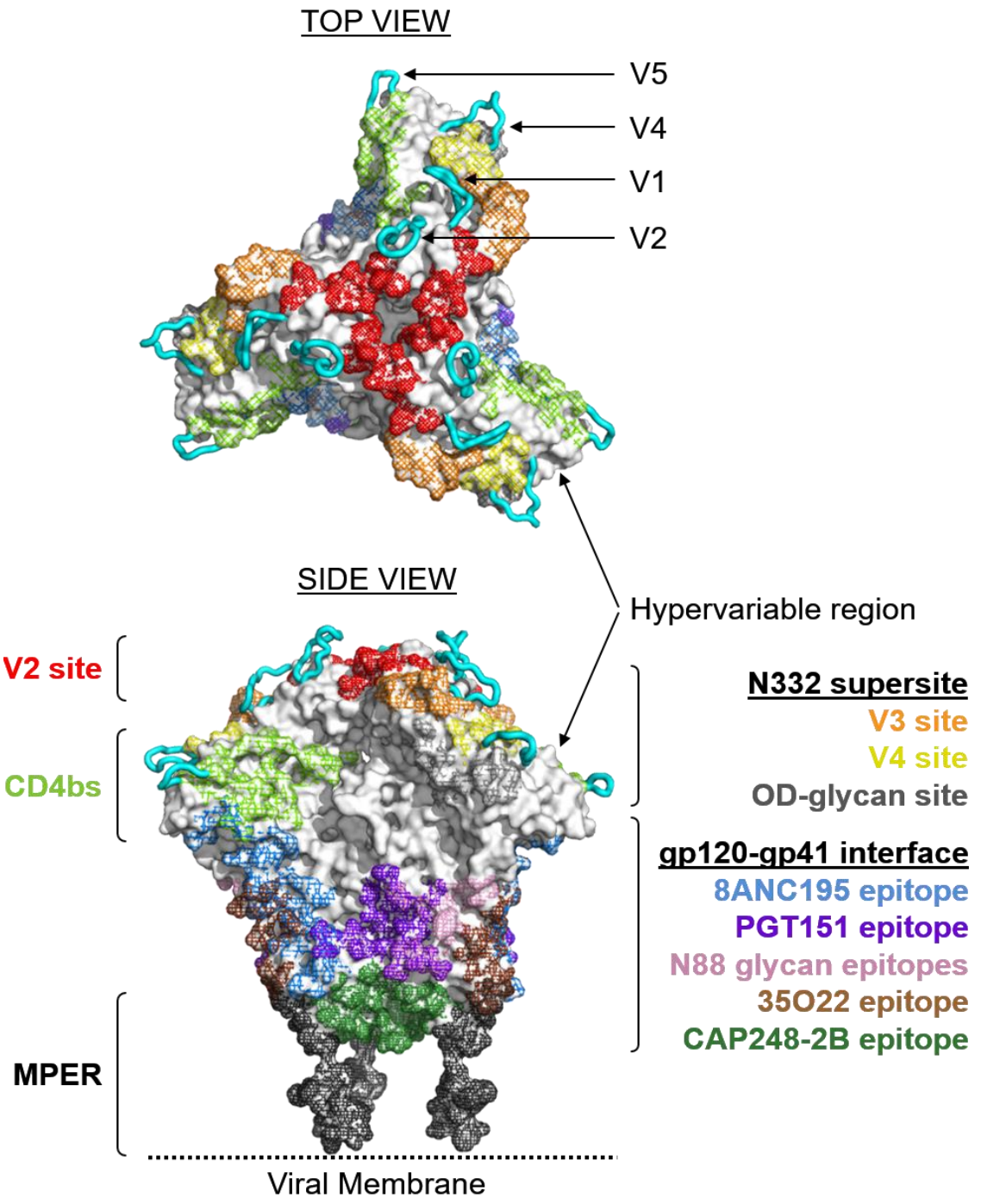

Figure 6: Broadly Neutralizing Antibody Epitopes
A surface view of the Env trimer is shown in grey, with various bNAb epitopes indicated with coloured mesh. The variable loops V1, V2, V4, and V5 are shown in cartoon and coloured cyan. An additional solvent-exposed, hypervariable region made up of the α2 helix and β14 sheet is indicated. Top view depicts the trimer from the angle of the host cell, while the side view shows an angle parallel with the viral membrane. BNAbs that bind to epitopes in V2 (red) or the CD4bs (light green) target highly overlapping surfaces and can be grouped into single sites of vulnerability. In contrast, bNAb epitopes in the N332 supersite or the gp120-gp41 interface overlap only marginally, and are shown with separate colours (labelled in the key). The MPER (black) is modelled in the 10E8 bound conformation, but is dynamic and can shift the rest of Env to vertically, bringing it closer to the viral membrane (indicated).

In contrast, and as presented as part of this thesis (Chapter 4), we describe N276 glycan dependent CD4bs bNAbs in the plasma of CAPRISA 002 participant CAP257, and together with work from another laboratory define a similar epitope for the monoclonal CD4bs bNAb HJ16 (172)***** (173). HJ16 forms part of a newly described class of CD4bs bNAbs that have CDR H3-dominated paratopes, allowing for a greater diversity in VH gene usage (171). The other current members of this class, VRC13, VRC16, and CH103 do not require the N276 glycan for effective neutralization, and all use positively charged amino acid side chains to interact directly with D368 in gp120. However, both HJ16 and the CAP257 plasma bNAbs described in this thesis are not dependent on interactions with D368 in gp120. More recently, yet another N276 glycan dependent bNAb, 179NC75, was isolated with a similar D368-independent epitope, suggesting a common mechanism of neutralization shared with HJ16, CAP257, and other CD4bs bNAbs that potentially have yet to be described (174). A better understanding of this glycan target in the CD4bs will expand our knowledge of the vulnerabilities that could be exploited for an effective HIV-1 vaccine immunogen. No crystal structure is currently available for 179NC75, and the structure of HJ16 bound to gp120 does not include the N276 glycan. Thus, in Chapter 5 of this thesis, we contribute to characterizing the N276 CD4bs target by determining the cocrystal structure of an N276 glycan dependent CD4bs neutralizing antibody isolated from CAP257, bound to gp120. While the CAP257 monoclonal antibody did not display broad neutralization against a panel of ~200 heterologous viruses, these data describe at the atomic level, one possible mechanism of how neutralizing CD4bs antibodies might recognize the N276 glycan.

The N276 glycan is also critical for the neutralization of bNAb 8ANC195, which binds to the gp120-gp41 interface (175). While 8ANC195 binds better to the pre-fusion closed conformation, it is also able to bind to Env after it has engaged CD4 and rearranged into a more open conformation (176). The epitopes for 8ANC195 and two other gp120-gp41 interface bNAbs, 35O22 and PGT151, were characterized in 2014, and represent three distinct but slightly overlapping epitopes that define a new bNAb target (58, 177-179). These are described in detail in Chapter 2 of this thesis (112)*****. Since the publication of that review, the epitope for PGT151 has been described at higher resolution (82), and additional bNAb epitopes have been identified in the gp120-gp41 interface (180). Remarkably, all of these antibodies make contacts with the

fusion peptide and fusion peptide proximal region, which are substantially more solvent exposed than previously thought, identifying these as common bNAb targets. 3BC315 is one such bNAb for which the epitope has been structurally characterized by cryogenic electron microscopy (cryo-EM). Like 35O22, 3BC315 approaches Env close to the viral membrane, but unlike previous interface bNAbs 3BC315 bridges both the gp120-gp41 and gp41-gp41 interfaces, destabilizing the interactions that hold together native pre-fusion Env trimers (180). 3BC315 also differs from the other interface bNAbs in that its mechanism of neutralization is not glycan dependent, despite having an epitope that is substantially occluded by the N88 glycan. This same glycan is the target of number of newly described gp120-gp41 interface bNAbs.

In Chapter 3 of this thesis, we describe the isolation and characterization of the monoclonal antibody CAP248-2B, which targets a distinct epitope in the vicinity of the gp120-gp41 interface. The antibody binds Env with the same membrane proximal angle of approach as 35O22 and 3BC315, and appears to partially overlap the gp41-gp41 bridging epitope of 3BC315, but also reaches under gp41 to make unique, critical contacts with the gp120 C terminus. The gp120 C terminus has not been targeted by previously described HIV-1 bNAbs, and CAP248-2B is unique amongst the interface targeting bNAbs in that it binds to the viral membrane proximal gp41-gp120 interface. Collectively, these antibodies completely encircle the Env trimer, implicating the entire pre-fusion gp41 protomer as a vaccine target (112)*****. CAP248-2B uses an unusually long CDR-L3 loop to bind to the viral membrane. Similarly, bNAbs that target the MPER all use long hydrophobic CDR-H3 loops to anchor themselves at the trimer-membrane interface (90, 181, 182). The MPER, as a bNAb target, can be further divided into three conformationally distinct epitopes: an N-terminal region (bound by 2F5 and m66.6), a C-terminal region (bound by 4E10 and 10E8) and an elbow region between the two epitopes (bound by Z13e1) (183-187). The conformational diversity of the MPER when visualized in complex with different bNAbs suggests that this region requires a highly plastic structure to facilitate its function in membrane fusion. This intrinsic flexibility allows the base of the trimer to lift up to 20 Å from the viral membrane, facilitating access to the MPER, as well as the epitopes for gp120-gp41 interface targeting bNAbs like CAP248-2B (82). Like 8ANC195, the MPER bNAbs are able to bind to both the open and closed forms of Env, but for MPER bNAbs the Env-CD4 interactions appear to enhance the frequency with which the MPER accessible

conformation is sampled (82, 179, 188). It should also be noted that while the MPER itself is a linear peptide epitope, more recent structural data of 4E10 in the presence of lipids and 10E8 bound to fully native pre-fusion trimers implicates other proximal regions of gp41, as well as the viral membrane, as components of the greater MPER site of vulnerability (82).

MAPPING PLASMA NEUTRALIZING RESPONSES

The identification of novel bNAb epitopes has traditionally been driven by the isolation and subsequent characterisation of monoclonal antibodies. Defining bNAb epitopes in plasma is more challenging, as these generally comprise only a minor fraction of the total antibody response to Env. Early attempts at mapping bNAb responses were flawed through the use of tier-1 isolates (189-192). These viruses have a number of normally non-neutralizing epitopes exposed in the context of their functional Env, for which multiple antibody lineages are often present at high titre in all HIV-1 infected plasma, and thus overwhelm any bNAb neutralization signals. Many of the newer bNAbs are glycan dependent, complicating the mapping data because removing these conserved components of the glycan shield can expose epitopes for non-neutralizing antibodies, or affect the processing of neighbouring glycans (193). Nevertheless, early plasma mapping studies defined key mapping strategies such as the use of chimeras between sensitive and resistant viruses to approximate general neutralization determinants (such as the TAD or MPER), or the use gp120 or MPER peptides to adsorb out the neutralizing fraction from the other plasma antibodies (191, 194). These experiments, coupled with alanine scanning mutagenesis or the introduction of key resistance mutations to known monoclonal bNAbs, allows for fine-mapping of the neutralization determinants. Despite this, most cohort mapping studies still list a large number of plasmas as targeting unknown epitopes (139, 142, 189, 191, 192, 195, 196). Our early efforts in this thesis suggested the existence of additional quaternary structure specific bNAb epitopes that were not V2-directed, which we and others postulated might target novel gp41 epitopes (172)***.** These observations were later confirmed through the isolation of gp120-gp41 interface monoclonal bNAbs by us and other research groups.

Using the CAPRISA 002 cohort we have previously identified seven individuals with broadly neutralizing plasma, and were able to map the bNAb epitopes of four of them (139). In this thesis, we map the bNAb epitopes for two additional CAPRISA 002 participants, CAP248 and CAP257, with a unique approach using longitudinally derived autologous Env sequences to identify bNAb selection pressure (172)*****(197)******. Escape mutations were validated when neutralization resistance was conferred by their introduction into sensitive heterologous viruses. While CAP248 plasma mapped to a novel gp120-gp41 interface epitope, we also identified additional confounders of plasma mapping for participant CAP257: the simultaneous presence of multiple bNAb lineages at similar time points, as well as the presence of previously undescribed dependencies within known bNAb targets (172)*****. In the latter example, the power of longitudinal sequences facilitated the identification of critical neutralization determinants, such as the N276 glycan dependent CD4bs bNAbs in CAP257 plasma, or the glycan independent V2 antibodies in CAP256 (172)*****(198). Multiple specificities could be accurately teased apart by introducing autologous mutations from each specificity into a single virus. Thus, mapping studies such as those described in this thesis have defined the bNAb targets of polyclonal plasma responses, characterized how viral escape influenced the development of bNAbs, and in turn have aided in the isolation monoclonal bNAbs from infected individuals (192, 198-201).

DESIGNING IMMUNOGENS TO TARGET BNAB PRECURSORS

In most instances, the UCAs or germline reverted (gHgL) precursors of bNAbs interact only weakly with an autologous virus from relatively early in infection (but these precursors are largely unable to bind or neutralize heterologous Envs), suggesting a requirement for specific germline reactive Env immunogens to engage naïve B cell precursors of bNAbs (156)******(202, 203). BNAbs that target the CD4bs bind primarily to the OD of gp120, and the use of OD minimalist antigens has been explored as a way to focus the immune response towards this epitope (67, 204-210). These OD constructs were extensively reengineered to produce proteins with high affinity for mature bNAbs, and reduced affinity for non-neutralizing CD4bs antibodies, but they still failed to bind bNAb precursors. More recently, the glycan at position N276 was identified a major obstruction for the engagement of gHgL reverted bNAbs from the VH-gene-restricted class of CD4bs bNAbs (211, 212). Antigens engineered without this glycan were able to activate B cells expressing these precursor antibodies in a

calcium flux assay. In addition, using these same antigens, immunization of mice engineered to express the heavy chain germline reverted genes for VRC01 or 3BNC60 (both VH1-2-gene-restricted CD4bs bNAbs), selected for neutralization compatible endogenous mouse light chains (211, 213, 214). Support for this immunization strategy has been found in archived viral sequences from donor 45, from whom VRC01 was isolated, which have similar potential bNAb-initiating immunotypes at positions 276 and 278 in loop D of Env (117, 199, 212, 215). These Env variants may represent a minor population of the total viral population at a given time point. Rare autologous viral variants that engage neutralizing antibody precursors have also been described for a V2 bNAb lineage (216), and for the CAP257-RH1 monoclonal antibody in this thesis. In the case of CAP257-RH1, this early N276 glycan dependent CD4bs antibody requires the absence of glycans in V5, a feature that also enhances binding to the gHgL version of VH-gene-restricted bNAbs. We suggest that these data might add to the design of vaccine immunogens that could activate B cells able to target N276-glycan dependent CD4bs epitopes, and might function cooperatively with N276 deleted immunogens to elicit a wider variety of CD4bs bNAb precursors. No doubt a major challenge for these types of immunization strategies will be the specific expansion of B cell clones that are able to evolve into bNAbs, over those that are intolerant of fully glycosylated Envs.

BNAB DEVELOPMENT *IN VIVO* AS A VACCINE BLUEPRINT

Understanding why bNAbs only develop after multiple years of infection, and how they acquire broad neutralizing activity has clear implications for HIV-1 vaccine design. From the current literature there are three mechanisms of virus-antibody co-evolution that contribute to bNAb development (217): the creation or exposure of a bNAb epitope through viral escape mutations, and the diversification of a bNAb epitope (and subsequently the bNAb) through the presentation of multiple viral immunotypes. In the first two instances, the creation or exposure of bNAb epitopes can be driven by selection pressure from both strain-specific, or broadly neutralizing antibodies (172)*****(197)******(202). These antibodies might target completely unrelated epitopes, such as the CAP257 escape mutations in V2 that potentially disrupted inter-protomer TAD interactions, and therefore possibly allowed for greater sampling of an open Env conformation which would in turn expose the CD4bs to bNAbs (172)*****, or CAP248 escape mutations in the gp120-gp41 interface that exposed the MPER. They may also

target epitopes that overlap significantly with bNAbs, but rely critically on unusual immunotypes or the rare absence of a conserved glycan (197)**(218-221), such as the strain-specific CD4bs antibody isolated from CAP257. In the latter case, the bNAb epitope diversifies to escape these early strain-specific antibodies, and this diversity almost always precedes the acquisition of some neutralization breadth in the plasma, whether the bNAb is from the same antibody lineage as the strain-specific antibodies or not (156)**(172)*(197)**(203, 222).

Three studies have now described how bNAbs can develop from a strain-specific precursor, and we have also documented the evolution of a broadly neutralizing antibody lineage targeting the V2 site, in CAPRISA 002 participant CAP256 (156)**. The CAP256-VRC26 bNAb lineage developed a maximum breadth of ~60% roughly 2.5 years after B cell transcripts could first be detected by deep sequencing (158)**. This was a substantially shorter timeframe than the 4 - 6 years it took for the CH103 and CH235 lineages, both CD4bs bNAbs isolated from the same donor (CH505), to develop to 55% and 90% breadth respectively (203, 223). Despite early CD4 mimicry by the CH235 unmutated common ancestor (UCA), this lineage still had mutations accumulating to 26% divergence from germline before achieving >90% neutralization breadth (223). These sequentially acquired mutations conferred breadth through tolerance for epitope diversity, or the ability to recognize other proximal conserved residues (217, 223). However, the requirement for such high levels of somatic hypermutation in natural infection probably contributes to the time it takes for bNAbs to develop significant breadth. Furthermore, in some instances epitope diversity also drives the bNAb lineage towards strain-specificity through critical interactions with rare escape residues. This results in highly mutated, off-track lineages that no longer contribute to plasma neutralization breadth (155, 216).

By designing immunogens that mimic selected pathways to breadth from natural infection, bNAbs with lower mutation levels might be elicited more rapidly by vaccination with sequential antigens expressing various common immunotypes. Understanding exactly which mutations are key to preferentially driving neutralization breadth may better inform vaccine design, and could prevent over engagement of the competing off-track lineages that will inevitably be co-stimulated by immunization.

CONCLUSIONS

In this thesis, we contribute to the identification of novel targets for bNAbs, and to understanding how viral escape mutations shape bNAb evolution *in vivo*. As a consequence of these data, we suggest several rare mutations in Env that might prove useful in increasing the antigenicity of B cell priming immunogens targeting bNAb precursors. These blueprints provided by natural infection may inform vaccine design, and future work will aim to characterize the responses elicited by these unusual immunogens in conjunction with their associated sequential immunization strategies.

REFERENCES

1. **Plotkin SA.** 2003. Vaccines, vaccination, and vaccinology. J Infect Dis **187:**1349-1359.
2. **Weiss RA, Esparza J.** 2015. The prevention and eradication of smallpox: a commentary on Sloane (1755) 'An account of inoculation'. Philos Trans R Soc Lond B Biol Sci **370**.
3. **Jenner E.** 1798. An Inquiry into the Causes and Effects of the Variolae Vaccinae, a Disease Discovered in Some of the Western Countries of England, Particularly Gloucestershire, and Known by the Name of “The Cow Pox”. Printed for the Author, by Sampson Low.
4. **Pasteur L.** 1880. [TRANSLATED] Of Infectious Diseases, Especially the Disease of Chicken Cholera. C R Acad Sci Paris **90:**248-249.
5. **Plotkin S.** 2014. History of vaccination. Proc Natl Acad Sci U S A **111:**12283-12287.
6. **Sabin AB, Ramos-Alvarez M, Alvarez-Amezquita J, Pelon W, Michaels RH, Spigland I, Koch MA, Barnes JM, Rhim JS.** 1960. Live, orally given poliovirus vaccine. Effects of rapid mass immunization on population under conditions of massive enteric infection with other viruses. JAMA **173:**1521-1526.
7. **Cann AJ, Stanway G, Hughes PJ, Minor PD, Evans DM, Schild GC, Almond JW.** 1984. Reversion to neurovirulence of the live-attenuated Sabin type 3 oral poliovirus vaccine. Nucleic Acids Res **12:**7787-7792.
8. **Chumakov K, Ehrenfeld E, Wimmer E, Agol VI.** 2007. Vaccination against polio should not be stopped. Nat Rev Microbiol **5:**952-958.
9. **McAleer WJ, Buynak EB, Maigetter RZ, Wampler DE, Miller WJ, Hilleman MR.** 1984. Human hepatitis B vaccine from recombinant yeast. Nature **307:**178-180.
10. **Valenzuela P, Medina A, Rutter WJ, Ammerer G, Hall BD.** 1982. Synthesis and assembly of hepatitis B virus surface antigen particles in yeast. Nature **298:**347-350.
11. **Faria NR, Rambaut A, Suchard MA, Baele G, Bedford T, Ward MJ, Tatem AJ, Sousa JD, Arinaminpathy N, Pepin J, Posada D, Peeters M, Pybus OG, Lemey P.** 2014. HIV epidemiology. The early spread and epidemic ignition of HIV-1 in human populations. Science **346:**56-61.
12. **Sharp PM, Hahn BH.** 2011. Origins of HIV and the AIDS pandemic. Cold Spring Harb Perspect Med **1:**a006841.

13. **Worobey M, Telfer P, Souquiere S, Hunter M, Coleman CA, Metzger MJ, Reed P, Makuwa M, Hearn G, Honarvar S, Roques P, Apetrei C, Kazanji M, Marx PA.** 2010. Island biogeography reveals the deep history of SIV. Science **329:**1487.
14. **Van Heuverswyn F, Li Y, Neel C, Bailes E, Keele BF, Liu W, Loul S, Butel C, Liegeois F, Bienvenue Y, Ngolle EM, Sharp PM, Shaw GM, Delaporte E, Hahn BH, Peeters M.** 2006. Human immunodeficiency viruses: SIV infection in wild gorillas. Nature **444:**164.
15. **Rowland-Jones SL, Whittle HC.** 2007. Out of Africa: what can we learn from HIV-2 about protective immunity to HIV-1? Nat Immunol **8:**329-331.
16. **Keele BF, Van Heuverswyn F, Li Y, Bailes E, Takehisa J, Santiago ML, Bibollet-Ruche F, Chen Y, Wain LV, Liegeois F, Loul S, Ngole EM, Bienvenue Y, Delaporte E, Brookfield JF, Sharp PM, Shaw GM, Peeters M, Hahn BH.** 2006. Chimpanzee reservoirs of pandemic and nonpandemic HIV-1. Science **313:**523-526.
17. **D'Arc M, Ayouba A, Esteban A, Learn GH, Boue V, Liegeois F, Etienne L, Tagg N, Leendertz FH, Boesch C, Madinda NF, Robbins MM, Gray M, Cournil A, Ooms M, Letko M, Simon VA, Sharp PM, Hahn BH, Delaporte E, Mpoudi Ngole E, Peeters M.** 2015. Origin of the HIV-1 group O epidemic in western lowland gorillas. Proc Natl Acad Sci U S A **112:**E1343-1352.
18. **Plantier JC, Leoz M, Dickerson JE, De Oliveira F, Cordonnier F, Lemee V, Damond F, Robertson DL, Simon F.** 2009. A new human immunodeficiency virus derived from gorillas. Nat Med **15:**871-872.
19. **Sauter D, Schindler M, Specht A, Landford WN, Munch J, Kim KA, Votteler J, Schubert U, Bibollet-Ruche F, Keele BF, Takehisa J, Ogando Y, Ochsenbauer C, Kappes JC, Ayouba A, Peeters M, Learn GH, Shaw G, Sharp PM, Bieniasz P, Hahn BH, Hatziioannou T, Kirchhoff F.** 2009. Tetherin-driven adaptation of Vpu and Nef function and the evolution of pandemic and nonpandemic HIV-1 strains. Cell Host Microbe **6:**409-421.
20. **Zhu T, Korber BT, Nahmias AJ, Hooper E, Sharp PM, Ho DD.** 1998. An African HIV-1 sequence from 1959 and implications for the origin of the epidemic. Nature **391:**594-597.
21. **Worobey M, Gemmel M, Teuwen DE, Haselkorn T, Kunstman K, Bunce M, Muyembe JJ, Kabongo JM, Kalengayi RM, Van Marck E, Gilbert MT, Wolinsky SM.** 2008. Direct evidence of extensive diversity of HIV-1 in Kinshasa by 1960. Nature **455:**661-664.
22. **Rambaut A, Robertson DL, Pybus OG, Peeters M, Holmes EC.** 2001. Human immunodeficiency virus. Phylogeny and the origin of HIV-1. Nature **410:**1047-1048.
23. **Hemelaar J.** 2012. The origin and diversity of the HIV-1 pandemic. Trends Mol Med **18:**182-192.
24. **Gilbert MT, Rambaut A, Wlasiuk G, Spira TJ, Pitchenik AE, Worobey M.** 2007. The emergence of HIV/AIDS in the Americas and beyond. Proc Natl Acad Sci U S A **104:**18566-18570.
25. **Ras GJ, Simson IW, Anderson R, Prozesky OW, Hamersma T.** 1983. Acquired immunodeficiency syndrome. A report of 2 South African cases. S Afr Med J **64:**140-142.
26. **van Harmelen J, Wood R, Lambrick M, Rybicki EP, Williamson AL, Williamson C.** 1997. An association between HIV-1 subtypes and mode of transmission in Cape Town, South Africa. Aids **11:**81-87.

27. **Abdool-Karim Q, Abdool-Karim SS.** 2002. The evolving HIV epidemic in South Africa. Int J Epidemiol **31:**37-40.
28. **Nel A, Mabude Z, Smit J, Kotze P, Arbuckle D, Wu J, van Niekerk N, van de Wijgert J.** 2012. HIV incidence remains high in KwaZulu-Natal, South Africa: evidence from three districts. PLoS One **7:**e35278.
29. **Abdool Karim SS, Abdool Karim Q, Baxter C.** 2015. Antibodies for HIV prevention in young women. Curr Opin HIV AIDS **10:**183-189.
30. **van Loggerenberg F, Mlisana K, Williamson C, Auld SC, Morris L, Gray CM, Abdool Karim Q, Grobler A, Barnabas N, Iriogbe I, Abdool Karim SS.** 2008. Establishing a cohort at high risk of HIV infection in South Africa: challenges and experiences of the CAPRISA 002 acute infection study. PLoS ONE **3:**e1954.
31. **Gifford RJ.** 2012. Viral evolution in deep time: lentiviruses and mammals. Trends Genet **28:**89-100.
32. **Gifford RJ, Katzourakis A, Tristem M, Pybus OG, Winters M, Shafer RW.** 2008. A transitional endogenous lentivirus from the genome of a basal primate and implications for lentivirus evolution. Proc Natl Acad Sci U S A **105:**20362-20367.
33. **Freed EO.** 2015. HIV-1 assembly, release and maturation. Nat Rev Microbiol **13:**484-496.
34. **Checkley MA, Luttge BG, Freed EO.** 2011. HIV-1 envelope glycoprotein biosynthesis, trafficking, and incorporation. J Mol Biol **410:**582-608.
35. **Lalonde MS, Sundquist WI.** 2012. How HIV finds the door. Proc Natl Acad Sci U S A **109:**18631-18632.
36. **Saad JS, Miller J, Tai J, Kim A, Ghanam RH, Summers MF.** 2006. Structural basis for targeting HIV-1 Gag proteins to the plasma membrane for virus assembly. Proc Natl Acad Sci U S A **103:**11364-11369.
37. **Hill CP, Worthylake D, Bancroft DP, Christensen AM, Sundquist WI.** 1996. Crystal structures of the trimeric human immunodeficiency virus type 1 matrix protein: implications for membrane association and assembly. Proc Natl Acad Sci U S A **93:**3099-3104.
38. **Zhao G, Perilla JR, Yufenyuy EL, Meng X, Chen B, Ning J, Ahn J, Gronenborn AM, Schulten K, Aiken C, Zhang P.** 2013. Mature HIV-1 capsid structure by cryo-electron microscopy and all-atom molecular dynamics. Nature **497:**643-646.
39. **Levin JG, Mitra M, Mascarenhas A, Musier-Forsyth K.** 2010. Role of HIV-1 nucleocapsid protein in HIV-1 reverse transcription. RNA Biol **7:**754-774.
40. **Muriaux D, Darlix JL.** 2010. Properties and functions of the nucleocapsid protein in virus assembly. RNA Biol **7:**744-753.
41. **Arts EJ, Hazuda DJ.** 2012. HIV-1 antiretroviral drug therapy. Cold Spring Harb Perspect Med **2:**a007161.
42. **Watts JM, Dang KK, Gorelick RJ, Leonard CW, Bess JW, Jr., Swanstrom R, Burch CL, Weeks KM.** 2009. Architecture and secondary structure of an entire HIV-1 RNA genome. Nature **460:**711-716.
43. **Kleiman L.** 2002. tRNA(Lys3): the primer tRNA for reverse transcription in HIV-1. IUBMB Life **53:**107-114.
44. **Katz RA, Skalka AM.** 1994. The retroviral enzymes. Annu Rev Biochem **63:**133-173.
45. **Chiu TK, Davies DR.** 2004. Structure and function of HIV-1 integrase. Curr Top Med Chem **4:**965-977.

46. **Bukrinsky M, Adzhubei A.** 1999. Viral protein R of HIV-1. Rev Med Virol **9:**39-49.
47. **Rose KM, Marin M, Kozak SL, Kabat D.** 2004. The viral infectivity factor (Vif) of HIV-1 unveiled. Trends Mol Med **10:**291-297.
48. **Sheehy AM, Gaddis NC, Choi JD, Malim MH.** 2002. Isolation of a human gene that inhibits HIV-1 infection and is suppressed by the viral Vif protein. Nature **418:**646-650.
49. **Neil SJ, Zang T, Bieniasz PD.** 2008. Tetherin inhibits retrovirus release and is antagonized by HIV-1 Vpu. Nature **451:**425-430.
50. **Jia B, Serra-Moreno R, Neidermyer W, Rahmberg A, Mackey J, Fofana IB, Johnson WE, Westmoreland S, Evans DT.** 2009. Species-specific activity of SIV Nef and HIV-1 Vpu in overcoming restriction by tetherin/BST2. PLoS Pathog **5:**e1000429.
51. **Strebel K.** 2014. HIV-1 Vpu - an ion channel in search of a job. Biochim Biophys Acta **1838:**1074-1081.
52. **Wildum S, Schindler M, Munch J, Kirchhoff F.** 2006. Contribution of Vpu, Env, and Nef to CD4 down-modulation and resistance of human immunodeficiency virus type 1-infected T cells to superinfection. J Virol **80:**8047-8059.
53. **Basmaciogullari S, Pizzato M.** 2014. The activity of Nef on HIV-1 infectivity. Front Microbiol **5:**232.
54. **Geyer M, Fackler OT, Peterlin BM.** 2001. Structure--function relationships in HIV-1 Nef. EMBO Rep **2:**580-585.
55. **Leonard CK, Spellman MW, Riddle L, Harris RJ, Thomas JN, Gregory TJ.** 1990. Assignment of intrachain disulfide bonds and characterization of potential glycosylation sites of the type 1 recombinant human immunodeficiency virus envelope glycoprotein (gp120) expressed in Chinese hamster ovary cells. J Biol Chem **265:**10373-10382.
56. **Zhu P, Liu J, Bess J, Jr., Chertova E, Lifson JD, Grise H, Ofek GA, Taylor KA, Roux KH.** 2006. Distribution and three-dimensional structure of AIDS virus envelope spikes. Nature **441:**847-852.
57. **Moore PL, Crooks ET, Porter L, Zhu P, Cayanan CS, Grise H, Corcoran P, Zwick MB, Franti M, Morris L, Roux KH, Burton DR, Binley JM.** 2006. Nature of nonfunctional envelope proteins on the surface of human immunodeficiency virus type 1. J Virol **80:**2515-2528.
58. **Pancera M, Zhou T, Druz A, Georgiev IS, Soto C, Gorman J, Huang J, Acharya P, Chuang GY, Ofek G, Stewart-Jones GB, Stuckey J, Bailer RT, Joyce MG, Louder MK, Tumba N, Yang Y, Zhang B, Cohen MS, Haynes BF, Mascola JR, Morris L, Munro JB, Blanchard SC, Mothes W, Connors M, Kwong PD.** 2014. Structure and immune recognition of trimeric pre-fusion HIV-1 Env. Nature **514:**455-461.
59. **Mao Y, Wang L, Gu C, Herschhorn A, Xiang SH, Haim H, Yang X, Sodroski J.** 2012. Subunit organization of the membrane-bound HIV-1 envelope glycoprotein trimer. Nat Struct Mol Biol doi:10.1038/nsmb.2351.
60. **Wyatt R, Kwong PD, Desjardins E, Sweet RW, Robinson J, Hendrickson WA, Sodroski JG.** 1998. The antigenic structure of the HIV gp120 envelope glycoprotein. Nature **393:**705-711.
61. **Kwong PD, Wyatt R, Robinson J, Sweet RW, Sodroski J, Hendrickson WA.** 1998. Structure of an HIV gp120 envelope glycoprotein in complex with the CD4 receptor and a neutralizing human antibody. Nature **393:**648-659.

62. **McLellan JS, Pancera M, Carrico C, Gorman J, Julien JP, Khayat R, Louder R, Pejchal R, Sastry M, Dai K, O'Dell S, Patel N, Shahzad-ul-Hussan S, Yang Y, Zhang B, Zhou T, Zhu J, Boyington JC, Chuang GY, Diwanji D, Georgiev I, Kwon YD, Lee D, Louder MK, Moquin S, Schmidt SD, Yang ZY, Bonsignori M, Crump JA, Kapiga SH, Sam NE, Haynes BF, Burton DR, Koff WC, Walker LM, Phogat S, Wyatt R, Orwenyo J, Wang LX, Arthos J, Bewley CA, Mascola JR, Nabel GJ, Schief WR, Ward AB, Wilson IA, Kwong PD.** 2011. Structure of HIV-1 gp120 V1/V2 domain with broadly neutralizing antibody PG9. Nature **480:**336-343.
63. **Cocchi F, DeVico AL, Garzino-Demo A, Cara A, Gallo RC, Lusso P.** 1996. The V3 domain of the HIV-1 gp120 envelope glycoprotein is critical for chemokine-mediated blockade of infection. Nat Med **2:**1244-1247.
64. **Bartesaghi A, Merk A, Borgnia MJ, Milne JL, Subramaniam S.** 2013. Prefusion structure of trimeric HIV-1 envelope glycoprotein determined by cryo-electron microscopy. Nat Struct Mol Biol **20:**1352-1357.
65. **Postler TS, Desrosiers RC.** 2013. The tale of the long tail: the cytoplasmic domain of HIV-1 gp41. J Virol **87:**2-15.
66. **Santos da Silva E, Mulinge M, Perez Bercoff D.** 2013. The frantic play of the concealed HIV envelope cytoplasmic tail. Retrovirology **10:**54.
67. **Joyce MG, Kanekiyo M, Xu L, Biertumpfel C, Boyington JC, Moquin S, Shi W, Wu X, Yang Y, Yang ZY, Zhang B, Zheng A, Zhou T, Zhu J, Mascola JR, Kwong PD, Nabel GJ.** 2013. Outer domain of HIV-1 gp120: antigenic optimization, structural malleability, and crystal structure with antibody VRC-PG04. J Virol **87:**2294-2306.
68. **Kwong PD, Doyle ML, Casper DJ, Cicala C, Leavitt SA, Majeed S, Steenbeke TD, Venturi M, Chaiken I, Fung M, Katinger H, Parren PW, Robinson J, Van Ryk D, Wang L, Burton DR, Freire E, Wyatt R, Sodroski J, Hendrickson WA, Arthos J.** 2002. HIV-1 evades antibody-mediated neutralization through conformational masking of receptor-binding sites. Nature **420:**678-682.
69. **Huang CC, Tang M, Zhang MY, Majeed S, Montabana E, Stanfield RL, Dimitrov DS, Korber B, Sodroski J, Wilson IA, Wyatt R, Kwong PD.** 2005. Structure of a V3-containing HIV-1 gp120 core. Science **310:**1025-1028.
70. **Gorry PR, Ancuta P.** 2011. Coreceptors and HIV-1 pathogenesis. Curr HIV/AIDS Rep **8:**45-53.
71. **Ray N, Doms RW.** 2006. HIV-1 coreceptors and their inhibitors. Curr Top Microbiol Immunol **303:**97-120.
72. **Gorry PR, Dunfee RL, Mefford ME, Kunstman K, Morgan T, Moore JP, Mascola JR, Agopian K, Holm GH, Mehle A, Taylor J, Farzan M, Wang H, Ellery P, Willey SJ, Clapham PR, Wolinsky SM, Crowe SM, Gabuzda D.** 2007. Changes in the V3 region of gp120 contribute to unusually broad coreceptor usage of an HIV-1 isolate from a CCR5 Delta32 heterozygote. Virology **362:**163-178.
73. **Bhattacharya J, Peters PJ, Clapham PR.** 2003. CD4-independent infection of HIV and SIV: implications for envelope conformation and cell tropism in vivo. AIDS **17 Suppl 4:**S35-43.
74. **Cilliers T, Nhlapo J, Coetzer M, Orlovic D, Ketas T, Olson WC, Moore JP, Trkola A, Morris L.** 2003. The CCR5 and CXCR4 coreceptors are both used by human immunodeficiency virus type 1 primary isolates from subtype C. J Virol **77:**4449-4456.

75. **Cilliers T, Willey S, Sullivan WM, Patience T, Pugach P, Coetzer M, Papathanasopoulos M, Moore JP, Trkola A, Clapham P, Morris L.** 2005. Use of alternate coreceptors on primary cells by two HIV-1 isolates. Virology **339:**136-144.
76. **Arthos J, Cicala C, Martinelli E, Macleod K, Van Ryk D, Wei D, Xiao Z, Veenstra TD, Conrad TP, Lempicki RA, McLaughlin S, Pascuccio M, Gopaul R, McNally J, Cruz CC, Censoplano N, Chung E, Reitano KN, Kottilil S, Goode DJ, Fauci AS.** 2008. HIV-1 envelope protein binds to and signals through integrin alpha4beta7, the gut mucosal homing receptor for peripheral T cells. Nat Immunol **9:**301-309.
77. **Haase AT.** 2005. Perils at mucosal front lines for HIV and SIV and their hosts. Nat Rev Immunol **5:**783-792.
78. **Cicala C, Martinelli E, McNally JP, Goode DJ, Gopaul R, Hiatt J, Jelicic K, Kottilil S, Macleod K, O'Shea A, Patel N, Van Ryk D, Wei D, Pascuccio M, Yi L, McKinnon L, Izulla P, Kimani J, Kaul R, Fauci AS, Arthos J.** 2009. The integrin alpha4beta7 forms a complex with cell-surface CD4 and defines a T-cell subset that is highly susceptible to infection by HIV-1. Proc Natl Acad Sci U S A **106:**20877-20882.
79. **Richardson SI, Gray ES, Mkhize NN, Sheward DJ, Lambson BE, Wibmer CK, Masson L, Werner L, Garrett N, Passmore JA, Karim QA, Karim SS, Williamson C, Moore PL, Morris L.** 2015. South African HIV-1 subtype C transmitted variants with a specific V2 motif show higher dependence on alpha4beta7 for replication. Retrovirology **12:**54.
80. **Geijtenbeek TB, Kwon DS, Torensma R, van Vliet SJ, van Duijnhoven GC, Middel J, Cornelissen IL, Nottet HS, KewalRamani VN, Littman DR, Figdor CG, van Kooyk Y.** 2000. DC-SIGN, a dendritic cell-specific HIV-1-binding protein that enhances trans-infection of T cells. Cell **100:**587-597.
81. **Geijtenbeek TB, van Kooyk Y.** 2003. DC-SIGN: a novel HIV receptor on DCs that mediates HIV-1 transmission. Curr Top Microbiol Immunol **276:**31-54.
82. **Lee JH, Ozorowski G, Ward AB.** 2016. Cryo-EM structure of a native, fully glycosylated, cleaved HIV-1 envelope trimer. Science **351:**1043-1048.
83. **Julien JP, Cupo A, Sok D, Stanfield RL, Lyumkis D, Deller MC, Klasse PJ, Burton DR, Sanders RW, Moore JP, Ward AB, Wilson IA.** 2013. Crystal structure of a soluble cleaved HIV-1 envelope trimer. Science **342:**1477-1483.
84. **Lyumkis D, Julien JP, de Val N, Cupo A, Potter CS, Klasse PJ, Burton DR, Sanders RW, Moore JP, Carragher B, Wilson IA, Ward AB.** 2013. Cryo-EM structure of a fully glycosylated soluble cleaved HIV-1 envelope trimer. Science **342:**1484-1490.
85. **Moore JP, McKeating JA, Weiss RA, Sattentau QJ.** 1990. Dissociation of gp120 from HIV-1 virions induced by soluble CD4. Science **250:**1139-1142.
86. **Weissenhorn W, Dessen A, Harrison SC, Skehel JJ, Wiley DC.** 1997. Atomic structure of the ectodomain from HIV-1 gp41. Nature **387:**426-430.
87. **Chan DC, Fass D, Berger JM, Kim PS.** 1997. Core structure of gp41 from the HIV envelope glycoprotein. Cell **89:**263-273.
88. **Tan K, Liu J, Wang J, Shen S, Lu M.** 1997. Atomic structure of a thermostable subdomain of HIV-1 gp41. Proc Natl Acad Sci U S A **94:**12303-12308.
89. **Binley JM, Cayanan CS, Wiley C, Schulke N, Olson WC, Burton DR.** 2003. Redox-triggered infection by disulfide-shackled human immunodeficiency virus type 1 pseudovirions. J Virol **77:**5678-5684.
90. **Alam SM, Morelli M, Dennison SM, Liao HX, Zhang R, Xia SM, Rits-Volloch**

S, Sun L, Harrison SC, Haynes BF, Chen B. 2009. Role of HIV membrane in neutralization by two broadly neutralizing antibodies. Proc Natl Acad Sci U S A **106:**20234-20239.

91. **Frey G, Peng H, Rits-Volloch S, Morelli M, Cheng Y, Chen B.** 2008. A fusion-intermediate state of HIV-1 gp41 targeted by broadly neutralizing antibodies. Proc Natl Acad Sci U S A **105:**3739-3744.
92. **Markosyan RM, Cohen FS, Melikyan GB.** 2003. HIV-1 envelope proteins complete their folding into six-helix bundles immediately after fusion pore formation. Mol Biol Cell **14:**926-938.
93. **Daniel MD, Kirchhoff F, Czajak SC, Sehgal PK, Desrosiers RC.** 1992. Protective effects of a live attenuated SIV vaccine with a deletion in the nef gene. Science **258:**1938-1941.
94. **Learmont J, Tindall B, Evans L, Cunningham A, Cunningham P, Wells J, Penny R, Kaldor J, Cooper DA.** 1992. Long-term symptomless HIV-1 infection in recipients of blood products from a single donor. Lancet **340:**863-867.
95. **Hofmann-Lehmann R, Vlasak J, Williams AL, Chenine AL, McClure HM, Anderson DC, O'Neil S, Ruprecht RM.** 2003. Live attenuated, nef-deleted SIV is pathogenic in most adult macaques after prolonged observation. AIDS **17:**157-166.
96. **Learmont JC, Geczy AF, Mills J, Ashton LJ, Raynes-Greenow CH, Garsia RJ, Dyer WB, McIntyre L, Oelrichs RB, Rhodes DI, Deacon NJ, Sullivan JS.** 1999. Immunologic and virologic status after 14 to 18 years of infection with an attenuated strain of HIV-1. A report from the Sydney Blood Bank Cohort. N Engl J Med **340:**1715-1722.
97. **Baba TW, Liska V, Khimani AH, Ray NB, Dailey PJ, Penninck D, Bronson R, Greene MF, McClure HM, Martin LN, Ruprecht RM.** 1999. Live attenuated, multiply deleted simian immunodeficiency virus causes AIDS in infant and adult macaques. Nat Med **5:**194-203.
98. **Whitney JB, Ruprecht RM.** 2004. Live attenuated HIV vaccines: pitfalls and prospects. Curr Opin Infect Dis **17:**17-26.
99. **Esparza J.** 2013. A brief history of the global effort to develop a preventive HIV vaccine. Vaccine **31:**3502-3518.
100. **Flynn NM, Forthal DN, Harro CD, Judson FN, Mayer KH, Para MF, rgp HIVVSG.** 2005. Placebo-controlled phase 3 trial of a recombinant glycoprotein 120 vaccine to prevent HIV-1 infection. J Infect Dis **191:**654-665.
101. **Pitisuttithum P, Gilbert P, Gurwith M, Heyward W, Martin M, van Griensven F, Hu D, Tappero JW, Choopanya K, Bangkok Vaccine Evaluation G.** 2006. Randomized, double-blind, placebo-controlled efficacy trial of a bivalent recombinant glycoprotein 120 HIV-1 vaccine among injection drug users in Bangkok, Thailand. J Infect Dis **194:**1661-1671.
102. **Buchbinder SP, Mehrotra DV, Duerr A, Fitzgerald DW, Mogg R, Li D, Gilbert PB, Lama JR, Marmor M, Del Rio C, McElrath MJ, Casimiro DR, Gottesdiener KM, Chodakewitz JA, Corey L, Robertson MN, Step Study Protocol T.** 2008. Efficacy assessment of a cell-mediated immunity HIV-1 vaccine (the Step Study): a double-blind, randomised, placebo-controlled, test-of-concept trial. Lancet **372:**1881-1893.
103. **Gray G, Buchbinder S, Duerr A.** 2010. Overview of STEP and Phambili trial results: two phase IIb test-of-concept studies investigating the efficacy of MRK adenovirus type 5 gag/pol/nef subtype B HIV vaccine. Curr Opin HIV AIDS **5:**357-361.

104. **Hammer SM, Sobieszczyk ME, Janes H, Karuna ST, Mulligan MJ, Grove D, Koblin BA, Buchbinder SP, Keefer MC, Tomaras GD, Frahm N, Hural J, Anude C, Graham BS, Enama ME, Adams E, DeJesus E, Novak RM, Frank I, Bentley C, Ramirez S, Fu R, Koup RA, Mascola JR, Nabel GJ, Montefiori DC, Kublin J, McElrath MJ, Corey L, Gilbert PB, Team HS.** 2013. Efficacy trial of a DNA/rAd5 HIV-1 preventive vaccine. N Engl J Med **369:**2083-2092.
105. **Rerks-Ngarm S, Pitisuttithum P, Nitayaphan S, Kaewkungwal J, Chiu J, Paris R, Premsri N, Namwat C, de Souza M, Adams E, Benenson M, Gurunathan S, Tartaglia J, McNeil JG, Francis DP, Stablein D, Birx DL, Chunsuttiwat S, Khamboonruang C, Thongcharoen P, Robb ML, Michael NL, Kunasol P, Kim JH.** 2009. Vaccination with ALVAC and AIDSVAX to prevent HIV-1 infection in Thailand. N Engl J Med **361:**2209-2220.
106. **Haynes BF, Gilbert PB, McElrath MJ, Zolla-Pazner S, Tomaras GD, Alam SM, Evans DT, Montefiori DC, Karnasuta C, Sutthent R, Liao HX, DeVico AL, Lewis GK, Williams C, Pinter A, Fong Y, Janes H, DeCamp A, Huang Y, Rao M, Billings E, Karasavvas N, Robb ML, Ngauy V, de Souza MS, Paris R, Ferrari G, Bailer RT, Soderberg KA, Andrews C, Berman PW, Frahm N, De Rosa SC, Alpert MD, Yates NL, Shen X, Koup RA, Pitisuttithum P, Kaewkungwal J, Nitayaphan S, Rerks-Ngarm S, Michael NL, Kim JH.** 2012. Immune-correlates analysis of an HIV-1 vaccine efficacy trial. N Engl J Med **366:**1275-1286.
107. **Rolland M, Edlefsen PT, Larsen BB, Tovanabutra S, Sanders-Buell E, Hertz T, deCamp AC, Carrico C, Menis S, Magaret CA, Ahmed H, Juraska M, Chen L, Konopa P, Nariya S, Stoddard JN, Wong K, Zhao H, Deng W, Maust BS, Bose M, Howell S, Bates A, Lazzaro M, O'Sullivan A, Lei E, Bradfield A, Ibitamuno G, Assawadarachai V, O'Connell RJ, deSouza MS, Nitayaphan S, Rerks-Ngarm S, Robb ML, McLellan JS, Georgiev I, Kwong PD, Carlson JM, Michael NL, Schief WR, Gilbert PB, Mullins JI, Kim JH.** 2012. Increased HIV-1 vaccine efficacy against viruses with genetic signatures in Env V2. Nature **490:**417-420.
108. **Plotkin SA.** 2015. Increasing Complexity of Vaccine Development. J Infect Dis **212 Suppl 1:**S12-16.
109. **Mascola JR, Lewis MG, Stiegler G, Harris D, VanCott TC, Hayes D, Louder MK, Brown CR, Sapan CV, Frankel SS, Lu Y, Robb ML, Katinger H, Birx DL.** 1999. Protection of Macaques against pathogenic simian/human immunodeficiency virus 89.6PD by passive transfer of neutralizing antibodies. J Virol **73:**4009-4018.
110. **Shibata R, Igarashi T, Haigwood N, Buckler-White A, Ogert R, Ross W, Willey R, Cho MW, Martin MA.** 1999. Neutralizing antibody directed against the HIV-1 envelope glycoprotein can completely block HIV-1/SIV chimeric virus infections of macaque monkeys. Nat Med **5:**204-210.
111. **Burton DR, Hessell AJ, Keele BF, Klasse PJ, Ketas TA, Moldt B, Dunlop DC, Poignard P, Doyle LA, Cavacini L, Veazey RS, Moore JP.** 2011. Limited or no protection by weakly or nonneutralizing antibodies against vaginal SHIV challenge of macaques compared with a strongly neutralizing antibody. Proc Natl Acad Sci U S A **108:**11181-11186.
112. **Wibmer CK, Moore PL, Morris L.** 2015. HIV broadly neutralizing antibody targets. Curr Opin HIV AIDS **10:**135-143.
113. **Moldt B, Rakasz EG, Schultz N, Chan-Hui PY, Swiderek K, Weisgrau KL, Piaskowski SM, Bergman Z, Watkins DI, Poignard P, Burton DR.** 2012.

Highly potent HIV-specific antibody neutralization in vitro translates into effective protection against mucosal SHIV challenge in vivo. Proc Natl Acad Sci U S A **109:**18921-18925.

114. **Pegu A, Yang ZY, Boyington JC, Wu L, Ko SY, Schmidt SD, McKee K, Kong WP, Shi W, Chen X, Todd JP, Letvin NL, Huang J, Nason MC, Hoxie JA, Kwong PD, Connors M, Rao SS, Mascola JR, Nabel GJ.** 2014. Neutralizing antibodies to HIV-1 envelope protect more effectively in vivo than those to the CD4 receptor. Sci Transl Med **6:**243ra288.
115. **Caskey M, Klein F, Lorenzi JC, Seaman MS, West AP, Jr., Buckley N, Kremer G, Nogueira L, Braunschweig M, Scheid JF, Horwitz JA, Shimeliovich I, Ben-Avraham S, Witmer-Pack M, Platten M, Lehmann C, Burke LA, Hawthorne T, Gorelick RJ, Walker BD, Keler T, Gulick RM, Fatkenheuer G, Schlesinger SJ, Nussenzweig MC.** 2015. Viraemia suppressed in HIV-1-infected humans by broadly neutralizing antibody 3BNC117. Nature **522:**487-491.
116. **Ledgerwood JE, Coates EE, Yamshchikov G, Saunders JG, Holman L, Enama ME, DeZure A, Lynch RM, Gordon I, Plummer S, Hendel CS, Pegu A, Conan-Cibotti M, Sitar S, Bailer RT, Narpala S, McDermott A, Louder M, O'Dell S, Mohan S, Pandey JP, Schwartz RM, Hu Z, Koup RA, Capparelli E, Mascola JR, Graham BS, Team VRCS.** 2015. Safety, pharmacokinetics and neutralization of the broadly neutralizing HIV-1 human monoclonal antibody VRC01 in healthy adults. Clin Exp Immunol **182:**289-301.
117. **Lynch RM, Wong P, Tran L, O'Dell S, Nason MC, Li Y, Wu X, Mascola JR.** 2015. HIV-1 fitness cost associated with escape from the VRC01 class of CD4 binding site neutralizing antibodies. J Virol **89:**4201-4213.
118. **Wagh K, Bhattacharya T, Williamson C, Robles A, Bayne M, Garrity J, Rist M, Rademeyer C, Yoon H, Lapedes A, Gao H, Greene K, Louder MK, Kong R, Karim SA, Burton DR, Barouch DH, Nussenzweig MC, Mascola JR, Morris L, Montefiori DC, Korber B, Seaman MS.** 2016. Optimal Combinations of Broadly Neutralizing Antibodies for Prevention and Treatment of HIV-1 Clade C Infection. PLoS Pathog **12:**e1005520.
119. **de Taeye SW, Ozorowski G, Torrents de la Pena A, Guttman M, Julien JP, van den Kerkhof TL, Burger JA, Pritchard LK, Pugach P, Yasmeen A, Crampton J, Hu J, Bontjer I, Torres JL, Arendt H, DeStefano J, Koff WC, Schuitemaker H, Eggink D, Berkhout B, Dean H, LaBranche C, Crotty S, Crispin M, Montefiori DC, Klasse PJ, Lee KK, Moore JP, Wilson IA, Ward AB, Sanders RW.** 2015. Immunogenicity of Stabilized HIV-1 Envelope Trimers with Reduced Exposure of Non-neutralizing Epitopes. Cell **163:**1702-1715.
120. **Kwon YD, Pancera M, Acharya P, Georgiev IS, Crooks ET, Gorman J, Joyce MG, Guttman M, Ma X, Narpala S, Soto C, Terry DS, Yang Y, Zhou T, Ahlsen G, Bailer RT, Chambers M, Chuang GY, Doria-Rose NA, Druz A, Hallen MA, Harned A, Kirys T, Louder MK, O'Dell S, Ofek G, Osawa K, Prabhakaran M, Sastry M, Stewart-Jones GB, Stuckey J, Thomas PV, Tittley T, Williams C, Zhang B, Zhao H, Zhou Z, Donald BR, Lee LK, Zolla-Pazner S, Baxa U, Schon A, Freire E, Shapiro L, Lee KK, Arthos J, Munro JB, Blanchard SC, Mothes W, Binley JM, et al.** 2015. Crystal structure, conformational fixation and entry-related interactions of mature ligand-free HIV-1 Env. Nat Struct Mol Biol **22:**522-531.
121. **Sanders RW, van Gils MJ, Derking R, Sok D, Ketas TJ, Burger JA, Ozorowski G, Cupo A, Simonich C, Goo L, Arendt H, Kim HJ, Lee JH,**

Pugach P, Williams M, Debnath G, Moldt B, van Breemen MJ, Isik G, Medina-Ramirez M, Back JW, Koff WC, Julien JP, Rakasz EG, Seaman MS, Guttman M, Lee KK, Klasse PJ, LaBranche C, Schief WR, Wilson IA, Overbaugh J, Burton DR, Ward AB, Montefiori DC, Dean H, Moore JP. 2015. HIV-1 VACCINES. HIV-1 neutralizing antibodies induced by native-like envelope trimers. Science **349:**aac4223.

122. **Tonegawa S.** 1983. Somatic generation of antibody diversity. Nature **302:**575-581.
123. **Harris LJ, Larson SB, Hasel KW, McPherson A.** 1997. Refined structure of an intact IgG2a monoclonal antibody. Biochemistry **36:**1581-1597.
124. **Satow Y, Cohen GH, Padlan EA, Davies DR.** 1986. Phosphocholine binding immunoglobulin Fab McPC603. An X-ray diffraction study at 2.7 A. J Mol Biol **190:**593-604.
125. **Li Z, Woo CJ, Iglesias-Ussel MD, Ronai D, Scharff MD.** 2004. The generation of antibody diversity through somatic hypermutation and class switch recombination. Genes Dev **18:**1-11.
126. **MacLennan IC.** 1994. Germinal centers. Annu Rev Immunol **12:**117-139.
127. **Muramatsu M, Sankaranand VS, Anant S, Sugai M, Kinoshita K, Davidson NO, Honjo T.** 1999. Specific expression of activation-induced cytidine deaminase (AID), a novel member of the RNA-editing deaminase family in germinal center B cells. J Biol Chem **274:**18470-18476.
128. **Euler Z, Schuitemaker H.** 2012. Cross-reactive broadly neutralizing antibodies: timing is everything. Front Immunol **3:**215.
129. **Tomaras GD, Yates NL, Liu P, Qin L, Fouda GG, Chavez LL, Decamp AC, Parks RJ, Ashley VC, Lucas JT, Cohen M, Eron J, Hicks CB, Liao HX, Self SG, Landucci G, Forthal DN, Weinhold KJ, Keele BF, Hahn BH, Greenberg ML, Morris L, Karim SS, Blattner WA, Montefiori DC, Shaw GM, Perelson AS, Haynes BF.** 2008. Initial B-cell responses to transmitted human immunodeficiency virus type 1: virion-binding immunoglobulin M (IgM) and IgG antibodies followed by plasma anti-gp41 antibodies with ineffective control of initial viremia. J Virol **82:**12449-12463.
130. **Trama AM, Moody MA, Alam SM, Jaeger FH, Lockwood B, Parks R, Lloyd KE, Stolarchuk C, Scearce R, Foulger A, Marshall DJ, Whitesides JF, Jeffries TL, Jr., Wiehe K, Morris L, Lambson B, Soderberg K, Hwang KK, Tomaras GD, Vandergrift N, Jackson KJ, Roskin KM, Boyd SD, Kepler TB, Liao HX, Haynes BF.** 2014. HIV-1 envelope gp41 antibodies can originate from terminal ileum B cells that share cross-reactivity with commensal bacteria. Cell Host Microbe **16:**215-226.
131. **Liao HX, Chen X, Munshaw S, Zhang R, Marshall DJ, Vandergrift N, Whitesides JF, Lu X, Yu JS, Hwang KK, Gao F, Markowitz M, Heath SL, Bar KJ, Goepfert PA, Montefiori DC, Shaw GC, Alam SM, Margolis DM, Denny TN, Boyd SD, Marshal E, Egholm M, Simen BB, Hanczaruk B, Fire AZ, Voss G, Kelsoe G, Tomaras GD, Moody MA, Kepler TB, Haynes BF.** 2011. Initial antibodies binding to HIV-1 gp41 in acutely infected subjects are polyreactive and highly mutated. J Exp Med **208:**2237-2249.
132. **Seaman MS, Janes H, Hawkins N, Grandpre LE, Devoy C, Giri A, Coffey RT, Harris L, Wood B, Daniels MG, Bhattacharya T, Lapedes A, Polonis VR, McCutchan FE, Gilbert PB, Self SG, Korber BT, Montefiori DC, Mascola JR.** 2010. Tiered categorization of a diverse panel of HIV-1 Env pseudoviruses for assessment of neutralizing antibodies. J Virol **84:**1439-1452.

133. **Moody MA, Gao F, Gurley TC, Amos JD, Kumar A, Hora B, Marshall DJ, Whitesides JF, Xia SM, Parks R, Lloyd KE, Hwang KK, Lu X, Bonsignori M, Finzi A, Vandergrift NA, Alam SM, Ferrari G, Shen X, Tomaras GD, Kamanga G, Cohen MS, Sam NE, Kapiga S, Gray ES, Tumba NL, Morris L, Zolla-Pazner S, Gorny MK, Mascola JR, Hahn BH, Shaw GM, Sodroski JG, Liao HX, Montefiori DC, Hraber PT, Korber BT, Haynes BF.** 2015. Strain-Specific V3 and CD4 Binding Site Autologous HIV-1 Neutralizing Antibodies Select Neutralization-Resistant Viruses. Cell Host Microbe **18:**354-362.
134. **Moore PL, Gray ES, Choge IA, Ranchobe N, Mlisana K, Abdool Karim SS, Williamson C, Morris L.** 2008. The C3-V4 region is a major target of autologous neutralizing antibodies in human immunodeficiency virus type 1 subtype C infection. J Virol **82:**1860-1869.
135. **Moore PL, Ranchobe N, Lambson BE, Gray ES, Cave E, Abrahams MR, Bandawe G, Mlisana K, Abdool Karim SS, Williamson C, Morris L.** 2009. Limited neutralizing antibody specificities drive neutralization escape in early HIV-1 subtype C infection. PLoS Pathog **5:**e1000598.
136. **Rong R, Bibollet-Ruche F, Mulenga J, Allen S, Blackwell JL, Derdeyn CA.** 2007. Role of V1V2 and Other Human Immunodeficiency Virus Type 1 Envelope Domains in Resistance to Autologous Neutralization during Clade C Infection. J Virol **81:**1350-1359.
137. **Rong R, Gnanakaran S, Decker JM, Bibollet-Ruche F, Taylor J, Sfakianos JN, Mokili JL, Muldoon M, Mulenga J, Allen S, Hahn BH, Shaw GM, Blackwell JL, Korber BT, Hunter E, Derdeyn CA.** 2007. Unique Mutational Patterns in the Envelope {alpha}2 Amphipathic Helix and Acquisition of Length in gp120 Hypervariable Domains Are Associated with Resistance to Autologous Neutralization of Subtype C Human Immunodeficiency Virus Type 1. J Virol **81:**5658-5668.
138. **Mikell I, Sather DN, Kalams SA, Altfeld M, Alter G, Stamatatos L.** 2011. Characteristics of the earliest cross-neutralizing antibody response to HIV-1. PLoS Pathog **7:**e1001251.
139. **Gray ES, Madiga MC, Hermanus T, Moore PL, Wibmer CK, Tumba NL, Werner L, Mlisana K, Sibeko S, Williamson C, Abdool Karim SS, Morris L.** 2011. The neutralization breadth of HIV-1 develops incrementally over four years and is associated with CD4+ T cell decline and high viral load during acute infection. J Virol **85:**4828-4840.
140. **Euler Z, van Gils MJ, Bunnik EM, Phung P, Schweighardt B, Wrin T, Schuitemaker H.** 2010. Cross-reactive neutralizing humoral immunity does not protect from HIV type 1 disease progression. J Infect Dis **201:**1045-1053.
141. **Doria-Rose NA, Klein RM, Manion MM, O'Dell S, Phogat A, Chakrabarti B, Hallahan CW, Migueles SA, Wrammert J, Ahmed R, Nason M, Wyatt RT, Mascola JR, Connors M.** 2009. Frequency and phenotype of human immunodeficiency virus envelope-specific B cells from patients with broadly cross-neutralizing antibodies. J Virol **83:**188-199.
142. **Sather DN, Stamatatos L.** 2010. Epitope specificities of broadly neutralizing plasmas from HIV-1 infected subjects. Vaccine **28 Suppl 2:**B8-12.
143. **Hraber P, Seaman MS, Bailer RT, Mascola JR, Montefiori DC, Korber BT.** 2014. Prevalence of broadly neutralizing antibody responses during chronic HIV-1 infection. AIDS **28:**163-169.
144. **Burton DR, Barbas CF, 3rd, Persson MA, Koenig S, Chanock RM, Lerner RA.** 1991. A large array of human monoclonal antibodies to type 1 human

immunodeficiency virus from combinatorial libraries of asymptomatic seropositive individuals. Proc Natl Acad Sci U S A **88:**10134-10137.

145. **Barbas CF, 3rd, Bjorling E, Chiodi F, Dunlop N, Cababa D, Jones TM, Zebedee SL, Persson MA, Nara PL, Norrby E, et al.** 1992. Recombinant human Fab fragments neutralize human type 1 immunodeficiency virus in vitro. Proc Natl Acad Sci U S A **89:**9339-9343.
146. **Trkola A, Purtscher M, Muster T, Ballaun C, Buchacher A, Sullivan N, Srinivasan K, Sodroski J, Moore JP, Katinger H.** 1996. Human monoclonal antibody 2G12 defines a distinctive neutralization epitope on the gp120 glycoprotein of human immunodeficiency virus type 1. J Virol **70:**1100-1108.
147. **Muster T, Steindl F, Purtscher M, Trkola A, Klima A, Himmler G, Ruker F, Katinger H.** 1993. A conserved neutralizing epitope on gp41 of human immunodeficiency virus type 1. J Virol **67:**6642-6647.
148. **Haynes BF, Fleming J, St Clair EW, Katinger H, Stiegler G, Kunert R, Robinson J, Scearce RM, Plonk K, Staats HF, Ortel TL, Liao HX, Alam SM.** 2005. Cardiolipin polyspecific autoreactivity in two broadly neutralizing HIV-1 antibodies. Science **308:**1906-1908.
149. **Walker LM, Phogat SK, Chan-Hui PY, Wagner D, Phung P, Goss JL, Wrin T, Simek MD, Fling S, Mitcham JL, Lehrman JK, Priddy FH, Olsen OA, Frey SM, Hammond PW, Kaminsky S, Zamb T, Moyle M, Koff WC, Poignard P, Burton DR.** 2009. Broad and potent neutralizing antibodies from an African donor reveal a new HIV-1 vaccine target. Science **326:**285-289.
150. **Liao HX, Bonsignori M, Alam SM, McLellan JS, Tomaras GD, Moody MA, Kozink DM, Hwang KK, Chen X, Tsao CY, Liu P, Lu X, Parks RJ, Montefiori DC, Ferrari G, Pollara J, Rao M, Peachman KK, Santra S, Letvin NL, Karasavvas N, Yang ZY, Dai K, Pancera M, Gorman J, Wiehe K, Nicely NI, Rerks-Ngarm S, Nitayaphan S, Kaewkungwal J, Pitisuttithum P, Tartaglia J, Sinangil F, Kim JH, Michael NL, Kepler TB, Kwong PD, Mascola JR, Nabel GJ, Pinter A, Zolla-Pazner S, Haynes BF.** 2013. Vaccine Induction of Antibodies against a Structurally Heterogeneous Site of Immune Pressure within HIV-1 Envelope Protein Variable Regions 1 and 2. Immunity **38:**176-186.
151. **Pan R, Gorny MK, Zolla-Pazner S, Kong XP.** 2015. The V1V2 Region of HIV-1 gp120 Forms a Five-Stranded Beta Barrel. J Virol **89:**8003-8010.
152. **Gorman J, Soto C, Yang MM, Davenport TM, Guttman M, Bailer RT, Chambers M, Chuang GY, DeKosky BJ, Doria-Rose NA, Druz A, Ernandes MJ, Georgiev IS, Jarosinski MC, Joyce MG, Lemmin TM, Leung S, Louder MK, McDaniel JR, Narpala S, Pancera M, Stuckey J, Wu X, Yang Y, Zhang B, Zhou T, Program NC, Mullikin JC, Baxa U, Georgiou G, McDermott AB, Bonsignori M, Haynes BF, Moore PL, Morris L, Lee KK, Shapiro L, Mascola JR, Kwong PD.** 2016. Structures of HIV-1 Env V1V2 with broadly neutralizing antibodies reveal commonalities that enable vaccine design. Nat Struct Mol Biol **23:**81-90.
153. **Bonsignori M, Hwang KK, Chen X, Tsao CY, Morris L, Gray E, Marshall DJ, Crump JA, Kapiga SH, Sam NE, Sinangil F, Pancera M, Yongping Y, Zhang B, Zhu J, Kwong PD, O'Dell S, Mascola JR, Wu L, Nabel GJ, Phogat S, Seaman MS, Whitesides JF, Moody MA, Kelsoe G, Yang X, Sodroski J, Shaw GM, Montefiori DC, Kepler TB, Tomaras GD, Alam SM, Liao HX, Haynes BF.** 2011. Analysis of a clonal lineage of HIV-1 envelope V2/V3 conformational epitope-specific broadly neutralizing antibodies and their inferred unmutated common ancestors. J Virol **85:**9998-10009.

154. **Walker LM, Huber M, Doores KJ, Falkowska E, Pejchal R, Julien JP, Wang SK, Ramos A, Chan-Hui PY, Moyle M, Mitcham JL, Hammond PW, Olsen OA, Phung P, Fling S, Wong CH, Phogat S, Wrin T, Simek MD, Koff WC, Wilson IA, Burton DR, Poignard P.** 2011. Broad neutralization coverage of HIV by multiple highly potent antibodies. Nature **477:**466-470.
155. **Sok D, van Gils MJ, Pauthner M, Julien JP, Saye-Francisco KL, Hsueh J, Briney B, Lee JH, Le KM, Lee PS, Hua Y, Seaman MS, Moore JP, Ward AB, Wilson IA, Sanders RW, Burton DR.** 2014. Recombinant HIV envelope trimer selects for quaternary-dependent antibodies targeting the trimer apex. Proc Natl Acad Sci U S A **111:**17624-17629.
156. **Doria-Rose NA, Schramm CA, Gorman J, Moore PL, Bhiman JN, DeKosky BJ, Ernandes MJ, Georgiev IS, Kim HJ, Pancera M, Staupe RP, Altae-Tran HR, Bailer RT, Crooks ET, Cupo A, Druz A, Garrett NJ, Hoi KH, Kong R, Louder MK, Longo NS, McKee K, Nonyane M, O'Dell S, Roark RS, Rudicell RS, Schmidt SD, Sheward DJ, Soto C, Wibmer CK, Yang Y, Zhang Z, Program NCS, Mullikin JC, Binley JM, Sanders RW, Wilson IA, Moore JP, Ward AB, Georgiou G, Williamson C, Abdool Karim SS, Morris L, Kwong PD, Shapiro L, Mascola JR.** 2014. Developmental pathway for potent V1V2-directed HIV-neutralizing antibodies. Nature **509:**55-62.
157. **Briney BS, Willis JR, Crowe JE, Jr.** 2012. Human peripheral blood antibodies with long HCDR3s are established primarily at original recombination using a limited subset of germline genes. PLoS One **7:**e36750.
158. **Doria-Rose NA, Bhiman JN, Roark RS, Schramm CA, Gorman J, Chuang GY, Pancera M, Cale EM, Ernandes MJ, Louder MK, Asokan M, Bailer RT, Druz A, Fraschilla IR, Garrett NJ, Jarosinski M, Lynch RM, McKee K, O'Dell S, Pegu A, Schmidt SD, Staupe RP, Sutton MS, Wang K, Wibmer CK, Haynes BF, Abdool-Karim S, Shapiro L, Kwong PD, Moore PL, Morris L, Mascola JR.** 2015. New Member of the V1V2-Directed CAP256-VRC26 Lineage That Shows Increased Breadth and Exceptional Potency. J Virol **90:**76-91.
159. **Pejchal R, Doores KJ, Walker LM, Khayat R, Huang PS, Wang SK, Stanfield RL, Julien JP, Ramos A, Crispin M, Depetris R, Katpally U, Marozsan A, Cupo A, Maloveste S, Liu Y, McBride R, Ito Y, Sanders RW, Ogohara C, Paulson JC, Feizi T, Scanlan CN, Wong CH, Moore JP, Olson WC, Ward AB, Poignard P, Schief WR, Burton DR, Wilson IA.** 2011. A potent and broad neutralizing antibody recognizes and penetrates the HIV glycan shield. Science **334:**1097-1103.
160. **Kong L, Lee JH, Doores KJ, Murin CD, Julien JP, McBride R, Liu Y, Marozsan A, Cupo A, Klasse PJ, Hoffenberg S, Caulfield M, King CR, Hua Y, Le KM, Khayat R, Deller MC, Clayton T, Tien H, Feizi T, Sanders RW, Paulson JC, Moore JP, Stanfield RL, Burton DR, Ward AB, Wilson IA.** 2013. Supersite of immune vulnerability on the glycosylated face of HIV-1 envelope glycoprotein gp120. Nat Struct Mol Biol **20:**796-803.
161. **Calarese DA, Scanlan CN, Zwick MB, Deechongkit S, Mimura Y, Kunert R, Zhu P, Wormald MR, Stanfield RL, Roux KH, Kelly JW, Rudd PM, Dwek RA, Katinger H, Burton DR, Wilson IA.** 2003. Antibody domain exchange is an immunological solution to carbohydrate cluster recognition. Science **300:**2065-2071.
162. **Garces F, Sok D, Kong L, McBride R, Kim HJ, Saye-Francisco KF, Julien JP, Hua Y, Cupo A, Moore JP, Paulson JC, Ward AB, Burton DR, Wilson**

IA. 2014. Structural evolution of glycan recognition by a family of potent HIV antibodies. Cell **159:**69-79.

163. **Sok D, Laserson U, Laserson J, Liu Y, Vigneault F, Julien JP, Briney B, Ramos A, Saye KF, Le K, Mahan A, Wang S, Kardar M, Yaari G, Walker LM, Simen BB, St John EP, Chan-Hui PY, Swiderek K, Kleinstein SH, Alter G, Seaman MS, Chakraborty AK, Koller D, Wilson IA, Church GM, Burton DR, Poignard P.** 2013. The effects of somatic hypermutation on neutralization and binding in the PGT121 family of broadly neutralizing HIV antibodies. PLoS Pathog **9:**e1003754.
164. **Scheid JF, Mouquet H, Ueberheide B, Diskin R, Klein F, Oliveira TY, Pietzsch J, Fenyo D, Abadir A, Velinzon K, Hurley A, Myung S, Boulad F, Poignard P, Burton DR, Pereyra F, Ho DD, Walker BD, Seaman MS, Bjorkman PJ, Chait BT, Nussenzweig MC.** 2011. Sequence and structural convergence of broad and potent HIV antibodies that mimic CD4 binding. Science **333:**1633-1637.
165. **Wu X, Zhou T, Zhu J, Zhang B, Georgiev I, Wang C, Chen X, Longo NS, Louder M, McKee K, O'Dell S, Perfetto S, Schmidt SD, Shi W, Wu L, Yang Y, Yang ZY, Yang Z, Zhang Z, Bonsignori M, Crump JA, Kapiga SH, Sam NE, Haynes BF, Simek M, Burton DR, Koff WC, Doria-Rose NA, Connors M, Program NCS, Mullikin JC, Nabel GJ, Roederer M, Shapiro L, Kwong PD, Mascola JR.** 2011. Focused evolution of HIV-1 neutralizing antibodies revealed by structures and deep sequencing. Science **333:**1593-1602.
166. **Zhou T, Georgiev I, Wu X, Yang ZY, Dai K, Finzi A, Do Kwon Y, Scheid JF, Shi W, Xu L, Yang Y, Zhu J, Nussenzweig MC, Sodroski J, Shapiro L, Nabel GJ, Mascola JR, Kwong PD.** 2010. Structural basis for broad and potent neutralization of HIV-1 by antibody VRC01. Science **329:**811-817.
167. **Chen L, Kwon YD, Zhou T, Wu X, O'Dell S, Cavacini L, Hessell AJ, Pancera M, Tang M, Xu L, Yang ZY, Zhang MY, Arthos J, Burton DR, Dimitrov DS, Nabel GJ, Posner MR, Sodroski J, Wyatt R, Mascola JR, Kwong PD.** 2009. Structural basis of immune evasion at the site of CD4 attachment on HIV-1 gp120. Science **326:**1123-1127.
168. **Wu X, Zhang Z, Schramm CA, Joyce MG, Kwon YD, Zhou T, Sheng Z, Zhang B, O'Dell S, McKee K, Georgiev IS, Chuang GY, Longo NS, Lynch RM, Saunders KO, Soto C, Srivatsan S, Yang Y, Bailer RT, Louder MK, Program NCS, Mullikin JC, Connors M, Kwong PD, Mascola JR, Shapiro L.** 2015. Maturation and Diversity of the VRC01-Antibody Lineage over 15 Years of Chronic HIV-1 Infection. Cell **161:**470-485.
169. **Zhou T, Zhu J, Wu X, Moquin S, Zhang B, Acharya P, Georgiev IS, Altae-Tran HR, Chuang GY, Joyce MG, Do Kwon Y, Longo NS, Louder MK, Luongo T, McKee K, Schramm CA, Skinner J, Yang Y, Yang Z, Zhang Z, Zheng A, Bonsignori M, Haynes BF, Scheid JF, Nussenzweig MC, Simek M, Burton DR, Koff WC, Program NCS, Mullikin JC, Connors M, Shapiro L, Nabel GJ, Mascola JR, Kwong PD.** 2013. Multidonor analysis reveals structural elements, genetic determinants, and maturation pathway for HIV-1 neutralization by VRC01-class antibodies. Immunity **39:**245-258.
170. **West AP, Jr., Diskin R, Nussenzweig MC, Bjorkman PJ.** 2012. Structural basis for germ-line gene usage of a potent class of antibodies targeting the CD4-binding site of HIV-1 gp120. Proc Natl Acad Sci U S A **109:**E2083-2090.
171. **Zhou T, Lynch RM, Chen L, Acharya P, Wu X, Doria-Rose NA, Joyce MG, Lingwood D, Soto C, Bailer RT, Ernandes MJ, Kong R, Longo NS, Louder**

MK, McKee K, O'Dell S, Schmidt SD, Tran L, Yang Z, Druz A, Luongo TS, Moquin S, Srivatsan S, Yang Y, Zhang B, Zheng A, Pancera M, Kirys T, Georgiev IS, Gindin T, Peng HP, Yang AS, Program NCS, Mullikin JC, Gray MD, Stamatatos L, Burton DR, Koff WC, Cohen MS, Haynes BF, Casazza JP, Connors M, Corti D, Lanzavecchia A, Sattentau QJ, Weiss RA, West AP, Jr., Bjorkman PJ, Scheid JF, Nussenzweig MC, et al. 2015. Structural Repertoire of HIV-1-Neutralizing Antibodies Targeting the CD4 Supersite in 14 Donors. Cell **161:**1280-1292.

172. **Wibmer CK, Bhiman JN, Gray ES, Tumba N, Abdool Karim SS, Williamson C, Morris L, Moore PL.** 2013. Viral escape from HIV-1 neutralizing antibodies drives increased plasma neutralization breadth through sequential recognition of multiple epitopes and immunotypes. PLoS Pathog **9:**e1003738.
173. **Balla-Jhagjhoorsingh SS, Corti D, Heyndrickx L, Willems E, Vereecken K, Davis D, Vanham G.** 2013. The N276 glycosylation site is required for HIV-1 neutralization by the CD4 binding site specific HJ16 monoclonal antibody. PLoS One **8:**e68863.
174. **Freund NT, Horwitz JA, Nogueira L, Sievers SA, Scharf L, Scheid JF, Gazumyan A, Liu C, Velinzon K, Goldenthal A, Sanders RW, Moore JP, Bjorkman PJ, Seaman MS, Walker BD, Klein F, Nussenzweig MC.** 2015. A New Glycan-Dependent CD4-Binding Site Neutralizing Antibody Exerts Pressure on HIV-1 In Vivo. PLoS Pathog **11:**e1005238.
175. **Scharf L, Scheid JF, Lee JH, West AP, Jr., Chen C, Gao H, Gnanapragasam PN, Mares R, Seaman MS, Ward AB, Nussenzweig MC, Bjorkman PJ.** 2014. Antibody 8ANC195 reveals a site of broad vulnerability on the HIV-1 envelope spike. Cell Rep **7:**785-795.
176. **Scharf L, Wang H, Gao H, Chen S, McDowall AW, Bjorkman PJ.** 2015. Broadly Neutralizing Antibody 8ANC195 Recognizes Closed and Open States of HIV-1 Env. Cell **162:**1379-1390.
177. **Falkowska E, Le KM, Ramos A, Doores KJ, Lee JH, Blattner C, Ramirez A, Derking R, van Gils MJ, Liang CH, McBride R, von Bredow B, Shivatare SS, Wu CY, Chan-Hui PY, Liu Y, Feizi T, Zwick MB, Koff WC, Seaman MS, Swiderek K, Moore JP, Evans D, Paulson JC, Wong CH, Ward AB, Wilson IA, Sanders RW, Poignard P, Burton DR.** 2014. Broadly Neutralizing HIV Antibodies Define a Glycan-Dependent Epitope on the Prefusion Conformation of gp41 on Cleaved Envelope Trimers. Immunity doi:10.1016/j.immuni.2014.04.009.
178. **Blattner C, Lee JH, Sliepen K, Derking R, Falkowska E, de la Pena AT, Cupo A, Julien JP, van Gils M, Lee PS, Peng W, Paulson JC, Poignard P, Burton DR, Moore JP, Sanders RW, Wilson IA, Ward AB.** 2014. Structural Delineation of a Quaternary, Cleavage-Dependent Epitope at the gp41-gp120 Interface on Intact HIV-1 Env Trimers. Immunity doi:10.1016/j.immuni.2014.04.008.
179. **Huang J, Kang BH, Pancera M, Lee JH, Tong T, Feng Y, Imamichi H, Georgiev IS, Chuang GY, Druz A, Doria-Rose NA, Laub L, Sliepen K, van Gils MJ, de la Pena AT, Derking R, Klasse PJ, Migueles SA, Bailer RT, Alam M, Pugach P, Haynes BF, Wyatt RT, Sanders RW, Binley JM, Ward AB, Mascola JR, Kwong PD, Connors M.** 2014. Broad and potent HIV-1 neutralization by a human antibody that binds the gp41-gp120 interface. Nature **515:**138-142.
180. **Lee JH, Leaman DP, Kim AS, Torrents de la Pena A, Sliepen K, Yasmeen**

A, Derking R, Ramos A, de Taeye SW, Ozorowski G, Klein F, Burton DR, Nussenzweig MC, Poignard P, Moore JP, Klasse PJ, Sanders RW, Zwick MB, Wilson IA, Ward AB. 2015. Antibodies to a conformational epitope on gp41 neutralize HIV-1 by destabilizing the Env spike. Nat Commun **6:**8167.

181. **Chen J, Frey G, Peng H, Rits-Volloch S, Garrity J, Seaman MS, Chen B.** 2014. Mechanism of HIV-1 neutralization by antibodies targeting a membrane-proximal region of gp41. J Virol **88:**1249-1258.
182. **Ofek G, McKee K, Yang Y, Yang ZY, Skinner J, Guenaga FJ, Wyatt R, Zwick MB, Nabel GJ, Mascola JR, Kwong PD.** 2010. Relationship between antibody 2F5 neutralization of HIV-1 and hydrophobicity of its heavy chain third complementarity-determining region. J Virol **84:**2955-2962.
183. **Pejchal R, Gach JS, Brunel FM, Cardoso RM, Stanfield RL, Dawson PE, Burton DR, Zwick MB, Wilson IA.** 2009. A conformational switch in HIV gp41 revealed by the structures of overlapping epitopes recognized by neutralizing antibodies. J Virol.
184. **Ofek G, Tang M, Sambor A, Katinger H, Mascola JR, Wyatt R, Kwong PD.** 2004. Structure and mechanistic analysis of the anti-human immunodeficiency virus type 1 antibody 2F5 in complex with its gp41 epitope. J Virol **78:**10724-10737.
185. **Cardoso RM, Zwick MB, Stanfield RL, Kunert R, Binley JM, Katinger H, Burton DR, Wilson IA.** 2005. Broadly neutralizing anti-HIV antibody 4E10 recognizes a helical conformation of a highly conserved fusion-associated motif in gp41. Immunity **22:**163-173.
186. **Huang J, Ofek G, Laub L, Louder MK, Doria-Rose NA, Longo NS, Imamichi H, Bailer RT, Chakrabarti B, Sharma SK, Alam SM, Wang T, Yang Y, Zhang B, Migueles SA, Wyatt R, Haynes BF, Kwong PD, Mascola JR, Connors M.** 2012. Broad and potent neutralization of HIV-1 by a gp41-specific human antibody. Nature **491:**406-412.
187. **Ofek G, Zirkle B, Yang Y, Zhu Z, McKee K, Zhang B, Chuang GY, Georgiev IS, O'Dell S, Doria-Rose N, Mascola JR, Dimitrov DS, Kwong PD.** 2014. Structural basis for HIV-1 neutralization by 2F5-like antibodies m66 and m66.6. J Virol **88:**2426-2441.
188. **Sun ZY, Oh KJ, Kim M, Yu J, Brusic V, Song L, Qiao Z, Wang JH, Wagner G, Reinherz EL.** 2008. HIV-1 broadly neutralizing antibody extracts its epitope from a kinked gp41 ectodomain region on the viral membrane. Immunity **28:**52-63.
189. **Gray ES, Taylor N, Wycuff D, Moore PL, Tomaras GD, Wibmer CK, Puren A, DeCamp A, Gilbert PB, Wood B, Montefiori DC, Binley JM, Shaw GM, Haynes BF, Mascola JR, Morris L.** 2009. Antibody specificities associated with neutralization breadth in plasma from human immunodeficiency virus type 1 subtype C-infected blood donors. J Virol **83:**8925-8937.
190. **Gray ES, Madiga MC, Moore PL, Mlisana K, Abdool Karim SS, Binley JM, Shaw GM, Mascola JR, Morris L.** 2009. Broad neutralization of human immunodeficiency virus type 1 mediated by plasma antibodies against the gp41 membrane proximal external region. J Virol **83:**11265-11274.
191. **Li Y, Svehla K, Louder MK, Wycuff D, Phogat S, Tang M, Migueles SA, Wu X, Phogat A, Shaw GM, Connors M, Hoxie J, Mascola JR, Wyatt R.** 2009. Analysis of neutralization specificities in polyclonal sera derived from human immunodeficiency virus type 1-infected individuals. J Virol **83:**1045-1059.
192. **Sather DN, Armann J, Ching LK, Mavrantoni A, Sellhorn G, Caldwell Z, Yu**

X, Wood B, Self S, Kalams S, Stamatatos L. 2009. Factors associated with the development of cross-reactive neutralizing antibodies during human immunodeficiency virus type 1 infection. J Virol **83:**757-769.

193. **Pritchard LK, Spencer DI, Royle L, Bonomelli C, Seabright GE, Behrens AJ, Kulp DW, Menis S, Krumm SA, Dunlop DC, Crispin DJ, Bowden TA, Scanlan CN, Ward AB, Schief WR, Doores KJ, Crispin M.** 2015. Glycan clustering stabilizes the mannose patch of HIV-1 and preserves vulnerability to broadly neutralizing antibodies. Nat Commun **6:**7479.
194. **Li Y, Migueles SA, Welcher B, Svehla K, Phogat A, Louder MK, Wu X, Shaw GM, Connors M, Wyatt RT, Mascola JR.** 2007. Broad HIV-1 neutralization mediated by CD4-binding site antibodies. Nat Med **13:**1032-1034.
195. **Walker LM, Simek MD, Priddy F, Gach JS, Wagner D, Zwick MB, Phogat SK, Poignard P, Burton DR.** 2010. A limited number of antibody specificities mediate broad and potent serum neutralization in selected HIV-1 infected individuals. PLoS Pathog **6:**e1001028.
196. **Tomaras GD, Binley JM, Gray ES, Crooks ET, Osawa K, Moore PL, Tumba N, Tong T, Shen X, Yates NL, Decker J, Wibmer CK, Gao F, Alam SM, Easterbrook P, Abdool Karim S, Kamanga G, Crump JA, Cohen M, Shaw GM, Mascola JR, Haynes BF, Montefiori DC, Morris L.** 2011. Polyclonal B cell responses to conserved neutralization epitopes in a subset of HIV-1-infected individuals. J Virol **85:**11502-11519.
197. **Moore PL, Gray ES, Wibmer CK, Bhiman JN, Nonyane M, Sheward DJ, Hermanus T, Bajimaya S, Tumba NL, Abrahams MR, Lambson BE, Ranchobe N, Ping L, Ngandu N, Abdool Karim Q, Abdool Karim SS, Swanstrom RI, Seaman MS, Williamson C, Morris L.** 2012. Evolution of an HIV glycan-dependent broadly neutralizing antibody epitope through immune escape. Nat Med **18:**1688-1692.
198. **Moore PL, Gray ES, Sheward D, Madiga M, Ranchobe N, Lai Z, Honnen WJ, Nonyane M, Tumba N, Hermanus T, Sibeko S, Mlisana K, Abdool Karim SS, Williamson C, Pinter A, Morris L, Study C.** 2011. Potent and broad neutralization of HIV-1 subtype C by plasma antibodies targeting a quaternary epitope including residues in the V2 loop. J Virol **85:**3128-3141.
199. **Wu X, Yang ZY, Li Y, Hogerkorp CM, Schief WR, Seaman MS, Zhou T, Schmidt SD, Wu L, Xu L, Longo NS, McKee K, O'Dell S, Louder MK, Wycuff DL, Feng Y, Nason M, Doria-Rose N, Connors M, Kwong PD, Roederer M, Wyatt RT, Nabel GJ, Mascola JR.** 2010. Rational design of envelope identifies broadly neutralizing human monoclonal antibodies to HIV-1. Science **329:**856-861.
200. **Morris L, Chen X, Alam M, Tomaras G, Zhang R, Marshall DJ, Chen B, Parks R, Foulger A, Jaeger F, Donathan M, Bilska M, Gray ES, Abdool Karim SS, Kepler TB, Whitesides J, Montefiori D, Moody MA, Liao HX, Haynes BF.** 2011. Isolation of a human anti-HIV gp41 membrane proximal region neutralizing antibody by antigen-specific single B cell sorting. PLoS One **6:**e23532.
201. **Gray ES, Moody MA, Wibmer CK, Chen X, Marshall D, Amos J, Moore PL, Foulger A, Yu JS, Lambson B, Abdool Karim S, Whitesides J, Tomaras GD, Haynes BF, Morris L, Liao HX.** 2011. Isolation of a monoclonal antibody that targets the alpha-2 helix of gp120 and represents the initial autologous neutralizing-antibody response in an HIV-1 subtype C-infected individual. J Virol **85:**7719-7729.

202. **Gao F, Bonsignori M, Liao HX, Kumar A, Xia SM, Lu X, Cai F, Hwang KK, Song H, Zhou T, Lynch RM, Alam SM, Moody MA, Ferrari G, Berrong M, Kelsoe G, Shaw GM, Hahn BH, Montefiori DC, Kamanga G, Cohen MS, Hraber P, Kwong PD, Korber BT, Mascola JR, Kepler TB, Haynes BF.** 2014. Cooperation of B cell lineages in induction of HIV-1-broadly neutralizing antibodies. Cell **158:**481-491.
203. **Liao HX, Lynch R, Zhou T, Gao F, Alam SM, Boyd SD, Fire AZ, Roskin KM, Schramm CA, Zhang Z, Zhu J, Shapiro L, Program NCS, Mullikin JC, Gnanakaran S, Hraber P, Wiehe K, Kelsoe G, Yang G, Xia SM, Montefiori DC, Parks R, Lloyd KE, Scearce RM, Soderberg KA, Cohen M, Kamanga G, Louder MK, Tran LM, Chen Y, Cai F, Chen S, Moquin S, Du X, Joyce MG, Srivatsan S, Zhang B, Zheng A, Shaw GM, Hahn BH, Kepler TB, Korber BT, Kwong PD, Mascola JR, Haynes BF.** 2013. Co-evolution of a broadly neutralizing HIV-1 antibody and founder virus. Nature **496:**469-476.
204. **Yang X, Tomov V, Kurteva S, Wang L, Ren X, Gorny MK, Zolla-Pazner S, Sodroski J.** 2004. Characterization of the outer domain of the gp120 glycoprotein from human immunodeficiency virus type 1. J Virol **78:**12975-12986.
205. **Chen H, Xu X, Jones IM.** 2007. Immunogenicity of the outer domain of a HIV-1 clade C gp120. Retrovirology **4:**33.
206. **Chen H, Xu X, Lin HH, Chen SH, Forsman A, Aasa-Chapman M, Jones IM.** 2008. Mapping the immune response to the outer domain of a human immunodeficiency virus-1 clade C gp120. J Gen Virol **89:**2597-2604.
207. **Wu L, Zhou T, Yang ZY, Svehla K, O'Dell S, Louder MK, Xu L, Mascola JR, Burton DR, Hoxie JA, Doms RW, Kwong PD, Nabel GJ.** 2009. Enhanced exposure of the CD4-binding site to neutralizing antibodies by structural design of a membrane-anchored human immunodeficiency virus type 1 gp120 domain. J Virol **83:**5077-5086.
208. **Bhattacharyya S, Rajan RE, Swarupa Y, Rathore U, Verma A, Udaykumar R, Varadarajan R.** 2010. Design of a non-glycosylated outer domain-derived HIV-1 gp120 immunogen that binds to CD4 and induces neutralizing antibodies. J Biol Chem **285:**27100-27110.
209. **Qin Y, Banasik M, Kim S, Penn-Nicholson A, Habte HH, LaBranche C, Montefiori DC, Wang C, Cho MW.** 2014. Eliciting neutralizing antibodies with gp120 outer domain constructs based on M-group consensus sequence. Virology **462-463:**363-376.
210. **Yokoyama M, Naganawa S, Yoshimura K, Matsushita S, Sato H.** 2012. Structural dynamics of HIV-1 envelope Gp120 outer domain with V3 loop. PLoS One **7:**e37530.
211. **McGuire AT, Hoot S, Dreyer AM, Lippy A, Stuart A, Cohen KW, Jardine J, Menis S, Scheid JF, West AP, Schief WR, Stamatatos L.** 2013. Engineering HIV envelope protein to activate germline B cell receptors of broadly neutralizing anti-CD4 binding site antibodies. J Exp Med doi:10.1084/jem.20122824.
212. **Jardine J, Julien JP, Menis S, Ota T, Kalyuzhniy O, McGuire A, Sok D, Huang PS, Macpherson S, Jones M, Nieusma T, Mathison J, Baker D, Ward AB, Burton DR, Stamatatos L, Nemazee D, Wilson IA, Schief WR.** 2013. Rational HIV Immunogen Design to Target Specific Germline B Cell Receptors. Science doi:10.1126/science.1234150.
213. **Dosenovic P, von Boehmer L, Escolano A, Jardine J, Freund NT, Gitlin**

AD, McGuire AT, Kulp DW, Oliveira T, Scharf L, Pietzsch J, Gray MD, Cupo A, van Gils MJ, Yao KH, Liu C, Gazumyan A, Seaman MS, Bjorkman PJ, Sanders RW, Moore JP, Stamatatos L, Schief WR, Nussenzweig MC. 2015. Immunization for HIV-1 Broadly Neutralizing Antibodies in Human Ig Knockin Mice. Cell **161:**1505-1515.

214. **Jardine JG, Ota T, Sok D, Pauthner M, Kulp DW, Kalyuzhniy O, Skog PD, Thinnes TC, Bhullar D, Briney B, Menis S, Jones M, Kubitz M, Spencer S, Adachi Y, Burton DR, Schief WR, Nemazee D.** 2015. HIV-1 VACCINES. Priming a broadly neutralizing antibody response to HIV-1 using a germline-targeting immunogen. Science **349:**156-161.
215. **Wu X, Wang C, O'Dell S, Li Y, Keele BF, Yang Z, Imamichi H, Doria-Rose N, Hoxie JA, Connors M, Shaw GM, Wyatt RT, Mascola JR.** 2012. Selection pressure on HIV-1 envelope by broadly neutralizing antibodies to the conserved CD4-binding site. J Virol **86:**5844-5856.
216. **Bhiman JN, Anthony C, Doria-Rose NA, Karimanzira O, Schramm CA, Khoza T, Kitchin D, Botha G, Gorman J, Garrett NJ, Abdool Karim SS, Shapiro L, Williamson C, Kwong PD, Mascola JR, Morris L, Moore PL.** 2015. Viral variants that initiate and drive maturation of V1V2-directed HIV-1 broadly neutralizing antibodies. Nat Med **21:**1332-1336.
217. **Moore PL, Williamson C, Morris L.** 2015. Virological features associated with the development of broadly neutralizing antibodies to HIV-1. Trends Microbiol **23:**204-211.
218. **Crooks ET, Tong T, Chakrabarti B, Narayan K, Georgiev IS, Menis S, Huang X, Kulp D, Osawa K, Muranaka J, Stewart-Jones G, Destefano J, O'Dell S, LaBranche C, Robinson JE, Montefiori DC, McKee K, Du SX, Doria-Rose N, Kwong PD, Mascola JR, Zhu P, Schief WR, Wyatt RT, Whalen RG, Binley JM.** 2015. Vaccine-Elicited Tier 2 HIV-1 Neutralizing Antibodies Bind to Quaternary Epitopes Involving Glycan-Deficient Patches Proximal to the CD4 Binding Site. PLoS Pathog **11:**e1004932.
219. **Wu X, Changela A, O'Dell S, Schmidt SD, Pancera M, Yang Y, Zhang B, Gorny MK, Phogat S, Robinson JE, Stamatatos L, Zolla-Pazner S, Kwong PD, Mascola JR.** 2011. Immunotypes of a quaternary site of HIV-1 vulnerability and their recognition by antibodies. J Virol **85:**4578-4585.
220. **Gorny MK, Stamatatos L, Volsky B, Revesz K, Williams C, Wang XH, Cohen S, Staudinger R, Zolla-Pazner S.** 2005. Identification of a new quaternary neutralizing epitope on human immunodeficiency virus type 1 virus particles. J Virol **79:**5232-5237.
221. **Bradley T, Fera D, Bhiman J, Eslamizar L, Lu X, Anasti K, Zhang R, Sutherland LL, Scearce RM, Bowman CM, Stolarchuk C, Lloyd KE, Parks R, Eaton A, Foulger A, Nie X, Karim SS, Barnett S, Kelsoe G, Kepler TB, Alam SM, Montefiori DC, Moody MA, Liao HX, Morris L, Santra S, Harrison SC, Haynes BF.** 2016. Structural Constraints of Vaccine-Induced Tier-2 Autologous HIV Neutralizing Antibodies Targeting the Receptor-Binding Site. Cell Rep **14:**43-54.
222. **Murphy MK, Yue L, Pan R, Boliar S, Sethi A, Tian J, Pfafferot K, Karita E, Allen SA, Cormier E, Goepfert PA, Borrow P, Robinson JE, Gnanakaran S, Hunter E, Kong XP, Derdeyn CA.** 2013. Viral Escape from Neutralizing Antibodies in Early Subtype A HIV-1 Infection Drives an Increase in Autologous Neutralization Breadth. PLoS Pathog **9:**e1003173.
223. **Bonsignori M, Zhou T, Sheng Z, Chen L, Gao F, Joyce MG, Ozorowski G,**

Chuang GY, Schramm CA, Wiehe K, Alam SM, Bradley T, Gladden MA, Hwang KK, Iyengar S, Kumar A, Lu X, Luo K, Mangiapani MC, Parks RJ, Song H, Acharya P, Bailer RT, Cao A, Druz A, Georgiev IS, Kwon YD, Louder MK, Zhang B, Zheng A, Hill BJ, Kong R, Soto C, Program NCS, Mullikin JC, Douek DC, Montefiori DC, Moody MA, Shaw GM, Hahn BH, Kelsoe G, Hraber PT, Korber BT, Boyd SD, Fire AZ, Kepler TB, Shapiro L, Ward AB, Mascola JR, Liao HX, et al. 2016. Maturation Pathway from Germline to Broad HIV-1 Neutralizer of a CD4-Mimic Antibody. Cell doi:10.1016/j.cell.2016.02.022.

CHAPTER TWO: HIV BROADLY NEUTRALIZING ANTIBODY TARGETS

A review published in Current Opinion in HIV and AIDS:
May 2015 - Volume 10 - Issue 3 - p 135-143.

REVIEW

HIV broadly neutralizing antibody targets

Constantinos Kurt Wibmer[a,b], Penny L. Moore[a,b,c], and Lynn Morris[a,b,c]

Purpose of review

To provide an update on neutralizing antibody targets in the context of the recent HIV-1 envelope trimer structure, describe new antibody isolation technologies, and discuss the implications of these data for HIV-1 prevention and therapy.

Recent findings

Recent advances in B-cell technologies have dramatically expanded the number of antibodies isolated from HIV-infected donors with broadly neutralizing plasma activity. These, together with the first high-resolution crystal and cryo-electron microscopy (cryo-EM) structures of a cleaved, prefusion HIV-1 trimer, have defined new regions susceptible to neutralization. This year, three epitopes in the gp120–gp41 interface were structurally characterized, highlighting the importance of prefusion gp41 as a target. Similar to many other broadly neutralizing antibody epitopes, these new antibodies define a target that is also highly glycan dependent. Collectively, the epitopes for broadly neutralizing antibodies now reveal a continuum of vulnerability spanning the length of the HIV-1 envelope trimer.

Summary

Progress in the last year has provided support for the use of rationally stabilized whole HIV-1 trimers as immunogens for eliciting antibodies to multiple epitopes. Furthermore, the increasing number of broad and potent antibodies with the potential for synergistic/complementary combinations opens up new avenues for preventing and treating HIV-1 infection.

Keywords

glycans, gp120–gp41 interface, HIV-1 envelope, neutralizing antibody epitopes

a Centre for HIV and STIs, National Institute for Communicable Diseases (NICD), National Health Laboratory Service (NHLS), **b** Faculty of Health Sciences, University of the Witwatersrand, Johannesburg and **c** Centre for the AIDS Programme of Research in South Africa (CAPRISA), University of KwaZulu-Natal, Durban, South Africa.
Correspondence to Prof. Lynn Morris, Centre for HIV and STIs, National Institute for Communicable Diseases, National Health Laboratory Service (NHLS), Private Bag X4, Sandringham 2131, Johannesburg, South Africa.
Tel: +27113866332; fax: +27113866456; e-mail: lynnm@nicd.ac.za

INTRODUCTION

The HIV-1 envelope (Env) glycoprotein spike mediates viral entry, and is the sole target of neutralizing antibodies. The entry-mediating form exists as a trimer composed of three host receptor binding gp120 molecules, noncovalently linked to three gp41 transmembrane fusion proteins. gp120 is heavily glycosylated and shielded by the hypervariable regions (loops V1–V5, the a2 helix, and b14 sheet), whereas gp41 is more conserved, less solvent exposed, and less glycosylated. As a result of host immune pressures Env is the most diverse of all HIV proteins with up to 30% variation between different genetic subtypes. Amino acid substitution, insertions /deletions, and glycan shifting occur predominantly in the variable regions that are most easily accessed by neutralizing antibodies. The dominant neutralizing antibody response is therefore strain specific, however over the course of HIV-1 infection most individuals develop antibodies with some level of cross-reactivity [1]. Those with the greatest breadth have been the source of new broadly neutralizing antibodies (bNAbs) [2]. Characterizing the epitopes of these bNAbs has led to high resolution structures of the HIV-1 Env trimer [3,4,5&&], allowing us to more clearly define sites of vulnerability that might be exploited for HIV-1 vaccine design and antibody mediated therapy.

KEY POINTS

- Technological advances have significantly improved our ability to map plasma bNAb specificities and isolate relevant mAbs.
- The gp120–gp41 interface is revealed as a new bNAb target.
- At least five broadly defined bNAb targets exist that form a continuum of vulnerability spanning the length of the HIV-1 Env trimer.
- New mAb combinations show unprecedented levels of cross-clade coverage and potency providing opportunities for preventive and therapeutic applications of bNAbs.
- Structure and immunogenicity studies of bNAb epitopes on the HIV-1 Env trimer may foster the design of better vaccines able to elicit bNAbs.

TECHNOLOGIES FOR THE ISOLATION OF NEW BROADLY NEUTRALIZING ANTIBODIES

The first bNAbs to HIV-1 (b12, 2G12, 2F5, and 4E10) were isolated by phage display or B-cell immortalization, selected for binding to Env peptides or monomeric proteins, and generally limited in breadth and/or potency. The ability to culture

memory B cells, together with high-throughput neutralization assays that allowed for direct functional screening, led to the isolation of several new antibodies targeting novel quaternary structure specific epitopes, as well as more potent antibodies to previously identified sites [6–8,9&&,10&&]. New bNAbs to previously known targets (but possessing greater breadth and potency) have also been identified using structure-guided methods to design sorting antigens for labelling B cells by flow cytometry [11,12]. Unlike B-cell culture this technique does not rely on potent neutralization to identify bNAbs, but it is limited by the specific mode of recognition. More recently, quaternary structure specific bNAbs have been isolated using native, cleaved, prefusion trimers as sorting antigens, which appear to preferentially bind neutralizing antibodies [13&&]. The successful isolation of bNAbs has been aided by first mapping the neutralization specificities in donor plasma, to tailor an appropriate selection technique [14,15]. In addition bioinformatics approaches have been used to predict specificities and design targeted approaches for the isolation of bNAbs [16–18]. Once a B-cell lineage has been identified the use of next-generation sequencing to mine the repertoire allows for literally hundreds of related variants to be identified [19–22]. A major obstacle of next-generation sequencing however is the inability to identify naturally occurring heavy-chain and light-chain antibody pairs. This was overcome when Georgiou et al. devised a method of pairing heavy-chain and light-chain PCR products prior to sequencing [23]. Information on the targets for bNAbs, as well as neutralization, sequence, and structural data on the monoclonal antibodies (mAbs) that have been isolated is being extensively catalogued into two new publically available databases: CATNAP on the LANL website: (http://www.hiv.lanl.gov/components/sequence/HIV/neutralization/main.comp) and bNAber [24], providing useful resources for the field.

BROADLY NEUTRALIZING ANTIBODY TARGETS

The isolation of exceptionally broad and potent bNAbs has enabled the identification of five roughly defined targets on the HIV-1 Env, such as the V2 site, the N332 supersite, the CD4 binding site (CD4bs), the gp120–gp41 interface, and the membrane proximal external region (MPER). Identifying multiple bNAbs with similar epitopes has pinpointed minimal sites of vulnerability, whose recognition confers the greatest neutralization breadth. However as

discussed below, new bNAbs with novel epitopes have revised our understanding of how these distinct sites partially merge in the context of the trimer.

THE V2 SITE

The V2 site at the trimer apex is formed from the converging, sequence conserved regions of the V1V2 domain and the V3 loop [3,4,25]. It is protected by densely packed glycans (particularly those at positions N156 and N160) and the hypervariable loops V1 and V2 [26]. Access to the underlying peptide epitope is only possible by antibodies with unusually long (between 26 and 39 amino acids), anionic heavy chain complementarity determining region loop three (CDR-H3) [7,14,26]. Anti-V2 bNAbs generally bind poorly to monomeric gp120 or scaffolded V1V2s [7,14]. In the case of the prototypical V2 antibody PG9, this quaternary specificity was partially explained by the fact that the antibody binds to N160 glycans from two separate protomers [27,28]. However, for some relatives of the CAP256-VRC26 lineage which targets a similar epitope, broad neutralization was not dependent on the N160 glycan [14]. Despite these differences, the actual peptide epitope determined by mutagenesis is minimal for both the PG9 and CAP256-VRC26 antibodies, made up of a short mostly cationic stretch of seven amino acids (position 165–171). For PG9 the underlying peptide comprises less than 25% of the epitope, with the rest of the epitope predominantly formed by the glycans at N156 and N160 [7,14,26,29]. The conserved nature of these glycans, and the small peptide footprint, likely contributes to the breadth of this class of antibodies.

THE N332 SUPERSITE

The N332 supersite is composed of a number of overlapping glycan-dependent epitopes [30]. V3 epitopes lie structurally proximal to the V2 site [4], and are the most well described within the N332 supersite. Antibodies targeting V3 show a similar mechanism to V2 site recognition, in that they access a minimal eight residue peptide epitope between positions 323 and 330 via long (20–26 amino acids) CDR-H3s [31]. Two such antibodies, PGT121 and PGT128, are highly dependent on the glycans at positions N301 and N332 [6], but somatic variants of PGT121 also depend on glycans in V1 (N137) and V2 (N156) [4]. In this way PGT121-like antibodies can recognize a different side of the N156 glycan that is critical to most anti-V2 bNAbs (Fig. 1). PGT130 was isolated from the same donor as PGT128, but

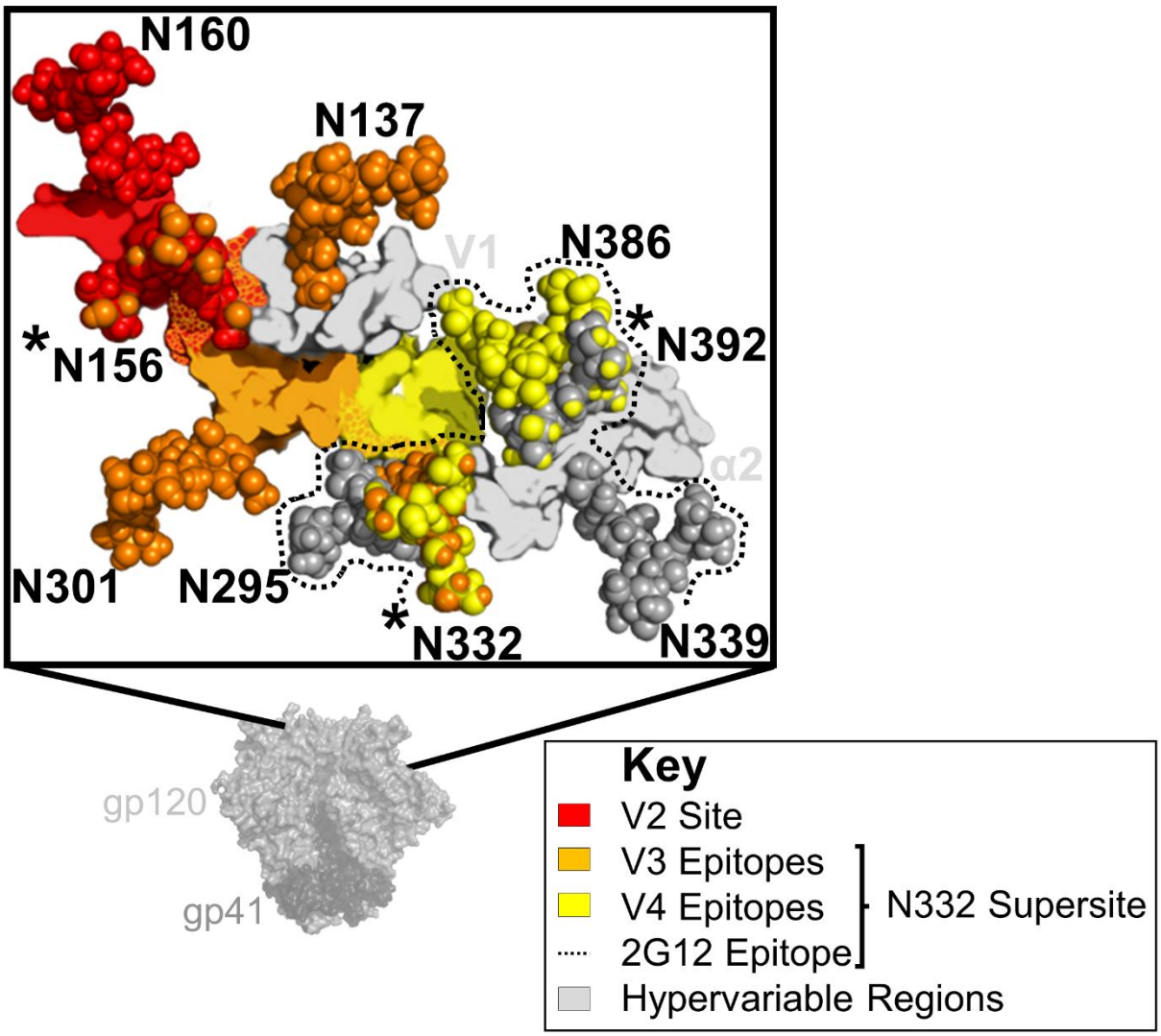

FIGURE 1. The V2 site overlaps with the N332 supersite. The HIV-1 envelope (Env) trimer is shown in light (gp120) and dark (gp41) grey surface view. An expanded graphic of the V2 and N332 sites is shown in the zoomed in box. Epitopes in V2 (red), V3 (orange), or V4 (yellow) are defined as residues within 5 Å of broadly neutralizing antibodies (bNAbs) PG9, PGT122/PGT128, or PGT135, respectively. Regions of overlap between epitopes are shown with mottled colours red/orange for V2-V3, and orange/yellow for V3–V4. Key glycans are shown as spheres, labelled, and coloured according to their epitopes. Glycans predicted to be a part of the 2G12 epitope are coloured dark grey, and bordered with a dotted line. Glycans N156, N332, and N392 that are bound by bNAbs targeting different epitopes are asterisked. Proximal hypervariable regions V1 and α2 are shown in light grey. Figure based on protein databank accession code 4TVP.

represents an alternate branch of the B-cell lineage that preferentially recognizes a glycan at N334 [6,32]. The N334 and N332 glycans are mutually exclusive, and thus in both donors somatic variants have evolved to recognize different immunotypes of the V3 site, indicative of the role for viral diversification in driving bNAb maturation, that ultimately accounts for total plasma neutralization breadth [32,33]. bNAb PGT135 defines a second epitope in the N332 supersite that does not involve V3, but rather contacts amino acids at the base of the V4 loop [30]. This mAb binds predominantly to the apolar face of the N332 glycan (unlike PGT128), and recognizes additional glycans at positions N295, N386, and N392 [30]. A third epitope, defined by the bNAb 2G12 overlaps the PGT135 epitope but unusually does not involve any peptide contact (Fig. 1). Rather, 2G12 uses a rare variable heavy (VH) chain domain swap to create a large paratope capable of binding to the terminal sugars of four glycans on the silent face of gp120 (N295, N332, N339, and N392) [34]. Thus, while 2G12 does not actually penetrate the glycan shield, it does share the recognition of key glycans with PGT135. The isolation of additional bNAbs with specificities similar to PGT135 or 2G12 will help to better define the vulnerabilities within this supersite.

THE CD4 BINDING SITE

In contrast to bNAbs targeting V2 or N332, antibodies targeting the CD4bs generally make minimal glycan contacts. Only one mode of recognition at the CD4bs has been extensively described, that of VH1-2 or VH1-46 derived bNAbs, typified by VRC01 and 8ANC131. The germline precursors of these bNAbs have specific genetic signatures that mimic CD4 binding, such as R71 in the heavy chain that, like R59 of CD4, interacts with D368 in the highly conserved CD4 binding loop of gp120 [12,35]. VH12 bNAbs also have unusually short CDR-L3 loops to avoid clashes with the glycan at position N276 in the D loop of gp120 [36–38]. Conversely the bNAb HJ16 derived from the VH3-30 gene does not interact with D368, and is entirely dependent on the glycan at position N276 for neutralization, defining a second subsite within the CD4bs [39,40]. This glycan is sometimes bound by VRC01-like antibodies, but is not critical to their neutralization [41]. HJ16 and other non-VH1-2/1-46 derived CD4bs bNAbs have long CDR-H3 loops important for their binding, but are still limited in their angle of approach to gp120 by extensive glycosylation and the quaternary nature of the trimer [15,42]. Cryoelectron microscopy (cryo-EM) structures have

shown that some CD4bs bNAbs such as PGV04 may actually interact with the glycans that closely border the CD4bs (N276, N363, and N386) as well as the N301 glycan from the V3 loop of an adjacent protomer [3]. These data also suggest contact between the positively charged amino acids in V3, and an anionic insertion in the PGV04 heavy-chain framework region 3 (FWR3). The contribution of these additional contacts to neutralization is unclear considering many CD4bs bNAbs induce a conformation of gp120 that would rearrange the V1V2 and V3 loops. Nonetheless the complexity of the CD4bs has previously been underestimated.

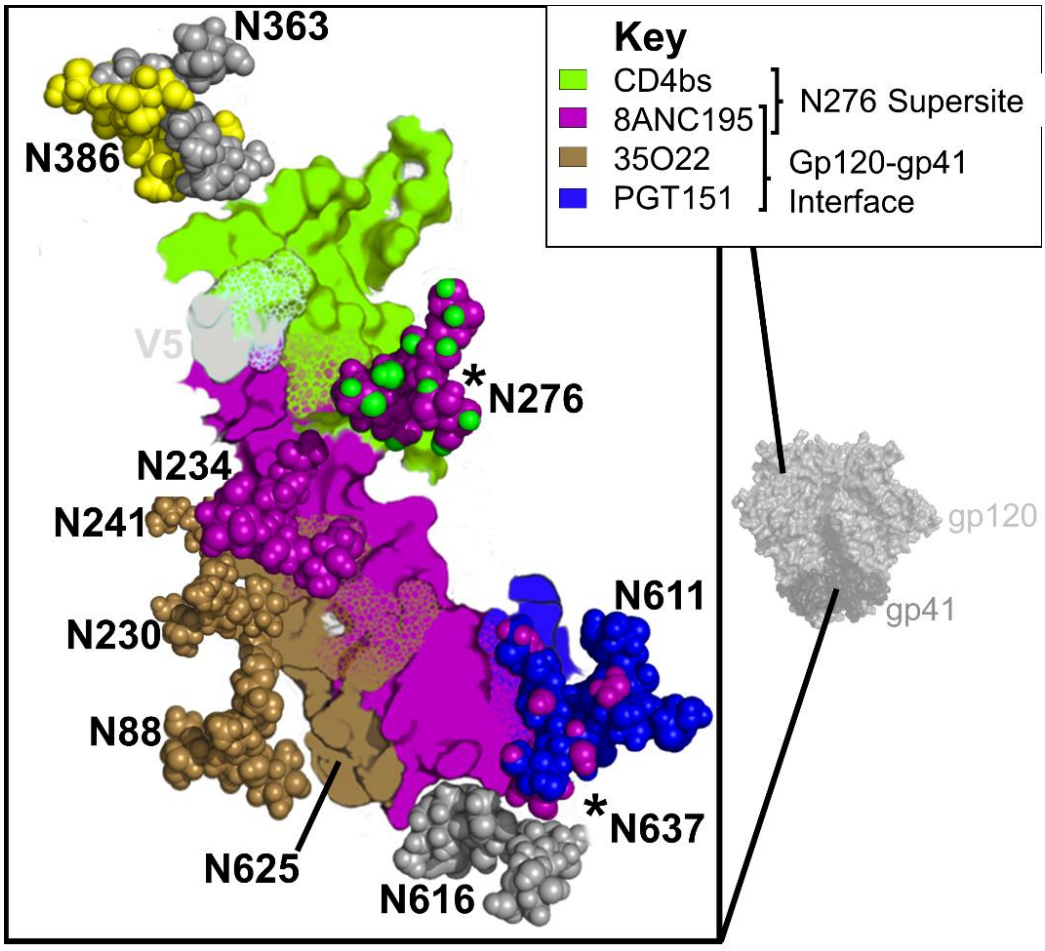

FIGURE 2. The CD4bs adjoins the gp120–gp41 interface. The HIV-1 envelope trimer is shown in light (gp120) and dark (gp41) grey surface view. An expanded graphic of the CD4bs and gp120–gp41 interface sites are shown in the zoomed out box. Epitopes for VRC01 (green), 8ANC195 (purple), 35O22 (brown), or PGT151 (blue) are defined as residues within 5 Å of each respective broadly neutralizing antibody (bNAb). Key glycans are shown as spheres, labelled, and coloured according to the epitopes they comprise. Regions that make up more than one epitope are shown with mottled colours, and glycans that are bound by bNAbs targeting different epitopes are asterisked. The hypervariable region V5 is shown in light grey.

THE gp120–gp41 INTERFACE

The N276 glycan described above is also the target for bNAb 8ANC195 (Fig. 2), recently shown to bind an epitope in the gp120–gp41 interface [43••]. This mAb is dependent on glycans at positions N234 and N276, and uses a four amino acid insertion to thrust the Fab heavy-chain FWR3 between these two glycans, contacting R456 at the distal most tip [43••]. The 8ANC195 CDR-H3 is 22 amino acids long, but is not used to penetrate the glycan shield. Rather the CDR-H3 folds back towards the light chain forming part of a wider paratope that makes significant contact with the 7-stranded b-sandwich (the gp41 interacting region) of gp120 [43••]. The affinity for gp120 is sufficient that 8ANC195 was isolated using a stabilized gp120 core, but docking of the Fab–gp120 complex into the prefusion trimer revealed potential interactions between the 8ANC195 light chain and gp41 near the N637 glycan. Deep sequencing in the 8ANC195 donor showed that the stabilized core specifically selected for a single branch of the bNAb lineage. More genetically diverse antibodies, created by pairing related heavy-chain and light-chain variants, exhibited increased potencies that were attributed almost entirely to light chain–gp41interactions [43••].

Thus, 8ANC195 was the first of several recently identified bNAbs targeting epitopes in the gp120– gp41 interface [9••,10••,43••,44]. Two new antibodies published in 2014, PGT151 and 35O22, were also shown to target the gp120–gp41 interface [5••,9••,10••,45••]. Unlike 8ANC195, these bNAbs do not bind monomeric gp120. bNAb 35O22 (isolated from the same donor as MPER bNAb 10E8) binds immediately adjacent to 8ANC195 near N234 (Fig. 2), close enough to contact the seven stranded b-sandwich via an eight amino acid FWR3 insertion [5••]. This bNAb epitope is remarkably low on the trimer, seemingly incompatible with the presence of the viral membrane, and it is speculated that certain rearrangements induced by CD4 are required for its binding [9••]. Neutralization by 35O22 was incompatible with glycosylation of the N625 sequon, but still critically dependent on the N625 residue [5••]. bNAb PGT151 binds between the 8ANC195 and 35O22 epitopes, over a cavity between gp160 protomers [45••]. Unlike 35O22, it has a specific requirement for cleaved trimers, and a maximum observed stoichiometry of two antigen binding fragments (Fabs) per trimer, suggesting an allosteric alteration of the third binding site after the first two Fabs have bound [45••].

This binding mechanism also allows PGT151 to stabilize native, cleaved Env trimers from cell membranes. Both 35O22 and PGT151 have highly glycan-dependent epitopes, with 35O22 neutralization dependent on the glycans at N88, N230, and N241 in gp120, and neutralization of PGT151 requiring gp41 glycans N611 and N637 [9••,10••]. Based on proximity, PGT151 was also predicted to interact with glycans in gp120 (N262, N276, N230, N234, N241, and N448) though these interactions are not critical for neutralization [45••]. This glycan dependence results in varied neutralization plateaus for both bNAbs. For 35O22, neutralization plateaus were improved (higher levels of maximum inhibition indicating enhanced potency) when pseudoviruses were grown in kifunensine, indicating a role for high mannose glycans in its epitope [9••]. In contrast, PGT151 could not neutralize kifunensine or 293S-grown pseudoviruses (glycosylated only with mannose rich glycans), and bound directly to triantennary and tetraantennary complex glycans [10••,45••]. As virus grown in peripheral blood mononuclear cells appears to have greater proportions of complex glycan, PGT151-like antibodies may exhibit better potencies *in vivo* [10••].

THE MEMBRANE PROXIMAL EXTERNAL REGION

Epitopes in the MPER of gp41 are almost exclusively contained within a linear, α-helical stretch of amino acids that links the transmembrane domain to the ectodomain of gp41. The MPER can be divided into an N-terminal and C-terminal helix around a kink at position 674, used to define various overlapping epitopes. bNAb 2F5 binds to the N-terminal helix, Z13e1 binds to the elbow between helices, while 4E10 and 10E8 bind to an epitope in the C-terminal helix. The hydrophobic C-terminus of the MPER is partially buried in the viral membrane and is thought to play a critical role in fusion with the host membrane. It is therefore highly conserved, and antibodies 4E10 and 10E8 are some of the broadest yet identified [8,46]. bNAbs targeting the MPER often interact with the viral membrane via long CDR-H3 loops, which may promote higher than normal levels of autoreactivity for these types of antibodies [47]. The precise location and conformation of the MPER in the prefusion HIV-1 trimer is not yet known, and further characterization will be necessary to determine the proximity of, and relationship between, epitopes in this site and those in the gp120–gp41 interface.

A CONTINUUM OF VULNERABILITY

The increased availability of bNAbs targeting novel sites, or variants of previously described sites, has blurred the definition of distinct bNAb epitopes. For instance CD4bs antibodies, once almost exclusively classified by their sensitivity to mutations at D368, now include a new group typified by HJ16 that are largely glycan dependent and insensitive to mutations at D368 [39,40]. Similarly V2 antibodies, previously defined as being N160 glycan dependent, now also include antibodies such as CAP256-VRC26 that target the same protein epitope but are not necessarily sensitive to glycan deletion [14]. These antibodies might be described as targeting subsites within the greater CD4bs or V2 site of vulnerability. This paradigm currently does not apply to the N332 dependent antibodies PGT128, PGT135, and 2G12, whose epitopes have mostly nonoverlapping peptide components (Figs. 1 and 3). One way to characterize these larger epitope clusters has been to define glycan supersites [30]. Based on these criteria, the glycan at position N276, which is the target for CD4bs antibodies (such as HJ16) and certain gp120–gp41 interface antibodies (e.g. 8ANC195) might now also be classified as a glycan supersite (Figs. 2 and 3). Other glycans, such as those at positions N156, N386, and in the newly described gp120–gp41 epitope cluster, are bound by antibodies targeting two distinct epitopes, but only form a critical component for one (Figs. 1 and 2). These glycans do not yet meet the requirements of a supersite (though isolation of additional mAbs may change this), but they may contribute towards the affinity maturation of bNAbs at both sites. Thus, it seems that bNAb epitopes form a continuum of vulnerability that includes conserved residues stretching from the trimer apex to the MPER (Fig. 3). The glycans which protect these regions, divide up the continuum into sites of vulnerability, but also because of their conservation become targets for neutralization themselves.

IMPROVED NEUTRALIZATION COVERAGE

Vaccine-induced bNAbs ideally need to protect against infection from all viral subtypes, and therefore those that target highly conserved epitopes are likely to be most effective. First-generation bNAbs, such as b12, 2F5, and 2G12, had fairly restricted breadth, and were often more effective against subtype-matched heterologous viruses [46]. More recently isolated bNAbs show much greater

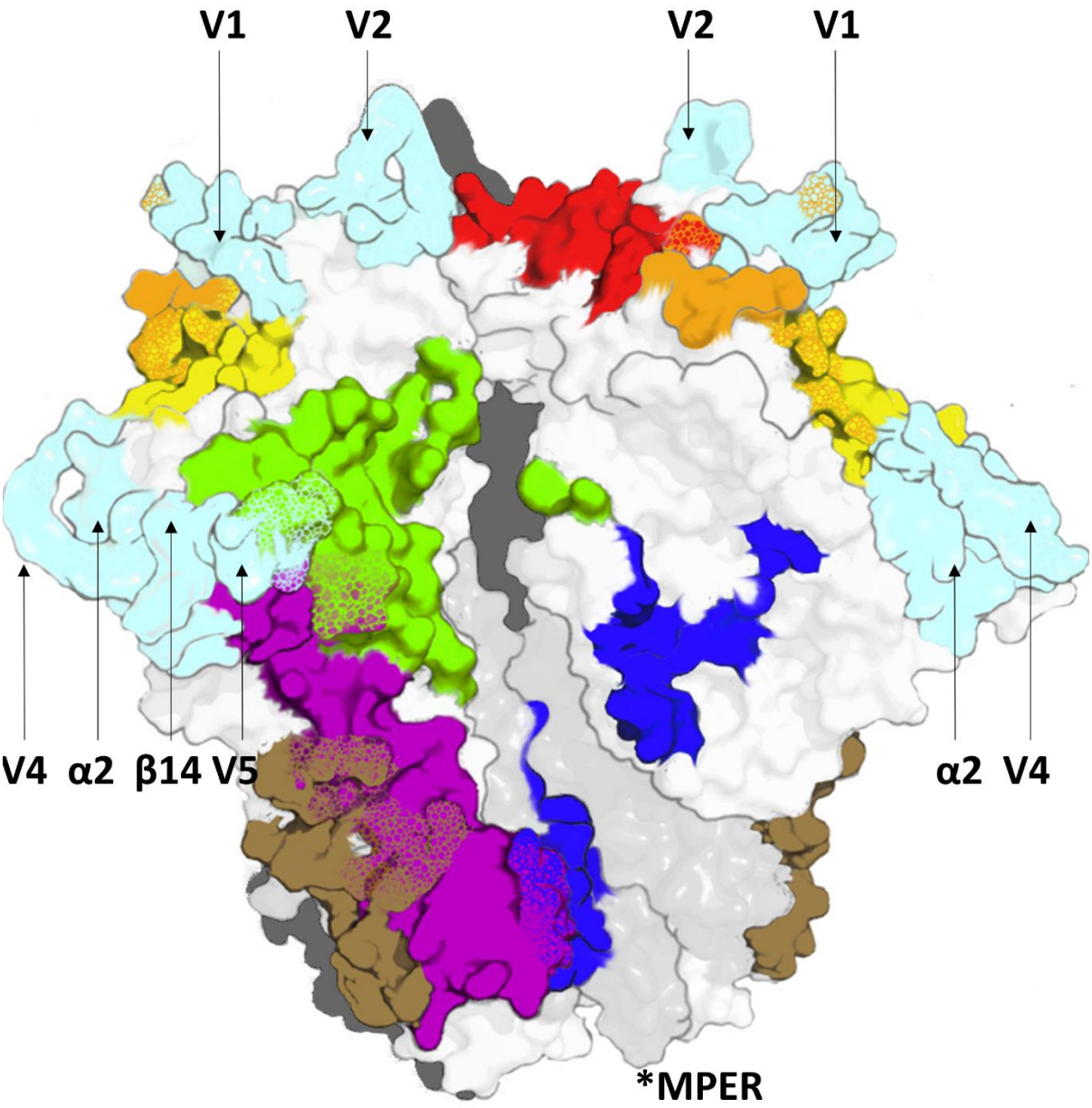

FIGURE 3. A continuum of broadly neutralizing antibody (bNAb) targets. A graphic of the HIV-1 envelope (Env) trimer is shown and surface coloured for broadly defined epitopes in V2 (red), V3 (orange), V4 (yellow), the CD4bs (green), and the gp120–gp41 interface (brown, purple, and blue for 8ANC195, 35O22, and PGT151, respectively). Overlap between these epitopes through recognition of common glycans or amino acids is indicated with mottling of the relevant colours. The highly accessible positions of hypervariable regions V1, V2, a2, V4, b14, and V5 (coloured in cyan) are indicated with arrows. The first residue of the MPER (truncated in the HIV-1 trimer structure 4TVP) is indicated with an asterisk.

breadth [2], although even among the broadest bNAbs coverage (and/or potency) varies between subtypes [7,9,14]. Subtype preference was also seen using large panels of chronic sera, which showed increased potency of plasmas against subtype matched viruses [48]. Notably, however, this effect was reduced in older and more diversified subtypes, suggesting that the significance of this observation for vaccine design will decrease overtime [48]. Differential coverage may occur for other reasons – bNAbs to the N332-supersite are less effective against viruses with the glycan at 334 despite some promiscuity in recognition [49], a finding that may be important as the 332 glycan is less common in subtype C founder viruses [50]. However, as a single antibody lineage could evolve to recognize both N332 and N334 variants (such as in the case of PGT128 and PGT130), inclusion of multiple immunotypes into vaccine design strategies may enhance coverage.

The availability of a large number of new more potent and cross-reactive mAbs has also enhanced prospects for passive immunotherapy. Early studies demonstrated that bNAbs could protect against infection in nonhuman primates and humanized mice [51–56]. However, these first-generation bNAbs were only able to transiently reduce viral loads in infected subjects [57–59]. The latest mAbs (mostly in combinations) resulted in more durable control of viremia while the mAbs were present, and in some cases thereafter [60–62]. Passively infused bNAbs will probably be used in combination. Indeed, mAbs targeting four different sites in double, triple, and quadruple combinations showed 98–100% coverage [63]. In addition to coverage, potency is likely to be important, with bNAbs engineered for greater *in vitro* potency associated with protection at lower plasma levels [64]. Lack of potency may be a particular concern for bNAbs with relatively low neutralization plateaus (incomplete neutralization even at high concentrations) such as 35O22, PGT151, and many V2-dependent antibodies. Ongoing human clinical trials will allow assessment of the dose of bNAb that is required (for protection and immunotherapy) and whether systemic infusion protects mucosal portals of infection.

CONCLUSION

The last year has brought significant advances in our understanding of the HIV-1 Env structure and its neutralization targets. New isolation technologies have allowed for less biased identification of

bNAbs targeting increasingly complex epitopes. These new antibodies have provided important insights, culminating in the near complete structural delineation of the HIV-1 Env spike. However, in many instances only a single mAb targeting a given site is available (e.g. PGT135, 2G12, 8ANC195, PGT151, and 35O22), and these often demonstrate some level of clade preference. Many more antibodies will need to be identified to properly characterize each of these new HIV-1 vulnerabilities. Additional bNAb–trimer complex structures will be necessary to define 'hotspots' or supersites for neutralization. Using the structural data from multiple bNAb–antigen complexes for a single target site will facilitate rational approaches to display specific sites of vulnerability, as is currently being done for the CD4bs and MPER epitope scaffolds. However, the extensive overlap between bNAb targets suggests that immunogen design may benefit from efforts to include whole, stabilized, cleaved HIV-1 trimers – perhaps rationally designed to expose the entire continuum of bNAb vulnerabilities while minimizing antigenicity to the hypervariable structures. The number of new bNAb targets, and our understanding of their structure have provided novel opportunities for preventing and treating HIV-1.

Acknowledgements

The authors thank Jinal Bhiman and Jay Gorman for helpful discussions.

Financial support and sponsorship

The authors receive research funding from the Centre for the AIDS Programme of Research (CAPRISA), the South African Medical Research Council (MRC) through the Flagship and SHIP programs, the National Institutes of Health (NIH) through an R01 Grant (R01 AI104387-01A1) and a U01 grant (AI116086-01), the Center for HIV/AIDS Vaccine Immunology (CHAVI grantAI067854), the Center for AIDS Vaccine Discovery (CAVD) of the Bill and Melinda Gates Foundation, the South African HIV/AIDS Research and Innovation Platform of the South African Department of Science and Technology and by a HIVRAD NIH grant (AI088610). CAPRISA was supported by NIAID, NIH, US Department of Health and Human Services (Grant U19 AI51794). P.L.M. is a Wellcome Trust Intermediate Fellow in Public Health and Tropical Medicine (Grant 089933/Z/ 09/Z). C.K.W. is supported by the Poliomyelitis Research Foundation (PRF) of South Africa and was the recipient of a Fogarty AITRP Fellowship.

Conflicts of interest

The authors declare no conflicts of interest.

REFERENCES AND RECOMMENDED READING

Papers of particular interest, published within the annual period of review, have been highlighted as: * of special interest ** of outstanding interest

1. Hraber P, Seaman MS, Bailer RT, et al. Prevalence of broadly neutralizing antibody responses during chronic HIV-1 infection. AIDS 2014; 28:163–169.
2. Klein F, Mouquet H, Dosenovic P, et al. Antibodies in HIV-1 vaccine development and therapy. Science 2013; 341:1199–1204.
3. Lyumkis D, Julien JP, de Val N, et al. Cryo-EM structure of a fully glycosylated soluble cleaved HIV-1 envelope trimer. Science 2013; 342:1484–1490.
4. Julien JP, Cupo A, Sok D, et al. Crystal structure of a soluble cleaved HIV-1 envelope trimer. Science 2013; 342:1477–1483.
5. Pancera M, Zhou T, Druz A, et al. Structure and immune recognition of trimeric prefusion HIV-1 Env. Nature 2014; 514:455–461.
** Using 35O22 and PGT122, the authors of this article crystallized the Env trimer in near entirety, building on work by Julien et al., 2013 [4], by resolving gp41. These data revealed the interactions that stabilize the prefusion trimer, and showed how HIV-1 Env proteins share remarkable mechanistic similarity with respiratory syncytial virus, Ebola, and influenza. The complex with 35O22 revealed binding to N625 that was incompatible with a glycan covalently linked to this side chain.
6. Walker LM, Huber M, Doores KJ, et al. Broad neutralization coverage of HIV by multiple highly potent antibodies. Nature 2011; 477:466–470.
7. Walker LM, Phogat SK, Chan-Hui PY, et al. Broad and potent neutralizing antibodies from an African donor reveal a new HIV-1 vaccine target. Science 2009; 326:285–289.
8. Huang J, Ofek G, Laub L, et al. Broad and potent neutralization of HIV-1 by a gp41-specific human antibody. Nature 2012; 491:406–412.
9. Huang J, Kang BH, Pancera M, et al. Broad and potent HIV-1 neutralization by a human antibody that binds the gp41-gp120 interface. Nature 2014; 515:138–142.
** This article detailed the third novel gp120–gp41 epitope to be described in 2014, that of 35O22. The authors did extensive mapping to show that this antibody was sensitive to mutations in potential N-linked glycosylation sites not associated with PGT151 or 8ANC195. The bNAb, isolated from the same donor as 10E8, has an unusual angle of approach that appears to clash with the viral membrane. Like PGT151, this antibody exhibited unusual neutralization plateaus that were explained by a preference for high mannose glycan.
10. Falkowska E, Le KM, Ramos A, et al. Broadly neutralizing HIV antibodies define a glycan-dependent epitope on the prefusion conformation of gp41 on cleaved envelope trimers. Immunity 2014; 40:657–668.
** Shortly after publication of the 8ANC195 epitope, this article detailed a second novel gp120–gp41 interface epitope targeted by the PGT151 lineage. This was the first article to confirm a role for gp41 glycans in the epitopes of bNAbs. These antibodies have unusually low neutralization plateaus that could be explained by a preference for complex glycan.
11. Wu X, Yang ZY, Li Y, et al. Rational design of envelope identifies broadly neutralizing human monoclonal antibodies to HIV-1. Science 2010; 329:856–861.
12. Scheid JF, Mouquet H, Ueberheide B, et al. Sequence and structural convergence of broad and potent HIV antibodies that mimic CD4 binding. Science 2011; 333:1633–1637.

13. Sok D, van Gils MJ, Pauthner M, et al. Recombinant HIV envelope trimer selects for quaternary-dependent antibodies targeting the trimer apex. Proc Natl Acad Sci U S A 2014; 111:17624–17629.
** This article describes for the first time the use of stabilized trimers for sorting single antigen specific B cells. Using the same donor as PGT145 they isolated somatic variants some of which had greater potency and breadth. This technological advance may make trimer specific bNAbs, or those of unknown specificity, easier to isolate in the future.
14. Doria-Rose NA, Schramm CA, Gorman J, et al. Developmental pathway for potent V1V2-directed HIV-neutralizing antibodies. Nature 2014; 509: 55–62.
15. Liao HX, Lynch R, Zhou T, et al. Co-evolution of a broadly neutralizing HIV-1 antibody and founder virus. Nature 2013; 496:469–476.
16. West AP Jr, Scharf L, Horwitz J, et al. Computational analysis of anti-HIV-1 antibody neutralization panel data to identify potential functional epitope residues. Proc Natl Acad Sci U S A 2013; 110:10598–10603.
17. Georgiev IS, Doria-Rose NA, Zhou T, et al. Delineating antibody recognition in polyclonal sera from patterns of HIV-1 isolate neutralization. Science 2013; 340:751–756.
18. Lacerda M, Moore PL, Ngandu NK, et al. Identification of broadly neutralizing antibody epitopes in the HIV-1 envelope glycoprotein using evolutionary models. Virol J 2013; 10:347.
19. He L, Sok D, Azadnia P, et al. Toward a more accurate view of human B-cell repertoire by next-generation sequencing, unbiased repertoire capture and single-molecule barcoding. Sci Rep 2014; 4:6778.
20. Xiao M, Prabakaran P, Chen W, et al. Deep sequencing and Circos analyses of antibody libraries reveal antigen-driven selection of Ig VH genes during HIV1 infection. Exp Mol Pathol 2013; 95:357–363.
21. Zhu J, Ofek G, Yang Y, et al. Mining the antibodyome for HIV-1-neutralizing antibodies with next-generation sequencing and phylogenetic pairing of heavy/light chains. Proc Natl Acad Sci U S A 2013; 110:6470–6475.
22. Zhu J, Wu X, Zhang B, et al. De novo identification of VRC01 class HIV-1neutralizing antibodies by next-generation sequencing of B-cell transcripts. Proc Natl Acad Sci U S A 2013; 110:E4088–E4097.
23. DeKosky BJ, Ippolito GC, Deschner RP, et al. High-throughput sequencing of the paired human immunoglobulin heavy and light chain repertoire. Nat Biotechnol 2013; 31:166–169.
24. Eroshkin AM, LeBlanc A, Weekes D, et al. bNAber: database of broadly neutralizing HIV antibodies. Nucleic Acids Res 2014; 42 (Database issue):D1133–D1139.
25. Bartesaghi A, Merk A, Borgnia MJ, et al. Prefusion structure of trimeric HIV-1 envelope glycoprotein determined by cryo-electron microscopy. Nat Struct Mol Biol 2013; 20:1352–1357.
26. McLellan JS, Pancera M, Carrico C, et al. Structure of HIV-1 gp120 V1/V2 domain with broadly neutralizing antibody PG9. Nature 2011; 480:336–343.
27. Julien JP, Lee JH, Cupo A, et al. Asymmetric recognition of the HIV-1 trimer by broadly neutralizing antibody PG9. Proc Natl Acad Sci U S A 2013; 110:4351–4356.
28. Loving R, Sjoberg M, Wu SR, et al. Inhibition of the HIV-1 spike by singlePG9/16-antibody binding suggests a coordinated-activation model for its three protomeric units. J Virol 2013; 87:7000–7007.
29. Doria-Rose NA, Georgiev I, O'Dell S, et al. A short segment of the HIV-1 gp120 V1/V2 region is a major determinant of resistance to V1/V2 neutralizing antibodies. J Virol 2012; 86:8319–8323.
30. Kong L, Lee JH, Doores KJ, et al. Supersite of immune vulnerability on the glycosylated face of HIV-1 envelope

glycoprotein gp120. Nat Struct Mol Biol 2013; 20:796–803.
31. Pejchal R, Doores KJ, Walker LM, et al. A potent and broad neutralizing antibody recognizes and penetrates the HIV glycan shield. Science 2011; 334:1097–1103.
32. Doores KJ, Kong L, Krumm SA, et al. Two classes of broadly neutralizing antibodies within a single lineage directed to the high-mannose patch of HIV Envelope. J Virol 2014; 89:1105–1118.
33. Moore PL, Williamson C, Morris L. Virological features associated with the development of broadly neutralizing antibodies to HIV-1. Trends Microbiol 2015; in press.
34. Calarese DA, Scanlan CN, Zwick MB, et al. Antibody domain exchange is an immunological solution to carbohydrate cluster recognition. Science 2003; 300:2065–2071.
35. Zhou T, Zhu J, Wu X, et al. Multidonor analysis reveals structural elements, genetic determinants, and maturation pathway for HIV-1 neutralization by VRC01-class antibodies. Immunity 2013; 39:245–258.
36. Zhou T, Xu L, Dey B, et al. Structural definition of a conserved neutralization epitope on HIV-1 gp120. Nature 2007; 445:732–737.
37. McGuire AT, Hoot S, Dreyer AM, et al. Engineering HIV envelope protein to activate germline B cell receptors of broadly neutralizing anti-CD4 binding site antibodies. J Exp Med 2013; 210:655–663.
38. Jardine J, Julien JP, Menis S, et al. Rational HIV immunogen design to target specific germline B cell receptors. Science 2013; 340:711–716.
39. Balla-Jhagjhoorsingh SS, Corti D, Heyndrickx L, et al. The N276 glycosylation site is required for HIV-1 neutralization by the CD4 binding site specific HJ16 monoclonal antibody. PLoS One 2013; 8:e68863.
40. Wibmer CK, Bhiman JN, Gray ES, et al. Viral escape from HIV-1 neutralizing antibodies drives increased plasma neutralization breadth through sequential recognition of multiple epitopes and immunotypes. PLoS Pathog 2013; 9:e1003738.
41. Diskin R, Klein F, Horwitz JA, et al. Restricting HIV-1 pathways for escape using rationally designed anti-HIV-1 antibodies. J Exp Med 2013; 210:1235–1249.
42. Corti D, Langedijk JP, Hinz A, et al. Analysis of memory B cell responses and isolation of novel monoclonal antibodies with neutralizing breadth from HIV-1infected individuals. PLoS One 2010; 5:e8805.
43. Scharf L, Scheid JF, Lee JH, et al. Antibody 8ANC195 reveals a site of broad vulnerability on the HIV-1 envelope spike. Cell Rep 2014; 7:785–795.
** This was the first article to show that bNAbs can bridge the gap between gp120 and gp41. It included the structural characterization of 8ANC195, including a crystal complex with gp120, and a cryo-EM co-localizing gp41 with the Fab light chain.
44. Wibmer CK, Sheward D, Bhiman JN, et al. Viral escape pathways from broadly neutralising antibodies targeting the HIV envelope cleavage site enhance MPER mediated neutralisation. AIDS Res Hum Retrovir 2014; 30:A20–A21.
45. Blattner C, Lee JH, Sliepen K, et al. Structural delineation of a quaternary, cleavage-dependent epitope at the gp41-gp120 interface on intact HIV-1 env trimers. Immunity 2014; 40:669–680.
** A structural characterization of the PGT151 lineage in complex with the HIV-1 trimer by cryo-EM, co-published with Falkowska et al., 2014 [10**]. These data largely supported the gp41 mapping from the linked article, as well as implicating additional gp120 glycans in the epitope. Interestingly PGT151 bound to the envelope trimer with a maximum stoichiometry of two Fabs.
46. Binley JM, Wrin T, Korber B, et al. Comprehensive cross-clade

neutralization analysis of a panel of antihuman immunodeficiency virus type 1 monoclonal antibodies. J Virol 2004; 78:13232–13252.
47. Verkoczy L, Kelsoe G, Haynes BF. HIV-1 envelope gp41 broadly neutralizing antibodies: hurdles for vaccine development. PLoS Pathog 2014; 10:e1004073.
48. Hraber P, Korber BT, Lapedes AS, et al. Impact of clade, geography, and age of the epidemic on HIV-1 neutralization by antibodies. J Virol 2014; 88:12623–12643.
49. Sok D, Doores KJ, Briney B, et al. Promiscuous glycan site recognition by antibodies to the high-mannose patch of gp120 broadens neutralization of HIV. Sci Transl Med 2014; 6:236ra63.
50. Moore PL, Gray ES, Wibmer CK, et al. Evolution of an HIV glycan-dependent broadly neutralizing antibody epitope through immune escape. Nat Med 2012; 18:1688–1692.
51. Hessell AJ, Poignard P, Hunter M, et al. Effective, low-titer antibody protection against low-dose repeated mucosal SHIV challenge in macaques. Nat Med 2009; 15:951–954.
52. Mascola JR, Stiegler G, VanCott TC, et al. Protection of macaques against vaginal transmission of a pathogenic HIV-1/SIV chimeric virus by passive infusion of neutralizing antibodies. Nat Med 2000; 6:207–210.
53. Moldt B, Rakasz EG, Schultz N, et al. Highly potent HIV-specific antibody neutralization in vitro translates into effective protection against mucosal SHIV challenge in vivo. Proc Natl Acad Sci U S A 2012; 109:18921–18925.
54. Parren PW, Marx PA, Hessell AJ, et al. Antibody protects macaques against vaginal challenge with a pathogenic R5 simian/human immunodeficiency virus at serum levels giving complete neutralization in vitro. J Virol 2001; 75:8340– 8347.
55. Balazs AB, Chen J, Hong CM, et al. Antibody-based protection against HIV infection by vectored immunoprophylaxis. Nature 2012; 481:81–84.
56. Balazs AB, Ouyang Y, Hong CM, et al. Vectored immunoprophylaxis protects humanized mice from mucosal HIV transmission. Nat Med 2014; 20:296–300.
57. Poignard P, Sabbe R, Picchio GR, et al. Neutralizing antibodies have limited effects on the control of established HIV-1 infection in vivo. Immunity 1999; 10:431–438.
58. Trkola A, Kuster H, Rusert P, et al. Delay of HIV-1 rebound after cessation of antiretroviral therapy through passive transfer of human neutralizing antibodies. Nat Med 2005; 11:615–622.
59. Mehandru S, Vcelar B, Wrin T, et al. Adjunctive passive immunotherapy in human immunodeficiency virus type 1-infected individuals treated with antiviral therapy during acute and early infection. J Virol 2007; 81:11016–11031.
60. Shingai M, Nishimura Y, Klein F, et al. Antibody-mediated immunotherapy of macaques chronically infected with SHIV suppresses viraemia. Nature 2013; 503:277–280.
61. Barouch DH, Whitney JB, Moldt B, et al. Therapeutic efficacy of potent neutralizing HIV-1-specific monoclonal antibodies in SHIV-infected rhesus monkeys. Nature 2013; 503:224–228.
62. Klein F, Halper-Stromberg A, Horwitz JA, et al. HIV therapy by a combination of broadly neutralizing antibodies in humanized mice. Nature 2012; 492:118–122.
63. Kong R, Louder MK, Wagh K, et al. Improving neutralization potency and breadth by combining broadly reactive HIV-1 antibodies targeting major neutralization epitopes. J Virol 2014; 89:2659–2671.
64. Rudicell RS, Kwon YD, Ko SY, et al. Enhanced potency of a broadly neutralizing HIV-1 antibody in vitro improves protection against lentiviral infection in vivo. J Virol 2014; 88:12669–12682.

CHAPTER THREE: STRUCTURE AND RECOGNITION OF A NOVEL HIV-1 GP120-GP41 INTERFACE ANTIBODY THAT CAUSED MPER EXPOSURE THROUGH VIRAL ESCAPE

Submitted to PLOS Pathogens: Feb 2016

Structure and Recognition of a Novel HIV-1 gp120-g41 Interface Antibody that Caused MPER Exposure through Viral Escape

Constantinos Kurt Wibmer[1,2], Jason Gorman[3], Gabriel Ozorowski[4], Jinal N. Bhiman[1,2], Daniel J. Sheward[5], Debra H. Elliott[6], Julie Rouelle[6], Ashley Smira[6], M. Gordon Joyce[3], Nonkululeko Ndabambi[5], Aliaksandr Druz[3], Dennis R. Burton[7,8], Mark Connors[3], Salim S. Abdool Karim[9,10], James E. Robinson[6], Andrew B. Ward[4], Carolyn Williamson[5,9], Peter D. Kwong[3], Lynn Morris*[1,2,9] and Penny L. Moore*[1,2,9]

---

1 Centre for HIV and STIs, National Institute for Communicable Diseases (NICD), of the National Health Laboratory Service (NHLS), Johannesburg, South Africa; **2** Faculty of Health Sciences, University of the Witwatersrand, Johannesburg, South Africa; **3** Vaccine Research Center, National Institute of Allergy and Infectious Diseases, National Institutes of Health, Bethesda, MD, United States of America; **4** Department of Integrative Structural and Computational Biology, CHAVI-ID, IAVI Neutralizing Antibody Center and Collaboration for AIDS Vaccine Discovery (CAVD), The Scripps Research Institute, La Jolla, CA, United States of America ; **5** Institute of Infectious Disease and Molecular Medicine (IDM) and Division of Medical Virology, University of Cape Town and NHLS, Cape Town, South Africa; **6** Department of Pediatrics, Tulane University Medical Center, New Orleans, United States of America; **7** Department of Immunology and Microbial Science, CHAVI-ID and IAVI Neutralizing Antibody Centre, The Scripps Research Institute, La Jolla, CA, United States of America; **8** Ragon Institute of Massachusetts General Hospital, MIT and Harvard, Cambridge, MA, United States of America; **9** Centre for the AIDS Programme of Research in South Africa (CAPRISA), University of KwaZulu-Natal, Durban, South Africa; **10** Department of Epidemiology, Columbia University, New York, United States of America

*Corresponding Authors: Penny Moore and Lynn Morris
E-mail: pennym@nicd.ac.za / lynnm@nicd.ac.za

Abstract

A comprehensive understanding of the regions on HIV-1 envelope trimers targeted by broadly neutralizing antibodies may contribute to rational design of an HIV-1 vaccine. We previously identified a participant in the CAPRISA cohort, CAP248, who developed trimer-specific antibodies capable of neutralizing 59% of heterologous viruses at three years post-infection. Here, we report the isolation by B cell culture of monoclonal antibody CAP248-2B, which targets a novel epitope in the gp120-gp41 trimer interface. Despite low maximum inhibition plateaus, often below 50% inhibitory concentrations, the breadth of CAP248-2B significantly correlated with donor plasma. Site-directed mutagenesis, X-ray crystallography, and negative-stain electron microscopy 3D reconstructions revealed how CAP248-2B recognizes a cleavage-dependent epitope that includes the gp120 C terminus. While this epitope was distinct, it did overlap in parts of gp41 with the epitopes of broadly neutralizing antibodies PGT151, 35O22, and 3BC315. CAP248-2B has a conformationally variable paratope with an unusually long 19 amino acid light chain third complementarity determining region. Two phenylalanines at the loop apex were shown by docking and mutagenesis data to interact with the viral membrane. Neutralization by CAP248-2B is not dependent on any single glycan proximal to its epitope, and low neutralization plateaus could not be completely explained by N- or O-linked glycosylation pathway inhibitors, furin co-transfection, or pre-incubation with soluble CD4. Viral escape from CAP248-2B involved a cluster of rare mutations in the gp120-gp41 cleavage sites. Simultaneous introduction of these mutations into heterologous viruses abrogated neutralization by CAP248-2B, but enhanced neutralization sensitivity to 35O22, 4E10, and 10E8 by 10-100 fold. Altogether, this study expands the region of the HIV-1 gp120-gp41 quaternary interface that is a target for broadly neutralizing antibodies and identifies a set of mutations in the gp120 C terminus that exposes the membrane proximal external region of gp41, with potential utility in HIV vaccine design.

Author Summary

Our understanding about which regions of the HIV-1 envelope are targets for broadly neutralizing antibodies (likely required for an HIV-1 vaccine) has expanded greatly in recent years, offering insights for vaccine design. For instance, much of solvent-exposed gp41 is now known to be targeted by antibodies at the gp120-gp41 interface. In this study, we isolated the neutralizing monoclonal antibody CAP248-2B, and used structural biology to characterize its epitope which spanned both the gp120-gp41 and gp41-gp41 interfaces in a manner distinct from other antibodies. CAP248-2B extends the interface target to include the gp120 C terminus, effectively encircling the base of native pre-fusion trimers. While CAP248-2B recapitulated the donor's plasma breadth, it had poor potency against some isolates as a consequence of low neutralization plateaus. Unlike many other broadly neutralizing antibodies, these plateaus did not appear to be a consequence of glycan heterogeneity, suggesting additional mechanisms that may contribute towards incomplete neutralization. Finally, we characterized viral escape pathways from CAP248-2B, and identified a cluster of unusual mutations in the gp160 cleavage sites that made HIV-1 viruses more sensitive to antibodies targeting highly conserved membrane-proximal epitopes. These mutations might improve the immunogenicity of gp41, and thereby inform HIV-1 immunogen design.

Introduction

The HIV-1 envelope glycoprotein trimer (Env) is the only known target for neutralizing antibodies and is thus a focus for vaccine design efforts. However, the development of an effective HIV-1 vaccine has been thwarted by the complex nature of Env, and the inability to produce soluble Env immunogens able to elicit broadly neutralizing antibodies (bNAbs) (1). Env is expressed as a single gp160 protomer that is extensively glycosylated and trimerized in the endoplasmic reticulum (2, 3). These gp160 oligomers are cleaved into gp120 (receptor binding subunit) and gp41 (transmembrane subunit), resulting in a trimer of heterodimers that is then subjected to extensive glycan processing in the Golgi apparatus (3, 4). The cleaving of gp160 occurs primarily through furin activity at position R511, but a fraction of Env is also cleaved at position R504 (4-6). During this process gp120 is often shed from non-covalently associated gp120-gp41 trimers, and the entry-competent form of Env may comprise only a small portion of the total Env content on the viral membrane (3, 4, 7). The remainder often exists as gp41 “stumps”, and incorrectly processed or prematurely triggered monomers and oligomers. The abundance of these aberrant forms of Env on the viral surface, and the consequent exposure of immunodominant regions not normally present on entry competent trimers, misdirects the humoral immune response toward non-protective epitopes (8). In addition Env is highly sequence variable, particularly within the V1-V5 variable loop regions, and heterogeneously glycosylated (even at conserved NxS/T sequons) because the densely packed glycans afford each other varied protection from the different glycan processing enzymes. This combination of factors favours the formation of strain-specific neutralizing antibodies (9-13).

Nevertheless some individuals develop HIV-1 bNAbs after several years of infection that are able to target more conserved regions of Env, and thus neutralize diverse viral strains (14-17). In some instances these bNAbs can neutralize 50% - 99% of globally circulating strains, and have been shown to prevent infection in animal models (18-24). HIV-1 bNAbs often display unusual characteristics such as high levels of somatic hypermutation, unusually long complementarity determining regions (CDRs), and insertions/deletions in both the CDRs and antibody framework regions (25-27). These features enable HIV-1 bNAbs to access epitopes that are often recessed or contain conserved glycan or membrane components. Interestingly, bNAbs that include

glycan(s) in their epitope frequently display incomplete neutralization, usually because they have evolved to recognise a specific glycoform not present on every trimer (28-32). More recently, incomplete neutralization has also been described for HIV-1 bNAbs with epitopes that do not appear to depend on glycan, suggesting that additional factors may contribute to neutralization potency (33).

To understand how these unusual bNAb specificities might be elicited by an HIV-1 vaccine, there has been a concerted effort to isolate bNAbs from HIV-1 infected individuals and to define their targets and developmental pathways (29, 34-47). The identification of bnAb-mediated immune selection pressures on Env, coupled with mutagenesis and structural biology techniques have been instrumental in our understanding of the epitopes susceptible to broad neutralization (48). These include the CD4 binding site (CD4bs), a cluster of epitopes surrounding the N332 glycan, the membrane proximal external region of gp41 (MPER), and a number of quaternary structure specific epitopes in either the V2 trimer apex or the gp120-gp41 interface. The more recently discovered gp120-gp41 interface bNAbs 8ANC195, PGT151, 35O22, and 3BC315 target distinct, usually glycan dependent epitopes, that overlap in gp41 (29, 43, 46, 47). For example, 8ANC195 requires glycans at positions N234 and N276, but prefers the absence of a glycan at position N230, while PGT151 requires glycan at positions N611 and N637 and 35O22 at positions N88 and N625. The identification of additional bNAbs that have epitopes within the gp120-gp41 interface could further enhance our understanding of this new site of vulnerability.

In a previous study we described CAP248, an HIV-1 subtype C infected participant in the CAPRISA 002 cohort who developed bNAbs to a trimer-specific epitope that could not be defined at the time (15). Here, we have isolated a monoclonal antibody (mAb) that was representative of the broadly neutralizing plasma response, but lacked potency due to low neutralization plateaus that could not be accounted for by glycan heterogeneity. Through the interrogation of autologous selection pressure in Env, together with X-ray crystallography and electron microscopy, we mapped the CAP248-2B target to a glycan independent epitope in the gp120-gp41 interface that overlaps with previously identified gp120-gp41 interface bNAbs, but is distinct in its recognition of the gp160 cleavage motifs in the gp120 C terminus. Escape from this antibody conferred a viral phenotype that was exceptionally sensitive to neutralization by MPER directed antibodies, suggesting a role for the C terminus of gp120 in the exposure of important bNAb epitopes in gp41.

Results

Isolation of antibody CAP248-2B, which recapitulates CAP248-plasma neutralization breadth

CAP248 first developed cross-neutralizing antibodies after one year of infection (Figure 1A). By three years, the neutralization breadth of CAP248 plasma increased incrementally, from 7% to 59% when tested against a 44 pseudovirus panel (15). This neutralization was largely subtype C specific with CAP248 plasma neutralizing 89% of 26 subtype C, 50% of 6 subtype A and 33% of 12 subtype B pseudoviruses (Figure 1A). As mapping of polyclonal plasma may be complicated by the presence of multiple overlapping specificities (49, 50), we used a stored peripheral blood mononuclear cell (PBMC) sample from 3.5 years post-infection to isolate a monoclonal antibody. B cells were enriched by negative selection with immunomagnetic beads, and B cell culture supernatants were screened after 14 days for neutralization of CAP45, a tier-2 pseudovirus sensitive to CAP248 plasma at ID50 titres of ~1:4,000. The isolated antibody, called CAP248-2B, was predicted to be derived from the IGHV4-31*05 and IGHJ3*01/02 heavy and IGLV2-14*01 and IGLJ1*01 lambda chain germline genes, and displayed modest levels of affinity maturation, with 13.5% and 9.7% nucleotide mutation in the heavy and light chains respectively (Supplementary Figure 1A). CAP248-2B potently neutralized CAP45 with an IC50 of 0.04 µg/mL (IC80 of 0.19 µg/mL), but against the same 44 pseudovirus panel on which CAP248 plasma displayed 59% neutralization breadth at three years post-infection, CAP248-2B neutralized only 23% of viruses with IC50 titres (Figure 1B). Examination of the neutralization curves indicated that the poor breadth of CAP248-2B was due to incomplete neutralization, e.g. the maximum inhibition of CAP45, CNE52, CAP228, and ZM249 plateaued at 95%, 69%, 54%, and 32% respectively (Figure 1C). When IC20 values were examined, CAP248-2B neutralized a much larger fraction of the panel, showing 57% breadth, equivalent to the plasma breadth (Figures 1B and 1D). Overall there was significant concordance ($p<0.00001$) between pseudoviruses neutralized by the plasma at 3 years (measured as ID50) and those neutralized by the monoclonal antibody at IC20 (Figure 1D). This suggested that CAP248-2B was representative of the dominant bNAb specificity in CAP248 plasma, though more potent variants of this mAb lineage remain to be isolated.

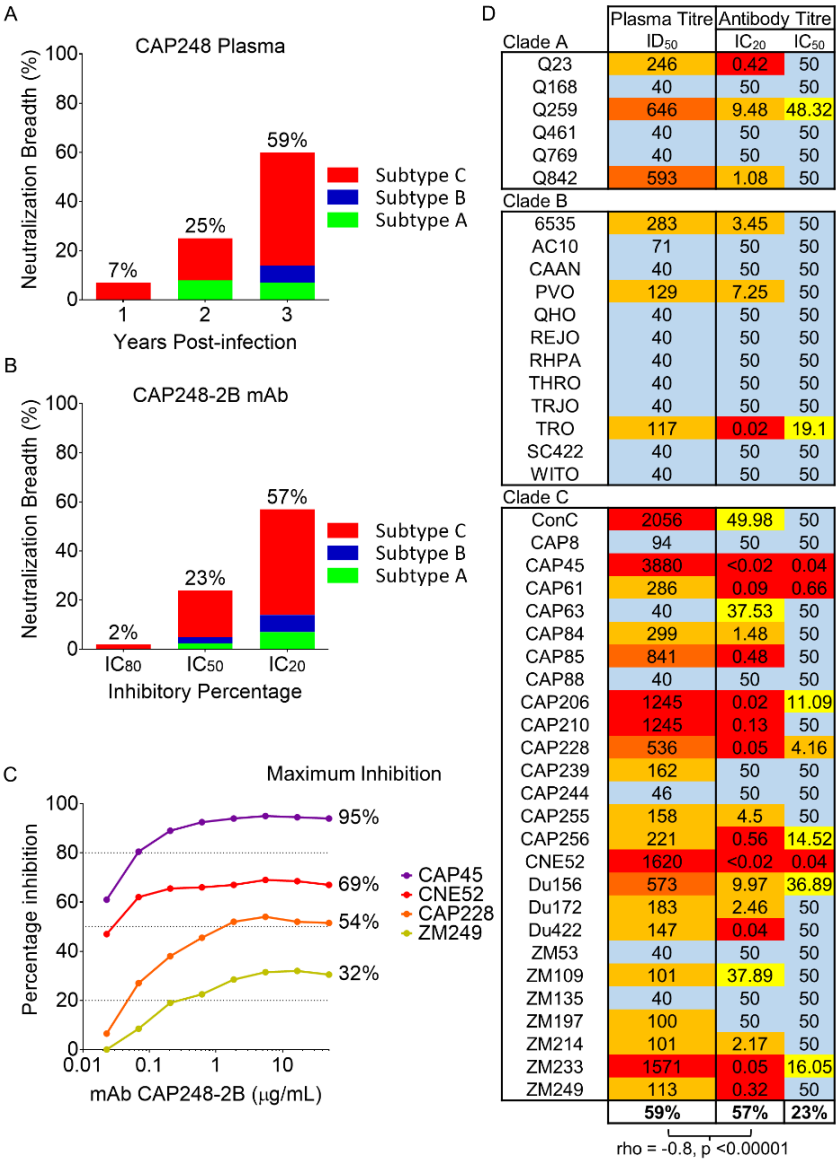

Figure 1: Isolated antibody CAP248-2B exhibits low neutralization plateaus, but recapitulates the plasma neutralization breadth

(A) Bar graph showing percentage neutralization breadth of CAP248 plasma at ID_{50} titers of >1:100 (y-axis) on a 44 virus panel at one, two, and three years post-infection (x-axis). The total breadth at each time point is indicated above the bars. The proportion of subtype C, B, and A viruses neutralized by CAP248 plasma is indicated in red, blue, and green respectively. (B) Percentage neutralization breadth of monoclonal antibody CAP248-2B (y-axis) on the same 44 virus panel as in A, when measured at IC_{80}, IC_{50}, and IC_{20} (x-axis), colored and labelled as above. (C) Neutralization curves of CAP248-2B against four viral strains (CAP45, CNE52, CAP228, and ZM249) plotted as percentage inhibition (y-axis) versus antibody concentration (x-axis). Dotted lines indicate y-axis intersections for IC_{80}, IC_{50}, and IC_{20}. The maximum inhibitory percentage achieved against each virus is listed to the right of each curve. (D) Comparison between the neutralization breadth of CAP248 plasma at three years, and CAP248-2B at IC_{20} and IC_{50}. Titers are colored yellow, orange and red by potency. A strong inverse spearman correlation with a rho value of -0.802 (p-value <0.00001) indicates good concordance between increasing plasma ID_{50} and decreasing antibody IC_{20}.

Structural characterization of monoclonal antibody CAP248-2B

CAP248-2B possessed an average length CDR-H3 of 15 amino acids, but had an unusually long CDR-L3 of 19 amino acids (Figure 2A). The typical length of a CDR-L3 is 8-12 amino acids, and there are no antibodies with CDR-L3s of greater than 15 amino acids in the Abysis database (http://www.bioinf.org.uk/abysis/index.html). In addition to the CDRs, there was also maturation away from germline in the framework region three (FR3) of the heavy chain (Figure 2A – blue). We determined two crystal structures of the unliganded CAP248-2B antigen binding fragment (Fab) to resolutions of 3.1 Å and 2.0 Å respectively (Figure 2B and Supplementary Figure 1). The CDR-H3 and CDR-L3 loops of the 2.0 Å resolution structure were influenced slightly by crystal packing (Supplementary Figure 1B and 1C), and a comparison of the CDR-H3 between the two structures revealed two distinct loop conformations that bent at residues Gly100D and Gly100E to flip the Asp100B and Asp100C anionic pair ~180° between CDR-L3 proximal and distal orientations (Figure 2B – top inset).

In the 3.1 Å resolution structure, the 19 amino acid CDR-L3 formed a β-hairpin which was stabilized along its length by seven hydrogen bonds, and protruded ~15Å at a right angle relative to the other CDR's. The tip of the CDR-L3 ended in hydrophobic residues Phe95C and Phe95D that were specifically angled by Pro95F and immediately flanked by residues Ser95B and Gly95E which may confer a degree of plasticity to this region. In all structures, the angle at which the CDR-L3 extended from the Fab was stabilized at its base by germline conserved hydrogen bonding interactions with CDR-L1, as well as a salt bridge formed between CDR-L3 residue Arg95I, and Asp50 in the CDR-H2. Ultimately, the CAP248-2B antigen binding site displayed substantial structural plasticity, an attribute that likely contributes to its mode of neutralization.

Viral escape from CAP248-2B was mediated by unusual mutations in the gp160 cleavage site

Previously, we have shown that CAP248 plasma bNAbs could not be adsorbed using recombinant monomeric gp140 or MPER peptides, and were not sensitive to V2 mutations at positions N160 and L165 (15). This suggested that CAP248 bNAbs targeted a quaternary epitope distinct from the V1V2 epitope. To identify potential escape mutations in response to CAP248 bNAbs, autologous gp160 sequences from nine weeks (study enrolment), as well as 1, 2, 3, and 3.5 years post-infection were

examined for accumulating mutations (indicative of selection pressure) in normally conserved regions of the envelope. Several autologous mutations were identified in, or proximal to, known bNAb epitopes within V2 (E164I/V, L165I/F), C1 (G87R/E) and C2 (D230N, N234T/S, T236K), V3 (D321E/G, N325D/K, E328K/D), and the MPER (N674G, K677N/Q, K683R) (Supplementary Figure 2A). However when these changes were made in the heterologous tier-2 virus CAP45, none affected CAP248-2B neutralization (Supplementary Figure 2B).

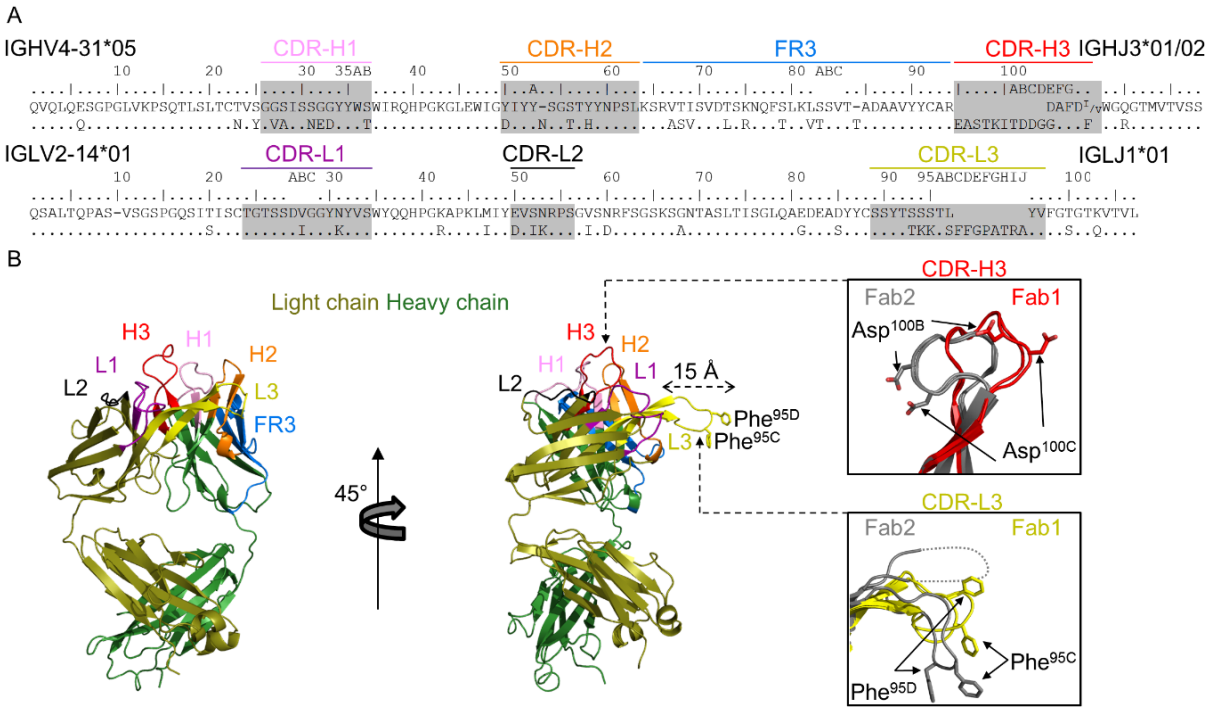

Figure 2: Crystal structure of CAP248-2B reveals an unusually long, protruding CDR-L3, with a hydrophobic tip

(A) Sequence alignment of the CAP248-2B heavy and light chain with their predicted V- and J-gene precursors. The CDRs are shaded, labelled, and colored. The heavy chain FR3 is similarly indicated in blue. (B) Crystal structure of the CAP248-2B Fab. The light and heavy chains are colored olive and forest green respectively, while CDR loops and FR-H3 are colored according to A. Two views are shown around a ~45° axis to highlight the long CDR-L3 (yellow). Insets show the conformational differences between the CDR-H3 and CDR-L3 loops between Fab structure 1 (shown here) and Fab structure 2 (shown in supplementary figure 1). Two Fabs were present in both asymmetric units, so four loops are shown per inset, two for Fab1 CDR-H3 (red) or L3 (yellow), and two for Fab2 CDR-H3 and L3 (both grey). Asp100B and Asp100C in the heavy chain and Phe95C and Phe95D in the light chain are shown with stick representations to highlight the conformational divergence between the two structures. Due to crystal packing all downstream analyses were based on the 3.1 Å structure.

To rule out these four epitopes as the target for CAP248-2B, we also assessed the effect of mutations known to confer resistance to bNAbs targeting these regions, but these mutations also failed to abrogate CAP248-2B neutralization (Supplementary Figure 2C). There were slight effects following the T303A and F672L/W673L mutations, but these are known to affect overall Env conformation (30, 51), and so may not form part of the CAP248-2B epitope. A cluster of unusual mutations were identified in the C terminus of gp120 at positions 500, 502, 505, 507, 508, and 509 within the gp160 furin cleavage motifs that separate gp120 from gp41 (Figure 3A). This region has not previously been implicated in viral escape from neutralizing antibodies, but analysis of 2,558 sequences from the Los Alamos National Laboratory HIV-1 database showed that while sequence variation at position 500 is common, mutations at the other five sites are rare, particularly amongst clade C viruses (Figure 3B). The simultaneous presence of these mutations in CAP248 viral sequences therefore suggested strong immune pressure on this region. When the six most common mutations at 3.5 years post-infection (E500K, R502Q, V505M, E507G, R508K, and E509G) were introduced individually into the heterologous virus CAP45, only the V505M mutation substantially reduced CAP248-2B neutralization (Figure 3C – blue line). However, the simultaneous introduction of all six mutations into CAP45, hereafter referred to as CAP45(CS-Mut), conferred complete resistance to CAP248-2B neutralization, confirming their collective role in escape from CAP248 bNAbs (Figure 3C – red line).

The gp120 C terminus is proximal to gp41, suggesting that the CAP248-2B epitope might be in the gp120-gp41 interface. To determine whether autologous gp41 mutations might contribute towards escape from CAP248-2B, we examined CAP248 gp41 ectodomain sequences over time. Of the thirteen changes identified (I515M, L519F, K588Q, N607T, Q619L, D621E, D624G, D632E, S636H, G640D, K644Q, N651I, and D659E), none drastically affected CAP248-2B neutralization when introduced into CAP45 (Figure 3D). Altogether, these data suggest that major escape mutations from the CAP248-2B lineage accumulated in the gp160 cleavage motifs, with the role of additional mutations accumulating in proximal regions of gp41 still to be defined.

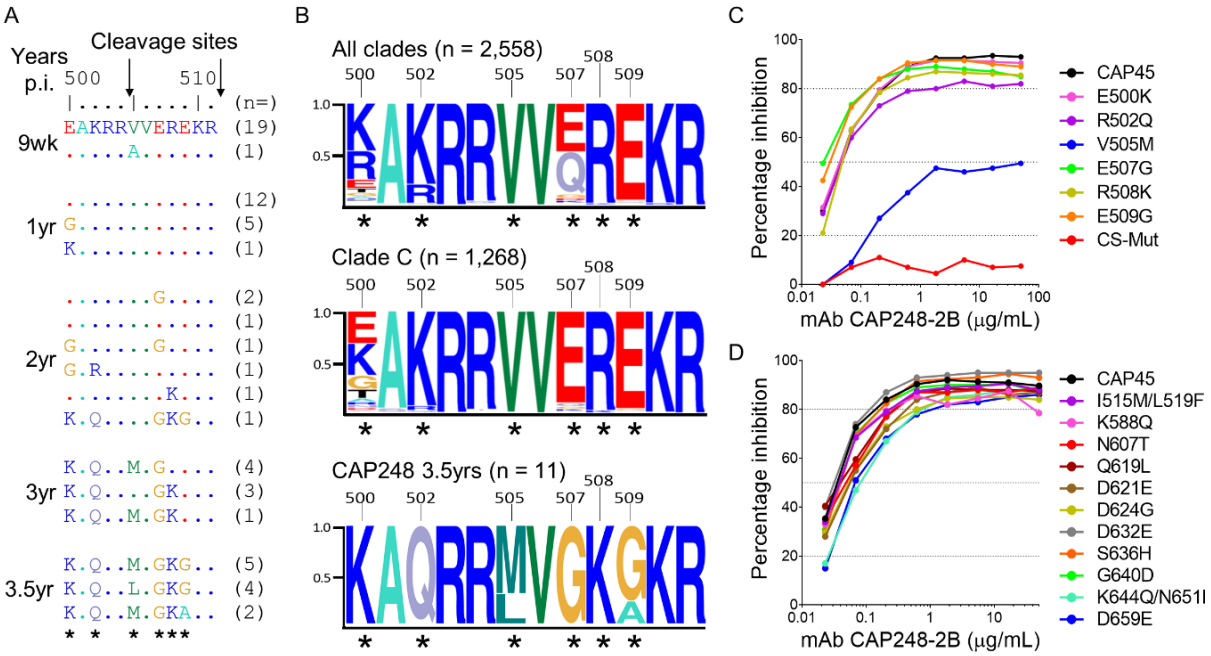

Figure 3: Escape mutations from CAP248-2B accumulate in the gp120 C terminus

(A) Sequence alignment of the gp120 C terminus from CAP248 autologous viruses at nine weeks (study enrolment), 1, 2, 3 and 3.5 years post-infection. The primary (position 511) and secondary (position 504) gp160 cleavage sites are indicated with arrows. The total number of viruses with identical amino acid sequence within this region are indicated in brackets to the right. Residues undergoing significant selection pressure are indicated with the asterisks. (B) Sequence logograms showing variation within the gp120 C terminus for all strains, and clade C only, from the LANL HIV sequence database, as well as from CAP248-2B at 3.5 years post-infection, colored and labelled as in A. The global frequencies for each of the autologous mutations identified in CAP248 sequences were: 500 (E8.88%, K46.56%, G3.56%), 502 (K79.35%, R18.73%, Q1.37%), 505 (V98.98%, A0.55%, M0.08%, L<0.01%), 507 (E47.5%, G3.87%, A0.7%), 508 (R98.24%, K1.49%), 509 (E95.11%, G1.53%, A0.27%). (C) Neutralization by CAP248-2B of the heterologous strain CAP45, when compared to gp120 C-terminal mutant viruses with changes identified from autologous CAP248 Env sequences. Data was plotted as percent inhibition (y-axis) against antibody concentration (x-axis). The wild-type virus is shown in black. Dotted lines indicate y-axis intersections for IC_{80}, IC_{50}, and IC_{20}. (D) Neutralization by CAP248-2B of CAP45 wild-type and mutant viruses with the gp41 changes identified from CAP248 autologous sequences, plotted as in C.

CAP248-2B targets a distinct membrane proximal epitope in the gp120-gp41 interface

To identify the binding site of CAP248-2B, we obtained structural information about the Fab bound to an Env trimer by electron microscopy (EM) (Figure 4 and Supplementary Figure 3). CAP248 plasma was unable to neutralize BG505, and CAP248-2B failed to bind recombinant BG505 SOSIP trimer in ELISA (Figure 4A – top

graph). Since it seemed likely that CAP248-2B targeted an epitope in the gp120-gp41 interface, we engineered the CAP248-2B epitope into a SOSIP trimer by designing a BG505(gp120)-CAP45(gp41) chimera. BG505 and CAP45 differed in gp41 by only 6.7% (23 amino acids), with most of these mutations not predicted to interact with gp120 in the pre-fusion structure. This chimeric SOSIP trimer was efficiently cleaved (data not shown), and bound well to trimer-specific bNAbs CAP256-VRC26.09 and CAP248-2B, but not to the non-neutralizing antibody F105, suggesting that it retained a native-like conformation (Figure 4A – bottom graph). Single particle negative stain EM reconstructions at ~20 Å showed a maximum stoichiometry of three CAP248-2B Fabs bound to the BG505(gp120)-CAP45(gp41) SOSIP trimer (Figure 4B – top view). Docking of the CAP248-2B Fab into the EM 3D reconstruction revealed a binding site that was extremely close to the viral membrane, similar to 35O22 and 3BC315 (43, 47), but approaching from an angle that was proximal to the gp120 C terminus (Figure 4B – side view). Since this is also the site of viral escape mutations, these data support the hypothesis that CAP248-2B binds to the C terminus of gp120, at the membrane proximal gp120-gp41 interface. In addition CAP248-2B appeared to interact with the α8 helix of one gp41 protomer and α9 helix of another gp41 protomer at the gp41-gp41 interface (Supplementary Figure 3E).

The CAP248-2B Fab structures could be docked into the EM reconstructions in two possible orientations. These placed the hydrophobic CDR-L3 tip in close proximity to either the viral membrane, or the fusion peptide (FP) of gp41, with approximately 1,100 $Å^2$ - 900 $Å^2$ of surface area buried by the paratope in Env respectively (Figure 4C). In the latter FP binding model, protein clashes would require flexible fitting of the CDR-L3 and/or FP, whereas in the lipid binding model Phe95C and Phe95D would insert into the core of the viral membrane, while Lys94 and Lys95 would be positioned to interact with the polar membrane lipid heads. To distinguish between these two binding orientations, we replaced the phenylalanine residues at the CAP248-2B CDR-L3 tip with either tryptophan or alanine (Figure 4D). The bulky, hydrophobic tryptophan side chains should interfere with specific FP interactions, negatively impacting on neutralization, whereas these same mutations would be expected to enhance interactions with the viral lipids, improving neutralization. The Trp95C/Trp95D CDR-L3 mutant was more potent against CAP45, CNE52, and CAP228, although neutralization plateaus were not improved. Similarly, mutating only one of the CDR-L3

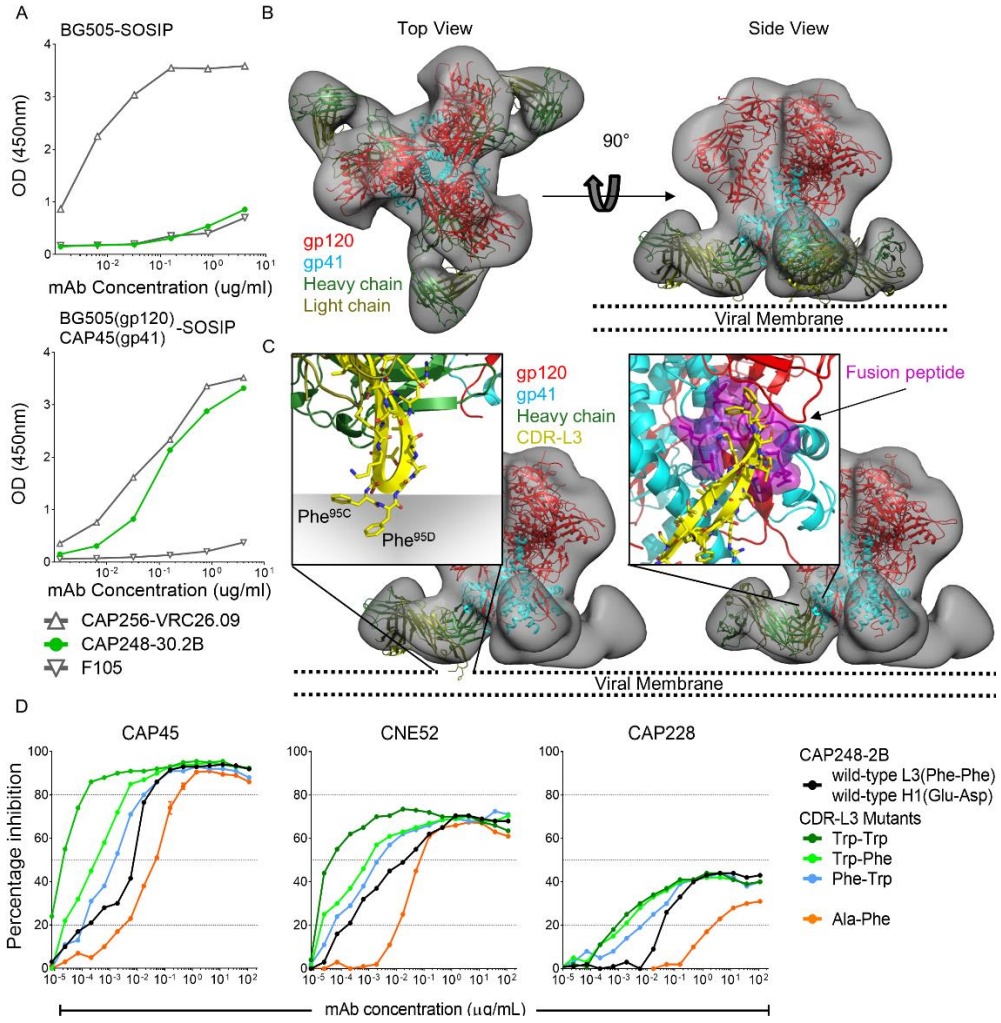

Figure 4: Negative-stain EM describes a distinct membrane proximal epitope for CAP248-2B in the gp120 C terminus and parts of gp41

(A) ELISA data comparing the binding of trimer-specific antibodies CAP256-VRC26.09 and CAP248-2B, and the non-neutralizing, gp120 binding antibody F105 to purified wild-type BG505 (top panel), and chimeric BG505(gp120)-CAP45(gp41) (bottom panel) SOSIP trimers. Absorbance readings are plotted on the y-axis and antibody concentration on the x-axis. (B) Negative stain EM 3D reconstruction of the CAP248-2B Fab bound trimers, shown in grey. The previously determined trimer structure with pdb ID: 4TVP was docked into the 3D reconstruction, and colored red for gp120 and cyan for gp41. Three CAP248-2B Fab structures were also docked, and colored forest and olive green for the heavy and light chains respectively. Two views are shown: As seen from the target cell (top view), and perpendicular to the viral membrane (side view). The approximate location of the viral membrane is indicated with dotted lines. (C) Two docking orientations for the CAP248-2B Fab are modelled and coloured as in B. In the two zoomed panel insets, the CDR-L3 (yellow) is shown in its predicted binding location with either the viral membrane (left panel inset) or interacting with the gp41 fusion peptide (right panel inset). The fusion peptide is colored purple and shown with surface representation. (D) Neutralization of three heterologous viruses by CAP248-2B and related CDR-L3 mutants. Percentage inhibition was plotted on the y-axis versus antibody concentration on the x-axis. Dotted lines indicate y-axis intersections for IC_{80}, IC_{50}, and IC_{20}.

Phe residues to generate Trp95C/Phe95D, or Phe95C/Trp95D mutants, also resulted in enhanced neutralization, with Trp95C showing the greater effect. In contrast the CDR-L3 Ala95C/Phe95D mutant showed decreased neutralization potency, confirming the importance of the CDR-L3 tip in effective neutralization of HIV-1. Binding of CAP248-2B to soluble SOSIP trimers was unaffected by any of these CDR-L3 substitutions (Supplementary Figure 3F). In contrast CDR-H1 mutations predicted to interfere with SOSIP binding in the membrane bound orientation, but not in the FP bound model, completely abrogated binding. Altogether, these data support a docking orientation where the CAP248-2B CDR-L3 makes critical hydrophobic interactions with the viral membrane.

The CAP248-2B binding site overlaps with broadly neutralizing antibody epitopes in gp41

Comparisons with previously determined structures showed CAP248-2B binding to be adjacent to the PGT151 epitope near N611/N637, the 35O22 epitope near to N88/N625, and overlap with the 3BC315 epitope at the gp41-gp41 interface (Supplementary Figure 4A and Figure 5A). To measure the extent to which these antibody epitopes overlapped, we assessed the ability of various bNAbs to block CAP248-2B binding to cell surface expressed CAP45 envelope trimers (Figure 5B). The gp120-gp41 interface antibodies PGT151 and 35O22 (but not 8ANC195) both competed for CAP248-2B binding, but 3BC315 only showed slight competition at the highest concentrations tested. In the reverse competition assay, CAP248-2B competed more substantially with 3BC315, consistent with the overlap observed by EM (Supplementary Figure 4B). Surprisingly, MPER bNAb 4E10 also competed for CAP248-2B binding to Env, while CAP248-2B binding did not affect 4E10 in the reverse assay (Figure 5B and Supplementary Figure 4B). Current trimer structures do not include the MPER, so it is not clear whether this region forms part of the CAP248-2B epitope, but this one-directional competition suggests MPER antibodies prevent CAP248-2B binding indirectly. Altogether, these data highlight the importance of the gp120-gp41 pre-fusion interface as a target for broadly neutralizing antibodies with multiple overlapping epitopes often in close proximity to the MPER.

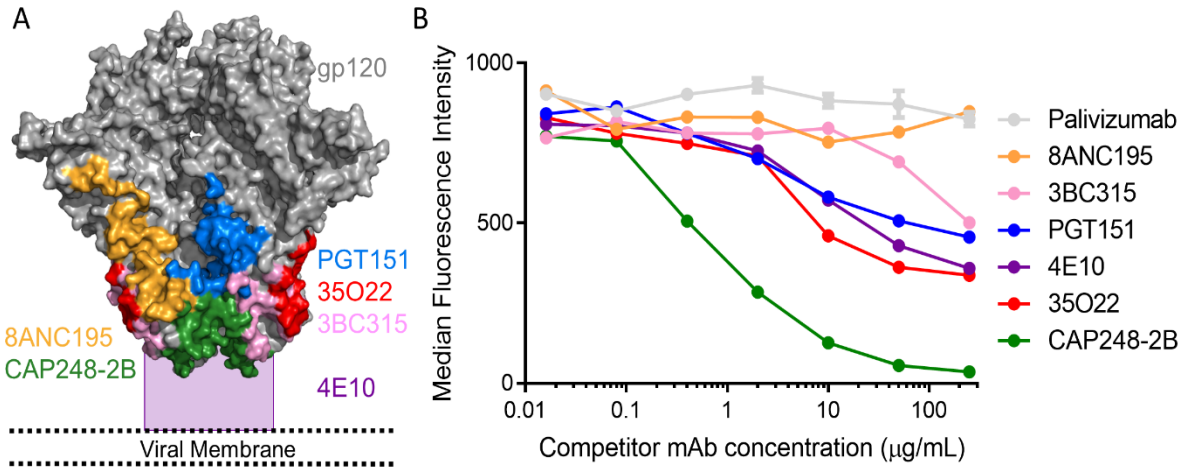

Figure 5: Broadly neutralizing antibodies that target gp41 compete with CAP248-2B for binding to cell-surface Env
(A) Surface view of the envelope trimer colored to show the core epitopes for bNAbs targeting the gp120-gp41 and gp41-gp41 interfaces. The approximate location of the MPER and the viral membrane are indicated. (B) Binding of labelled CAP248-2B to cell-surface anchored HIV-1 Env by flow cytometry, in the presence of increasing concentrations of unlabeled competitor antibody. Median fluorescence intensity (MFI) is shown on the y-axis, and increasing concentrations of each competitor antibody is plotted on the x-axis. Decreasing MFI signals correspond to increasing competition with CAP248-2B.

CAP248-2B is not dependent on glycans proximal to the gp120-gp41 interface

With the exception of 3BC315, all bNAbs targeting the gp120-gp41 interface identified to date depend on various highly conserved glycosylation sites for neutralization. Docking of the CAP248-2B Fab into the EM 3D reconstruction showed that CAP248-2B does not use long CDRs to penetrate the glycan shield, but instead glycans proximal to the epitope (particularly N88 and N611) need to shift to facilitate CAP248-2B binding (Figure 6A). The 35O22 bound orientation of the N88 glycan was incompatible with CAP248-2B binding, suggesting that similarly to 3BC315 (47), the N88 glycan must first be relocated. To assess whether glycans in gp120 or gp41 that were proximal to the CAP248 epitope were required for CAP248-2B neutralization, knock-out mutants were generated in CAP45 and tested for altered sensitivity to CAP248-2B, 8ANC195, 35O22, PGT151, and 3BC315 (Figure 6B and Supplementary Figure 5A). As expected from previous studies, 8ANC195 neutralization was abrogated by T236K and N276A mutations but enhanced by an N230A mutation,

35O22 neutralization was reduced by N88A, N230A, T236K, and N625A mutations, and PGT151 was negatively affected by N611D and N637A mutations (Supplementary Figure 5A) (29, 43, 52). However unlike these three bNAbs, but similar to 3BC315, CAP248-2B neutralization titres were not negatively affected by any of these glycan deleting mutations (Figure 6B).

N276D and N611D changes did result in slightly lower neutralization plateaus, but did not affect the CAP248-2B IC50. To test whether CAP248-2B neutralization was dependent on the N611 glycan, a S613A mutation (that also removes the N611 glycan) was introduced into CAP45. While similarly resistant to PGT151 (when compared to N611D), the S613A mutation had no effect on CAP248-2B neutralization, suggesting that unlike PGT151, CAP248-2B does not interact with the N611 glycan but rather with the amino acid side chain at position 611 (Figure 6B and Supplementary Figure 5A – dashed red line). In contrast, the N88A, N230A, and N625A glycan mutants did not affect neutralization plateaus, but were more potently neutralized by CAP248-2B at IC_{50} than the wild-type CAP45, supporting the observation that these glycans obscure the CAP248-2B epitope. The N88A glycan mutant was also more sensitive to 3BC315 neutralization, consistent with published data showing that this glycan partially occludes the 3BC315 epitope (47). These data suggest that CAP248-2B was not critically dependent on any single glycan in the gp120-gp41 interface for effective neutralization.

PGT151 is only partially affected by the individual N611D/S613A or N637A mutations, and simultaneous mutation at both N611 and N637 glycan sites is required to completely abrogate neutralization (29). To test whether the removal of an additional glycan, in conjunction with the N611D mutation, was similarly required to knock out CAP248-2B activity, each of the glycan mutants was also made in the N611D mutant backbone (Figure 6C and Supplementary Figure 5B). None of these double glycan mutant pseudoviruses showed increased resistance to CAP248-2B, though all showed partially elevated plateaus relative to the N611D mutant for CAP248-2B, with a T90A mutation (that removes the N88 glycan) having the greatest effect. Altogether these data suggest that CAP248-2B binds to a glycan-independent epitope, but that this binding must overcome steric occlusion by several glycans at positions N88, N230, N611, and N625.

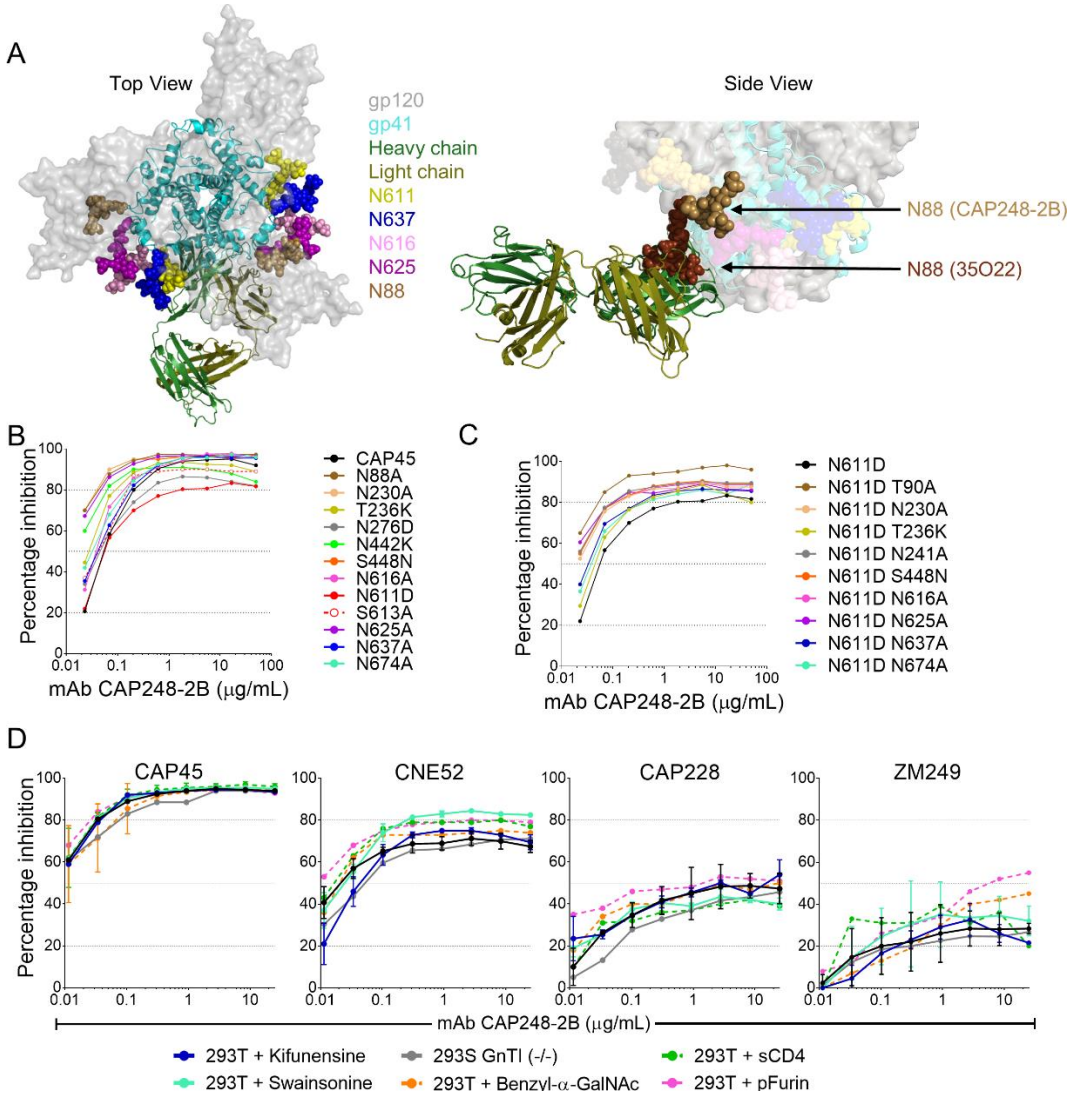

Figure 6: The CAP248-2B epitope is proximal to Env glycans, but not affected by glycan heterogeneity

(A) Schematic of CAP248-2B bound trimer (colored as in Figure 4 with gp120 shown in transparent surface grey scale) including modelled (NAG)2MAN3 basic glycans at epitope proximal N88, N611, N616, N625, and N637 residues (colored brown, yellow, pink, purple, and blue respectively). Two views are shown: Top view (left panel), and a side view zoom (right panel). Relocation of the N88 glycan between 35O22 and CAP248-2B bound states is indicated. (B) Neutralization of CAP45 by CAP248-2B when compared to epitope proximal glycan mutants. The S613A mutant that removed the glycan at N611 but maintains the amino acid side chain properties is shown with red dashed lines and open circles. Percentage inhibition was plotted on the y-axis versus CAP248-2B antibody concentration on the x-axis. (C) Neutralization of the CAP45 N611D single mutant, and various N611D including double glycan mutants, plotted as in B. (D) Neutralization of heterologous tier-2 strains CAP45, CNE52, CAP228, and ZM249 when grown normally (black lines), with co-transfected furin (dashed pink lines), or in the presence of kifunensine (blue lines), swainsonine (cyan lines), and an O-linked glycosylation inhibitor (dashed orange lines), or in a GnTI deficient cell line (grey lines). Neutralization was also assessed in the presence of sCD4 at predetermined IC_{40} concentrations for each virus (dashed green lines). Graphs are plotted as in B.

CAP248-2B neutralization plateaus could not be explained by glycan heterogeneity, cleavage, or soluble CD4

While CAP248-2B did not appear to be critically dependent on glycans surrounding the gp120-gp41 interface, incomplete inhibition by HIV-1 bNAbs is often attributed to heterogeneous glycosylation within or proximal to bNAb epitopes (33). To test whether CAP248-2B had a preference for particular N-linked glycoforms of Env, we evaluated CAP248-2B neutralization of pseudoviruses grown in the presence of N-glycosylation pathway inhibitors kifunensine or swainsonine, or grown in a GnTI deficient cell line (Figure 6D). Four sensitive strains representing different neutralization maxima (from Figure 1B) were used. Except for the slightly enhanced sensitivity of swainsonine-grown CNE52 to CAP248-2B, there was no substantial change in the CAP248-2B neutralization plateaus when enriching for high mannose (kifunensine), medium-high mannose (GnTI (-/-)) or pre-complex only (swainsonine) glycans (Figure 6D). Therefore, the unusually low neutralization plateaus of CAP248-2B could not be completely explained by overall envelope N-linked glycan heterogeneity.

Other factors for intra-strain heterogeneity could potentially include O-linked glycosylation of Env, inefficient gp160 cleavage, or an exclusive preference for a CD4 activated form of envelope. While the potential role of O-linked glycosylation in envelope heterogeneity has not been extensively characterized, recombinant gp120 expressed as a monomer can be O-glycosylated in the C terminus at position T499, and at least some forms of gp160 might be O-glycosylated at position T606 in gp41 (53-57). Both of these sites were proximal to the CAP248-2B epitope, but manipulating Env O-linked glycosylation pathways by growing pseudoviruses in the presence of benzyl 2-acetamido-2-deoxy-α-D-galactopyranoside (a modulator of mucin-like O-linked glycosylation pathways, preventing N-acetyl glucosamine addition) did not affect CAP248-2B maximum inhibition plateaus (Figure 6D – orange dashed curves). Similarly, increasing gp160 cleavage efficacy by co-transfecting pEnv and pFurin during pseudovirus production (Figure 6D – pink dashed curves), or increasing the sampling of a CD4-bound conformation during the neutralization assays by pre-incubating pseudovirions with soluble CD4 at a previously determined IC_{40} value (data not shown) for 30 minutes, did not substantially affect CAP248-2B neutralization (Figure 6D – green dashed curves). These data suggest that gp160 cleavage, sampling of the CD4 bound conformation, or O-linked glycan processing also do not contribute to the low neutralization plateaus of CAP248-2B.

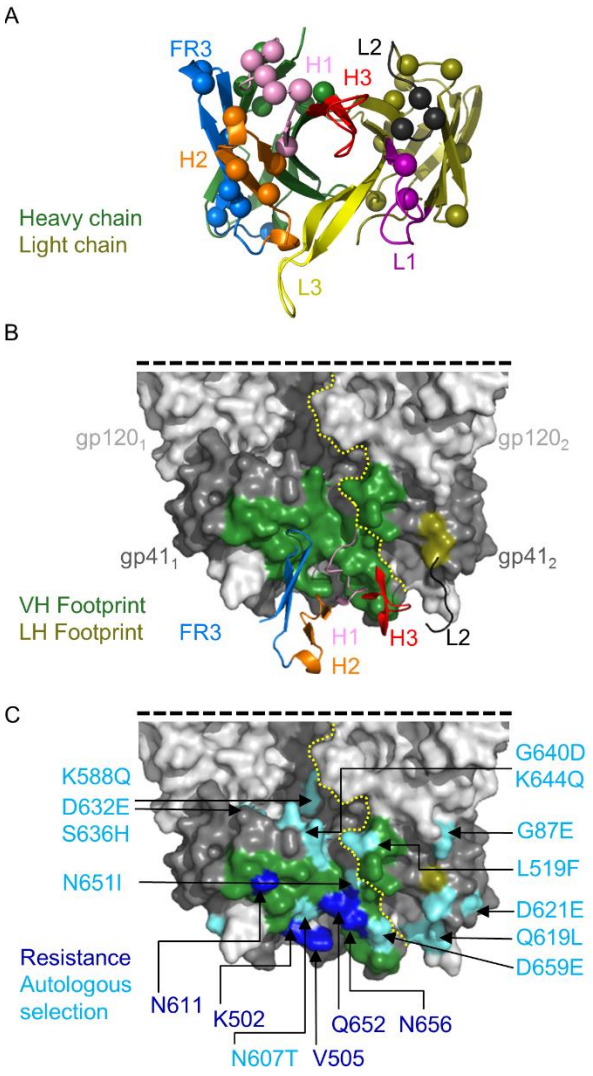

D

	Amino Acid Position	Interface Broadly Neutralizing Antibodies				
		CAP248-2B	PGT151	3BC315	35O22	8ANC195
		IC_{50}	IC_{50}	IC_{50}	IC_{50}	IC_{50}
	WT	0.04	0.03	1.14	0.05	38.56
gp41 Mutants	K601R	0.04	0.05	1.45	0.03	33.57
gp41 Mutants	L602F	0.04	0.06	1.23	0.02	36.51
gp41 Mutants	T605A	0.04	0.03		0.04	35.18
gp41 Mutants	N607A	0.05	0.13		0.01	37.35
gp41 Mutants	P609A	0.06	0.03		0.03	31.85
gp41 Mutants	S612A	0.06	0.03		0.06	30.34
gp41 Mutants	S613A	0.03	3.53	1.41	0.02	31.45
gp41 Mutants	Q619A	0.04	0.05	1.76	0.11	34.3
gp41 Mutants	T620A	0.06	0.02		0.04	31.91
gp41 Mutants	D621A	0.06	0.05		0.02	32.08
gp41 Mutants	D624A	0.05	0.09		0.03	32.57
gp41 Mutants	T641A	0.02	12.89	1.56	0.01	12.85
gp41 Mutants	E647A	0.04	>50	0.98	0.05	47.04
gp41 Mutants	S649A	0.04	0.06	1.41	0.07	33.1
gp41 Mutants	Q650A	0.04	0.18	1.21	0.14	69.46
gp41 Mutants	N651A	0.04	0.06	1.48	0.06	35.83
gp41 Mutants	Q652A	0.34	0.07	1.43	0.06	45.21
gp41 Mutants	Q653A	0.05	0.13	1.63	0.06	48.48
gp41 Mutants	E654A	0.02	50	0.33	0.07	40.48
gp41 Mutants	Q655A	0.05	0.15	1.18	0.07	54.42
gp41 Mutants	N656A	>50	0.13	1.66	0.55	59.04
gp41 Mutants	E657A	0.02	50	0.37	0.07	43.26
gp41 Mutants	K658A	0.02	0.03	0.36	0.05	28.44
gp41 Mutants	D659A	0.07	0.16	1.08	0.06	43.65
gp41 Mutants	L661A	0.12**	30.35	0.9	0.03	17.18
gp41 Mutants	L663A	0.10**	0.97	1.06	0.03	15.00
gp41 Mutants	D664A	0.02	0.07	0.35	0.07	23.47
gp120 Mutants	E500A	0.02	0.04	0.42	0.03	19.68
gp120 Mutants	A501C	>50	>50	0.44	>50	36.52
gp120 Mutants	R502A	0.23	>50	0.48	0.03	29.03
gp120 Mutants	R504A	0.05	0.2	0.22	0.06	25.71
gp120 Mutants	V505A	0.46	0.05	0.35	0.06	24.07
gp120 Mutants	V506A	0.11**	0.06	0.2	0.05	25.42
gp120 Mutants	E507A	<0.02	0.05	0.59	0.1	30.79
gp120 Mutants	R508A	>50	0.09	0.39	0.14	16.85
gp120 Mutants	E509A	<0.02	0.09	0.38	0.06	20.34
gp120 Mutants	K510R	<0.02	0.07	0.46	0.07	17.33
gp120 Mutants	K510A	0.02	0.09	0.33	0.26	13.23
gp120 Mutants	R511K	<0.02	0.04	0.31	0.09	4.53
gp120 Mutants	CS-MUT	>50	>50	0.62	<<0.02	63.71

** Mutations that affect CAP248-2B plateaus, but do not affect titre by >3 Fold

Key	>3 Fold	>30 Fold	Knock out

Figure 7: Fine mapping of the CAP248-2B epitope
(A) Cartoon of the CAP248-2B paratope (shown as a mirror image of the docked model in B, and colored as in Figure 2), showing amino acids that have affinity matured relative to the predicted germline genes with main chain Cα spheres. (B) A surface view schematic of gp41 (dark grey) and proximal regions in gp120 (light grey) showing predicted heavy chain (dark green) and light chain (olive green) binding footprints. The interface between two separate gp120-gp41 heterodimers is indicated with the dotted line. CDR loops and the heavy chain FR3 predicted to interact with envelope are shown in cartoon and colored as in A. (C) The envelope trimer is shown and colored as in B. Point mutants shown to significantly affect CAP248-2B neutralization are shown in dark blue, relative to the CAP248-2B predicted binding footprint. The autologous mutations in gp41 that were identified in Figure 4 are shown in cyan, with many in close proximity to the CAP248-2B predicted binding footprint. (D) Table showing neutralization IC50 titers for CAP248-2B, PGT151, 3BC315, 35O22, and 8ANC195 against CAP45 and various mutants. The location of each mutant in either gp41 or the gp120 C terminus is shown on the left. Fold effects on IC_{50} are colored.

Fine mapping of the CAP248-2B epitope

Most of the CAP248-2B affinity maturation occurred in the heavy chain CDRs and FR3, with limited maturation occurring in the CDR-L1 (Figure 2A and Figure 7A). In accordance with these data the CAP248-2B heavy and light chain footprint (based on the SOSIP bound EM analyses) was dominated by interactions with CDR-H1, H2, and H3, as well as the heavy chain (FR3), with limited predicted peptide interactions for the CDR-L1 or L3 (which interacts with viral lipids) (Figure 7B). To characterize the CAP248 epitope in finer detail, we made mutants in the gp120 C terminus (the location of escape mutations) and proximal regions of gp41 to compare neutralization of CAP248-2B to 8ANC195, PGT151, 35O22, and 3BC315 (Figure 7D). None of the mutations universally abrogated neutralization of all the bNAbs tested, suggesting that trimer conformation was not compromised, however the A501C mutation negatively affected the neutralization of PGT151, CAP248-2B, and 35O22. A mutation at position Q652 substantially affected CAP248-2B neutralization, while N656A completely abrogated its activity. These sites are close enough to interact with CDR-H1 residues Glu32/Asp33 that were shown above to be critical to the CAP248-2B interaction with SOSIP trimer (Supplementary Figure 3). Mutations between positions 640-660 in the α9-helix of gp41 affected PGT151 neutralization, and the N656A mutation also moderately affected 35O22 neutralization, though this residue does not form part of the 35O22 epitope. Three mutations, V506A, L661A, and L663A appeared to affect CAP248-2B maximum inhibition percentages, but did not affect CAP248-2B IC_{50} values more than three-fold (within the error of the assay), suggesting that hydrophobic interactions play a role in modulating CAP248-2B neutralization plateaus. Mutations in the gp120 C terminus affected both CAP248-2B and PGT151 neutralization, though the exact sites/effects differed between the two antibodies. Interestingly, although PGT151 does not appear to bind the gp120 C terminus directly (its access is occluded by gp41) the CAP45(CS-Mut) virus, that is completely resistant to CAP248-2B, was also resistant at IC50 to PGT151 (neutralization plateaus just under 50%). Conversely, 35O22 neutralization of CAP45(CS-Mut) was considerably more potent than the wild-type CAP45 virus. All of the mutations affecting CAP248-2B overlapped with the predicted antibody binding footprint, confirming their importance in the CAP248-2B epitope (Figure 7C – dark blue). In addition to these resistance mutations, we also examined the location of autologous mutations in gp41 identified

from longitudinal viral sequences. While these mutations were not implicated in CAP248-2B escape, half of them (N607T, Q619L, K644Q, N651I, and D659E) were proximal to the predicted CAP248-2B epitope, and may play a role in resistance to other members of the CAP248-2B lineage present in CAP248 plasma (Figure 7C – light blue).

Escape from CAP248-2B exposes proximal epitopes for anti-gp41 broadly neutralizing antibodies

The enhancement of 35O22 neutralization after the introduction of cleavage site mutations into CAP45 suggested a role for the gp120 C terminus in Env conformation. To investigate this, the neutralization of CAP45(CS-Mut) was compared to wild type CAP45 for bNAbs with diverse epitopes on HIV-1 Env (Figure 8A). CAP45(CS-Mut) neutralization by V2 and N332 antibodies remained unchanged relative to wildtype. The neutralization of CD4bs antibodies VRC01 and b12 was marginally enhanced, but neutralization of MPER bNAbs 4E10 and 10E8 was enhanced by 26- and 38-fold respectively. CAP45 is resistant to 2F5 and Z13e1, so these bNAbs were not tested. To determine whether this effect was specific to CAP45, the six CAP248 autologous escape mutations (CS-Mut) were simultaneously introduced into four additional heterologous pseudoviruses. Similar to CAP45, all four of these mutant pseudoviruses were between 10- and 100-fold more sensitive to 35O22, 4E10, and 10E8 neutralization (Figure 8B). In some instances introduction of the CS-mutations conferred sensitivity to 35O22 or 4E10, where the wild-type virus was completely resistant at the concentrations tested. These data show that mutations in the C terminus of gp120 induce localised effects in trimer conformation that specifically enhance sensitivity to MPER bNAbs.

Discussion

The identification of HIV-1 bNAbs with overlapping epitopes in the gp120-gp41 interface has greatly expanded our knowledge of the regions of the envelope trimer susceptible to neutralization (29, 43, 46, 47, 58-60). Here, we isolated a monoclonal antibody called CAP248-2B that targeted a membrane proximal epitope in the gp120-gp41 and gp41-gp41 interfaces overlapping with, but distinct from the epitopes for bNAbs PGT151, 35O22, and 3BC315. Together with 8ANC195, these epitopes surround the base of the HIV-1 envelope trimer, forming a continuum of neutralization

A

Epitope	bNAb	CAP45 WT	CAP45(CS-Mut)	Effect
V2	PG9	0.001	0.001	None
	PGT145	0.001	0.001	None
	CAP256-VRC26.08	0.11	0.12	None
N332	PGT121	12.9	24	None
CD4bs	b12	2.38	0.41	6X Enhanced
	VRC01	12	3.89	3X Enhanced
MPER	4E10	24	0.93	26X Enhanced
	10E8	1.13	<0.03	>38X Enhanced
gp120-gp41 Interface	CAP248-2B	0.03	>50	Knock out
	PGT151	0.03	>50	Knock out
	3BC315	0.75	0.76	None
	8ANC195	29.7	44.9	None
	35O22	0.05	<0.003	>17X Enhanced

B

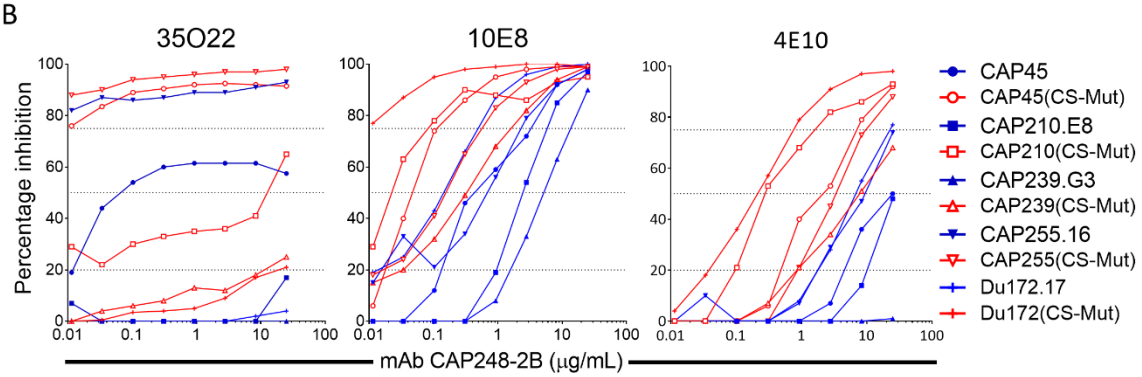

Figure 8: Escape mutations from CAP248-2B enhance the neutralization of broadly neutralizing antibodies that bind to gp41
(A) Neutralization of CAP45 and a mutant variant that includes the six gp120 C-terminal mutations identified in CAP248 autologous sequences (CS-Mut), by broadly neutralizing antibodies with epitopes in V2, V3, the CD4bs, the MPER, and the gp120-gp41 interface. Fold changes that were less than three were regarded as being within the error of the assay (no effect). Fold enhancement in neutralization sensitivity to CAP248-2B is indicated in orange (3 – 10 fold increased sensitivity) and red (> 10 fold increased sensitivity). Conferred resistance to the mutant virus at IC_{50} is shown by grey shading. (B) Neutralization of five paired WT (blue) and CS-Mut (red) viruses by 35O22, 10E8, and 4E10.

vulnerability (Figure 5A) (48). Unlike many other bNAbs, CAP248-2B neutralization plateaus could not be completely explained by glycan heterogeneity. Furthermore, rare mutations in the gp120 C terminus that mediated escape from CAP248-2B increased the sensitivity of HIV-1 viruses to MPER antibodies. Thus the identification of new antibodies targeting this supersite of vulnerability may provide important insights for vaccine design.

CAP248-2B was isolated from a CAPRISA donor (CAP248) who showed plasma neutralization breadth of nearly 60% against a multi-subtype panel and 80% against subtype C viruses. While CAP248-2B did not recapitulate the donor's plasma breadth

at IC_{50}, the neutralization profile at IC20 strongly suggested that this lineage was responsible for CAP248 broad neutralization The CAP248-2B epitope was structurally proximal to glycans at N88, N230, N611, and N625, but CAP248-2B neutralization was not dependent on any single glycan, or any double glycan knock-outs that included N611D. These data would support recent evidence for the common occurrence of neutralization plateaus across all bNAb classes, including those that do not require glycan for effective neutralization (33). Potential confounders such as the rate of furin cleavage or random sampling of CD4-induced transition intermediates were also tested, but did not affect the low plateaus for CAP248-2B. It is possible that CAP248-2B neutralization plateaus were the result of a preference for different glycoforms at two or more N-linked glycan sites. This could explain why shifting the overall glycosylation profile of a viral strain in one direction (e.g. by growing a pseudovirus in the presence of a glycosylation pathway inhibitor) had no substantial effect on the neutralization plateau. Alternatively, our data suggest an additional contributor to envelope heterogeneity, which could be an important confounder for vaccine immunogen design.

Structural analysis indicated that the CAP248-2B paratope was conformationally variable. Divergent CDR-H3 conformations that were only seen because of crystal packing may represent a level of plasticity that could have evolved to better accommodate Env sequence variation. Many bNAb epitopes are composed of structurally dynamic components, such as lipid membranes or large glycan moieties. For instance, the N88 glycan is oriented towards the viral membrane when bound by 35O22, but must shift into an orientation that would clash with 35O22 binding to allow for 3BC315 to access its epitope (47, 60). As a result, bNAb affinity maturation often rigidifies the paratope by hydrogen bonding and/or disulphide bonds within the CDRs. This optimization of the “lock-and-key” fit between antigen and antibody, can result in increased potency by reductions in binding entropy. Conversely the additional flexibility observed for CAP248-2B may contribute to its potency through low neutralization plateaus.

The unusually long CDR-L3 of CAP248-2B was specifically angled towards the viral membrane but its tip retains a level of plasticity that may assist in interacting with dynamic viral lipids. In this way, the CAP248-2B light chain CDR-L3 performs a similar function to the heavy chain CDR-H3 of MPER targeting bNAbs 2F5, Z13e1, 4E10, and 10E8 which all extend hydrophobic residues at the CDR-H3 loop tips to anchor the

antibody in the viral membrane. In addition to sharing a common mechanism of lipid recognition, CAP248-2B, 35O22, and MPER bNAbs all approach the HIV-1 trimer very close to the viral membrane. These antibodies may require the trimer to alter its orientation or position relative to the viral membrane for them to access their epitopes (43). As a consequence of this epitope occlusion, MPER bNAbs may not bind well to pre-fusion native trimers (61). From our EM docking analyses, it appears that CAP248-2B recognizes the pre-fusion "closed" state of the HIV-1 envelope trimer. These data are supported by the observations that firstly, CAP248-2B binding to Env was not enhanced in the presence of sCD4, and secondly, that CAP248-2B could not compete with the MPER bNAb 4E10, which prefers recognition of the CD4-induced transition intermediate. It remains to be determined what structural rearrangements (if any) in the trimer are required for CAP248-2B to properly access its epitope.

In accordance with its low angle of binding, escape from CAP248-2B occurred in both the gp160 cleavage motifs. Of the six identified mutations, only V505M individually affected CAP248-2B neutralization. In autologous viruses, mutations at positions 500, 502, 507, 508, and 509 all occurred by two years post-infection, while variants at position 505 were only detectable after three years of infection. Based on these kinetics, it is likely that mutations at positions 500, 502, 507, 508, and 509 accumulated first in response to earlier members of the CAP248 bNAb lineage, with the eventual selection of extremely rare mutations at position 505 by later members of the antibody lineage. Similarly, we identified a cluster of autologous gp41 mutations that overlap the CAP248-2B epitope, and while these did not affect CAP248-2B neutralization they may have played a role in escaping earlier lineage members. Future experiments to isolate these early members of the lineage will help to understand how virus-antibody co-evolution led to the development of CAP248-2B. In addition, the isolation of more potent variants of CAP248-2B should help to explain the mechanisms of incomplete neutralization for this new interface targeting antibody.

In addition to mediating escape from CAP248-2B, mutations in the gp120 C terminus conferred partial resistance to PGT151. Based on EM 3D reconstructions PGT151 does not bind the gp120 C terminus (58), suggesting that these mutations have the ability to affect envelope conformation in a way that confers resistance to PGT151. Conversely, the gp120 C-terminal mutations also had the unexpected effect of dramatically enhancing the neutralization of 35O22 (targeting a membrane proximal epitope) and bNAbs targeting the MPER, suggesting that these conformational effects

may assist in raising gp41 relative to the membrane (43, 62-65), perhaps by increasing the frequency at which membrane associated Env trimers sample a CD4-induced conformation, without first having to engage the CD4 receptor. Importantly, this effect did not make viruses globally sensitive to HIV-1 antibodies, but was specific for bNAbs with membrane proximal epitopes. Incorporating these mutations into membrane bound HIV-1 trimer immunogens may therefore improve the antigenicity of bNAb epitopes in gp41.

Overall these data expand the recently identified gp120-gp41 interface supersite to include the gp120 C terminus, highlighting the importance of this region as a vaccine target. Future experiments should aim to determine whether membrane-bound CS-Mut trimers successfully engage MPER bNAb precursors, thus overcoming an important barrier to the induction of MPER bNAbs. Furthermore, defining additional glycan independent mechanisms of envelope heterogeneity will have implications for the use of bNAbs in both passive and active immunization strategies.

Materials and Methods

Ethics statement

The CAPRISA Acute Infection study received ethical approval from the Universities of KwaZulu-Natal (E013/04), Cape Town (025/2004), and the Witwatersrand (MM040202). CAP248 provided written informed consent for study participation.

CAPRISA 002 Acute Infection cohort

The CAPRISA Acute Infection cohort is comprised of women at high risk of HIV-1 infection in KwaZulu-Natal, South Africa (15). Blood samples collected at regular intervals from seroconversion through to the initiation of antiretroviral therapy were cryopreserved as individually processed PBMC, serum and plasma samples.

B cell culture

Cryopreserved CAP248 PBMC were thawed, washed and suspended in medium containing 10% foetal bovine serum (FBS) and antibiotics. B cells were enriched by negative selection with immunomagnetic beads (Miltenyi), and were cultured at 25 cells per well in Iscove's Modified Dulbecco's Medium (IMDM) containing 10% FBS, 2 µg/mL CpG2006, 100 units/mL rIL-2, rIL-21 (50 ng/mL) with 3T3msCD40L as feeder cells (a gift of Mark Connors) (44), plated at 2500 cells/well in multiple 96 well plates. rIL-2 was obtained from the NIH AIDS Reagent Program as provided by Maurice Gately (Hoffmann-La Roche). Fresh medium containing growth factors was added

after 7 days of culture and after each antibody screening procedure. B cell culture fluids were screened from day 14 for neutralizing activity against CAP45 pseudovirus in an adaptation of the single-cycle TZM-bl neutralization assay as previously described (66).

Cloning and expression of human immunoglobulin genes

B cells from wells testing positive for antibody were stored in RNAlater (Ambion). VH, Vκ, or Vλ genes were amplified in separate reactions from RNA using a one-step RT-PCR (Invitrogen SuperScript III kit with Platinum Taq High Fidelity polymerase) with previously described primer mixes (67). For expression vector assembly, forward primers included a 25 nucleotide non-annealing 5' tag sequence, which was homologous to the immunoglobulin leader sequence at the 3' end of the CMV promoter fragment. Reverse primers were designed to overlap the 5' end of the immunoglobulin constant region for each vector. Linear expression constructs were assembled by overlapping PCR between two DNA fragments containing the CMV promoter and immunoglobulin leader sequence or the constant region sequences for IgG1, kappa or lambda genes followed by a C-terminal BGH poly A sequence. These were co-transfected into 293T cells, and supernatant fluids were tested for neutralization activity. This step allowed rapid detection of pairs of VH and VL chain genes that functioned together to produce antibody. To produce monoclonal antibodies, the In-Fusion cloning system (Clontech) was used to insert re-amplified pairs of VH and VL gene fragments into pLM2 expression plasmids similar to previously described (68), but modified to contain the immunoglobulin leader sequence in the linear vectors. Expression plasmids were linearized by restriction enzymes acting on sites within the multiple cloning site of plasmid (EcoRI for IgG1 and lambda, BsiWI for kappa). Linearized vectors were then PCR amplified with primer pairs designed to create terminal sequences that were homologous to 5' and 3' terminal sequences of the variable region insert fragments, allowing insertion of the VH and VL fragments into linearized plasmids by the activity of the In-Fusion enzyme as described (69). The resulting plasmids were transformed in *E.coli* JM109 cells. A previously described strategy was used to identify the correct pair of VH and VL clones responsible for antibody production (70). Subsequent sequencing of multiple clones showed that only one heavy and one light chain were capable of directing mAb synthesis.

Cell lines

CD4+/CCR5+ TZM-bl HeLa cells were obtained from the NIH AIDS Research and Reference Reagent Program, Division of AIDS, NIAID, NIH (developed by Dr. John C. Kappes, and Dr. Xiaoyun Wu [79,80]). 293T cells were obtained from Dr George Shaw (University of Alabama, Birmingham, AL). Adherent cell lines were cultured at 37°C, 5% CO2, in DMEM containing 10% heat-inactivated fetal bovine serum (Gibco BRL Life Technologies) and supplemented with 50 ug/ml gentamicin (Sigma). Cells were routinely disrupted at confluency with 0.25% trypsin in 1 mM EDTA (Sigma) every 48-72 hours. 293F suspension cells were cultured in 293Freestlye media (Gibco BRL Life Technologies) at 37°C, 10% CO^2, 125 RPM and diluted twice a week to between 0.2 and 0.5 million cells/mL.

Single genome amplification

The single genome amplification of HIV Env has been previously described (71). Briefly, CAP248 viral RNA was isolated using the Viral RNA Extraction Kit (QIAGEN), to serve as a template for Superscript III Reverse Transcriptase (Invitrogen) in cDNA generation. Residual RNA was degraded with RNaseH (Invitrogen) and CAP248 envelope genes were amplified by a nested PCR approach using Platinum Taq (Invitrogen). PCR products were cleaned up (QIAGEN) and sequenced with the ABI Prism Big Dye Terminator Cycle Sequencing Ready Reaction kit (Applied Biosystems) on the ABI 3100 automated genetic analyser, assembled using Sequencher v.4.5 (Genecodes), and compiled into working alignments in Bioedit v.7.0.5.3.

Pseudovirus production and site-directed mutagenesis

Plasmids expressing the HIV Env of interest were co-transfected with pSG3DEnv backbone expressing plasmids (obtained from the NIH AIDS Research and Reference Reagent Program, Division of AIDS, NIAID, NIH) into 293T cells using PEI-MAX 40,000 (Polysciences). Cultures were incubated for 48 hours at 37°C, then filtered through 0.45 µm and frozen in DMEM, 20% FBS to yield Env-pseudotyped viruses capable of a single round of infection only. Mutant envelope genes were generated with the QuikChange Lightning Kit (Stratagene), confirmed by DNA sequencing, and transfected as above. For the glycan heterogeneity experiments, pseudoviruses were grown as above in the presence of 25 M glycosylation inhibitor, or in 293S GnTI(-/-) cells.

Neutralization assays

Neutralization assays were performed in TZM-bl cells as previously described (12, 72). Neutralization is measured as a reduction in relative light units after a single round of pseudovirus infection in the presence of the monoclonal antibody or plasma sample of interest. Samples were serially diluted 1:3 and the ID_{50}/IC_{50} calculated as the dilution at which the infection was reduced by 50%.

Protein production

For CAP248-2B antibody expression, plasmids separately encoding heavy and light chain genes were co-transfected into 293F cells with PEI-MAX 40,000 (Polysciences). To make CAP248-2B Fab, the HRV-3C protein cleavage site (GLEVLFQGP) was introduced into the heavy chain gene between Fab and Fc fragments by PCR. Expressed full length mAb was digested with HRV-3C enzyme (Merck Millipore) at 25°C for four hours, and then the separated Fab fragments were purified by sequential negative selection over protein A, and positive selection by gel filtration using a superdex 200 (GE Healthcare). Cells were cultured for seven days in 293Freestyle media at 37°C, 10% CO^2, then harvested supernatants were 0.22 µm filtered and purified using protein A. Trimers were expressed previously described (60), and purified from 0.22 µm filtered supernatants with an Ni-NTA column (30 mM Imidazole wash and 400 mM Imidazole elution buffers at pH 7), and then by CAP248-2B mAb bound to protein A. The Fab-trimer complexes were eluted by digestion with HRV-3C (which also removed the His6 tag from gp41), and further purified by gel filtration using a superdex 200 column (GE Healthcare).

Enzyme-Linked Immunosorbent Assay (ELISA)

HisTagged trimers were coated at 2 µg/mL in PBS onto nickel coated 96 well plates (Thermo) for one hour at 25°C. Plates were washed and then probed with serial dilutions of HIV-1 monoclonal antibody for one hour at 25°C. This process was repeated using an anti-Fc/HRP conjugate to detect trimer-bound antibodies. Antigen-antibody complexes were detected by incubating with 100 µL of enzyme substrate for five minutes and then the reaction was stopped with 25 µL of 1 M HCl. Absorbance was read at 450 nm.

Protein X-ray crystallography

Concentrated aliquots were stored at 4°C. 576 crystallization conditions were screened in 96 well plates (Corning) using the Cartesian Honeybee crystallization robot by sitting drop vapour diffusion in 400 nL drops at 25°C containing 50% mother

liquor. Crystal hits were hand-optimised in 15 well hanging drop diffusion plates at 25°C in 1 µL drops containing 50% mother liquor. All crystallographic diffraction data was collected at the Advanced Photon Source (Argonne National Laboratory) SER-CAT ID-22 beamline, at a wavelength of 1.00 Å, 100 K, and processed with HKL2000. Model building and refinement was handled with COOT v0.8 and PHENIX v1.9-1692 software packages respectively, using 5% of the data as an R-free cross validation test set, and hydrogens were refined to minimise clashes. The unliganded CAP248-2B Fab was first crystallized in 10.25% PEG4000, 87.5 mM ammonium sulphate, and flash frozen in 25% PEG400 as a cryoprotectant. This crystal diffracted to a resolution of 2.0 Å and phasing by molecular replacement was done using PDB-IDs: 4QHK and 3B2U as search models. We could not reliably build the constant domain for one of the two Fabs in the asymmetric unit, which appeared to have considerable mobility within the crystal lattice, resulting in poor RSRZ scores for regions of these chains. This first structure served as the search model for the second crystal structure obtained in 7.5% PEG4000, 12.5% isopropanol, 0.1 M sodium citrate (pH5.6), and flash frozen in 30% ethylene glycol as a cryoprotectant, which diffracted with I/αI >2 to a resolution of 3.1 Å, with data up to 2.8 Å (PDB-ID: 5F89). All structural images were generated in PyMOL Molecular Graphics System, Version 1.3r1edu, Schrödinger LLC., or UCSF Chimera (73).

Negative stain Electron Microscopy (EM)

BG505-CAP45 SOSIP trimers were incubated with a 6 molar excess of CAP248-2B Fab overnight at room temperature and the complexes were diluted to ~0.03 mg/mL in Tris-buffered saline prior to application onto a carbon-coated 400 Cu mesh grid (Electron Microscopy Sciences) that had been glow discharged at 20 mA for 30 seconds. The grids were stained with 2% (w/v) NanoW (Nanoprobes) for 7 s, blotted, and stained for an additional 15 s. Samples were imaged on an FEI T12 electron microscope operating at 120 keV, with an electron dose of ~25 electrons/Å2 and a magnification of 52,000x that resulted in a pixel size of 2.05 Å at the specimen plane. Images were acquired with Leginon (74), using a Tietz TemCam F416 camera and a nominal defocus range of 1000-1500 nm. Stage tilts between -50° and 0° using 10° increments were performed to increase the amount of unique views to aid with 3D reconstruction. Automated particle picking, stack creation, and initial 2D classification were performed in the Appion software suite (75). Classes representing noisy alignments, neighboring particles, unbound Fab, or ligand-free trimers were discarded

and representative class averages with unique views of the SOSIP-CAP248-2B complex were used to generate an initial common-lines model using EMAN2 (76), followed by refinement against all 28,215 particles in Sparx (77), with *C3*-symmetry imposed. The resolution of the final reconstruction is ~20 Å based on a Fourier shell correlation of 0.5. Two-dimensional back projections of the final 3D models were generated using EMAN (76).

Cell-surface binding assay

The CAP45.2.00.G3J (Genbank: EF203960) env plasmid was codon optimised (GenScript) and truncated at the cytoplasmic tail to increase surface Env content (78). Following restriction digest cloning this plasmid was transiently transfected using TrueFect-MAX (United Biosystems) into HEK/293T cells. Two days after transfection, cells were labelled with Live/Dead Fixable Aqua Dead Cell Stain (Life Technologies) followed by biotinylated CAP248-2B and serially diluted unlabelled competitor antibodies (CAP248-2B, 3BC315, 35O22, PGT151. 8ANC195, 4E10, and control antibody Palivizumab). After incubation and three washes with 5% FBS in PBS, cells were stained with Streptavidin-PE (Life Technologies) at a 1:300 dilution. Reverse competition assays were also performed with biotinylated 3BC315, 35O22, PGT151, 8ANC195 and 4E10 and serially diluted CAP248-2B or Palivizumab. Cells were analysed on a BD FACS Aria II (Becton Dickinson) and binding was measured as the median fluorescence intensity (MFI) for each sample minus the MFI of the cells stained with the detection antibody only.

Acknowledgements

We are grateful to CAPRISA Acute Infection cohort participant CAP248, and the clinical and laboratory staff at CAPRISA for their continued commitment to the study, as well as to the staff at sector 22 (Southeast Region Collaborative Access Team) at the Advanced Photon Source. We thank Dr. Elin S. Gray and Maphuti Madiga who ran the initial neutralization screens that identified CAP248 as a potential broadly neutralizing antibody donor with quaternary structure specificity, and acknowledge Dr. Florian Klein for providing the antibody 3BC315.

References

1. Mascola JR, Montefiori DC. The role of antibodies in HIV vaccines. Annu Rev Immunol. 2010;28:413-44.
2. Earl PL, Doms RW, Moss B. Oligomeric structure of the human immunodeficiency virus type 1 envelope glycoprotein. Proceedings of the National Academy of Sciences of the United States of America. 1990;87(2):648-52.
3. Earl PL, Moss B, Doms RW. Folding, interaction with GRP78-BiP, assembly, and transport of the human immunodeficiency virus type 1 envelope protein. Journal of virology. 1991;65(4):2047-55.
4. McCune JM, Rabin LB, Feinberg MB, Lieberman M, Kosek JC, Reyes GR, et al. Endoproteolytic cleavage of gp160 is required for the activation of human immunodeficiency virus. Cell. 1988;53(1):55-67.
5. Freed EO, Myers DJ, Risser R. Mutational analysis of the cleavage sequence of the human immunodeficiency virus type 1 envelope glycoprotein precursor gp160. Journal of virology. 1989;63(11):4670-5.
6. Kieny MP, Lathe R, Riviere Y, Dott K, Schmitt D, Girard M, et al. Improved antigenicity of the HIV env protein by cleavage site removal. Protein Eng. 1988;2(3):219-25.
7. Moore JP, McKeating JA, Weiss RA, Sattentau QJ. Dissociation of gp120 from HIV-1 virions induced by soluble CD4. Science. 1990;250(4984):1139-42.
8. Tomaras GD, Yates NL, Liu P, Qin L, Fouda GG, Chavez LL, et al. Initial B-cell responses to transmitted human immunodeficiency virus type 1: virion-binding immunoglobulin M (IgM) and IgG antibodies followed by plasma anti-gp41 antibodies with ineffective control of initial viremia. Journal of virology. 2008;82(24):12449-63.
9. Gray ES, Moore PL, Choge IA, Decker JM, Bibollet-Ruche F, Li H, et al. Neutralizing antibody responses in acute human immunodeficiency virus type 1 subtype C infection. Journal of virology. 2007;81(12):6187-96.
10. Richman DD, Wrin T, Little SJ, Petropoulos CJ. Rapid evolution of the neutralizing antibody response to HIV type 1 infection. Proceedings of the National Academy of Sciences of the United States of America. 2003;100(7):4144-9.
11. Li B, Decker JM, Johnson RW, Bibollet-Ruche F, Wei X, Mulenga J, et al. Evidence for potent autologous neutralizing antibody titers and compact envelopes in early infection with subtype C human immunodeficiency virus type 1. Journal of virology. 2006;80(11):5211-8.
12. Wei X, Decker JM, Wang S, Hui H, Kappes JC, Wu X, et al. Antibody neutralization and escape by HIV-1. Nature. 2003;422(6929):307-12.
13. Moog C, Fleury HJ, Pellegrin I, Kirn A, Aubertin AM. Autologous and heterologous neutralizing antibody responses following initial seroconversion in human immunodeficiency virus type 1-infected individuals. Journal of virology. 1997;71(5):3734-41.
14. Hraber P, Seaman MS, Bailer RT, Mascola JR, Montefiori DC, Korber BT. Prevalence of broadly neutralizing antibody responses during chronic HIV-1 infection. Aids. 2014;28(2):163-9.
15. Gray ES, Madiga MC, Hermanus T, Moore PL, Wibmer CK, Tumba NL, et al. The neutralization breadth of HIV-1 develops incrementally over four years and is associated with CD4+ T cell decline and high viral load during acute infection. Journal of virology. 2011;85(10):4828-40.
16. Doria-Rose NA, Klein RM, Manion MM, O'Dell S, Phogat A, Chakrabarti B, et al.

Frequency and phenotype of human immunodeficiency virus envelope-specific B cells from patients with broadly cross-neutralizing antibodies. Journal of virology. 2009;83(1):188-99.
17. Sather DN, Armann J, Ching LK, Mavrantoni A, Sellhorn G, Caldwell Z, et al. Factors associated with the development of cross-reactive neutralizing antibodies during human immunodeficiency virus type 1 infection. Journal of virology. 2009;83(2):757-69.
18. Moldt B, Rakasz EG, Schultz N, Chan-Hui PY, Swiderek K, Weisgrau KL, et al. Highly potent HIV-specific antibody neutralization in vitro translates into effective protection against mucosal SHIV challenge in vivo. Proceedings of the National Academy of Sciences of the United States of America. 2012;109(46):18921-5.
19. Pegu A, Yang ZY, Boyington JC, Wu L, Ko SY, Schmidt SD, et al. Neutralizing antibodies to HIV-1 envelope protect more effectively in vivo than those to the CD4 receptor. Science translational medicine. 2014;6(243):243ra88.
20. Baba TW, Liska V, Hofmann-Lehmann R, Vlasak J, Xu W, Ayehunie S, et al. Human neutralizing monoclonal antibodies of the IgG1 subtype protect against mucosal simian-human immunodeficiency virus infection. Nature medicine. 2000;6(2):200-6.
21. Hessell AJ, Poignard P, Hunter M, Hangartner L, Tehrani DM, Bleeker WK, et al. Effective, low-titer antibody protection against low-dose repeated mucosal SHIV challenge in macaques. Nature medicine. 2009;15(8):951-4.
22. Mascola JR, Stiegler G, VanCott TC, Katinger H, Carpenter CB, Hanson CE, et al. Protection of macaques against vaginal transmission of a pathogenic HIV-1/SIV chimeric virus by passive infusion of neutralizing antibodies. Nature medicine. 2000;6(2):207-10.
23. Parren PW, Marx PA, Hessell AJ, Luckay A, Harouse J, Cheng-Mayer C, et al. Antibody protects macaques against vaginal challenge with a pathogenic R5 simian/human immunodeficiency virus at serum levels giving complete neutralization in vitro. Journal of virology. 2001;75(17):8340-7.
24. Veazey RS, Shattock RJ, Pope M, Kirijan JC, Jones J, Hu Q, et al. Prevention of virus transmission to macaque monkeys by a vaginally applied monoclonal antibody to HIV-1 gp120. Nature medicine. 2003;9(3):343-6.
25. Kwong PD, Mascola JR. Human antibodies that neutralize HIV-1: identification, structures, and B cell ontogenies. Immunity. 2012;37(3):412-25.
26. Verkoczy L, Kelsoe G, Moody MA, Haynes BF. Role of immune mechanisms in induction of HIV-1 broadly neutralizing antibodies. Curr Opin Immunol. 2011;23(3):383-90.
27. Klein F, Diskin R, Scheid JF, Gaebler C, Mouquet H, Georgiev IS, et al. Somatic mutations of the immunoglobulin framework are generally required for broad and potent HIV-1 neutralization. Cell. 2013;153(1):126-38.
28. Doores KJ, Burton DR. Variable loop glycan dependency of the broad and potent HIV-1 neutralizing antibodies PG9 and PG16. Journal of virology. 2010.
29. Falkowska E, Le KM, Ramos A, Doores KJ, Lee JH, Blattner C, et al. Broadly Neutralizing HIV Antibodies Define a Glycan-Dependent Epitope on the Prefusion Conformation of gp41 on Cleaved Envelope Trimers. Immunity. 2014.
30. Kim AS, Leaman DP, Zwick MB. Antibody to gp41 MPER alters functional properties of HIV-1 Env without complete neutralization. PLoS pathogens. 2014;10(7):e1004271.
31. Pritchard LK, Spencer DI, Royle L, Vasiljevic S, Krumm SA, Doores KJ, et al. Glycan Microheterogeneity at the PGT135 Antibody Recognition Site on HIV-1

gp120 Reveals a Molecular Mechanism for Neutralization Resistance. Journal of virology. 2015;89(13):6952-9.
32. Doores KJ. The HIV glycan shield as a target for broadly neutralizing antibodies. FEBS J. 2015.
33. McCoy LE, Falkowska E, Doores KJ, Le K, Sok D, van Gils MJ, et al. Incomplete Neutralization and Deviation from Sigmoidal Neutralization Curves for HIV Broadly Neutralizing Monoclonal Antibodies. PLoS pathogens. 2015;11(8):e1005110.
34. Doria-Rose NA, Schramm CA, Gorman J, Moore PL, Bhiman JN, DeKosky BJ, et al. Developmental pathway for potent V1V2-directed HIV-neutralizing antibodies. Nature. 2014;509(7498):55-62.
35. Liao HX, Lynch R, Zhou T, Gao F, Alam SM, Boyd SD, et al. Co-evolution of a broadly neutralizing HIV-1 antibody and founder virus. Nature. 2013;496(7446):469-76.
36. Walker LM, Huber M, Doores KJ, Falkowska E, Pejchal R, Julien JP, et al. Broad neutralization coverage of HIV by multiple highly potent antibodies. Nature. 2011;477(7365):466-70.
37. Walker LM, Phogat SK, Chan-Hui PY, Wagner D, Phung P, Goss JL, et al. Broad and potent neutralizing antibodies from an African donor reveal a new HIV-1 vaccine target. Science. 2009;326(5950):285-9.
38. Sok D, van Gils MJ, Pauthner M, Julien JP, Saye-Francisco KL, Hsueh J, et al. Recombinant HIV envelope trimer selects for quaternary-dependent antibodies targeting the trimer apex. Proceedings of the National Academy of Sciences of the United States of America. 2014;111(49):17624-9.
39. Bonsignori M, Montefiori DC, Wu X, Chen X, Hwang KK, Tsao CY, et al. Two distinct broadly neutralizing antibody specificities of different clonal lineages in a single HIV-1-infected donor: implications for vaccine design. Journal of virology. 2012;86(8):4688-92.
40. Wu X, Yang ZY, Li Y, Hogerkorp CM, Schief WR, Seaman MS, et al. Rational design of envelope identifies broadly neutralizing human monoclonal antibodies to HIV-1. Science. 2010;329(5993):856-61.
41. Corti D, Langedijk JP, Hinz A, Seaman MS, Vanzetta F, Fernandez-Rodriguez BM, et al. Analysis of memory B cell responses and isolation of novel monoclonal antibodies with neutralizing breadth from HIV-1-infected individuals. PloS one. 2010;5(1):e8805.
42. Scheid JF, Mouquet H, Feldhahn N, Walker BD, Pereyra F, Cutrell E, et al. A method for identification of HIV gp140 binding memory B cells in human blood. J Immunol Methods. 2009;343(2):65-7.
43. Huang J, Kang BH, Pancera M, Lee JH, Tong T, Feng Y, et al. Broad and potent HIV-1 neutralization by a human antibody that binds the gp41-gp120 interface. Nature. 2014;515(7525):138-42.
44. Huang J, Ofek G, Laub L, Louder MK, Doria-Rose NA, Longo NS, et al. Broad and potent neutralization of HIV-1 by a gp41-specific human antibody. Nature. 2012;491(7424):406-12.
45. Klein F, Gaebler C, Mouquet H, Sather DN, Lehmann C, Scheid JF, et al. Broad neutralization by a combination of antibodies recognizing the CD4 binding site and a new conformational epitope on the HIV-1 envelope protein. The Journal of experimental medicine. 2012;209(8):1469-79.
46. Scharf L, Scheid JF, Lee JH, West AP, Jr., Chen C, Gao H, et al. Antibody 8ANC195 reveals a site of broad vulnerability on the HIV-1 envelope spike. Cell reports. 2014;7(3):785-95.

47. Lee JH, Leaman DP, Kim AS, Torrents de la Pena A, Sliepen K, Yasmeen A, et al. Antibodies to a conformational epitope on gp41 neutralize HIV-1 by destabilizing the Env spike. Nat Commun. 2015;6:8167.
48. Wibmer CK, Moore PL, Morris L. HIV broadly neutralizing antibody targets. Curr Opin HIV AIDS. 2015;10(3):135-43.
49. Wibmer CK, Bhiman JN, Gray ES, Tumba N, Abdool Karim SS, Williamson C, et al. Viral escape from HIV-1 neutralizing antibodies drives increased plasma neutralization breadth through sequential recognition of multiple epitopes and immunotypes. PLoS pathogens. 2013;9(10):e1003738.
50. Mikell I, Stamatatos L. Evolution of Cross-Neutralizing Antibody Specificities to the CD4-BS and the Carbohydrate Cloak of the HIV Env in an HIV-1-Infected Subject. PloS one. 2012;7(11):e49610.
51. Wang W, Nie J, Prochnow C, Truong C, Jia Z, Wang S, et al. A systematic study of the N-glycosylation sites of HIV-1 envelope protein on infectivity and antibody-mediated neutralization. Retrovirology. 2013;10:14.
52. West AP, Jr., Scharf L, Horwitz J, Klein F, Nussenzweig MC, Bjorkman PJ. Computational analysis of anti-HIV-1 antibody neutralization panel data to identify potential functional epitope residues. Proceedings of the National Academy of Sciences of the United States of America. 2013.
53. Guttman M, Kahn M, Garcia NK, Hu SL, Lee KK. Solution structure, conformational dynamics, and CD4-induced activation in full-length, glycosylated, monomeric HIV gp120. Journal of virology. 2012;86(16):8750-64.
54. Go EP, Hewawasam G, Liao HX, Chen H, Ping LH, Anderson JA, et al. Characterization of glycosylation profiles of HIV-1 transmitted/founder envelopes by mass spectrometry. Journal of virology. 2011;85(16):8270-84.
55. Stansell E, Panico M, Canis K, Pang PC, Bouche L, Binet D, et al. Gp120 on HIV-1 Virions Lacks O-Linked Carbohydrate. PloS one. 2015;10(4):e0124784.
56. Go EP, Herschhorn A, Gu C, Castillo-Menendez L, Zhang S, Mao Y, et al. Comparative Analysis of the Glycosylation Profiles of Membrane-Anchored HIV-1 Envelope Glycoprotein Trimers and Soluble gp140. Journal of virology. 2015;89(16):8245-57.
57. Yang W, Shah P, Toghi Eshghi S, Yang S, Sun S, Ao M, et al. Glycoform analysis of recombinant and human immunodeficiency virus envelope protein gp120 via higher energy collisional dissociation and spectral-aligning strategy. Anal Chem. 2014;86(14):6959-67.
58. Blattner C, Lee JH, Sliepen K, Derking R, Falkowska E, de la Pena AT, et al. Structural Delineation of a Quaternary, Cleavage-Dependent Epitope at the gp41-gp120 Interface on Intact HIV-1 Env Trimers. Immunity. 2014.
59. Scharf L, Wang H, Gao H, Chen S, McDowall AW, Bjorkman PJ. Broadly Neutralizing Antibody 8ANC195 Recognizes Closed and Open States of HIV-1 Env. Cell. 2015;162(6):1379-90.
60. Pancera M, Zhou T, Druz A, Georgiev IS, Soto C, Gorman J, et al. Structure and immune recognition of trimeric pre-fusion HIV-1 Env. Nature. 2014;514(7523):455-61.
61. Chen J, Frey G, Peng H, Rits-Volloch S, Garrity J, Seaman MS, et al. Mechanism of HIV-1 neutralization by antibodies targeting a membrane-proximal region of gp41. Journal of virology. 2014;88(2):1249-58.
62. Rathinakumar R, Dutta M, Zhu P, Johnson WE, Roux KH. Binding of anti-membrane-proximal gp41 monoclonal antibodies to CD4-liganded and -unliganded human immunodeficiency virus type 1 and simian immunodeficiency

virus virions. Journal of virology. 2012;86(3):1820-31.
63. Frey G, Peng H, Rits-Volloch S, Morelli M, Cheng Y, Chen B. A fusion-intermediate state of HIV-1 gp41 targeted by broadly neutralizing antibodies. Proceedings of the National Academy of Sciences of the United States of America. 2008;105(10):3739-44.
64. Chakrabarti BK, Walker LM, Guenaga JF, Ghobbeh A, Poignard P, Burton DR, et al. Direct antibody access to the HIV-1 membrane-proximal external region positively correlates with neutralization sensitivity. Journal of virology. 2011;85(16):8217-26.
65. Irimia A, Sarkar A, Stanfield RL, Wilson IA. Crystallographic Identification of Lipid as an Integral Component of the Epitope of HIV Broadly Neutralizing Antibody 4E10. Immunity. 2016;44(1):21-31.
66. Robinson JE, Franco K, Elliott DH, Maher MJ, Reyna A, Montefiori DC, et al. Quaternary epitope specificities of anti-HIV-1 neutralizing antibodies generated in rhesus macaques infected by the simian/human immunodeficiency virus SHIVSF162P4. Journal of virology. 2010;84(7):3443-53.
67. Liao HX, Levesque MC, Nagel A, Dixon A, Zhang R, Walter E, et al. High-throughput isolation of immunoglobulin genes from single human B cells and expression as monoclonal antibodies. J Virol Methods. 2009;158(1-2):171-9.
68. Smith K, Garman L, Wrammert J, Zheng NY, Capra JD, Ahmed R, et al. Rapid generation of fully human monoclonal antibodies specific to a vaccinating antigen. Nat Protoc. 2009;4(3):372-84.
69. Benoit RM, Wilhelm RN, Scherer-Becker D, Ostermeier C. An improved method for fast, robust, and seamless integration of DNA fragments into multiple plasmids. Protein Expr Purif. 2006;45(1):66-71.
70. Guan Y, Sajadi MM, Kamin-Lewis R, Fouts TR, Dimitrov A, Zhang Z, et al. Discordant memory B cell and circulating anti-Env antibody responses in HIV-1 infection. Proceedings of the National Academy of Sciences of the United States of America. 2009;106(10):3952-7.
71. Salazar-Gonzalez JF, Bailes E, Pham KT, Salazar MG, Guffey MB, Keele BF, et al. Deciphering human immunodeficiency virus type 1 transmission and early envelope diversification by single-genome amplification and sequencing. Journal of virology. 2008;82(8):3952-70.
72. Montefiori DC. Evaluating neutralizing antibodies againts HIV, SIV and SHIV in luciferase reporter gene assays. In: Coligan JE, Kruisbeek AM, Margulies DH, Shevach EM, Strober W, Coico R, editors. Current Protocols in Immunology: John Wiley * Sons; 2004.
73. Pettersen EF, Goddard TD, Huang CC, Couch GS, Greenblatt DM, Meng EC, et al. UCSF Chimera--a visualization system for exploratory research and analysis. J Comput Chem. 2004;25(13):1605-12.
74. Suloway C, Pulokas J, Fellmann D, Cheng A, Guerra F, Quispe J, et al. Automated molecular microscopy: the new Leginon system. J Struct Biol. 2005;151(1):41-60.
75. Lander GC, Stagg SM, Voss NR, Cheng A, Fellmann D, Pulokas J, et al. Appion: an integrated, database-driven pipeline to facilitate EM image processing. J Struct Biol. 2009;166(1):95-102.
76. Tang G, Peng L, Baldwin PR, Mann DS, Jiang W, Rees I, et al. EMAN2: an extensible image processing suite for electron microscopy. J Struct Biol. 2007;157(1):38-46.
77. Penczek PA, Grassucci RA, Frank J. The ribosome at improved resolution: new techniques for merging and orientation refinement in 3D cryo-electron microscopy

of biological particles. Ultramicroscopy. 1994;53(3):251-70.
78. Pancera M, Wyatt R. Selective recognition of oligomeric HIV-1 primary isolate envelope glycoproteins by potently neutralizing ligands requires efficient precursor cleavage. Virology. 2005;332(1):145-56.
79. Lefranc MP, Giudicelli V, Ginestoux C, Jabado-Michaloud J, Folch G, Bellahcene F, et al. IMGT, the international ImMunoGeneTics information system. Nucleic acids research. 2009;37(Database issue):D1006-12.

A

CAP248-2B Heavy Chain

IGHV	IGHD	IGHJ	CDR3 Length (amino acid)	Mutation Frequency (nucleotide)
4-31*05	6-13*01	3*01/02	15	13.54%

CAP248-2B Light Chain

IGLV	IGLJ	CDR3 Length (amino acid)	Mutation Frequency (nucleotide)
2-14*01	1*01	19	9.72%

Germline alleles determined from IMGT

B

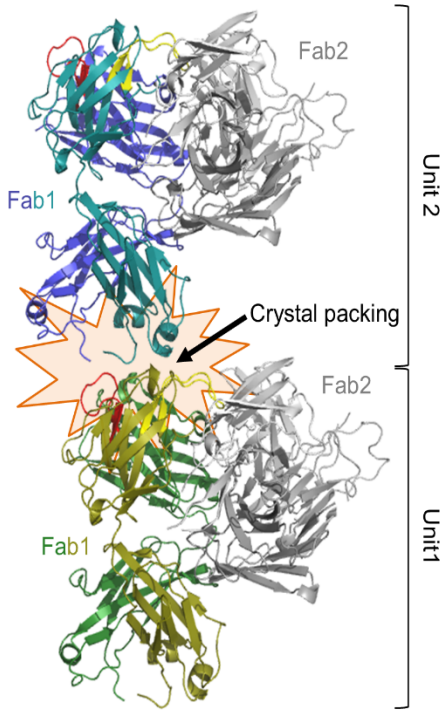

C

Table 1: **Data collection and refinement statistics (molecular replacement)**

	CAP248-2B $F_{ab}1$	CAP248-2B $F_{ab}2$
Data collection		
Space group	P1	P212121
Cell dimensions□□		
a, *b*, *c* (Å)	42.0, 68.3, 85.7	73, 85.9, 126.3
α, β, γ (°)	95.6, 99.8, 102.5	90, 90, 90
Resolution (Å)	50–2.78 (3.15-3.08, 3.08-3.02, 3.02-2.96, 2.96-2.90, 2.90-2.85, 2.85-2.78)[a]	50-1.95 (1.98-1.95)
R_{merge}	10.8 (30.5, 30, 32.5, 32.8, 34.1, 40)	10.6 (67.9)
$I / \sigma I$	6.75 (2.04, 1.95, 1.87, 1.98, 1.57, 1.44)	17.25 (2.1)
Completeness (%)	88.9 (83.1, 80.1, 72, 67.4, 61.9, 57.9)	99.9 (99.9)
Redundancy	1.9 (1.8, 1.7, 1.7, 1.7, 1.7, 1.6)	7.2 (5.7)
Refinement		
Resolution (Å)	41.8224-2.78424 (3.14-3, 3-2.88, 2.88-2.78)	41.7482-1.9593 (2.01-1.96)
No. reflections		
R_{work} / R_{free}	0.228 / 0.279	0.204 / 0.239
No. atoms	13,329	13,575
Protein	13,306	13,248
Ligand	0	5
Water	23	322
B factors (noH)	59.83	49
Protein	59.85	49
Ligand	0	
Water	54.29	39
Average B-factor (Å^2), all atoms	65.0	53
Wilson B-factor (Å^2), all atoms	45.6	27.1
Bond lengths (Å)	0.004	0.004
Bond angles (°)	0.812	0.869
Ramachandran Favoured %	93.1	95.6
Ramachandran Outliers %	0.0%	0.4
Rotamer Outliers	0.0%	0.1
Molprobity All-atoms Clashscore	1.35	1.1
Molprobity Score	1.31	1.1
PDB ID	**5F89**	

[a]Values in parentheses are for highest-resolution shell.

Supplementary Figure 1: Conformational differences between unliganded structures of CAP248-2B explained by crystal packing

(A) Predicted germline alleles, CDR3 lengths, and mutation frequencies for CAP248-2B from the IMGT database (79). (B) Cartoon representation of neighboring asymmetric units from the 2 Å resolution dataset showing crystal packing in the antibody paratope. The heavy and light chains of Fab1 in the first unit are colored forest and olive green respectively, and in the second unit dark and light blue. The CDR-H3 (red), and CDR-L3 (yellow) are indicated. (C) Data collection and refinement statistics for the two unliganded CAP248-2B Fab crystal structures.

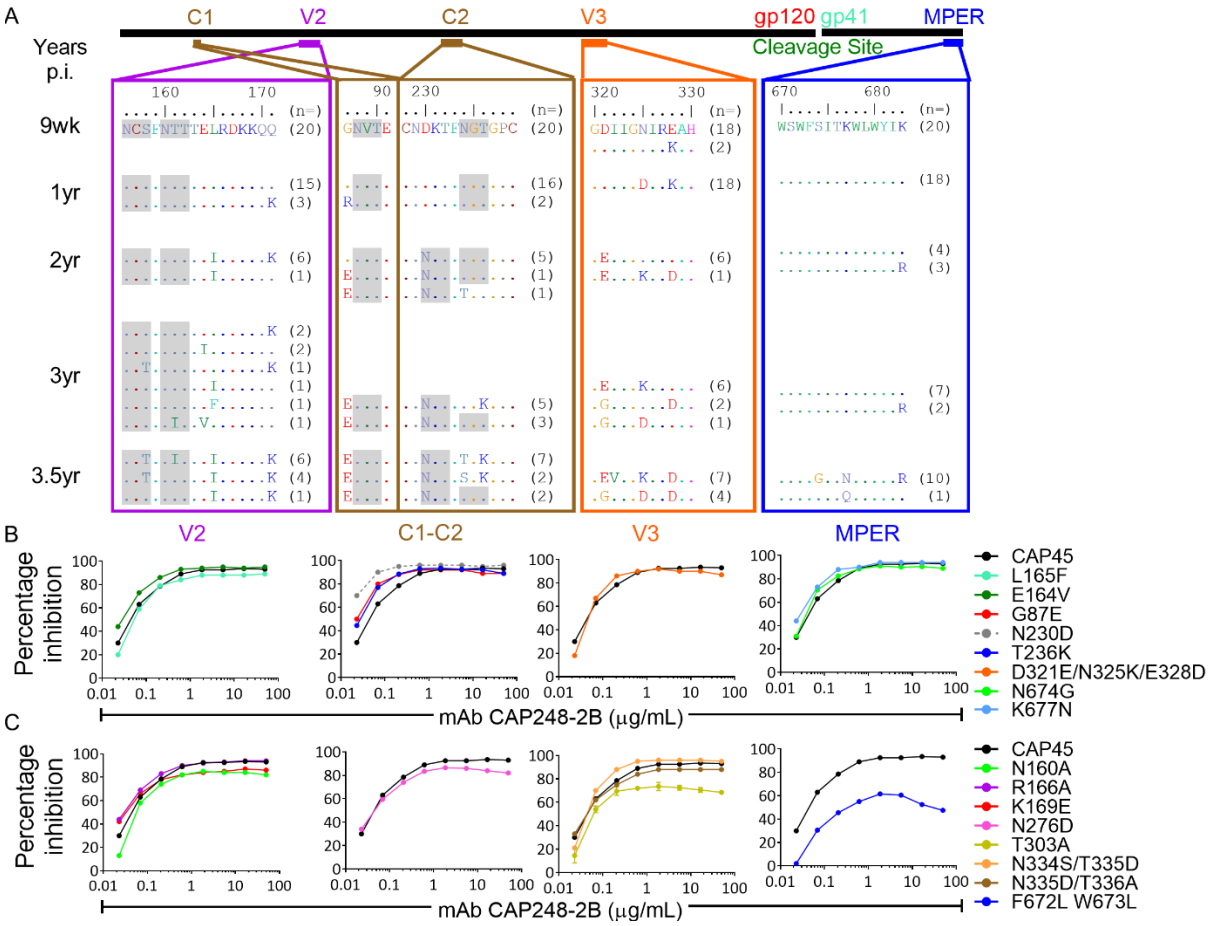

Supplementary Figure 2: Selection pressure in conserved bNAb epitopes does not contribute to escape from CAP248-2B

(A) Alignments of five different regions in CAP248 autologous envelope sequences at nine weeks (study enrolment), 1, 2, 3 and 3.5 years post-infection, that overlap with previously described broadly neutralizing antibody epitopes in V2 (boxed in purple), C1/C2 (boxed in brown), V3 (boxed in orange), and the MPER (boxed in blue). N-linked glycosylation sequons are shaded grey. (B) CAP248-2B neutralization of the heterologous strain CAP45, compared to mutants containing potential autologous escape mutations identified from CAP248 sequences. CAP45 already had the N230 glycan, so the N230D reverse mutation was tested (grey dashed line). Percent inhibition (y-axis) is plotted against CAP248-2B concentration (x-axis). (C) CAP248-2B neutralization of CAP45 and mutants with known resistance mutations to common bNAbs (not identified in CAP248 sequences), plotted as in B.

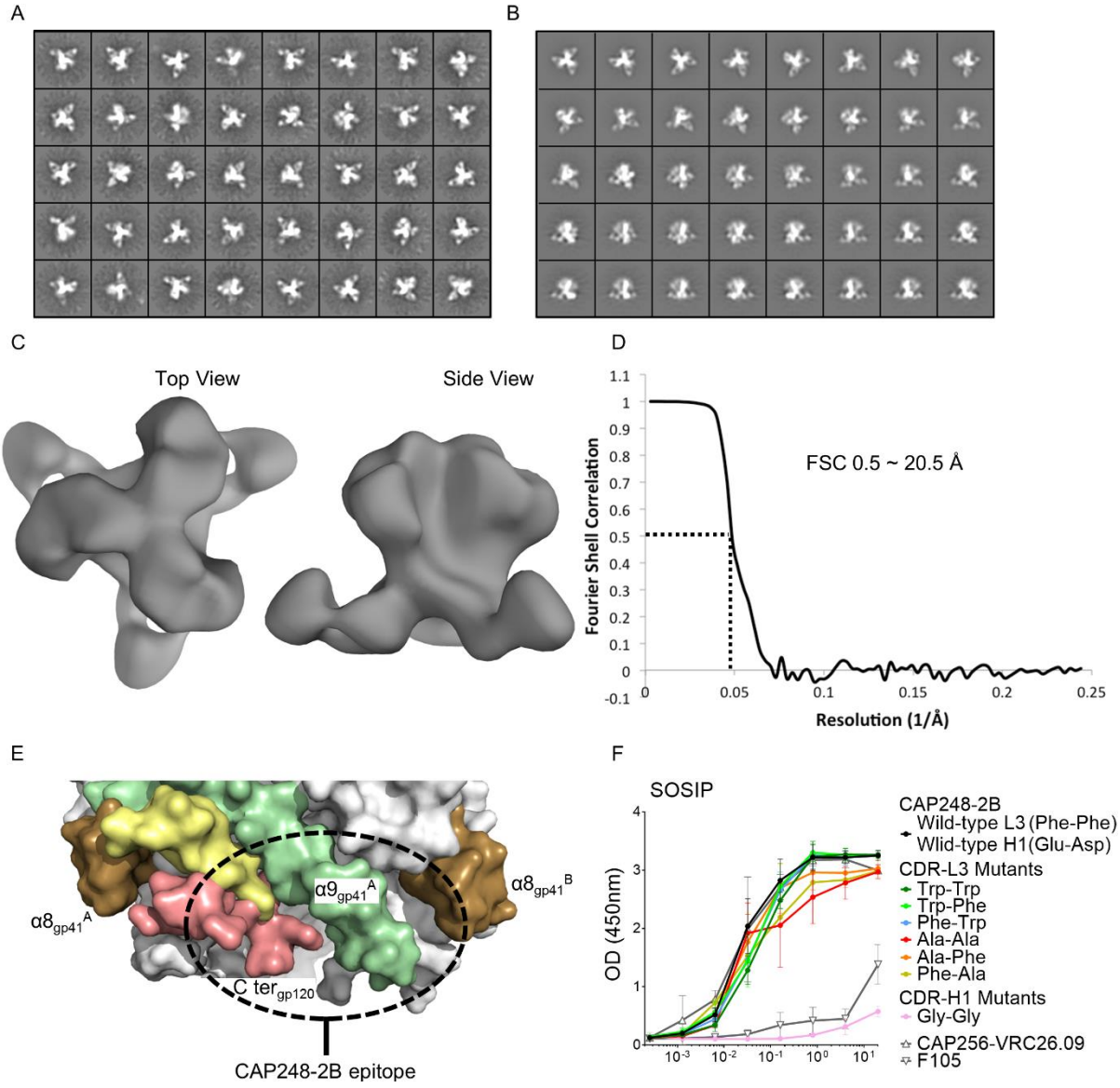

Supplementary Figure 3: Negative stain EM data, and approximation of the CAP248-2B epitope.
(A) Reference-free 2D class averages (B) 2D back-projections of the final model (C) 3D reconstructions (top and side views) (D) Fourier Shell Correlation (FSC) curves with estimated resolution using an FSC cut-off of 0.5. Samples were stained with NanoW. (E) Elements of gp120 and gp41 within 5 Å of CAP248-2B, based on EM docking. Different gp41 protomers are labelled as A and B superscript (F) ELISA binding of CAP248-2B and related CDR-L3/H1 mutants to chimeric BG505gp120-CAP45gp41 SOSIP trimer. Positive and negative controls CAP256-VRC26.09 and F105 are shown. The wild-type amino acids are indicated in the legend for both CDR-L3 and CDR-H1.

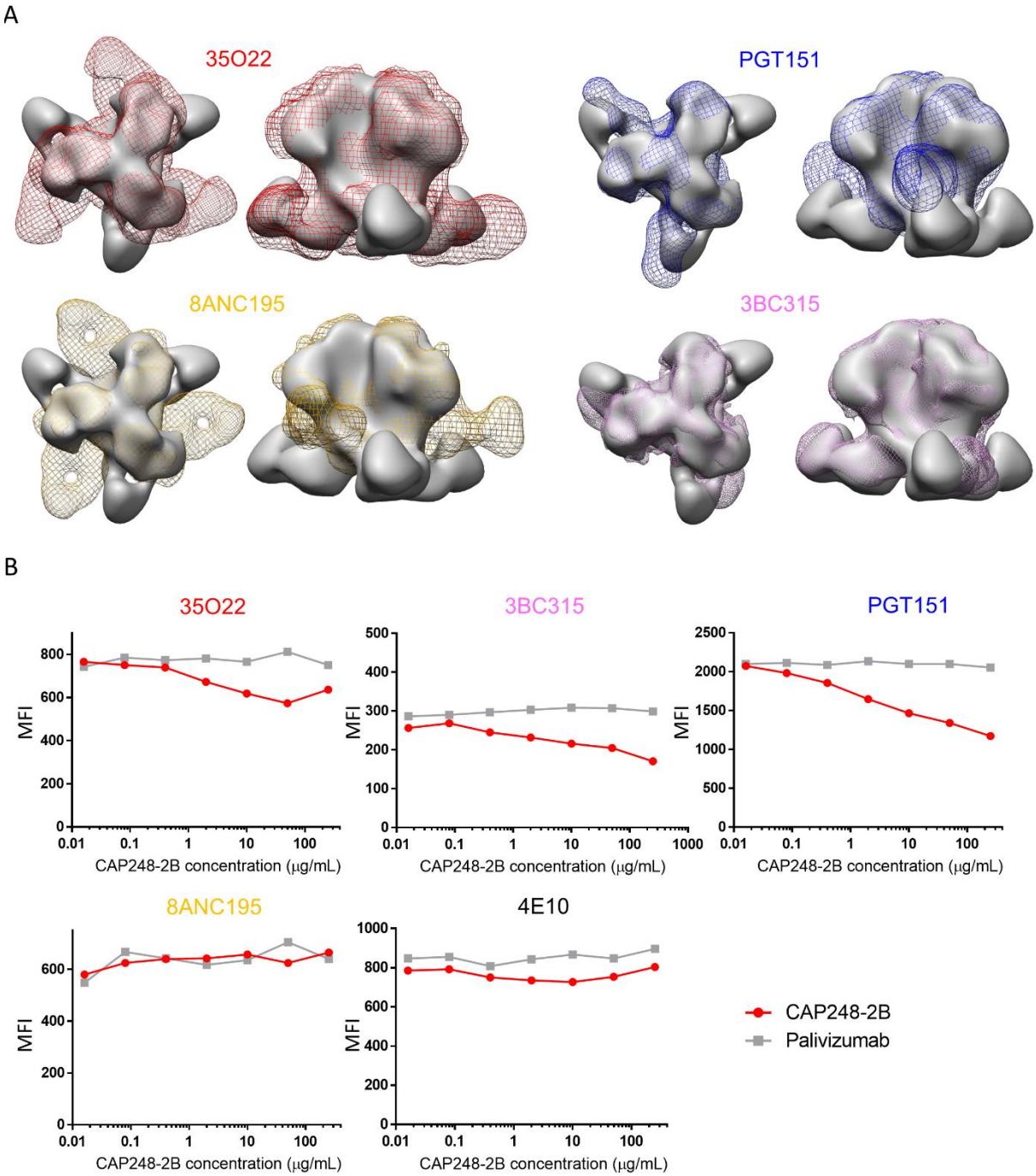

Supplementary Figure 4: CAP248-2B blocks the binding of 35O22, 3BC315, and PGT151 to cell surface envelope trimers

(A) Comparisons of gp120-gp41 interface bNAbs bound to SOSIP trimers by EM. The CAP248-2B bound trimers are shown in solid grey surface, while 35O22, PGT151, 8ANC195, and 3BC315 bound trimers are shown with mesh representation colored as in Figure 5. Both top views and side views are shown. (B) Binding of labelled HIV-1 bNAbs 35O22, 3BC315, PGT151, 8ANC195, and 4E10 to cell-surface anchored HIV-1 trimers by flow cytometry, in the presence of increasing concentration of unlabeled CAP248-2B. Median fluorescence intensity (MFI) is shown on the y-axis, and increasing concentrations of CAP248-2B or palivizumab are plotted on the x-axis. Decreasing MFI signals correspond to increasing competition by CAP248-2B.

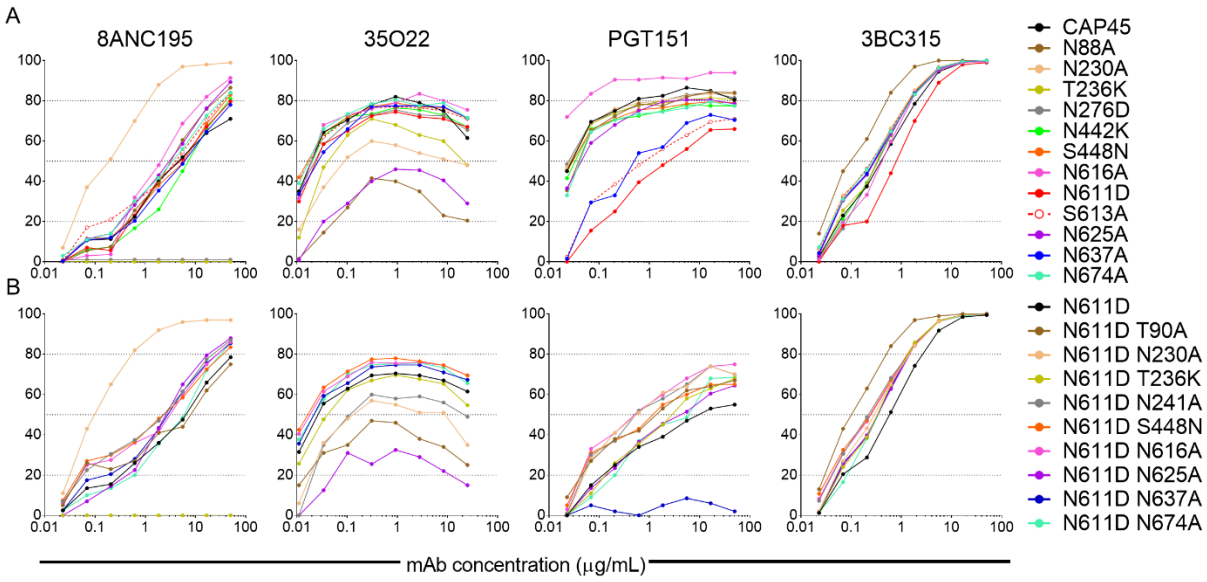

Supplementary Figure 5: Glycan dependence of known gp120-gp41 interface targeting bNAbs.
(A) Neutralization of CAP45 by broadly neutralizing antibodies that target the gp120-gp41 interface, when compared to CAP248-2B epitope proximal glycan mutants. The S613A mutant that removed the glycan at N611 but maintains the amino acid side chain properties is shown with red dashed lines and open circles. Percentage inhibition is plotted on the y-axis versus CAP248-2B antibody concentration on the x-axis. (B) Neutralization of the CAP45 N611D single mutant, and various N611D including double glycan mutants, plotted as in A.

CHAPTER FOUR: VIRAL ESCAPE FROM HIV-1 NEUTRALIZING ANTIBODIES DRIVES INCREASED PLASMA NEUTRALIZATION BREADTH THROUGH SEQUENTIAL RECOGNITION OF MULTIPLE EPITOPES AND IMMUNOTYPES

Published in PLOS Pathogens: 31 October 2013 9(10), e1003738.

OPEN ACCESS Freely available online PLOS | PATHOGENS

Viral Escape from HIV-1 Neutralizing Antibodies Drives Increased Plasma Neutralization Breadth through Sequential Recognition of Multiple Epitopes and Immunotypes

Constantinos Kurt Wibmer[1,2], Jinal N. Bhiman[1,2], Elin S. Gray[1¤], Nancy Tumba[1], Salim S. Abdool Karim[3], Carolyn Williamson[4], Lynn Morris[1,2], Penny L. Moore[1,2*]

Abstract

Identifying the targets of broadly neutralizing antibodies to HIV-1 and understanding how these antibodies develop remain important goals in the quest to rationally develop an HIV-1 vaccine. We previously identified a participant in the CAPRISA Acute Infection Cohort (CAP257) whose plasma neutralized 84% of heterologous viruses. In this study we showed that breadth in CAP257 was largely due to the sequential, transient appearance of three distinct broadly neutralizing antibody specificities spanning the first 4.5 years of infection. The first specificity targeted an epitope in the V2 region of gp120 that was also recognized by strain-specific antibodies 7 weeks earlier. Specificity for the autologous virus was determined largely by a rare N167 antigenic variant of V2, with viral escape to the more common D167 immunotype coinciding with the development of the first wave of broadly neutralizing antibodies. Escape from these broadly neutralizing V2 antibodies through deletion of the glycan at N160 was associated with exposure of an epitope in the CD4 binding site that became the target for a second wave of broadly neutralizing antibodies. Neutralization by these CD4 binding site antibodies was almost entirely dependent on the glycan at position N276. Early viral escape mutations in the CD4 binding site drove an increase in wave two neutralization breadth, as this second wave of heterologous neutralization matured to recognize multiple immunotypes within this site. The third wave targeted a quaternary epitope that did not overlap any of the four known sites of vulnerability on the HIV-1 envelope and remains undefined. Altogether this study showed that the human immune system is capable of generating multiple broadly neutralizing antibodies in response to a constantly evolving viral population that exposes new targets as a consequence of escape from earlier neutralizing antibodies.

1 Centre for HIV and STIs, National Institute for Communicable Diseases (NICD), of the National Health Laboratory Service (NHLS), Johannesburg, South Africa, **2** Faculty of

Health Sciences, University of the Witwatersrand, Johannesburg, South Africa, **3** Centre for the AIDS Programme of Research in South Africa (CAPRISA), University of KwaZulu-Natal, Durban, South Africa, **4** Institute of Infectious Disease and Molecular Medicine (IIDMM) and Division of Medical Virology, University of Cape Town and NHLS, Cape Town, South Africa

Citation: Wibmer CK, Bhiman JN, Gray ES, Tumba N, Abdool Karim SS, et al. (2013) Viral Escape from HIV-1 Neutralizing Antibodies Drives Increased Plasma Neutralization Breadth through Sequential Recognition of Multiple Epitopes and Immunotypes. PLoS Pathog 9(10): e1003738. doi:10.1371/journal.ppat.1003738

Editor: Alexandra Trkola, University of Zurich, Switzerland

Received June 23, 2013; Accepted September 14, 2013; Published October 31, 2013

Funding: This work was funded by CAPRISA, the NIAID Center for HIV/AIDS Vaccine Immunology (CHAVI) grant AI067854, the South African HIV/AIDS Research and Innovation Platform of the South African Department of Science and Technology and by a HIVRAD NIH grant AI088610. CAPRISA was supported by the National Institute of Allergy and Infectious Diseases (NIAID), National Institutes for Health (NIH), U.S. Department of Health and Human Services (Grant U19 AI51794).). PLM and JNB were supported by the Columbia University-Southern African Fogarty AIDS International Training and Research Program (AITRP) through the Fogarty International Center, National Institutes of Health (grant # 5 D43 TW000231). CKW received bursary funding from the National Research Foundation and the Poliomyelitis Research Foundation. JNB received a University of the Witwatersrand Post-graduate Merit Award as well as a bursary from the Poliomyelitis Research Foundation. PLM is a Wellcome Trust Intermediate Fellow in Public Health and Tropical Medicine (Grant 089933/Z/09/Z). The funders had no role in study design, data collection and analysis, decision to publish, or preparation of the manuscript.

Competing Interests: The authors have declared that no competing interests exist.

* E-mail: pennym@nicd.ac.za

¤ Current address: The Melanoma Research Foundation, Edith Cowan University, Perth, Australia.

Introduction

Neutralizing antibodies are the principal correlate of protection for most preventative vaccines. Designing suitable vaccine immunogens to elicit these types of antibodies has been relatively simple for conserved pathogens such as smallpox and other DNA viruses. For more diverse pathogens like HIV-1, the neutralizing antibodies elicited by vaccination or during natural infection are largely strain-specific and therefore would not be protective against globally circulating viral variants [1–5]. The HIV-1 envelope glycoprotein spikes mediate viral entry and are the sole targets for neutralizing antibodies. The spikes are trimeric, made up of three non-covalently associated gp41-gp120 heterodimers, each with a conserved core that mediates infection of $CD4^+$ T cells. Functionally conserved sites are protected by extensive glycosylation, and large solvent exposed hypervariable structures (the V1–V5 loops, and the a2-helix in C3) [6]. All HIV-1 infected individuals develop strain-specific neutralizing antibodies which target these sequence variable regions, but only a quarter develop broadly neutralizing antibodies [7–11], which will likely be needed for a preventative HIV-1 vaccine.

Author Summary

Four sites of vulnerability for broadly neutralizing antibodies to HIV-1 have been identified thus far. How these broadly reactive antibodies arise, and the host-pathogen interactions that drive the affinity maturation necessary for neutralization breadth are poorly understood. This study details the sequential development of three distinct broadly neutralizing antibody responses within a single HIV-1 infected individual over 4.5 years of infection. We show how escape from the first wave of antibodies targeting V2 exposed a second site that was the stimulus for a new wave of glycan dependent broadly neutralizing antibodies against the CD4 binding site. These data highlight how antibody evolution in response to viral escape mutations served to broaden the host immune response to these two epitopes. Finally, we document a third wave of neutralization that targets an undefined epitope that did not appear to overlap with the four known sites of vulnerability on the HIV-1 envelope. These data support the design of templates for sequential immunization strategies aimed at increasing neutralization breadth through the recognition of multiple epitopes and their immunotypes.

To engineer an envelope immunogen that can specifically elicit these antibodies, the HIV-1 vaccine research field has adopted a strategy based largely on rational design: identifying the targets for these broadly cross-reactive antibodies, and elucidating the pathways that promoted their development.

Plasma mapping strategies and the isolation of monoclonal antibodies have defined four major targets for broadly neutralizing antibodies on the HIV-1 glycoprotein [7–10,12–20]. The CD4 binding site (CD4bs) of gp120 and the membrane proximal external region (MPER) of gp41 are glycan independent epitopes, while the V1/V2 sub-domain and the co-receptor/V3 site on gp120 are sites of vulnerability for glycan binding antibodies (predominantly at positions N156/N160 and N301/N332 respectively) [14–16]. Both CD4bs antibodies and co-receptor/V3 antibodies bind well to monomeric gp120, while MPER antibodies bind to a linear peptide in gp41. This makes it possible to adsorb out their neutralization activity from plasma with various recombinant proteins. In contrast the epitope for V2 antibodies (such as PG9/16) consists of two anti-parallel b-sheets (B- and C- strands) of a Greek key motif, and the glycans therein, that is preferentially formed on the native trimer. This region is critically important for the gp120-gp120 interactions that stabilize the envelope glycoprotein spike in its unliganded conformation, and therefore cannot be readily adsorbed [16,21]. Various sub-epitopes within each of these four major sites of vulnerability have also been identified through subtle differences in the mechanism of neutralization [22]. For instance antibodies targeting the CD4bs can be sub-divided into two groups: those that are sensitive to the D368A and/or E370A mutations in the CD4 binding loop a3 (such as VRC01); and those that are dependent on amino acids D474, M475, and/or R476 in a5 termed CD4bs/DMR (such as HJ16) [23–26]. Despite this detailed knowledge, epitope mapping strategies have failed to identify the neutralization targets in a subset of plasma samples [7– 9,17,19,27,28]. The antibodies mediating breadth in these samples could target sub-epitopes within one of the four sites of vulnerability or they may target entirely novel epitopes.

In the CAPRISA 002 Acute Infection Cohort, we previously identified seven individuals with broadly neutralizing antibodies. In five cases we were able to map the plasma antibody specificities to known epitopes (two targeted N332, two the V2 epitope, and one the MPER) [7]. In this study we have focused on one of the individuals (CAP257) for which the target

was undefined. Heterologous and autologous neutralization data as well as viral sequences from longitudinal samples were used to identify the epitopes for CAP257 broadly neutralizing antibodies. We showed that heterologous neutralization in CAP257 was conferred by three distinct, sequentially occurring antibody waves, two of which were mapped to epitopes in V2 and the CD4bs respectively. While individuals with more than one broadly neutralizing antibody specificity have been previously identified [29–31], there is little information on how the dynamic relationship between host and pathogen contributed to the development of antibodies targeting multiple epitopes. We have shown previously that escape from strain-specific neutralizing antibodies can drive the formation of epitopes for broadly neutralizing antibodies [32]. Here we found that viral escape from broadly neutralizing antibodies targeting V2 promoted the development of a second broadly neutralizing antibody response targeting a glycan dependent epitope in the CD4bs. We also identified early escape mutations from both the V2 and CD4bs antibodies that drove an increase in the neutralization breadth of CAP257 plasma. These findings have implications for the design of HIV-1 vaccine antigens and sequential immunization strategies.

Results

The broadly neutralizing activity of CAP257 develops in three distinct waves

We have previously described the development of neutralization breadth in CAP257 using longitudinal plasma samples from HIV1 seroconversion to three years post-infection (p.i.) [7]. Here, we extended this analysis until the start of anti-retroviral therapy at four and a half years p.i. (Figure 1A). Longitudinal plasma was tested against the autologous CAP257 virus amplified from the earliest available time point (7 weeks p.i.), the subtype C consensus sequence (ConC) [33], 4 Tier 1b viruses, and 39 Tier 2 viruses [34]. Autologous neutralizing antibodies appeared by 14 weeks of infection with a peak titer at two years of 1:6,754. This was followed by the neutralization of heterologous viruses 30 weeks after infection. CAP257 neutralized 84% of the heterologous viruses at three years (174 weeks) with neutralization breadth of 100% against subtype A (6/6 viruses), 96% against subtype C (25/26 viruses, including ConC), and 50% against subtype B (6/12 viruses). The titers of these broadly neutralizing antibodies peaked and waned in three separate waves.

The first wave of neutralization breadth

(typified by CAP63) peaked at 67 weeks p.i. with a maximum titer of 1:1,493 and exclusively neutralized subtype C viruses (Figures 1A and 1B – red curves). Wave 1 titers dropped to as low as 1:145 by 149 weeks of infection. As this early heterologous neutralization began to wane, CAP257 plasma gained the capacity to neutralize additional subtype C viruses as well as several subtype A and B viruses (Figures 1A and 1B – blue and green curves). This second wave (typified by Q842) peaked at 122 weeks p.i. with titers as high as 1:8,565 against RHPA that dropped to 1:1,254 by 213 weeks of infection. Finally, a third wave of heterologous neutralization (represented by Du156) appeared by 149 weeks p.i. and peaked at 213 weeks p.i. (Figure 1B – brown curve). This third wave was also largely subtype C specific. These data suggested that the neutralization breadth of CAP257 plasma was mediated by at least three distinct antibody specificities.

To identify the targets of each of the three broadly neutralizing antibody specificities in CAP257 plasma we first assessed whether they targeted epitopes in monomeric gp120 (such as the CD4bs or N301/N332 glycans). We adsorbed out the gp120 binding antibodies in plasma samples from the peak neutralizing activity of each wave using recombinant ConC gp120 coupled to tosyl-activated magnetic beads (Figure 1C). The adsorbed plasma was compared with untreated plasma for activity against a heterologous virus neutralized by each wave. Neutralization by wave 1 (67 weeks p.i.) and wave 3 (213 weeks p.i.) was not affected by adsorption with monomeric gp120 (Figure 1C – red and brown curves), however neutralization by wave 2 antibodies (122 weeks p.i.) could be partially adsorbed with the ConC gp120 protein (Figure 1C – blue curve). The neutralizing activity of wave 2 could also be equally adsorbed with a core gp120 lacking the hypervariable loops V1/V2 and V3 (Figure 1C – green curve). These data supported our hypothesis that CAP257 heterologous neutralization was mediated by more than one neutralizing antibody specificity, two of which were largely subtype C specific and targeted an epitope not present on monomeric gp120, and a third whose epitope in gp120 was more conserved across clades and did not require the hypervariable loops V1/V2 or V3.

Wave 1 broadly neutralizing antibodies target V2

The inability of gp120 to adsorb out wave 1 neutralization suggested these antibodies might recognize the trimer specific epitope in V1/V2 defined by

PG9/16 [16]. Therefore, we performed mapping studies using ConC, which was neutralized by all three waves of neutralizing antibodies (Figure 2A – red curve). Seven mutations in the V2 region (F159A, N160A, R166A, K168A, K169E, K171A, and I181A) each abrogated wave 1 neutralization, but did not significantly affect the titers of waves 2 or 3 (Figure 2A – purple curves). In contrast, a D167N mutation resulted in enhanced neutralization by wave 1 antibodies, but did not significantly affect the titers of waves 2 or 3 (Figure 2A – orange curve).

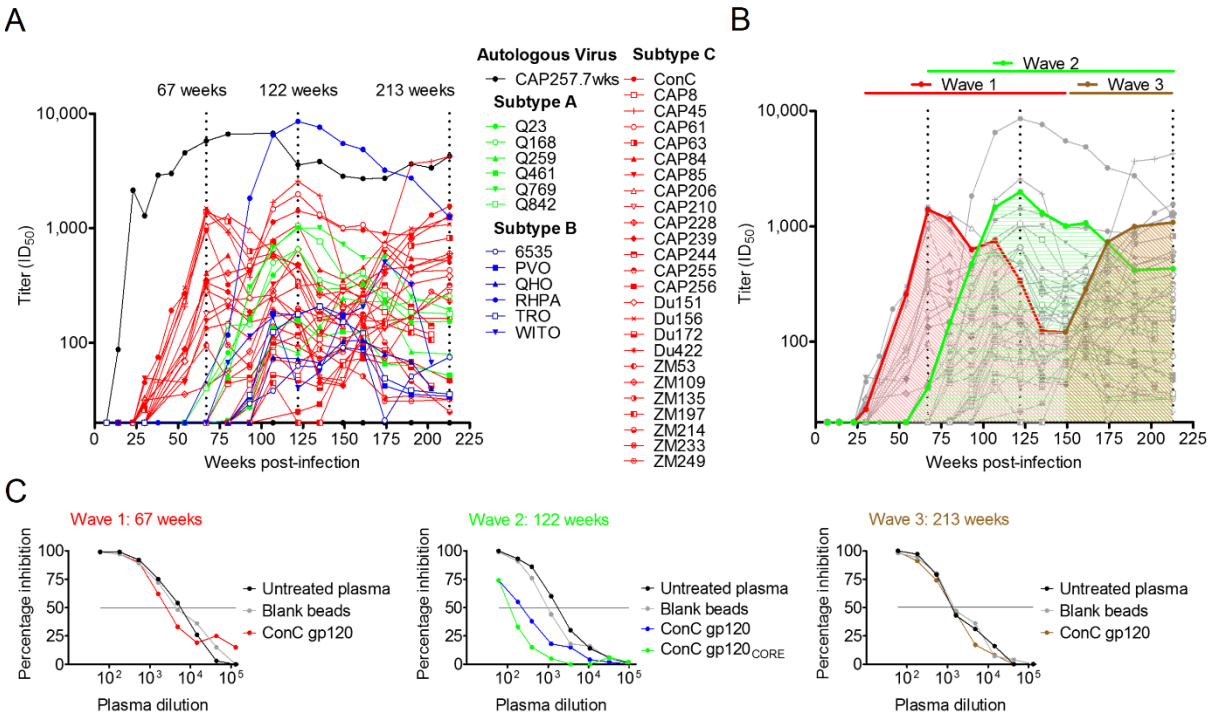

Figure 1. CAP257 broadly neutralizing antibodies develop sequentially in three distinct waves.

A) Longitudinal neutralization of the autologous CAP257 virus (black) and 37 heterologous viruses neutralized by CAP257 plasma at titers .1:100. The ID_{50} titers (y-axis) are shown versus weeks p.i. (x-axis). Three peaks in heterologous neutralization titers at 67, 122, and 213 weeks p.i. are indicated with dotted lines. Heterologous viruses are colored according to subtype (A = green, B = blue, C = red). **B)** A summary of the three waves of heterologous neutralization defined by a representative virus, superimposed over the neutralization kinetics shown in Figure 1A. Wave 1 was subtype C specific and is colored red. Wave 2 neutralized viruses from all three clades and is colored green. Wave 3 is colored brown. **C)** Adsorption of heterologous neutralization at the peak of each of the three waves. Percentage inhibition (y-axis) is shown versus plasma dilution (x-axis). Untreated plasma is shown in black, blank beads in grey and beads coated with recombinant proteins are shown in red (wave 1), blue/green (wave 2) or brown (wave 3).

A second mutation (L165A) also resulted in significant neutralization enhancement at all the time points tested, including those preceding breadth (Figure 2A – grey curve), suggesting that this mutation resulted in general neutralization sensitivity. Overall, these data indicated that wave 1 antibodies (but not waves 2 or 3) targeted residues in the V2 region. To define whether the V2 epitope recognized by CAP257 plasma antibodies overlapped with that of known broadly neutralizing antibodies to this site, we tested the sensitivity of PG9/16, CH01-04, and PGT145 to the same ConC V2 mutations described above and compared them to CAP257 neutralizing antibodies at the peak of wave 1 activity, 67 weeks p.i. (Figure 2B). Of the seven mutations that abrogated CAP257 neutralization only two (N160A and K169E) resulted in complete resistance to all the antibodies tested, consistent with previous data [35,36]. Neither the monoclonal antibodies nor CAP257 wave 1 antibodies were sensitive to deletion of the N156 glycan (through the S158A mutation) in ConC. Lastly, mutations at two hydrophobic amino acids in V2 (F159A and I181A) that do not form part of the PG9 epitope as defined by the crystal structure [37], had a significant effect on the neutralization of monoclonal antibodies targeting V2, and CAP257 wave 1 antibodies.

Immunotype switching within V2 precedes the development of wave 1 antibodies

To define escape from wave 1 neutralizing antibodies, we examined sequences from the V2 region of CAP257 over time. Using single genome amplification (SGA) we obtained 125 full envelope sequences from twelve time points between 7 and 213 weeks p.i., and focused on the N160 glycan and the cationic C-strand in V2 that are the targets of wave 1 antibodies (Figure 3A). Interestingly, the earliest virus (7 weeks p.i.) had an asparagine at position 167. This N167 residue is rare, occurring in only 5.6% (196 of 3,478) of sequences in the Los Alamos National Laboratory (LANL) HIV sequence database. By the time of the earliest detectable heterologous neutralization (30 weeks p.i., maximum titer of 1:49) mutations in sites forming part of the wave 1 V2 epitope were already apparent in 6/14 autologous sequences at positions R166, K169, and Q170 (Figure 3A). Of the remaining eight sequences, six exhibited other mutations either in the N160 glycosylation sequon or the V1/V2 C-strand. This rapid selection pressure in the C-strand of V1/V2 was sometimes an N167D mutation (4/14 autologous sequences) that was unlikely to be

A

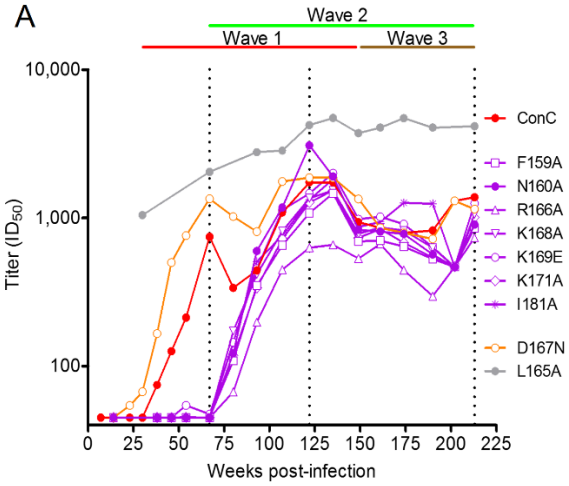

B

ConC V2 mutants	CAP257 plasma	PGT145	CH01	CH02	CH03	CH04	PG9	PG16
	ID 50 fold change	*IC 50 fold change*						
S158A	1	3	1	2	1	1	1	1
F159A	>20	>200	>100	>100	>100	>100	11	266
N160A	>20	>200	>100	>100	>100	>100	>1000	>1000
L165A	0.5	139	1	2	2	1	2	2
R166A	>20	>200	1	16	1	5	0	1
D167N	0.7	1	1	1	1	1	1	1
K168A	>20	156	13	22	20	15	0	0
K169E	>20	>200	>100	>100	>100	>100	>1000	>1000
K171A	>20	>200	>100	>100	>100	>100	6	24
I181A	>20	>200	>100	>100	>100	>100	13	17

Figure 2. The first wave of broadly neutralizing antibodies targets residues in the V2 region.

A) Longitudinal neutralization of ConC V2 mutants. ConC wild-type (wt) is shown in red. V2 mutants F159A, N160A, R166A, K168A, K169E, K171A, and I181A that abrogated wave 1 neutralization are shown in purple. The D167N mutation that enhanced wave 1 neutralization is shown in orange, while the L165A mutation that resulted in universal neutralization sensitivity is shown in grey. The timing of wave 1 (red), wave 2 (green), and wave 3 (brown) neutralization is summarized above as horizontal lines, while the peak titers at each wave are indicated with dotted lines. ID50 titers (y-axis) are shown versus weeks p.i. (x-axis). **B)** The dependence of CAP257 wave 1 neutralizing antibodies (at 67 weeks p.i.) on V2 residues in ConC, compared to monoclonal antibodies PGT145, CH01-04, and PG9/16. Complete abrogation of neutralization is colored red, 2–10 fold reductions in IC_{50} are colored yellow, and >10 fold reductions in IC_{50} are coloured orange.

selected for by wave 1 broadly neutralizing antibodies, as all the heterologous viruses neutralized by wave 1 had a D167 residue. Since the V1/V2 region is a common target of strain-specific neutralizing responses [38–41], these data suggested the possibility of an earlier neutralizing response targeting N167 in V2 that preceded the development of broadly neutralizing antibodies. Wave 1 mapping data (Figure 2A) further supported this possibility because the reverse D167N mutation enhanced the neutralization of ConC by wave 1 antibodies only, and resulted in earlier neutralization kinetics (Figure 2A – orange curve).To test this we selected an envelope from 174 weeks p.i. (CAP257 3 yr) that was completely resistant to CAP257 neutralizing antibodies (consistent with ongoing neutralization escape), and back-mutated the V1/V2 region to match the earliest sequence from 7 weeks p.i. (Figure 3B). The neutralization sensitivity of the back-mutated virus, CAP257 3 yr($V1/V2_S$), was

then compared to the parental CAP257 3 yr virus using longitudinal plasma samples. In contrast with the resistant CAP257 3 yr virus, the back-mutated V1/V2 virus (CAP257 3 yr(V1/V2s)) became sensitive to neutralization at 23 weeks p.i. (Figure 3B – black curve). This suggested the emergence of a strain-specific V1/V2 response 7 weeks prior to the development of wave 1 broadly neutralizing antibodies at 30 weeks p.i.

To establish whether these strain-specific V1/V2 neutralizing antibodies targeted the same epitope as wave 1 broadly neutralizing antibodies, we introduced selected escape mutations (N167D, N160D/ S and K169E) into the sensitive CAP257 3 yr($V1/V2_S$) back-mutated envelope. Introduction of the N167D mutation (Figure 3B – orange curve), a common V2 change at 30 weeks p.i., shifted the timing of autologous V1/V2 neutralization to overlap with the emergence of wave 1 broad neutralization. The introduction of N160D/S mutations that deleted the N160 glycan (Figure 3B – purple curves), further shifted autologous neutralization to overlap with the emergence of wave 2 neutralizing antibodies. Finally, when the K169E mutation was introduced (Figure 3B – pink curve), autologous V1/V2 neutralization titers were completely abrogated. As the N160A and K169E mutations in ConC also completely abrogated neutralization by CAP257 wave 1 broadly neutralizing antibodies (Figure 2B) these data suggest that the strain-specific V2 neutralizing antibodies in CAP257 plasma targeted the same site of vulnerability that was later targeted by wave 1 broadly neutralizing antibodies. However the strain-specific V2 antibodies recognized the rare N167 immunotype of V2 present in the CAP257 infecting virus. Following an early N167D escape mutation at this site, V1/V2 neutralization became N167 independent, allowing recognition of the more common D167 immunotype. This switch in the fine specificity of CAP257 V2 antibodies correlated with the emergence of broadly neutralizing wave 1 antibodies.

Escape from wave 1 antibodies exposed the epitope for wave 2 neutralization

Wave 1 broadly neutralizing antibodies were completely dependent on the glycan at N160 (Figure 2A). Viral escape from wave 1 neutralizing antibodies by deletion of this glycan first occurred at 54 weeks p.i. (in 37.5% of the sequences), immediately prior to the development of wave 2 neutralizing antibodies (Figure 3A – pie charts). This escape pathway persisted at 93 weeks p.i. (in 30% of sequences), but by 122 weeks p.i., at the peak of wave 2 activity, alternative

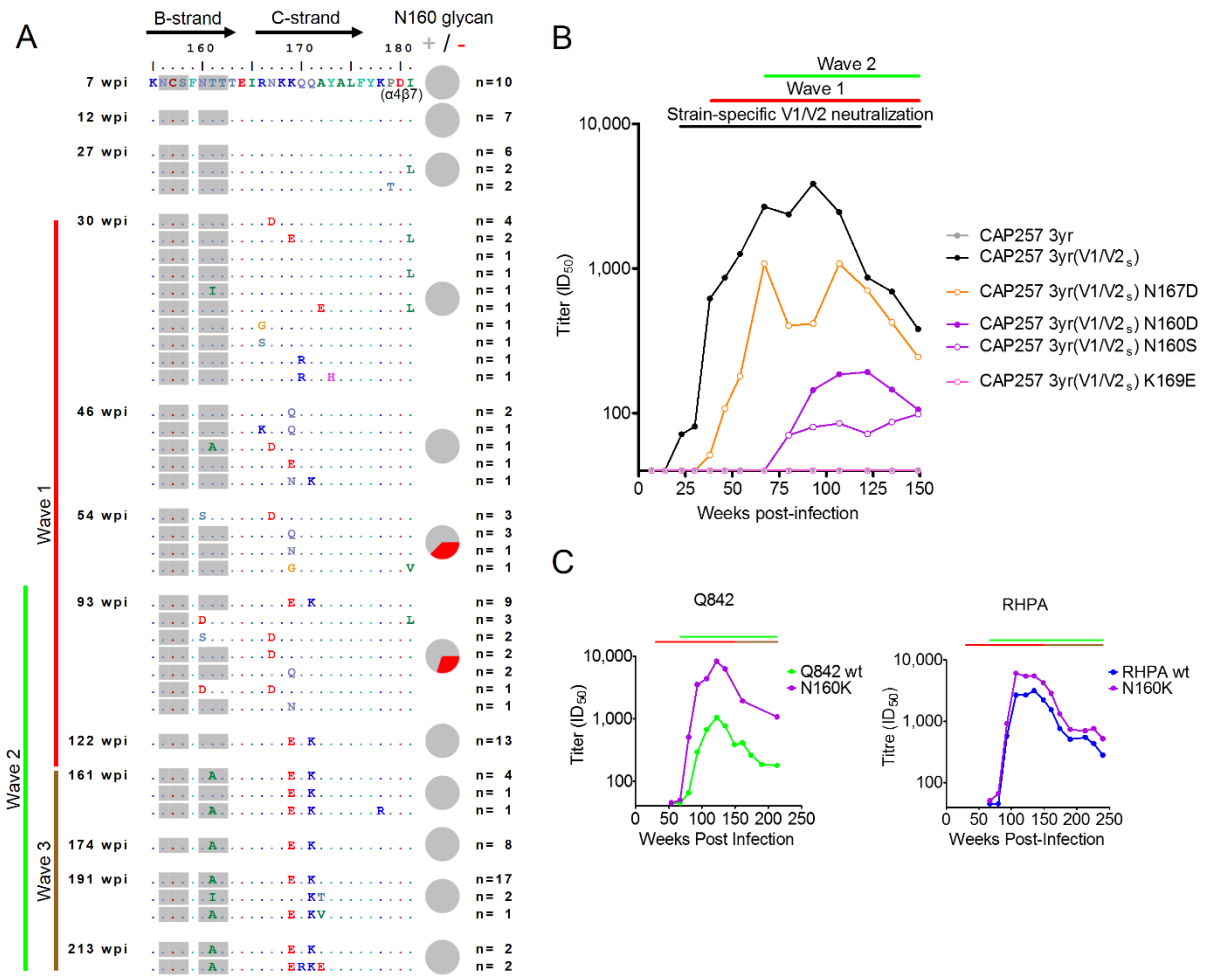

Figure 3. Escape from V2 neutralizing antibodies drives the formation/exposure of broadly neutralizing antibody epitopes in the CD4bs.

A) Amino acid sequence alignment of the CAP257 B- and C- strands in the V1/V2 sub-domain of gp120, from twelve time points. The number of envelopes per unique V2 sequence is shown on the right. The timing of wave 1 (red), wave 2 (green), and wave 3 (brown) neutralization is summarized to the left with vertical lines. Potential N-linked glycans are shaded grey, and the presence (grey slices) or absence (red slices) of the N160 glycan within the population at each time point is shown with pie charts to the right. **B)** CAP257 develops a strain-specific V2 response prior to wave 1 broadly neutralizing antibodies. Neutralization of an autologous virus amplified from 174 weeks p.i. (CAP257 3 yr), is shown in grey. The V1/V2 region of this virus was back-mutated to the earliest known sequence (CAP257 3 yr(V1/V2s)) shown in black. Longitudinal neutralization of the N167D, N160D/S, and K169E mutants is shown in orange, purple, and pink respectively. The timing of wave 1 (red), wave 2 (green), and preceding strain-specific V2 (black) neutralization is summarized above with horizontal lines. ID50 titers (y-axis) are shown versus weeks p.i. (x-axis). **C)** Wave 2 neutralization of Q842 (green) or RHPA (blue) wild-type (wt) viruses, and their N160K mutants (purple). The timing of wave 1 (red), wave 2 (green), and wave 3 (brown) neutralization is summarized above as in Figure 1B. ID50 titers (y-axis) are shown versus weeks p.i. (x-axis).

escape pathways existed, and all sequences contained the N160 glycan. The transient nature of this highly effective escape pathway suggested that deletion of the N160 glycan had a deleterious effect on the virus.

A potential mechanism for this came from the observation that deleting the N160 glycan (critical to wave 1 neutralization) in the CAP257 3 yr(V1V2s) virus conferred slight neutralization sensitivity coinciding temporally with wave 2 (Figure 3B – purple curves). These data suggested that mutations at N160 exposed the wave 2 epitope. To examine whether loss of the N160 glycan enhanced CAP257 wave 2 neutralization we selected two viruses, Q842 and RHPA, which were neutralized at high titer by wave 2 but resistant to wave 1, and deleted the N160 glycan in each. The effect of these N160K mutations was assessed longitudinally using CAP257 plasma. While the timing of RHPA N160K and Q842 N160K neutralization by CAP257 was not altered compared to the wild-type viruses, these mutant viruses were neutralized 2–8 fold more potently by wave 2 antibodies (Figure 3C – purple curves). A similar 2 fold increase in titer was shown at the peak of wave 2 activity when the N160 glycan was deleted in ConC (Figure 2A – purple closed circles). As deletion of the N160 glycan in the autologous virus occurred prior to the development of wave 2 neutralizing antibodies, these data suggest that this particular escape pathway from wave 1 neutralizing antibodies may have contributed to the development of wave 2 antibodies, possibly by better exposing the epitope. Therefore, after the development of wave 2, the K169E mutation that also allowed escape from wave 1 broadly neutralizing antibodies, but did not enhance wave 2 neutralization, was preferentially selected over deletion of the N160 glycan (Figure 3A).

Wave 2 neutralizing antibodies target the CD4bs

The V1/V2 sub-domain of gp120 plays an important role in shielding the envelope from neutralization. More specifically, several modifications in V1/V2 (particularly at N-glycosylation sites) have been implicated in either shielding or exposing the CD4bs to neutralizing antibodies [42–51]. As escape from wave 1 at N160 enhanced neutralization by wave 2, these data suggested the CD4bs as the target for wave 2 antibodies. This was supported by the adsorption data (Figure 1C), showing that wave 2 neutralizing antibodies bound the core gp120 protein. Therefore we examined envelope sequences from 191 weeks p.i. for selection pressure in the conserved CD4bs (Figure 4). Three mutations in the

D-loop (N276D/S, T278A/K and N279D) and one at the base of V5 in the b23 sheet of C4 (R456W) dominated the viral population at this time point. Both the D-loop and V5 have been previously implicated in resistance to CD4bs antibodies [52–54]. To assess whether these CD4bs mutations mediated resistance to wave 2 neutralization, we introduced the three most common mutations (T278A, N279D and R456W) simultaneously into two heterologous viruses (Q842 and RHPA) neutralized by wave 2 but not by wave 1 (Figure 1A), and tested them against plasma from the peak of wave 2 activity (122 weeks p.i.). The mutants were at least 20 fold more resistant to neutralization at this time point than the wild-type viruses, confirming the role of CD4bs mutations in escape from wave 2 antibodies (Figure 5A).

To further characterize the epitope targeted by wave 2 antibodies, we assessed the dependence of wave 2 binding on the D368 residue in a3 (critical for VRC01-like antibodies), and residues 474/475/476 in a5 (critical for HJ16-like antibodies) by adsorption studies. The D368R or D474A / M475A / R476A mutations were separately introduced into ConC gp120, and compared to the wild-type protein for their ability to adsorb out the neutralizing activity against Q842 and RHPA at peak wave 2 titers. Both mutant gp120s (Figure 5B – yellow and brown bars) adsorbed out a significant fraction of the neutralizing activity against Q842 and RHPA, equivalent to that adsorbed by wild-type gp120 (Figure 5B – white bars). These data suggested that CAP257 antibody binding was not dependent on these residues in the a3 and a5 helices. CAP257 neutralization could not be adsorbed with the RSC3 protein used to isolate VRC01, which binds weakly to the HJ16 class of CD4bs antibodies [55].

CAP257 wave 2 antibodies recognize a glycan dependent epitope in the CD4bs, also recognized by the monoclonal antibody HJ16

Of the three changes identified above as mediating escape from wave 2 antibodies, N279 and R456 make contact with CD4, while T278 forms part of an adjacent glycosylation sequon [6]. This glycosylation sequon is conserved in 96% (n=3,475) of envelope sequences in the LANL HIV sequence database. Its deletion via N276D/S or T278A/K mutations in later viruses (Figure 4) for wave 2 escape was therefore striking, and suggested a possible role for glycan recognition by CAP257 wave 2 antibodies. To examine wave 2 glycan binding, we expressed an RHPA core gp120 in GnTI(-/-) 293S cells, which allowed for deglycosylation of the protein using Endo-H, and assessed the ability of

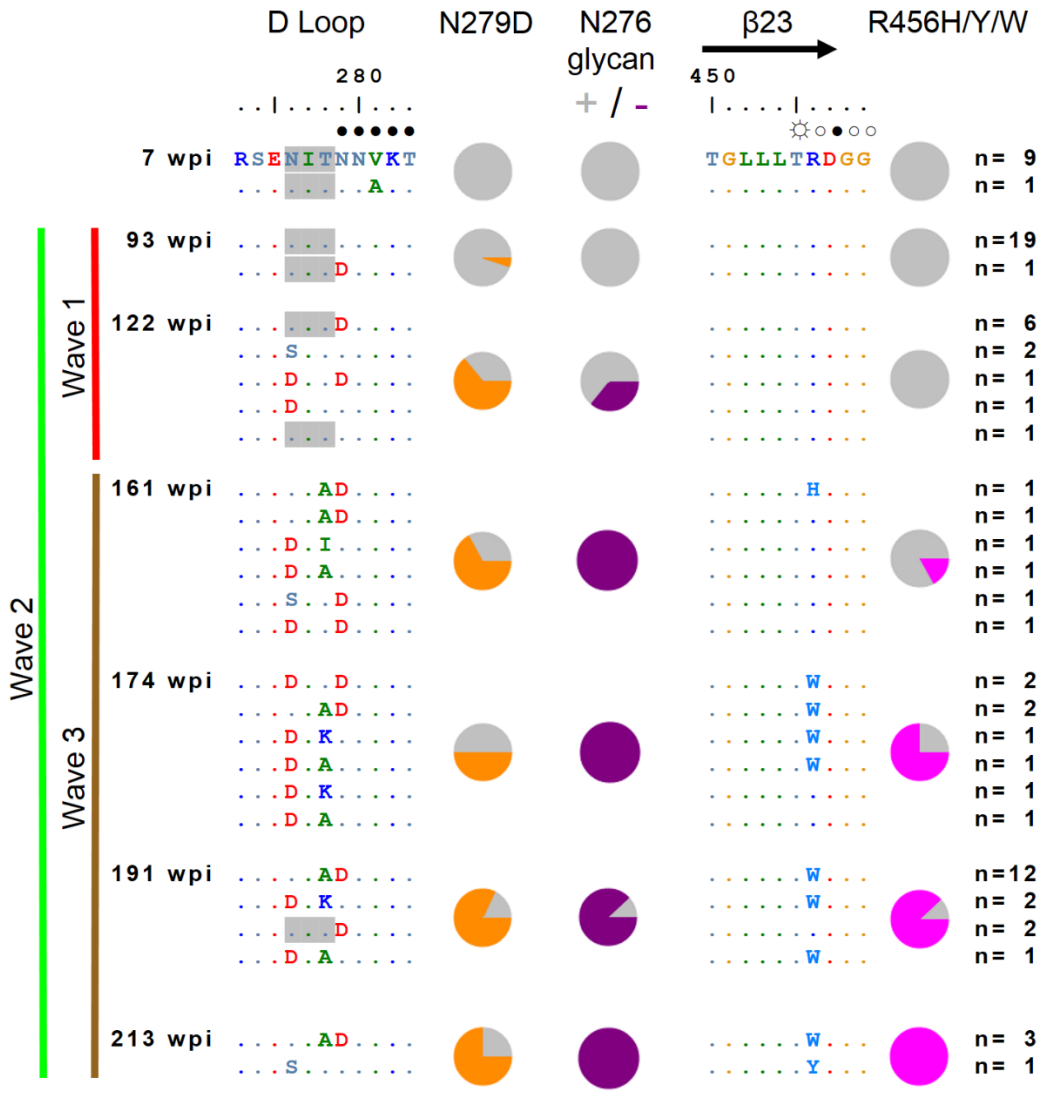

Figure 4. Accumulating escape mutations from wave 2 broadly neutralizing antibodies occur in the CD4 binding site.

Amino acid sequence alignment of the CAP257 D loop and b23 regions of gp120 from seven time points. The number of envelopes per unique sequence is shown on the right. The timing of wave 1 (red), wave 2 (green), and wave 3 (brown) neutralization is summarized to the left with vertical lines. Amino acids contacting CD4 (as described in [57]) are indicated above the sequence alignment, with ○ denoting backbone only contacts, ☼ denoting side chain contacts, and ● denoting main chain and side chain contacts. Potential N-linked glycans are shaded grey. The frequency of escape mutations at position 279 (orange slices), in the N276/T278 glycosylation sequon (purple slices), or at position 456 (pink slices) for each time point is shown with pie charts.

both glycosylated and deglycosylated proteins to adsorb out wave 2 neutralization activity. While neutralizing activity against RHPA was efficiently adsorbed with the glycosylated RHPA gp120 core (Figure 5C – white bars), the deglycosylated protein only adsorbed out a fraction of that activity (Figure 5C – purple bars) confirming the importance of glycans in wave 2 antibody binding. Similarly HJ16 was not adsorbed by the deglycosylated protein suggesting glycan dependence. In contrast, VRC01 was adsorbed equally effectively by both proteins.

To assess in more detail the role of the N276 glycan in wave 2 neutralization, we generated four mutants in RHPA, comparing the effects of two conservative mutations (N276Q, T278S) with the effects of two alanine substitutions (N276A, T278A) in the N276 glycosylation sequon (Figure 5D – boxed in purple). Both alanine mutations significantly affected wave 2 peak titers by 18- and 30-fold respectively. The N276Q mutation which deleted the glycan but retained the amino acid properties at position 276 also affected wave 2 neutralization by 21-fold (a similar effect to the N276A mutation), while the T278S mutation that retained the N276 glycan had no effect on neutralization. These data suggested that sensitivity to wave 2 neutralization was largely dependent on the glycan at position 276, rather than the N276 amino acid side chain. We also assessed the effect of the remaining two autologous mutations in the CD4bs (N279D and R456W) identified above (Figure 5D). The N279D mutation alone had a relatively small 2 fold effect on neutralization, suggesting only a minor role in escape from wave 2. When an alanine was substituted at position 279 instead, wave 2 neutralization was enhanced. The R456W mutation had a more significant 10-fold effect on CAP257 neutralization, but was still less effective than the glycan deleting mutations at positions 276/278 which were the major escape mutations.

We next compared the epitope for CAP257 wave 2 neutralizing antibodies with that of HJ16 (CD4bs/DMR) and VRC01 (CD4bs). Both monoclonal antibodies were profoundly affected by the R456W mutation (514- and 30-fold respectively). Like CAP257, HJ16 neutralization was significantly dependent on the glycan at position 276 with glycan deleting mutations (N276Q/A and T278A) resulting in a 74–106 fold increase in IC_{50} (Figure 5D). This dependence on the N276 glycan distinguished both CAP257 and HJ16 from VRC01, for which neutralization was slightly enhanced (2–3 fold) when the glycan was removed. This effect on VRC01 is consistent with

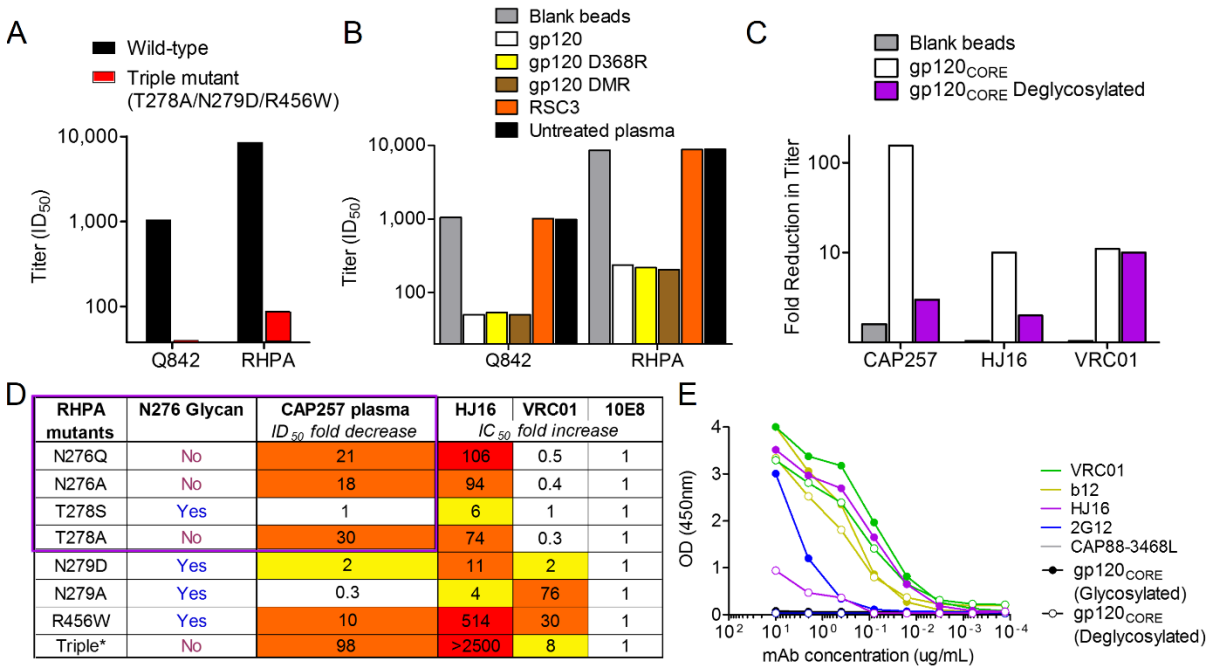

RHPA mutants	N276 Glycan	CAP257 plasma *ID50 fold decrease*	HJ16 *IC50 fold increase*	VRC01 *IC50 fold increase*	10E8 *IC50 fold increase*
N276Q	No	21	106	0.5	1
N276A	No	18	94	0.4	1
T278S	Yes	1	6	1	1
T278A	No	30	74	0.3	1
N279D	Yes	2	11	2	1
N279A	Yes	0.3	4	76	1
R456W	Yes	10	514	30	1
Triple*	No	98	>2500	8	1

Figure 5. CAP257 broadly neutralizing antibodies bind a glycan-dependent epitope in the CD4bs, also targeted by mAb HJ16.

A) Effect of escape mutations T278A, N279D, and R456W in the CD4bs on wave 2 neutralization. ID_{50} titers at 122 weeks p.i. (y-axis) are shown for Q842 and RHPA (black bars), or the corresponding triple mutants (red bars). **B)** Adsorption of peak wave 2 titers (122 weeks p.i.) with wild-type or mutant gp120 proteins. The residual neutralizing activity in the adsorbed plasma samples is shown as ID_{50} titers (y-axis) for the heterologous viruses Q842 and RHPA. Untreated plasma is shown in black, plasma adsorbed with blank beads in grey, plasma adsorbed with ConC gp120 in white, plasma adsorbed with D368R mutant gp120 in yellow, plasma adsorbed with D474A/M475A/R476A triple mutant gp120 in brown, and plasma adsorbed with RSC3 protein in orange. **C)** Effect of glycosylation on the CAP257 wave 2 epitope in RHPA. The fold reduction in titer (y-axis) of adsorbed samples from 122 weeks p.i. are shown for CAP257 wave 2, HJ16, and VRC01. Plasma adsorbed with blank beads is shown in grey, gp120 core in white, and deglycosylated gp120 core in purple. **D)** The dependence of CAP257 wave 2 neutralizing antibodies (at 122 weeks p.i.) on D-loop and b23 residues/ glycans in RHPA, compared to the monoclonal antibodies HJ16, VRC01, and 10E8. The effect of N276 glycan mutations on CAP257 plasma is boxed in purple, and the presence or absence of a glycan at N276 for each mutation is indicated. Fold effects between 2–10 are yellow, 10–100 colored orange, and .100 colored red. Triple* is the triple mutant described in A. **E)** Effect of glycosylation on the HJ16 epitope. The ELISA OD at 450 nm is shown (yaxis) versus antibody concentration (x-axis). Binding to glycosylated or deglycosylated gp120 core is shown with solid or open circles respectively. The monoclonal antibodies tested were VRC01 (green), b12 (yellow), HJ16 (purple), 2G12 (blue), and CAP88-3468L (grey).

previous studies showing that deleting the N276 glycan exposes the CD4 binding site to neutralization by VRC01 or b12 [52,56]. Introducing all three CAP257 escape mutations identified above therefore had a compensatory effect on VRC01 resistance (8-fold compared to 30-fold effect for R456W alone), but completely abrogated HJ16 neutralization, confirming the similarities between HJ16 and CAP257 plasma. Despite these overall similarities, some differences were apparent between CAP257 wave 2 antibodies and HJ16, such as the preference of HJ16 for the threonine at position 278 and the asparagine at position 279. Unlike CAP257, the N279A mutation did not enhance HJ16 neutralization but rather resulted in a 4-fold reduction in titer. These data may suggest minor contacts between HJ16 and the amino acid side chain at position 279. The N279A mutation also significantly affected VRC01 neutralization (76-fold), consistent with either asparagine or aspartic acid residues at position 279 being directly contacted by $W100^B$ in the CDR3-H3 of VRC01 [52,57].

To clarify the role of glycan binding we tested three CD4bs neutralizing antibodies (VRC01, b12, and HJ16) in ELISA for binding to either the glycosylated or deglycosylated RHPA gp120 core proteins (Figure 5E). The neutralizing antibody 2G12 has a well-defined glycan epitope and was used as a positive control [58– 62], while CAP88-3468L (a V3 binding antibody) served as a negative control [63]. Deglycosylation significantly affected the binding of both 2G12 and HJ16 (Figure 5E – blue and purple curves), but did not significantly affect binding of either VRC01 or b12 (Figure 5E – green and yellow curves) to the RHPA gp120 core. These data confirmed the glycan binding properties of HJ16, and suggest that both CAP257 wave 2 neutralizing antibodies and HJ16 have a glycan dependent mechanism of neutralization at the CD4bs.

Early wave 2 escape mutations drive an increase in neutralization breadth

While the simultaneous introduction of T278A, N279D, and R456W mutations into heterologous viruses Q842 and RHPA made them resistant to wave 2 neutralization at 122 weeks p.i. (Figure 5A), when each mutation was introduced individually into RHPA the results were varied (2–30-fold reductions in titer) with no single mutation resulting in complete escape (Figure 5D). These data suggested that escape from wave 2 required a combination of all three mutations. Longitudinal sequence analysis showed that the N279D mutation emerged first at 93 weeks in 5% of the

population, followed by N276D/S glycan deleting mutations at 122 weeks in 36% of the population, and then by substitution of the R456 residue with a bulky amino acid side chain (H, Y, or W) at 161 weeks p.i. in 17% of the population (Figure 4).

To better characterize their contributions to escape from wave 2 antibodies, each mutation (T278A, N279D, and R456W) was introduced separately into Q842 and RHPA and compared to the wild-type viruses. The N279D mutation (Figure 6 – orange curves) had a significant effect only at the beginning of wave 2 activity against Q842, shifting the earliest heterologous neutralization of Q842 from 80 weeks to 93 weeks p.i. (with a 5-fold effect on titers at 107 weeks p.i.). The mutation also affected the titers against RHPA by 2–3 fold. This suggested an initial dependence on N279, with later wave 2 antibodies being less vulnerable to mutations at this residue. This reduced dependence on N279 coincided with the emergence of the N279D mutation at 93 weeks p.i. (Figure 6 – orange dotted lines) providing a mechanism for maturation of the antibody response. The T278A mutation (Figure 6 – purple curves) that deleted the N276 glycan conferred almost complete resistance in Q842, and shifted the earliest neutralization of RHPA from 67 to 122 weeks p.i. The R456W mutation (Figure 6 – pink curves) did not result in a further right shift in the neutralization curves for RHPA relative to the T278A mutation, but did affect the neutralization kinetics of Q842 relative to the wild-type or N279D mutant viruses. As with the N279D mutation, these changes in the fine specificity of the maturing antibody response reflected the emergence of either T278A or R456W mutations in longitudinal autologous sequences (Figure 6 – purple and pink dotted lines respectively).

These data are consistent with accumulating resistance to wave 2, and suggest that after each successive round of escape, new antibody variants emerged that were able to neutralize first the N279D mutant, and then later autologous viruses with additional polymorphisms at positions 276, 278, or 456. We wished to determine whether the ability to neutralize escaped viral variants correlated with increased wave 2 neutralization breadth. Heterologous viruses neutralized by wave 2 were divided into two groups, those neutralized at 67 weeks p.i. (early wave 2 neutralization), and those first neutralized at 93 weeks p.i. (late wave 2 neutralization) after the emergence of initial wave 2 escape mutations (Figure 7A). Viruses also neutralized by wave 1 were omitted as the overlapping titers confounded this analysis.

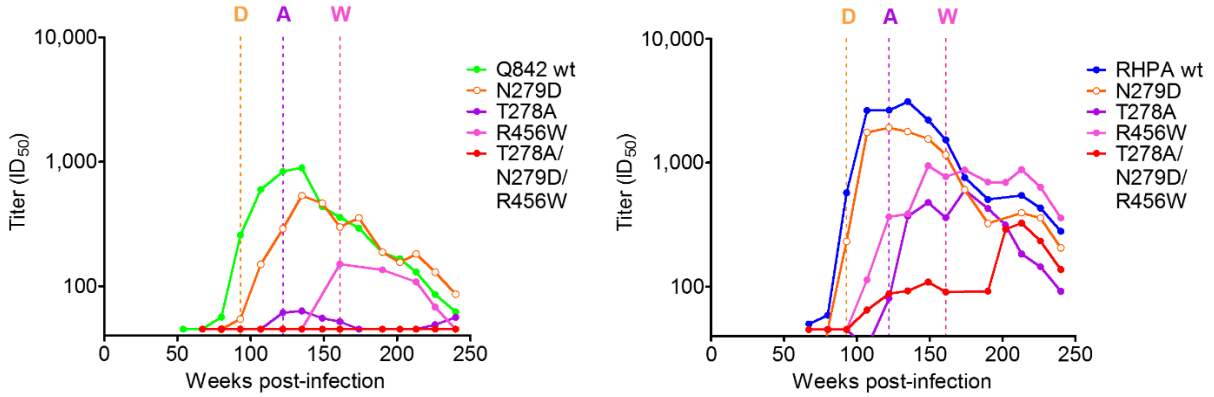

Figure 6. Changes in the fine specificity of CAP257 CD4bs antibodies in response to autologous escape mutations.

The longitudinal neutralization of Q842 (green) or RHPA (blue) wild-type (wt) viruses was compared to the neutralization of N279D (orange), T278A (purple), and R456W (pink) mutant viruses. The triple mutant (T278A/N279D/R456W) from Figure 5A is also shown in red. ID_{50} titers (y-axis) are shown versus weeks p.i. (x-axis). Dotted lines indicate the time points at which each mutation (D=N279D, A=T278A, W=R456W) first appears in the autologous sequences (colored as above).

Inspection of the envelope sequences (particularly in the D-loop) showed that all of the viruses neutralized by early wave 2 antibodies had the N279 immunotype (Figure 7B – boxed in orange). In contrast 44% of viruses neutralized by later wave 2 antibodies had the D279 immunotype. Furthermore, of the viruses neutralized by later wave 2 antibodies, one (Q259) lacked the N276 glycan and four others also had additional non-conservative mutations at positions 273–275 in the N-terminus of the D-loop. (Figure 7B – boxed in blue) that may also affect early wave 2 neutralization. These data suggest that wave 2 escape mutations guided maturation of the CD4bs response, enabling later wave 2 antibodies to neutralize additional heterologous viruses and ultimately resulting in the increased neutralization breadth of CAP257 plasma.

The wave 3 neutralizing antibody target is distinct but undefined

Like wave 1, wave 3 neutralization could not be adsorbed with monomeric gp120, suggesting that these antibodies targeted a quaternary epitope, or an epitope in gp41. To assess whether wave 3 was a distinct antibody specificity, or a re-emergence of wave 1 antibodies, we selected a virus (Du156) that was sensitive to waves 1 and 3, and less sensitive to wave 2 (Figure 8A – red curve). Resistance to wave 1 (V2) and wave 2 (CD4bs) neutralizing antibodies

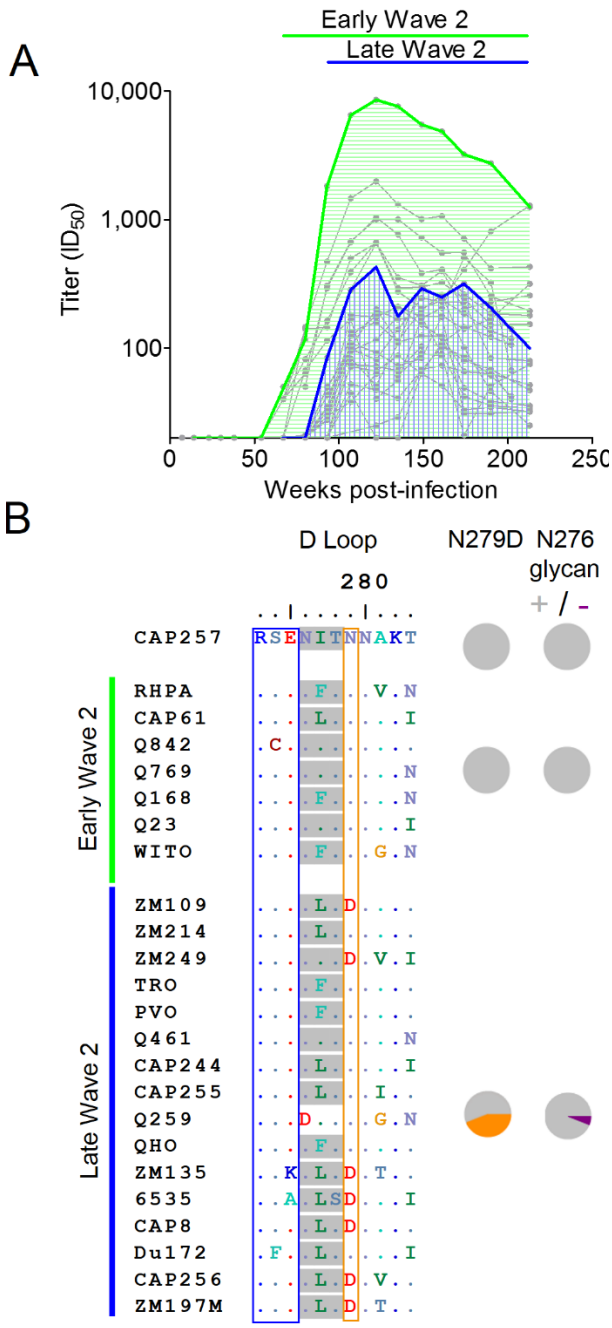

was established by introducing the N160K and T278A mutations identified above. The resulting virus (Du156 N160K/ T278A) remained sensitive to wave 3 neutralization only (Figure 8A – brown curve), suggesting that wave 3 differed from wave 1 (which was completely abrogated by the N160K mutation). To confirm this, we introduced additional V2 mutations (R166A, K168A, K169E, K171A) known to abolish wave 1 neutralization, into the Du156 double mutant. None of these mutations significantly affected the titers of wave 3 neutralizing antibodies (Figure 8A – yellow curves), confirming that the epitope for wave 3 antibodies did not overlap with the wave 1 V2 epitope. An N332A mutation was also introduced to confirm that wave 3 antibodies did not target this glycan.

Figure 7. Maturation of the wave 2 CD4bs response results in the increased neutralization breadth of CAP257 plasma.

A) Summary of early (green) and late (blue) heterologous neutralization by wave 2 antibodies superimposed over the individual virus neutralization kinetics (grey). Viruses neutralized by V2 antibodies in wave 1 have been excluded. ID_{50} titers (y-axis) are shown versus weeks p.i. (x-axis). **B)** Amino acid sequence alignment of heterologous viruses depicted in (A). The timing of early or late heterologous neutralization is shown on the left with horizontal lines. The N276 glycan is shaded grey, and position 279 is boxed in orange. The frequency of the N279D mutation or disrupted N276 glycosylation within the two groups is shown with orange or purple pie slices respectively. The N-terminal region of the D loop is boxed in blue.

To test whether CAP257 wave 3 neutralizing antibodies targeted the MPER region of gp41, we coupled MPER peptides to magnetic beads and used them to adsorb out MPER specific binding antibodies in CAP257 plasma. The adsorption of MPER binding antibodies (Figure 8B) did not affect neutralization of Du156 or the double mutant Du156 N160K/T278A (with wave 1 and 2 resistance mutations) when compared to untreated plasma (Figure 8C). Thus, while we cannot exclude the possibility that wave 3 antibodies target V2 or gp41, these neutralizing antibodies appear to target an epitope distinct from any of the four known sites of vulnerability in the HIV-1 envelope.

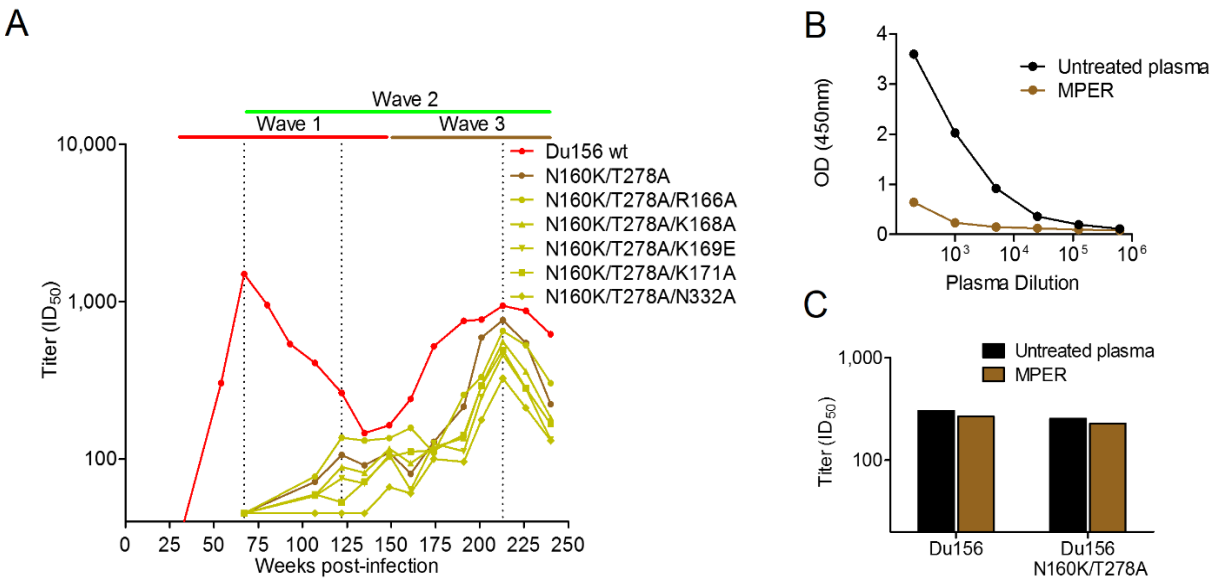

Figure 8. Wave 3 neutralizing antibodies target a novel epitope.

A) Neutralization of Du156 wild-type (wt) virus by longitudinal CAP257 serum is shown in red. The timing of wave 1 (red), wave 2 (green), and wave 3 (brown) neutralization is summarized above as horizontal lines, with peak titers of each wave indicated with dotted lines. The Du156 N160K/T278A double mutant is shown in brown. Du156 triple mutants N160K/ T278A/(R166A, K168A, K169E, K171A, or N332A) are shown in yellow. ID_{50} titers (y-axis) are shown versus weeks p.i. (x-axis). **B)** Adsorption of MPER binding antibodies. OD (450 nm) against the MPER peptide is shown (y-axis) versus plasma dilution (x-axis). Untreated plasma is shown in black, and MPER adsorbed plasma in brown. C) Adsorption of wave 3 neutralization by MPER (colored as above). ID_{50} neutralization titers at 213 weeks p.i. (yaxis) are shown for Du156 and Du156 N160K/T278A.

CAP257 viruses develop resistance to known broadly neutralizing antibodies

We hypothesized that the selection pressure exerted by these broadly neutralizing antibodies would impact on the overall neutralization phenotype of CAP257 viruses over time. Therefore we tested the sensitivity of envelopes from 7, 30, 54, 93, and 174 weeks p.i. to broadly neutralizing monoclonal antibodies targeting the four major epitopes (Figure 9). The 7 week clone from CAP257 was sensitive to neutralization by anti-V2 antibodies, but following the development of wave 1 V2 neutralizing antibodies, CAP257 viruses became more resistant to PG9 and PGT145 neutralization. The 7 week clone was also highly sensitive to HJ16 (0.02 mg/mL) and VRC01 (1.79 mg/mL), however clones isolated after the emergence of wave 2 neutralization were increasingly resistant to neutralization by antibodies targeting the CD4bs. CAP257 viruses from all the time points selected were sensitive to neutralization by antibodies targeting the MPER or N301/N332, neither of which was targeted by broadly neutralizing antibodies in CAP257 plasma. These data confirm that CAP257 developed broadly neutralizing antibodies targeting the CD4bs and V2. Furthermore, the finding that CAP257 viruses remained sensitive to neutralization by antibodies targeting N301/N332 and the MPER supports our hypothesis that wave 3 antibodies target a novel epitope on the HIV-1 envelope.

Discussion

A preventative HIV-1 vaccine remains the most likely way to end the HIV pandemic, but current envelope immunogens have so far failed to elicit broadly neutralizing antibodies. Nonetheless, the development of cross-reactive antibodies in approximately a quarter of HIV-1 infected individuals has confirmed that the human immune system can make such antibodies. Much emphasis has been placed on mapping the targets for these broadly neutralizing antibodies in an attempt to define viral vulnerabilities for immunogen design. Here we analyzed CAP257 heterologous neutralization over a 4.5 year period, describing the sequential evolution of three distinct broadly neutralizing antibody specificities within a single HIV-1 subtype C infected individual. We further showed how early viral evolution in the context of broadly reactive antibodies may profoundly shape the maturing antibody response towards enhanced neutralization breadth, in a process that may inform immunogen design.

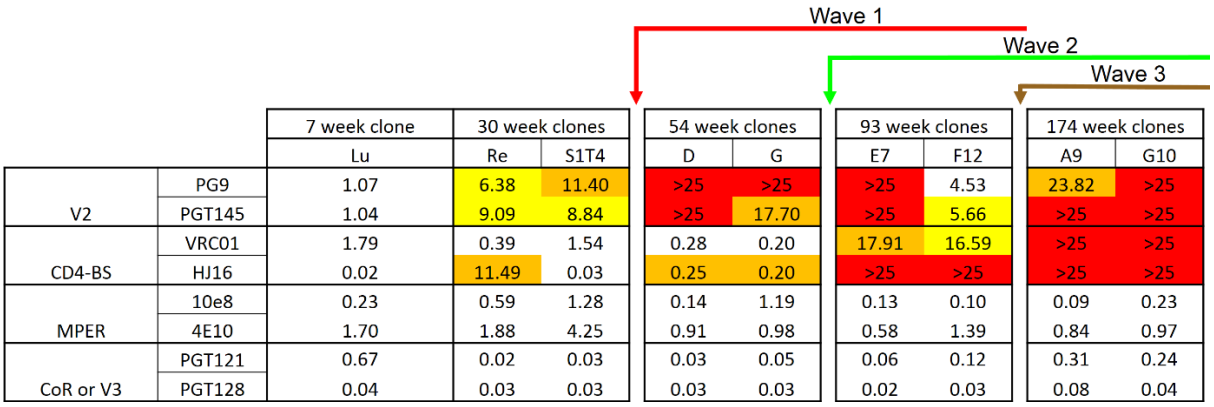

		7 week clone	30 week clones		54 week clones		93 week clones		174 week clones	
		Lu	Re	S1T4	D	G	E7	F12	A9	G10
V2	PG9	1.07	6.38	11.40	>25	>25	>25	4.53	23.82	>25
	PGT145	1.04	9.09	8.84	>25	17.70	>25	5.66	>25	>25
CD4-BS	VRC01	1.79	0.39	1.54	0.28	0.20	17.91	16.59	>25	>25
	HJ16	0.02	11.49	0.03	0.25	0.20	>25	>25	>25	>25
MPER	10e8	0.23	0.59	1.28	0.14	1.19	0.13	0.10	0.09	0.23
	4E10	1.70	1.88	4.25	0.91	0.98	0.58	1.39	0.84	0.97
CoR or V3	PGT121	0.67	0.02	0.03	0.03	0.05	0.06	0.12	0.31	0.24
	PGT128	0.04	0.03	0.03	0.03	0.03	0.02	0.03	0.08	0.04

Figure 9. Accumulating resistance of CAP257 clones to broadly neutralizing monoclonal antibodies targeting V2 and the CD4bs.

The sensitivity of nine CAP257 clones from 7, 30, 54, 93, and 174 weeks p.i. to broadly neutralizing antibodies targeting the four known sites of vulnerability was measured in a TZM-bl assay. The timing of wave 1 (red), wave 2 (green), and wave 3 (brown) neutralization is summarized above with arrows. Increases in IC_{50} relative to the 7 week clone are colored as follows: 5–10-fold (yellow), .10-fold (orange), and complete neutralization resistance (red).

These data have been summarized in Figure 10. The CAP257 autologous virus efficiently escaped all three specificities. As a consequence the antigenic stimulus for these broadly neutralizing antibodies declined, and antibody titers dropped at least ten fold within a three year period. The waxing and waning of the broadly neutralizing specificities in CAP257 confounded our previous attempts to map the targets at 174 weeks p.i. [7], when the titers of the three waves overlapped significantly. As most mapping studies are cross-sectional, the number of individuals who mount multiple broadly neutralizing antibody responses may therefore be underestimated, and may make up a significant proportion of those plasma samples that remain undefined. Nonetheless we were able to finely map 2 of the 3 specificities in this study and showed that they targeted known sites of vulnerability on the HIV-1 envelope. Wave 1 antibodies targeted the site defined by PG9/16 and were completely dependent on N160 and K169, consistent with previous data describing PG9/16 dependence on the N160 glycan and the positively charged amino acids in the C-strand of V1/V2 [16,37]. In general the epitope for wave 1 antibodies showed a larger footprint in V2 when compared to the epitopes of other monoclonal antibodies targeting this site, but behaved most similarly to PGT145.

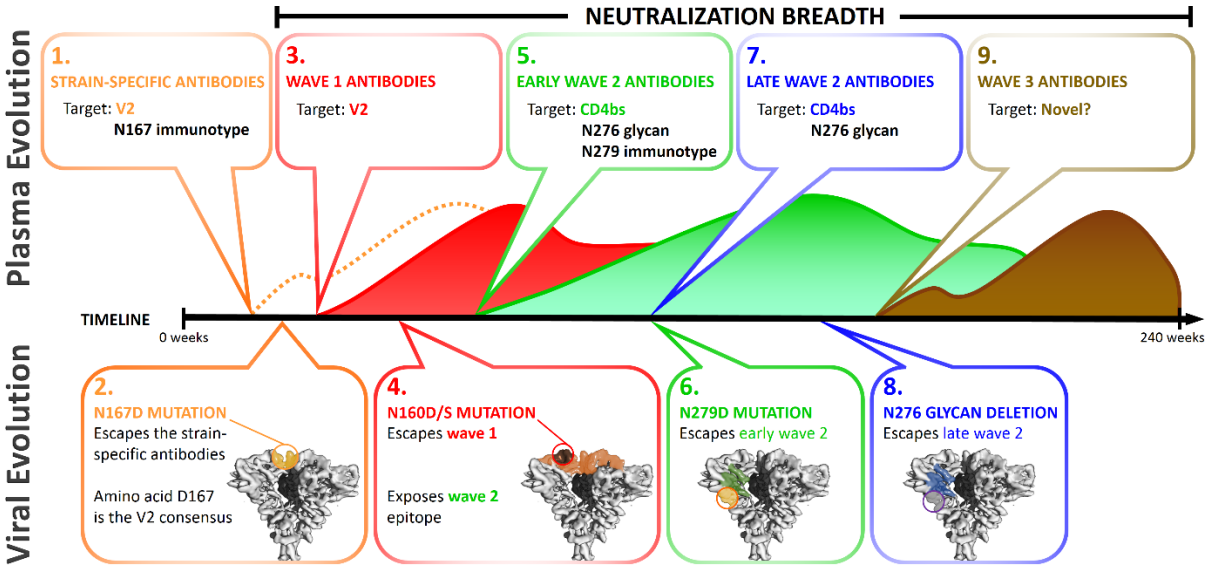

Figure 10. Summary of the role of CAP257 viral evolution in shaping broadly neutralizing antibody responses.

The schema depicts the evolution of plasma neutralizing antibodies and viral escape mutations over 240 weeks. Each of the three waves of CAP257 broadly neutralizing antibodies is shown. Text boxes highlight the key events described herein. Env trimers (EMD-5447) were drawn in UCSF-Chimera, and spheres were used to approximate the location of escape mutations. 1) Strain-specific antibodies (dotted orange line) developed at 23 weeks, targeting a V2 epitope overlapping with known V2 antibodies (eg: PG9). 2) Strain-specific V2 antibodies were escaped by an N167D mutation (D being the global consensus at this site). 3) Broadly neutralizing antibodies targeting V2 (wave 1 – red curve) developed at 30 weeks. 4) Escape from wave 1 antibodies through deletion of the N160 glycan was associated with exposure of an epitope in the CD4bs. 5) At 67 weeks broadly neutralizing antibodies targeting the CD4bs (wave 2 – green curve) develop. Neutralization was N276 glycan dependent and sensitive to an N279D mutation. 6) The N279D change emerges at 93 weeks, significantly affecting wave 2 neutralization at this time point. 7) Wave 2 neutralization becomes independent of position 279, which was associated with increased neutralization breadth. 8) Mutations that delete the N276 glycan (as well as an R456W change) escape wave 2 antibodies. 9) CAP257 develops a third broadly neutralizing antibody specificity that could not be mapped to any of the four known antibody targets.

However none of the antibodies or plasma tested was sensitive to removal of the N156 glycan. While the crystal structure of PG9 with V2 showed interactions with the N156 glycan [37], the effect of deleting the N156 glycan is variable [16,35,36]. This effect might be explained by recent data suggesting that PG9 recognizes two N160 glycans (from two adjacent gp120 monomers) but only one N156 glycan [64]. The requirement for a lysine at position 169 explains the

subtype C specificity of CAP257 wave 1 antibodies, as this residue is less common in subtypes A and B [35]. Wave 2 antibodies targeted a known site of vulnerability, the CD4bs, but these antibodies had an unusual glycan dependent mechanism of neutralization. CAP257 wave 2 and HJ16 neutralization were both highly dependent on interactions with the N276 glycan. N276 is also the recently described target of the broadly neutralizing antibody 8ANC195, but this antibody does not appear to interact with the CD4bs [65]. While glycan dependence for neutralization has not previously been described for CD4bs antibodies, including HJ16, Balla-Jhagjhoorsingh et al. reported that resistance to HJ16 involved an N276D mutation (deleting the glycan) with a hundred-fold drop in titer [66], providing support for our observations. The glycan dependence of both HJ16 and CAP257 wave 2 antibodies suggests that they target a similar sub-epitope of the CD4bs that may be better defined as an N276 glycan dependent class of neutralizing antibodies, which is distinct from the VRC01 class. Recently it was shown that related variants of VRC01 do bind the glycan at N276 [67], however this glycan is not a major determinant of neutralization sensitivity to VRC01 [52,56,57,68]. Rather, N276 has been described as a protective shield for the CD4bs, and deleting this glycan enhances the neutralization of CD4bs antibodies VRC01 and b12 [52,56]. Removing N276 from gp120 also enabled binding to the predicted germline antibody for VRC01, which otherwise did not bind to gp120, and has been suggested as a modification for candidate vaccine immunogens [69,70]. However, the glycan shield is increasingly recognized as a major site of vulnerability on the HIV-1 envelope [15,16], and as with the glycans at N156/N160 and N301/N332, conservation of the N276 glycan bordering the CD4bs may make it a promising target for vaccine design. Characterization of viral escape from CAP257 CD4bs antibodies indicated that deletion of the N276 glycan alone did not confer complete resistance. Escape required accumulating mutations in the CD4bs site, consistent with the functional conservation of this epitope. In addition to deletion of the N276 glycan, CAP257 escape occurred through a R456W mutation that also significantly affected neutralization by VRC01 (30 fold) and HJ16 (514-fold). This mutation likely contributed towards the evolution of VRC01 resistant virus by 174 weeks. W456 is extremely rare, occurring in only 0.78% (27 of 3,481) of sequences in the LANL HIV-1 sequence database. A

crystal complex for HJ16 is not available, however the structure of VRC01 bound to its epitope showed that this antibody does not make significant contact with the R456 side chain in gp120, but rather hydrogen bonds with the R456 backbone carbonyl group. This suggests that the R456W mutation provides an indirect mechanism for resistance. The highly conserved R456 side chain can make hydrogen bonds with backbone carbonyl groups of amino acids at position 277 and 278 in the D-loop, as well as hydrogen bonds with E466 side chain in b24, C-terminal to V5 (Figure 11). Loss of these bonds and localized conformational changes to accommodate a bulky tryptophan residue may destabilize this critical component of the CD4bs epitope [52,56,71]. This study adds to data showing that the immune system can target multiple conserved epitopes [29–31]. It is striking that in three of these four studies, antibodies targeted both V2 and the CD4bs (donors CH219, AC053, and CAP257), suggesting an association between these two epitopes. Indeed, there is a well-documented relationship between V1/V2 and the CD4bs. The V1/V2 region protects the receptor binding sites from neutralization [42–51], and also interacts with V3 at the trimerization domain to hold the CD4bs in its pre-liganded conformation [21]. The crystal structures of monoclonal antibodies PG9, CH58, and CH59 bound to their epitopes in V2 show that the conformation of the V1/V2 sub-domain may vary significantly, but the factors that govern these conformational states are not known [37,72]. In CAP257, deletion of the N160 glycan increased exposure of the CD4bs. It is possible that certain immunotypes of the V1/V2 epitope, such as the rare mutations at N160 or D167 described here, shifted the equilibrium of V1/V2 toward conformations that better exposed the CD4bs to neutralizing antibodies. This is supported by previous observations that introduction of the N160K and D167N mutations simultaneously into JR-FL resulted in a 50-fold increase in neutralization sensitivity to CD4bs antibodies [73]. CAP257 was infected with the less common N167 variant, and therefore following escape from V2 wave 1 antibodies a similar conformational state (D/S160, N167) would have been presented to the immune system. Our data suggest that this escape pattern further exposed the glycan dependent CD4bs sub-epitope. Although vaccination with the K160 and/or N167 immunotype may improve antibody responses to the CD4bs site, antibodies induced to the V2 epitope would be relatively strain-specific, like monoclonal antibody 2909 that

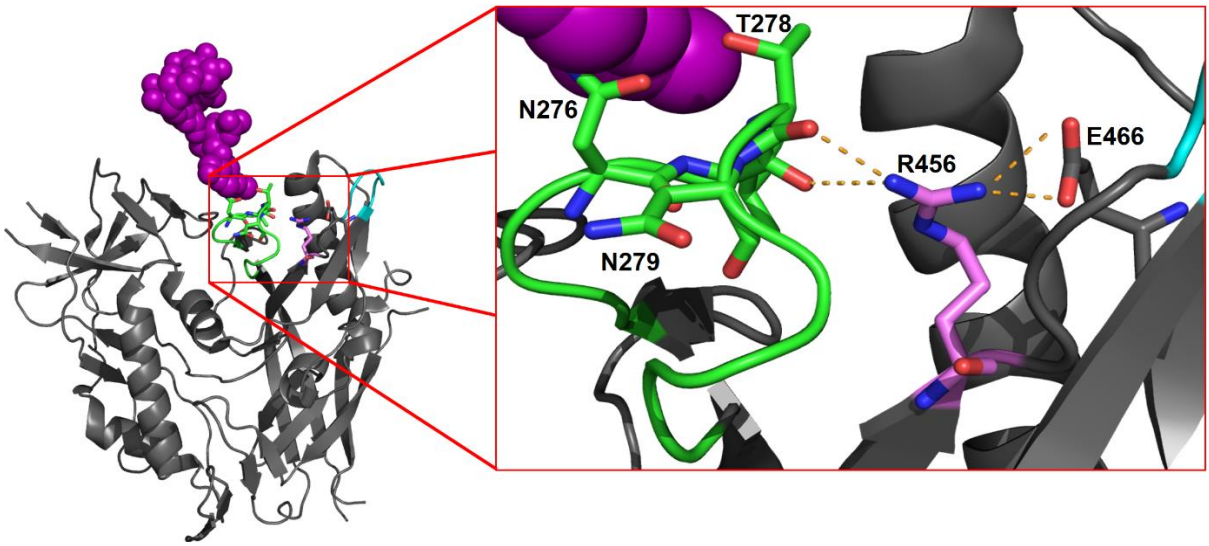

Figure 11. The R456 side chain stabilizes the CD4bs epitope through hydrogen bonding. A diagram of the 93TH057 gp120 crystal structure (pdb file 4JKP) shown in an orientation similar to the angle of approach for CD4. The crystalized part of the N276 attached glycan (GlcNAc2Man4) is shown with purple spheres. The D-loop is shown in green, the V5 loop is shown in cyan, and the R456 residue is shown in pink. Oxygen atoms are colored red, and nitrogen atoms blue. The inset shows a magnified view of the interaction between R456 and residues in the Dloop or the b24 strand. Putative hydrogen bonds are shown with dotted orange lines. The image was created using The PyMOL Molecular Graphics System, Version 1.3r1edu, Schrodinger LLC

recognizes the K160 immunotype and is therefore specific for SF162 [74]. In CAP257, switching from N167 to the more common D167 residue resulted in escape from the strain-specific response to V2, and this coincided with the development of a much broader response targeting the same epitope. Sequential immunization may be a useful strategy to promote the broadening of the B-cell response. Recently Murphy et al. showed that two light chain variants paired with a single heavy chain of a strain-specific neutralizing antibody differentially neutralized early autologous envelopes [75]. While evolution of that strain-specific epitope did not affect the development of broadly neutralizing antibodies in this individual, the data supports the possibility that viral evolution might facilitate the neutralization of amino acid variants within a given epitope. Similarly, we have previously shown in an individual who developed broadly neutralizing antibodies to the V2 region that viral escape drove a maturation of the antibody response towards recognizing multiple V2 variants [35]. Here we show that emergence of an aspartic acid at position 279 preceded a broadening of the B-cell response to the CD4bs. The N279 and D279 amino acid variants of the CD4bs

are equally common among sequences in the LANL HIV-1 database (50% and 48% respectively, n=3,479), and preferential neutralization of either immunotype would halve the neutralization breadth of an antibody. CAP257 wave 2 neutralizing antibodies and HJ16 were somewhat sensitive to the N279D change. However the resistance of D279 containing viruses to CAP257 antibodies was rapidly lost after the emergence of the N279D escape mutation. Therefore, like the N167D mutation in V2 described for wave 1, this change in the fine specificity of CAP257 antibodies coincided with an increase in the neutralization breadth of the CD4bs response. We hypothesize that position N279 was non-critical for antibody binding, and despite temporarily facilitating neutralization escape, the N279D mutation then promoted affinity maturation by reducing the dependence of CAP257 antibodies on this amino acid. This adds to recent data suggesting a major role for viral evolution in the development of neutralization breadth to the CD4bs [76]. These data support the possibility that a sequential immunization strategy would enhance neutralization breadth by systematically presenting common variants in a given epitope. Such residues would have to be noncritical to antibody binding allowing for the evolution of higher affinity variants that would in turn recognize multiple immunotypes. Overall these data highlight how interactions between the host immune system and viral escape mutations shaped the development of broadly neutralizing antibodies. The escape pathways identified here that led to the increased breadth of neutralization for both V2 and CD4bs antibodies provide potential pathways for generating broadly neutralizing antibodies. Further defining these pathways through the isolation of monoclonal antibodies will provide valuable insight into how these types of antibodies could be elicited using sequential immunization in a vaccine setting.

Materials and Methods

Ethics statement

The CAPRISA Acute Infection study received ethical approval from the Universities of KwaZulu-Natal (E013/04), Cape Town (025/2004), and the Witwatersrand (MM040202). CAP257 provided written informed consent for study participation.

CAPRISA 002 Acute Infection cohort participant

The CAPRISA Acute Infection cohort is comprised of women at high risk of HIV-1 infection in KwaZulu-Natal, South Africa [77]. Here we studied one individual

(CAP257) from seven weeks p.i. through four and a half years of infection, until she started anti-retroviral therapy. During this time she had an average viral load of 60,784 copies/mL and an average CD4 count of 498 cells/ mL. Plasma samples collected at 30 time points were used in this study.

Single genome amplification

The amplification of envelope genes from single HIV-1 RNA genomes has been previously described [78]. Viral RNA was isolated from CAP257 plasma using a Viral RNA Extraction Kit (QIAGEN), and cDNA was synthesized with Superscript III Reverse Transcriptase (Invitrogen). The reaction product was treated with RNase H (Invitrogen) and envelope genes were amplified by nested PCR with Platinum Taq (Invitrogen). Amplicons were purified with a PCR Clean-up Kit (QIAGEN) and single genome amplification confirmed by DNA sequencing using the ABI PRISM Big Dye Terminator Cycle Sequencing Ready Reaction kit (Applied Biosystems) and an ABI 3100 automated genetic analyzer. The full-length env sequences were assembled and edited using Sequencher v.4.5 (Genecodes) and Bioedit v.7.0.5.3.

Cell lines

The TZM-bl cell line engineered from CXCR4-positive HeLa cells to express CD4, CCR5, and a firefly luciferase reporter gene (under control of the HIV-1 LTR) was obtained from the NIH AIDS Research and Reference Reagent Program, Division of AIDS, NIAID, NIH (developed by Dr. John C. Kappes, and Dr. Xiaoyun Wu [79,80]). The 293T cell line was obtained from Dr George Shaw (University of Alabama, Birmingham, AL). Cells were cultured at 37°C, 5% CO^2 in DMEM containing 10% heatinactivated fetal bovine serum (Gibco BRL Life Technologies) with 50 ug/ml gentamicin (Sigma) and disrupted at confluency by treatment with 0.25% trypsin in 1 mM EDTA (Sigma).

Pseudovirus production

Selected envelope sequences were re-amplified from first round nested PCR products (described above) with PfuUltra II (Stratagene), purified by a Gel Extraction Kit (QIAGEN) and cloned into pcDNA3.1 (Invitrogen). The envelope plasmids were co-transfected into 293T cells using FuGENE 6 (Roche) with the pSG3DEnv backbone (obtained from the NIH AIDS Research and Reference Reagent Program, Division of AIDS, NIAID, NIH). Cultures were incubated for 48 hours to produce Envpseudotyped viral stocks that were filtered through 0.45 mm and frozen in DMEM supplemented with 20% FBS. Mutant envelopes were generated with the QuikChange Lightning Kit (Stratagene) and confirmed by DNA

sequencing (as above).

Neutralization assay

The TZM-bl neutralization assay has been described previously [4,81]. It measures a reduction in relative light units generated by a single round of infection in TZM-bl cells with Env-pseudotyped viruses after pre-incubation with monoclonal antibodies or a plasma sample of interest. Samples were serially diluted 1:3 and the ID_{50} calculated as the dilution at which the infection was reduced by 50%.

Protein expression and adsorptions

Plasmids encoding Histidine tagged recombinant envelope proteins were transfected into 293T cells using polyethylenimine 25 kDa (Polysciences). Recombinant proteins were expressed and purified as previously described [9]. Aliquots of 400 mg each were coupled to MyOne Tosyl-activated magnetic Dynabeads (Invitrogen) at 37°C pH 9.5 overnight, and then blocked with 0.5% BSA in 0.05% Tween20 PBS overnight at 37uC. Protein coupled beads were incubated with 200 mL of plasma (diluted 1:20) for two hours at 37°C, then the beads were removed magnetically and the remaining plasma assessed for binding and neutralizing antibodies using ELISA and neutralization assays respectively.

Enzyme Linked Immunosorbent Assay (ELISA)

Protein antigens were coated at 4 mg/mL onto high binding 96 well ELISA plates (Corning) overnight at 4°C. All subsequent steps were carried out in 5% fat-free milk, 0.05% Tween20 in PBS for 1 hour at 37°C. The plates were blocked and then probed with serial dilutions of the adsorbed plasma or specific monoclonal antibodies, biotinylated goat anti-human polyclonal antibodies (KPL), and an anti-biotin monoclonal conjugated to HRP (Calbiochem). Antigen-antibody complexes were detected by incubating with 100 mL 1-Step Ultra TMB-ELISA (Thermoscientific) for five minutes and then the reaction was stopped with 25 mL 1 M H_2SO_4. Absorbance was read at 450 nm on a VERSAmax tunable microplate reader (Molecular devices).

Protein deglycosylation

Plasmid encoding the RHPA gp120 core was transfected with polyethylenimine-MAX 40 kDa (Polysciences) into GnTI(-/-) 293S cells and purified using two step lectin chromatography and Ni-NTA affinity chromatography. Protein was assessed for purity and conformation by SDS-PAGE and ELISA. 1 mg of the RHPA core gp120 was deglycosylated overnight at 37°C in 500 mM sodium chloride, 100 mM sodium acetate pH 5.5 with 0.5 U of Endo-H. Glycans were removed through buffer exchange into PBS using Vivaspin 20 mL

concentrators (Sartorius stedim). Deglycosylation was confirmed by SDS-PAGE and sandwich ELISA (described above) using lectins as a capture protein.

Acknowledgments

We are grateful to participant CAP257 in the CAPRISA Acute Infection cohort for providing samples, and to the clinical/laboratory staff at CAPRISA for their commitment to the study. We thank Ruwayda Thebus and Dr. Bronwen E. Lambson for amplifying CAP257 envelope sequences from 93, 174, and 191 weeks p.i., and Daniel Sheward for generating statistics on the amino acid frequencies among envelope sequences in the LANL HIV sequence database. We also thank Maphuti Madiga for running the initial screen on CAP257 that identified the broadly neutralizing activity of her plasma. Lastly we are grateful to Joseph Sodroski for the GnTI(-/-) 293S cell line, and Robin Weiss, David Corti and the Collaboration for AIDS Vaccine Discovery (supported in part by the Bill and Melinda Gates Foundation) for supplying the monoclonal antibody HJ16.

Author Contributions

Conceived and designed the experiments: CKW ESG LM PLM. Performed the experiments: CKW JNB NT. Analyzed the data: CKW JNB ESG NT LM PLM. Wrote the paper: CKW JNB CW LM PLM. Conceived, implemented and led the CAPRISA 002 Acute Infection study: SSAK CW.

References

1. Gray ES, Moore PL, Choge IA, Decker JM, Bibollet-Ruche F, et al. (2007) Neutralizing antibody responses in acute human immunodeficiency virus type 1 subtype C infection. J Virol 81: 6187–6196.
2. Richman DD, Wrin T, Little SJ, Petropoulos CJ (2003) Rapid evolution of the neutralizing antibody response to HIV type 1 infection. Proc Natl Acad Sci U S A 100: 4144–4149.
3. Li B, Decker JM, Johnson RW, Bibollet-Ruche F, Wei X, et al. (2006) Evidence for potent autologous neutralizing antibody titers and compact envelopes in early infection with subtype C human immunodeficiency virus type 1. J Virol 80: 5211–5218.
4. Wei X, Decker JM, Wang S, Hui H, Kappes JC, et al. (2003) Antibody neutralization and escape by HIV-1. Nature 422: 307–312.
5. Moog C, Fleury HJ, Pellegrin I, Kirn A, Aubertin AM (1997) Autologous and heterologous neutralizing antibody responses following initial seroconversion in human immunodeficiency virus type 1-infected individuals. J Virol 71: 3734–3741.
6. Kwong PD, Wyatt R, Robinson J, Sweet RW, Sodroski J, et al. (1998) Structure of an HIV gp120 envelope glycoprotein in complex with the CD4 receptor and a neutralizing human antibody. Nature 393: 648–659.
7. Gray ES, Madiga MC, Hermanus T, Moore PL, Wibmer CK, et al. (2011) The neutralization breadth of HIV-1 develops

incrementally over four years and is associated with CD4+ T cell decline and high viral load during acute infection. J Virol 85: 4828–4840.
8. Sather DN, Stamatatos L (2010) Epitope specificities of broadly neutralizing plasmas from HIV-1 infected subjects. Vaccine 28 Suppl 2: B8–12.
9. Gray ES, Taylor N, Wycuff D, Moore PL, Tomaras GD, et al. (2009) Antibody specificities associated with neutralization breadth in plasma from human immunodeficiency virus type 1 subtype C-infected blood donors. J Virol 83: 8925–8937.
10. Doria-Rose NA, Klein RM, Manion MM, O'Dell S, Phogat A, et al. (2009) Frequency and phenotype of human immunodeficiency virus envelope-specific B cells from patients with broadly cross-neutralizing antibodies. J Virol 83: 188–199.
11. Euler Z, van Gils MJ, Bunnik EM, Phung P, Schweighardt B, et al. (2010) Crossreactive neutralizing humoral immunity does not protect from HIV type 1 disease progression. J Infect Dis 201: 1045–1053.
12. Burton DR, Barbas CF, (1991) A large array of human monoclonal antibodies to type 1 human immunodeficiency virus from combinatorial libraries of asymptomatic seropositive individuals. Proc Natl Acad Sci U S A 88: 10134–10137.
13. Muster T, Steindl F, Purtscher M, Trkola A, Klima A, et al. (1993) A conserved neutralizing epitope on gp41 of human immunodeficiency virus type 1. J Virol 67: 6642–6647.
14. Trkola A, Purtscher M, Muster T, Ballaun C, Buchacher A, et al. (1996) Human monoclonal antibody 2G12 defines a distinctive neutralization epitope on the gp120 glycoprotein of human immunodeficiency virus type 1. J Virol 70: 1100– 1108.
15. Walker LM, Huber M, Doores KJ, Falkowska E, Pejchal R, et al. (2011) Broad neutralization coverage of HIV by multiple highly potent antibodies. Nature 477: 466–470.
16. Walker LM, Phogat SK, Chan-Hui PY, Wagner D, Phung P, et al. (2009) Broad and potent neutralizing antibodies from an African donor reveal a new HIV-1 vaccine target. Science 326: 285–289.
17. Sather DN, Armann J, Ching LK, Mavrantoni A, Sellhorn G, et al. (2009) Factors associated with the development of cross-reactive neutralizing antibodies during human immunodeficiency virus type 1 infection. J Virol 83: 757–769.
18. Tomaras GD, Binley JM, Gray ES, Crooks ET, Osawa K, et al. (2011) Polyclonal B cell responses to conserved neutralization epitopes in a subset of HIV-1-infected individuals. J Virol 85: 11502–11519.
19. Walker LM, Simek MD, Priddy F, Gach JS, Wagner D, et al. (2010) A limited number of antibody specificities mediate broad and potent serum neutralization in selected HIV-1 infected individuals. PLoS Pathog 6. e1001028.
20. Scheid JF, Mouquet H, Feldhahn N, Seaman MS, Velinzon K, et al. (2009) Broad diversity of neutralizing antibodies isolated from memory B cells in HIVinfected individuals. Nature 458: 636–640.
21. Mao Y, Wang L, Gu C, Herschhorn A, Xiang SH, et al. (2012) Subunit organization of the membrane-bound HIV-1 envelope glycoprotein trimer. Nat Struct Mol Biol 19(9):893–9.
22. Kwong PD, Mascola JR (2012) Human antibodies that neutralize HIV-1: identification, structures, and B cell ontogenies. Immunity 37: 412–425.
23. Corti D, Langedijk JP, Hinz A, Seaman MS, Vanzetta F, et al. (2010) Analysis of memory B cell responses and isolation of novel monoclonal antibodies with neutralizing breadth from HIV-1-infected individuals. PLoS One 5: e8805.
24. Wu X, Yang ZY, Li Y, Hogerkorp CM, Schief WR, et al. (2010) Rational design of envelope identifies broadly neutralizing human monoclonal antibodies to HIV-1.

Science 329: 856–861.
25. Roben P, Moore JP, Thali M, Sodroski J, Barbas CF, . (1994) Recognition properties of a panel of human recombinant Fab fragments to the CD4 binding site of gp120 that show differing abilities to neutralize human immunodeficiency virus type 1. J Virol 68: 4821–4828.
26. Pietzsch J, Scheid JF, Mouquet H, Klein F, Seaman MS, et al. (2010) Human anti-HIV-neutralizing antibodies frequently target a conserved epitope essential for viral fitness. J Exp Med 207: 1995–2002.
27. Binley J (2009) Specificity of broadly neutralizing antibodies in sera from HIV-1 infected individuals. Current Opinion in HIV and AIDS 4: 364–372.
28. Li Y, Svehla K, Louder MK, Wycuff D, Phogat S, et al. (2009) Analysis of neutralization specificities in polyclonal sera derived from human immunodeficiency virus type 1-infected individuals. J Virol 83: 1045–1059.
29. Bonsignori M, Montefiori DC, Wu X, Chen X, Hwang KK, et al. (2012) Two distinct broadly neutralizing antibody specificities of different clonal lineages in a single HIV-1-infected donor: implications for vaccine design. J Virol 86: 4688– 4692.
30. Mikell I, Stamatatos L (2012) Evolution of Cross-Neutralizing Antibody Specificities to the CD4-BS and the Carbohydrate Cloak of the HIV Env in an HIV-1-Infected Subject. PLoS One 7: e49610.
31. Klein F, Gaebler C, Mouquet H, Sather DN, Lehmann C, et al. (2012) Broad neutralization by a combination of antibodies recognizing the CD4 binding site and a new conformational epitope on the HIV-1 envelope protein. J Exp Med 209: 1469–1479.
32. Moore PL, Gray ES, Wibmer CK, Bhiman JN, Nonyane M, et al. (2012) Evolution of an HIV glycan-dependent broadly neutralizing antibody epitope through immune escape. Nat Med 18: 1688–1692.
33. Kothe DL, Li Y, Decker JM, Bibollet-Ruche F, Zammit KP, et al. (2006) Ancestral and consensus envelope immunogens for HIV-1 subtype C. Virology 352: 438–449.
34. Seaman MS, Janes H, Hawkins N, Grandpre LE, Devoy C, et al. (2010) Tiered categorization of a diverse panel of HIV-1 Env pseudoviruses for assessment of neutralizing antibodies. J Virol 84: 1439–1452.
35. Moore PL, Gray ES, Sheward D, Madiga M, Ranchobe N, et al. (2011) Potent and broad neutralization of HIV-1 subtype C by plasma antibodies targeting a quaternary epitope including residues in the V2 loop. J Virol 85: 3128–3141.
36. Bonsignori M, Hwang KK, Chen X, Tsao CY, Morris L, et al. (2011) Analysis of a clonal lineage of HIV-1 envelope V2/V3 conformational epitope-specific broadly neutralizing antibodies and their inferred unmutated common ancestors. J Virol 85: 9998–10009.
37. McLellan JS, Pancera M, Carrico C, Gorman J, Julien JP, et al. (2011) Structure of HIV-1 gp120 V1/V2 domain with broadly neutralizing antibody PG9. Nature 480: 336–343.
38. Lynch RM, Rong R, Boliar S, Sethi A, Li B, et al. (2011) The B cell response is redundant and highly focused on V1V2 during early subtype C infection in a Zambian seroconverter. J Virol 85: 905–915.
39. Moore PL, Ranchobe N, Lambson BE, Gray ES, Cave E, et al. (2009) Limited neutralizing antibody specificities drive neutralization escape in early HIV-1 subtype C infection. PLoS Pathog 5: e1000598.
40. Honnen WJ, Krachmarov C, Kayman SC, Gorny MK, Zolla-Pazner S, et al. (2007) Type-specific epitopes targeted by monoclonal antibodies with exceptionally potent neutralizing activities for selected strains of human immunodeficiency virus type 1 map to a common region of the V2 domain of gp120 and differ only at single

positions from the clade B consensus sequence. J Virol 81: 1424–1432.
41. Moore PL, Gray ES, Choge IA, Ranchobe N, Mlisana K, et al. (2008) The C3V4 region is a major target of autologous neutralizing antibodies in human immunodeficiency virus type 1 subtype C infection. J Virol 82: 1860–1869.
42. Zolla-Pazner S (2004) Identifying epitopes of HIV-1 that induce protective antibodies. Nat Rev Immunol 4: 199–210.
43. Stamatatos L, Cheng-Mayer C (1998) An envelope modification that renders a primary, neutralization-resistant clade B human immunodeficiency virus type 1 isolate highly susceptible to neutralization by sera from other clades. J Virol 72: 7840–7845.
44. O'Rourke SM, Schweighardt B, Phung P, Fonseca DP, Terry K, et al. (2010) Mutation at a single position in the V2 domain of the HIV-1 envelope protein confers neutralization sensitivity to a highly neutralization-resistant virus. J Virol 84: 11200–11209.
45. Ly A, Stamatatos L (2000) V2 loop glycosylation of the human immunodeficiency virus type 1 SF162 envelope facilitates interaction of this protein with CD4 and CCR5 receptors and protects the virus from neutralization by anti-V3 loop and anti-CD4 binding site antibodies. J Virol 74: 6769–6776.
46. Guttman M, Kahn M, Garcia NK, Hu SL, Lee KK (2012) Solution structure, conformational dynamics, and CD4-induced activation in full-length, glycosylated, monomeric HIV gp120. J Virol 86: 8750–8764.
47. Li Y, Cleveland B, Klots I, Travis B, Richardson BA, et al. (2008) Removal of a single N-linked glycan in human immunodeficiency virus type 1 gp120 results in an enhanced ability to induce neutralizing antibody responses. J Virol 82: 638– 651.
48. van Gils MJ, Bunnik EM, Boeser-Nunnink BD, Burger JA, Terlouw-Klein M, et al. (2011) Longer V1V2 region with increased number of potential N-linked glycosylation sites in the HIV-1 envelope glycoprotein protects against HIVspecific neutralizing antibodies. J Virol 85: 6986–6995.
49. Watkins JD, Diaz-Rodriguez J, Siddappa NB, Corti D, Ruprecht RM (2011) Efficiency of neutralizing antibodies targeting the CD4-binding site: influence of conformational masking by the V2 loop in R5-tropic clade C simian-human immunodeficiency virus. J Virol 85: 12811–12814.
50. Ye Y, Si ZH, Moore JP, Sodroski J (2000) Association of structural changes in the V2 and V3 loops of the gp120 envelope glycoprotein with acquisition of neutralization resistance in a simian-human immunodeficiency virus passaged in vivo. J Virol 74: 11955–11962.
51. Pinter A, Honnen WJ, He Y, Gorny MK, Zolla-Pazner S, et al. (2004) The V1/V2 domain of gp120 is a global regulator of the sensitivity of primary human immunodeficiency virus type 1 isolates to neutralization by antibodies commonly induced upon infection. J Virol 78: 5205–5215.
52. Li Y, O'Dell S, Walker LM, Wu X, Guenaga J, et al. (2011) Mechanism of neutralization by the broadly neutralizing HIV-1 monoclonal antibody VRC01. J Virol 85: 8954–8967.
53. Sather DN, Carbonetti S, Kehayia J, Kraft Z, Mikell I, et al. (2012) Broadly neutralizing antibodies developed by an HIV-positive elite neutralizer exact a replication fitness cost on the contemporaneous virus. J Virol 86: 12676–12685.
54. Wu X, Wang C, O'Dell S, Li Y, Keele BF, et al. (2012) Selection pressure on HIV-1 envelope by broadly neutralizing antibodies to the conserved CD4binding site. J Virol 86: 5844–5856.
55. Lynch RM, Tran L, Louder MK, Schmidt SD, Cohen M, et al. (2012) The development of CD4 binding site antibodies during HIV-1 infection. J Virol 86: 7588–7595.

56. Pantophlet R, Ollmann Saphire E, Poignard P, Parren PW, Wilson IA, et al. (2003) Fine mapping of the interaction of neutralizing and nonneutralizing monoclonal antibodies with the CD4 binding site of human immunodeficiency virus type 1 gp120. J Virol 77: 642–658.
57. Zhou T, Georgiev I, Wu X, Yang ZY, Dai K, et al. (2010) Structural basis for broad and potent neutralization of HIV-1 by antibody VRC01. Science 329: 811–817.
58. Calarese DA, Lee HK, Huang CY, Best MD, Astronomo RD, et al. (2005) Dissection of the carbohydrate specificity of the broadly neutralizing anti-HIV-1 antibody 2G12. Proc Natl Acad Sci U S A 102: 13372–13377.
59. Calarese DA, Scanlan CN, Zwick MB, Deechongkit S, Mimura Y, et al. (2003) Antibody domain exchange is an immunological solution to carbohydrate cluster recognition. Science 300: 2065–2071.
60. Sanders RW, Venturi M, Schiffner L, Kalyanaraman R, Katinger H, et al. (2002) The mannose-dependent epitope for neutralizing antibody 2G12 on human immunodeficiency virus type 1 glycoprotein gp120. J Virol 76: 7293–7305.
61. Scanlan CN, Pantophlet R, Wormald MR, Ollmann Saphire E, Stanfield R, et al. (2002) The broadly neutralizing anti-human immunodeficiency virus type 1 antibody 2G12 recognizes a cluster of alpha1R2 mannose residues on the outer face of gp120. J Virol 76: 7306–7321.
62. Scanlan CN, Pantophlet R, Wormald MR, Saphire EO, Calarese D, et al. (2003) The carbohydrate epitope of the neutralizing anti-HIV-1 antibody 2G12. Adv Exp Med Biol 535: 205–218.
63. Gray ES, Moody MA, Wibmer CK, Chen X, Marshall D, et al. (2011) Isolation of a monoclonal antibody that targets the alpha-2 helix of gp120 and represents the initial autologous neutralizing-antibody response in an HIV-1 subtype Cinfected individual. J Virol 85: 7719–7729.
64. Julien JP, Lee JH, Cupo A, Murin CD, Derking R, et al. (2013) Asymmetric recognition of the HIV-1 trimer by broadly neutralizing antibody PG9. Proc Natl Acad Sci U S A 110: 4351–4356.
65. West AP, Jr., Scharf L, Horwitz J, Klein F, Nussenzweig MC, et al. (2013) Computational analysis of anti-HIV-1 antibody neutralization panel data to identify potential functional epitope residues. Proc Natl Acad Sci U S A [epub ahead of print].
66. Balla-Jhagjhoorsingh SS, Corti D, Heyndrickx L, Willems E, Vereecken K, et al. (2013) The N276 Glycosylation Site Is Required for HIV-1 Neutralization by the CD4 Binding Site Specific HJ16 Monoclonal Antibody. PLoS One 8: e68863.
67. Diskin R, Klein F, Horwitz JA, Halper-Stromberg A, Sather DN, et al. (2013) Restricting HIV-1 pathways for escape using rationally designed anti-HIV-1 antibodies. J Exp Med 210: 1235–1249.
68. Zhou T, Xu L, Dey B, Hessell AJ, Van Ryk D, et al. (2007) Structural definition of a conserved neutralization epitope on HIV-1 gp120. Nature 445: 732–737.
69. Jardine J, Julien JP, Menis S, Ota T, Kalyuzhniy O, et al. (2013) Rational HIV Immunogen Design to Target Specific Germline B Cell Receptors. Science 340(6133):711–6.
70. McGuire AT, Hoot S, Dreyer AM, Lippy A, Stuart A, et al. (2013) Engineering HIV envelope protein to activate germline B cell receptors of broadly neutralizing anti-CD4 binding site antibodies. J Exp Med 210(4):655–63.
71. West AP, Jr., Diskin R, Nussenzweig MC, Bjorkman PJ (2012) Structural basis for germ-line gene usage of a potent class of antibodies targeting the CD4binding site of HIV-1 gp120. Proc Natl Acad Sci U S A 109: E2083–2090.
72. Liao HX, Bonsignori M, Alam SM, McLellan JS, Tomaras GD, et al. (2013) Vaccine Induction of Antibodies against a Structurally Heterogeneous Site of Immune Pressure within HIV-1 Envelope

Protein Variable Regions 1 and 2. Immunity 38: 176–186.
73. Krachmarov C, Lai Z, Honnen WJ, Salomon A, Gorny MK, et al. (2011) Characterization of structural features and diversity of variable-region determinants of related quaternary epitopes recognized by human and rhesus macaque monoclonal antibodies possessing unusually potent neutralizing activities. J Virol 85: 10730–10740.
74. Wu X, Changela A, O'Dell S, Schmidt SD, Pancera M, et al. (2011) Immunotypes of a quaternary site of HIV-1 vulnerability and their recognition by antibodies. J Virol 85: 4578–4585.
75. Murphy MK, Yue L, Pan R, Boliar S, Sethi A, et al. (2013) Viral Escape from Neutralizing Antibodies in Early Subtype A HIV-1 Infection Drives an Increase in Autologous Neutralization Breadth. PLoS Pathog 9: e1003173.
76. Liao HX, Lynch R, Zhou T, Gao F, Alam SM, et al. (2013) Co-evolution of a broadly neutralizing HIV-1 antibody and founder virus. Nature 496: 469–476.
77. van Loggerenberg F, Mlisana K, Williamson C, Auld SC, Morris L, et al. (2008) Establishing a cohort at high risk of HIV infection in South Africa: challenges and experiences of the CAPRISA 002 acute infection study. PLoS ONE 3: e1954.
78. Salazar-Gonzalez JF, Bailes E, Pham KT, Salazar MG, Guffey MB, et al. (2008) Deciphering human immunodeficiency virus type 1 transmission and early envelope diversification by single-genome amplification and sequencing. J Virol 82: 3952–3970.
79. Platt EJ, Wehrly K, Kuhmann SE, Chesebro B, Kabat D (1998) Effects of CCR5 and CD4 cell surface concentrations on infections by macrophagetropic isolates of human immunodeficiency virus type 1. J Virol 72: 2855–2864.
80. Wei X, Decker JM, Liu H, Zhang Z, Arani RB, et al. (2002) Emergence of resistant human immunodeficiency virus type 1 in patients receiving fusion inhibitor (T-20) monotherapy. Antimicrob Agents Chemother 46: 1896–1905.
81. Montefiori D (2004) Evaluating neutralizing antibodies againts HIV, SIV and SHIV in luciferase reporter gene assays. In: J. E. . Coligan AMK, D. H. . Margulies, E. M. . Shevach, W. . Strober, and R. . Coico, editor. Current Protocols in Immunology. New York, NY.: John Wiley * Sons. pp. 12.11.11– 12.11.15.

CHAPTER FIVE: STRUCTURE AND RECOGNITION OF A STRAIN-SPECIFIC GLYCAN-DEPENDENT CD4 BINDING SITE HIV-1 NEUTRALIZING ANTIBODY

Submitted to Journal of Virology: July 2016

Structure of an N276-dependent HIV-1 Neutralizing Antibody Targeting a Rare V5 Glycan Hole adjacent to the CD4 Binding Site

Constantinos Kurt Wibmer[1,2,3], Jason Gorman[3], Colin S. Anthony[4], Nonhlanhla N. Mkhize[1,2], Aliaksandr Druz[3], Talita York[4], Stephen D. Schmidt[3], Phillip Labuschagne[5], Mark K. Louder[3], Robert T. Bailer[3], Salim S. Abdool Karim[6,7], John R. Mascola[3], Carolyn Williamson[4,6], Penny L. Moore[1,2,6], Peter D. Kwong[#3], and Lynn Morris[#1,2,6]

---

1 *Centre for HIV and STIs, National Institute for Communicable Diseases (NICD), of the National Health Laboratory Service (NHLS), Johannesburg, South Africa;* **2** *Faculty of Health Sciences, University of the Witwatersrand, Johannesburg, South Africa;* **3** *Vaccine Research Center, National Institute of Allergy and Infectious Diseases, National Institutes of Health, Bethesda, MD, United States of America;* **4** *Institute of Infectious Disease and Molecular Medicine (IDM) and Division of Medical Virology, University of Cape Town and NHLS, Cape Town, South Africa;* **5** *South African National Bioinformatics Institute, University of the Western Cape, Cape Town, South Africa;* **6** *Centre for the AIDS Programme of Research in South Africa (CAPRISA), University of KwaZulu-Natal, Durban, South Africa;* **7** *Department of Epidemiology, Columbia University, New York, NY, United States of America*

[#]Corresponding Authors: Peter D. Kwong, and Lynn Morris

E-mail: pdkwong@nih.gov / lynnm@nicd.ac.za

Running Title: N276-dependent CD4bs Antibody Targets a V5 Glycan Hole

Abstract

All HIV-1 infected individuals develop strain-specific neutralizing antibodies to their infecting virus, which in some cases mature into broadly neutralizing antibodies. Defining the epitopes of strain-specific antibodies that overlap with conserved sites of vulnerability might provide mechanistic insights into how broadly neutralizing antibodies arise. We have previously described an HIV-1 clade C infected donor, CAP257, who developed broadly neutralizing plasma antibodies targeting an N276 glycan-dependent epitope in the CD4 binding site. The initial CD4 binding site response potently neutralized the heterologous tier-2 clade B viral strain RHPA, which was used to design resurfaced gp120 antigens for single B cell sorting. We report the isolation and structural characterization of CAP257-RH1, an N276 glycan-dependent CD4 binding site antibody, representative of the early CD4 binding site plasma response in CAP257. A cocrystal structure of CAP257-RH1 bound to RHPA gp120 revealed critical interactions with the N276 glycan, loop D, and V5, but not with aspartic acid 368, similar to HJ16 and 179NC75. This antibody was derived from IGHV3-33 and IGLV3-10 genes, and neutralized RHPA but not the CAP257 transmitted/founder virus. Its narrow neutralization breadth was attributed to a binding angle that was incompatible with glycosylated V5 loops, present in almost all HIV-1 strains including the CAP257 transmitted/founder virus. Deep sequencing of autologous CAP257 viruses however, revealed minority variants early in infection that lacked V5 glycans. These glycan-free V5 loops likely resulted in unusual holes in the glycan shield that may have been necessary for initiating this N276 glycan-dependent CD4 binding site B cell lineage.

Importance

The conserved CD4 binding site on gp120 is a major target for HIV-1 vaccine design, but key events in the elicitation and maturation of different antibody lineages to this site remain elusive. Studies have shown that strain-specific antibodies can evolve into broadly neutralizing antibodies, or in some cases act as helper lineages. Therefore characterizing the epitopes of strain-specific antibodies will help to inform the design of HIV-1 immunogens to elicit broadly neutralizing antibodies. In this study we isolate a narrowly neutralizing N276 glycan-dependent antibody, and use x-ray crystallography and viral deep sequencing to describe how gp120 lacking glycans in V5 might have elicited these early glycan-dependent CD4 binding site antibodies. These data highlight the importance of glycan holes in the elicitation of B cell lineages targeting the CD4 binding site.

Introduction

Neutralizing antibodies to the HIV-1 envelope (Env) glycoprotein generally appear in all individuals within months of infection (1-4). These antibodies target highly sequence variable epitopes that are fully accessible on pre-fusion Env trimers, such as the immunodominant, solvent exposed, hypervariable regions V1 to V5 (2, 3, 5-8). As a result, these early neutralizing antibodies are strain-specific for the transmitted/founder virus, and rapidly select for escape mutants that drive Env diversification (6). Broadly neutralizing antibodies (bNAbs) that are able to cross-neutralize diverse HIV-1 strains by targeting structurally/functionally conserved regions of Env develop in some individuals later in infection (9-14). Animal studies have shown that bNAbs have the capacity to prevent infection, and are likely the types of antibodies that will need to be elicited by an HIV-1 vaccine (15, 16). Significant effort has therefore gone into designing bNAb-initiating immunogens, and understanding how bNAb precursors become broadly neutralizing. Studies defining the ontogeny of bNAbs have shown that they can develop from strain-specific precursors through affinity maturation, suggesting that in addition to recognising hypervariable loop regions, strain-specific neutralizing antibodies might also overlap the conserved epitopes recognised by bNAbs (17-20). Furthermore, strain-specific or narrowly neutralizing antibodies have the potential to cooperate with other lineages in driving overall viral diversity, which in turn creates stimuli for the diversification of bNAbs (21, 22). Thus studies of strain-specific antibodies are providing important insights for understanding how antibody lineages acquire neutralization breadth.

A large number of bNAbs targeting the CD4 binding site (CD4bs) have been isolated from HIV-1 infected individuals (18, 23-28). These antibodies can be adsorbed out of complex polyclonal sera by gp120 monomers, making them ideal candidates for isolation by flow cytometry. High resolution crystal structures in complex with Env antigens have made this the most well characterized site of vulnerability on the HIV-1 envelope (25, 26, 29). Two classes of CD4bs bNAbs have been described: the VH-gene-restricted class, and the CDR-H3-dominated class. VH-gene-restricted bNAbs all develop from the germline-encoded immunoglobulin heavy chain variable genes IGHV1-2 or IGHV1-46, and were defined by prototypical antibodies VRC01 and 8ANC131 (25, 26, 29, 30). This class has a germline-encoded arginine residue at position 71 in the heavy chain complementarity determining region two (CDR-H2) that

mimics an arginine at position 59 in CD4 by interacting with aspartic acid 368 in the CD4 binding loop of gp120. Over half of the VRC01 interaction with gp120 is mediated by the CDR-H2 (30). As a result, VH-gene-restricted CD4bs bNAbs are all similarly oriented with respect to Env. This angle of approach positions the light chains of IGVH1-2/46 derived CD4bs antibodies proximal to loop D in gp120, causing steric clashes with loop D and/or the glycan at position N276, which is thought to severely hamper the initiation of VH-gene-restricted CD4bs bNAb lineages (31, 32). In contrast, the CDR-H3 dominated class of CD4bs antibodies are derived from a wider variety of IGHV genes, and bind to Env with diverse angles of approach that are not impeded by the N276 glycan (26). Antibodies VRC13 (IGVH1-69), VRC16 (IGVH3-23), and CH103 (IGVH4-59) all form important interactions with D368 that develop through affinity maturation or germline V-D-J recombination, similar to VH1-2/46 class antibodies. A sub-group of the CDR-H3 dominated class, that includes HJ16 (IGVH3-30) and the more recently described 179NC75 (IGVH3-21), have a different mode of recognition where neutralization is independent of interactions with D368, but critically dependent on the N276 glycan (the same glycan that obstructs VH1-2/46 binding) (28, 33). Recombinant Env-derived proteins with a glycan deletion at position N276 are able to engage the germline reverted antibodies of many IGVH1-2/46 derived CD4bs bNAbs, and have been proposed as HIV-1 vaccine immunogens (34, 35). Additional glycan deletions in V5 enable even better binding to VH-gene-restricted bNAb precursors (32). These glycan deletions create large holes in the glycan shield, but their effects on Env antigenicity, and the immunogenicity of the CD4bs, remain to be determined

We have previously characterized the bNAb responses in the plasma of CAP257, a participant of the CAPRISA cohort (36). CAP257 developed three distinct waves of bNAbs that appeared sequentially in the plasma, first targeting the V2 epitope, then the CD4bs, and finally a third as yet undefined epitope. The CAP257 CD4bs bNAbs appeared between 50 and 60 weeks post-infection, peaking in titre at 122 weeks post-infection and declining thereafter. They were critically dependent on the N276 glycan, and unlike most previously described CD4bs bNAbs could be readily adsorbed with D368R mutant gp120s. This CD4bs plasma bNAb response could be further divided into early and late CD4bs antibodies based on sensitivity to an N279D escape mutation that arose in the viral quasispecies at 93 weeks post-infection. Early CD4bs antibodies potently neutralized the tier-2 clade B strain RHPA, but had very narrow

neutralization breadth and were abrogated by the D279 immunotype. Late CD4bs antibodies were tolerant of the D279 immunotype, and this coincided with the acquisition of greater neutralization breadth. These broader antibodies were escaped first by mutations that removed the N276 glycan at 122 weeks post-infection, and then by bulky aromatic side chain substitutions at position R456 in the base of V5 by 163 weeks post-infection.

Here, we designed RHPA-derived sorting antigens to isolate an early member of the CD4bs neutralizing antibody response, called CAP257-RH1, from CAP257 memory B cells. A cocrystal structure of CAP257-RH1 in complex with an RHPA gp120 that included the N276 glycan revealed a CDR-H3-dominated interface that overlapped significantly with the epitopes of CD4bs bNAbs. CAP257-RH1 neutralized one virus, RHPA, out of a large multi-clade panel, and this heterologous strain-specificity was explained by a binding angle that was incompatible with the V5 glycans present in most HIV-1 strains. Analysis of CAP257 autologous viruses by deep sequencing revealed a minority population with glycan-free V5 loops similar to RHPA, which may have initiated this lineage, or provided the antigenic stimuli that allowed it to mature. These findings provide a mechanism for the strain-specificity of early CD4bs neutralizing antibodies in CAP257, which target a rare glycan hole in V5, and have implications for the use of HIV-1 immunogens that are aimed at activating CD4bs bNAb precursors by removing key glycans loop D and/or the V5 loop.

Materials and Methods

Ethics statement

The CAPRISA 002 Acute Infection cohort is comprised of women at high risk of HIV-1 infection in KwaZulu-Natal, South Africa. The CAPRISA Acute Infection study received ethical approval from the Universities of KwaZulu-Natal (E013/04), Cape Town (025/2004), and the Witwatersrand (MM040202). Donor CAP257 provided written informed consent for study participation. Blood samples were collected at regular intervals from seroconversion through to the initiation of antiretroviral therapy, processed, and cryopreserved individually.

Cell culture and pseudovirus preparation

293F suspension cells were cultured in 293Freestyle media (Gibco BRL Life Technologies) at 37°C, 10% CO2, 125RPM. 293S (GntI-/-) cells were cultured in suspension as above, but supplemented with 2% heat-inactivated fetal bovine serum

(FBS). Adherent $CD4^+/CCR5^+$ TZM-bl HeLa and HEK293T cells were grown to confluency in DMEM supplemented with 10% FBS, 22.7 mM HEPES (Gibco BRL Life Technologies), and 50 ug/ml gentamicin (Sigma) at 37°C, 5% CO2. Monolayers were disrupted with 0.25% trypsin in 1 mM EDTA (Sigma). For pseudoviruses, 293T cells were seeded in 10 mL at $2x10^6$ cells/mL in 10 cm^2 dishes. 24 hours later plasmids expressing the Env of interest and the pSG3ΔEnv backbone (obtained from the NIH AIDS Research and Reference Reagent Program, Division of AIDS, NIAID, NIH) were co-transfected using a 3:1 ratio of PEI-MAX 40,000 (Polysicences). Cultures were incubated for 48 hours at 37°C, filtered through 0.45 µm, and frozen in 20% FBS. Mutant Env plasmids were made with the QuikChange Lightning Kit (Stratagene).

ELISA

Recombinant gp120 was coated onto high-binding ELISA plates at 2 µg/mL in Carb/Bicarb buffer at 4°C, pH 10 overnight. Plates were washed between each subsequent step four times with PBS containing 0.05% Tween20. Blocking was done with 5% skim milk powder in PBS for 1 hour at 37°C. Serial dilutions of HIV-1 monoclonal antibodies in 5% skim milk powder in PBS were added for 1 hour at 37°C, and complexes were detected with an anti-Fc/HRP conjugate. ELISA reactions were propagated in 100 µL of enzyme substrate for five minutes and stopped with 25 µL of 1 M HCl. Absorbance was read at 450 nm.

Neutralization Assays

Neutralization assays (as previously described (3, 37)) measured the reduction in relative light units after a single round of pseudovirus infection in the presence of a monoclonal antibody or plasma sample. Samples were serially diluted 1:3 and the ID_{50}/IC_{50} calculated as the dilution at which the infection was reduced by 50%.

Adsorption Assays

Protein aliquots of 400 µg each were coupled to MyOne Tosyl-activated magnetic Dynabeads (Invitrogen) at 37°C, pH 9.5 overnight, and then blocked with 0.5% BSA in 0.0 5% Tween20 PBS overnight at 37°C. Protein conjugated beads were incubated with 200 µL of plasma (diluted 1:20) for two hours at 37°C, then the beads were removed magnetically and the remaining plasma assessed for binding and neutralizing antibodies using ELISA and neutralization assays respectively.

B-cell Sorting

The RHPA-RC positive and RHPA-ADW negative gp120 antigens were engineered with a C-terminal AviTag, and the proteins were biotinylated post-expression using

bulk BirA biotinylation kit (Avidity). Biotinylated sorting antigens were conjugated to streptavidin labelled with Alexafluor (AF647) or brilliant violet (BV420) and titrated for flow cytometry. Thawed PBMCs were stained with sorting probes as well as viability marker Aqua vital (Invitrogen, Carlsbad, CA), CD3 phycoerythrin (PE), CD14 PE, CD16 PE, IgD Fluorescein isothiocyanate (FITC), and CD19 allophycocyanin (APC)-Cy7 (BD Biosciences). Single sorted cells were frozen in RNase-free buffer. Flow cytometric data were acquired on a BD Aria 2 fluorescence-activate cell sorter (FACS), and the data were analyzed using FlowJo software (Tree Star).

Immunoglobulin Gene Amplification

Single B-cell heavy and light chain mRNA transcripts were reverse transcribed using random hexamers, and amplified by nested PCR in five different primer pools (three distinct sets for groups of variable heavy chain genes) as previously described (38, 39). Second round PCR reactions introduced restriction sites that were used to clone the antibodies into mammalian expression vectors for IgG expression.

X-ray Protein Crystallography

CAP257-RH1 monoclonal antibody containing the HRV3C site was bound to protein A, and used to purify an RHPA gp120 core that had already been enriched for by Ni-NTA chromatography (30 mM Imidazole wash and 400 mM Imidazole elution buffers at pH 7). The Fab-gp120 complexes were eluted with HRV3C, and further purified by gel filtration using a superdex 200 column (GE Healthcare). Complexes were concentrated to ~8 mg/mL, aliquoted, and flash frozen in the presence of Endo H at ~200 U/mL. Aliquots were thawed immediately before setting up crystallization drops. 400 nL crystallization screens (containing 50% mother liquor) were set-up over 576 conditions in 96 well sitting drop vapour diffusion plates (Corning) at 25°C, using the Cartesian Honeybee and TTP Labtech Mosquito crystallization robots. A single crystal hit was hand-optimised in 15 well hanging drop diffusion plates using 1 µL drops at 25°C. The final crystallization conditions were 0.1 M HEPES (pH 7.5), 8% PEG4000, 10% isopropanol, and crystals were flash frozen in 15% 2R3R or 25% MPD as a cryoprotectant. Once mounted onto the goniometer only 5% of the crystals yielded measurable x-ray diffraction, and this was considerably improved after these crystals were annealed in situ by diverting the cryostream for three seconds. Two of the crystals diffracted to a final resolution of 3.2 Å. Diffraction data were collected at the Advanced Photon Source (Argonne National Laboratory) SER-CAT ID-22 beamline, at a wavelength of 1.00 Å, 100K, and processed with HKL2000. The structure was

solved by molecular replacement using the PHENIX v1.9-1692 software package and search models 4JZZ, 1NL0, 4HPY. Models were refined with hydrogens to minimise clashes in COOT v0.8 using 5% of the data as an R-free cross validation test set. All structural images were generated in PyMOL Molecular Graphics System, Version 1.3r1edu, Schrodinger LLC.

Next-generation sequencing library preparation.

RNA extraction, cDNA synthesis and subsequent amplification were carried out as described previously (40), with the following modifications: A minimum of 5,000 HIV-1 RNA copies were isolated from longitudinal plasma samples spanning ~3.5 years of infection, using the QIAamp Viral RNA kit (Qiagen). The cDNA synthesis primer was designed to bind to the C5 region of the HIV-1 envelope gene (HXB2 gp160 DNA position 1,408–1,431) and included a randomly assigned 9-mer tag (Primer ID method) to uniquely label each cDNA molecule, followed by a universal primer binding site to allow out-nested PCR amplification of cDNA templates. First-round amplification primers were designed to bind to the end of the V3 loop (HXB2 gp160 DNA position 890-911) and contained a template-specific binding region, followed by a variable-length spacer of 0–3 randomly assigned bases to increase sample complexity. In addition, PCR primers contained 5′ overhangs, introducing binding sites for the Nextera XT indexing primers (Illumina). This allowed the amplification of the C3 to V5 region of the envelope spanning HXB2 gp160 positions 911 to 1408. Nested PCR reactions were carried out using the Nextera XT indexing kit. After indexing, samples were purified using SPIRselect magnetic beads (Beckman Coulter) with a sample volume to bead ratio of 1:0.65, for the removal of <300bp fragments. Samples were quantified using the Qubit dsDNA HS assay (ThermoFisher) and pooled in equimolar concentrations. The pooled amplicons were gel extracted using the QIAquick gel purification kit (Qiagen) to ensure primer removal before the final library was submitted for sequencing on an Illumina MiSeq, using 2 × 300 paired-end chemistry.

Next-generation sequencing data processing and analysis.

Raw reads were processed using a custom pipeline housed within the University of Cape Town High-Performance Computing core. Read quality was assessed using fastqc (http://www.bioinformatics.babraham.ac.uk/projects/fastqc). Short reads (<150 bp) were filtered out using Trimmomatic (41), and reads with an average quality of >Q20 were removed using a custom python script. A low Q-score cut off was used, as the Primer-ID method removes sequencing and PCR error during the consensus

sequence generation step. The overlapping forward and reverse reads were merged using PEAR (42), and the forward primer sequence was stripped out of all reads using a custom python script. Reads where the forward primer could not be found were discarded. An in-house program, developed in R, was used to bin all reads containing an identical Primer ID tag, align the reads within each bin using MAFFT (43), and to produce a consensus sequence based on a majority rule. Consensus sequences from bin of sizes > n (where n is proportional to the size of the largest bin, and had a mean value of 15 for this dataset) were filtered out using the cut-off model previously described in (44). Consensus sequences containing degenerate bases, frame shift mutations, or stop codons were also removed. Custom python scripts were used to calculate and plot the number and frequency of glycosylation sites in the V5 loop.

Results

Design of a resurfaced gp120 core sorting antigen based on the tier-2 strain RHPA

We have previously shown that the CD4bs neutralizing antibodies in CAP257 plasma were similar to HJ16 (36), and could not be adsorbed with the Resurfaced Stabilised gp120 Core (RSC3) sorting antigen used to isolate VRC01. Therefore a new sorting antigen was engineered for CAP257 B-cell isolation based on the tier-2 strain RHPA, which was highly sensitive (ID_{50} titer of ~1:8,000) to the CAP257 CD4bs antibodies. Similar to RSC3, the RHPA gp120 sorting antigens were truncated in the V1-V3 loops as well as the N and C termini, and resurfaced with 47 rare mutations in surface exposed, but normally conserved residues outside the CD4bs (Figure 1A and Supplementary Figure 1A) (24). Hypervariable regions are unlikely to be reactive with heterologous antibodies, and were not resurfaced. The RSC3 cavity filling mutations (M95W, T257S, S375W, A433M) and cystine bonds near loop D (W96C/V275C) that were previously designed to stabilize gp120 in the CD4-bound conformation were avoided, because it was not known how these might affect the CAP257 epitope which differed from VRC01-like antibodies (36). This resurfaced core gp120, called RHPA-RC, bound to the conformation sensitive neutralizing antibodies VRC01 and 2G12, confirming that resurfacing mutations did not compromise protein folding (Supplementary Figure 1B). To enhance the specificity for CAP257 CD4bs antibodies, we also created a negative sorting antigen, called RHPA-ADW, which included three mutations in the gp120 loop D and the base of V5 (T278A, N279D, and R456W) that

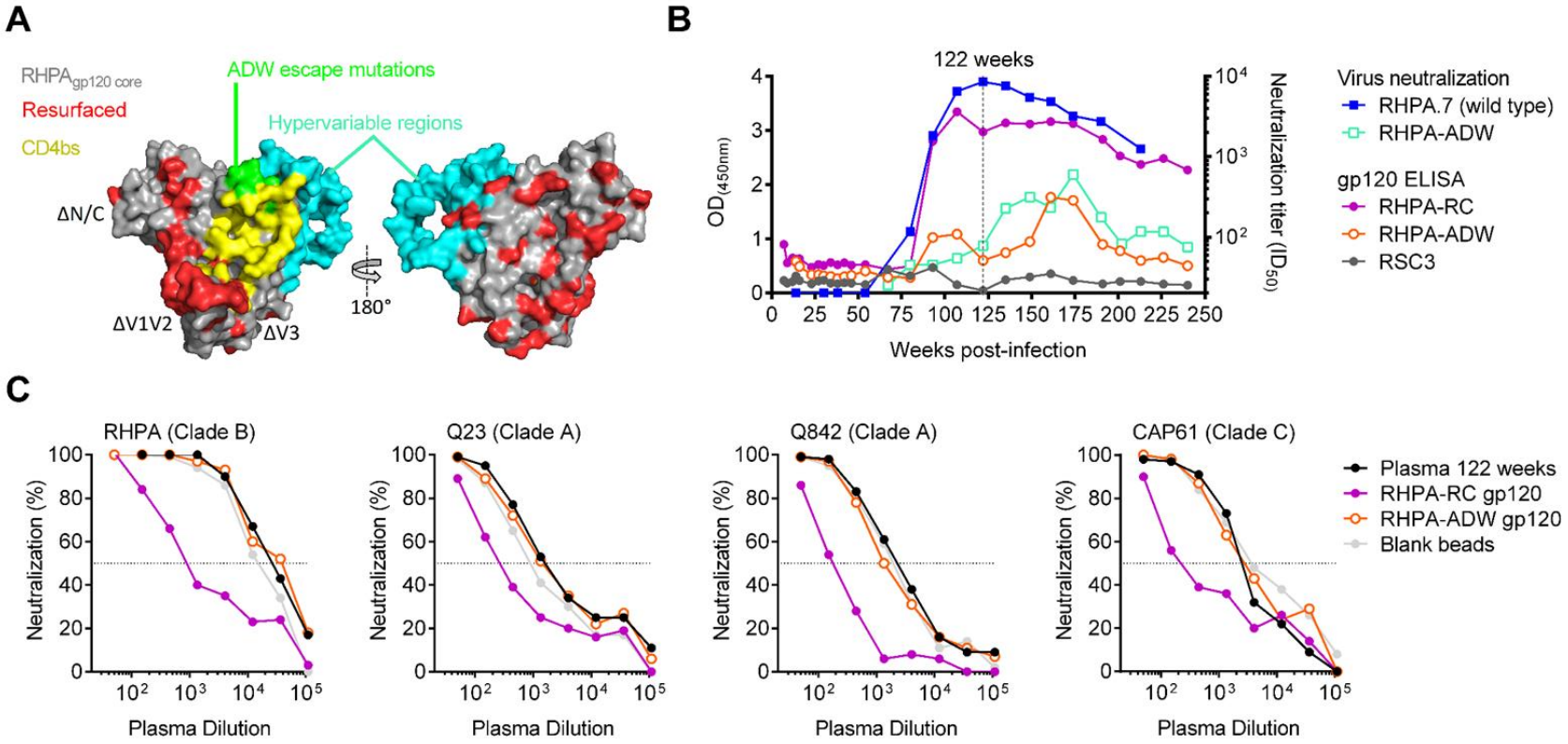

Figure 1: Resurfaced RHPA gp120 antigens bind differentially to CAP257 CD4bs plasma antibodies
A) Surface view of a modelled RHPA gp120 core (grey) showing the location of N/C terminal truncations, deleted V1, V2, or V3 loops, resurfacing mutations (red), and the N276D/T278A, N279D, R456W escape mutations (green), relative to the CD4 binding site (yellow). The hypervariable regions α2, β14, V4, and V5 were not resurfaced and are shown in cyan. B) A comparison of the ability of longitudinal CAP257 plasma samples to bind to the newly designed gp120 core sorting antigens RHPA-RC (purple) and RHPA-ADW (orange) by ELISA, and the neutralization of the heterologous tier 2 strain RHPA (blue) or the RHPA-ADW mutant variant resistant to CAP257 CD4bs antibodies (cyan). The lack of binding to RSC3 is shown in grey. Absorbance readings are plotted on the left y-axis, neutralization titers on the right y-axis, and time course post-infection on the x-axis. The vertical dotted line indicates the 122 week time point at which the adsorption experiments in C were performed. C) Adsorption of CAP257 peak CD4bs neutralizing titers by the positive gp120 antigen RHPA-RC (purple), but not the negative gp120 antigen RHPA-ADW (orange) or uncoated beads (grey). The neutralization of four HIV-1 strains by CAP257 plasma that had been adsorbed with blank beads, or beads coated in the positive gp120 antigen RHPA-RC, or the negative gp120 antigen RHPA-ADW, is plotted on the y-axis as percentage inhibition. Serial dilutions of the adsorbed plasma are indicated on the x-axis.

we have previously shown to contribute to escape from the CD4bs neutralizing antibodies in CAP257 plasma (Figure 1A, green) (36). The negative antigen RHPA-ADW did not bind strongly to the CD4bs antibody VRC01 as expected, but still bound well to 2G12, confirming the antigens conformational integrity and ability to select for CD4bs antibody responses (Supplementary Figure 1C).

The ability of CAP257 CD4bs antibodies to bind to either the RHPA-RC positive antigen or RHPA-ADW negative antigen was assessed by ELISA and adsorption assays. Remarkably, the longitudinal kinetics of CAP257 plasma antibody binding to the positive antigen RHPA-RC tracked with the neutralization of the RHPA parent strain, increasing or decreasing in titre at similar time points throughout infection (Figure 1B). Similarly, CAP257 plasma antibodies did not bind well to the negative antigen RHPA-ADW, although they did show weak binding between 161 and 174 weeks post-infection that tracked with the neutralization of the more resistant RHPA-ADW mutant virus (Figure 1B). Adsorption experiments using CAP257 plasma from 122 weeks post-infection, when the CD4bs antibody titres had peaked, showed that the positive antigen RHPA-RC could efficiently adsorb out the CD4bs neutralizing antibodies against RHPA (a clade B virus), Q23 and Q842 (clade A) and CAP61 (clade C) respectively, while the negative antigen RHPA-ADW could not (Figure 1C). Altogether these data suggested highly specific selection for CAP257 CD4bs neutralizing antibodies by the RHPA-RC positive, RHPA-ADW negative sorting probe combination.

Isolation of an N276 glycan-dependent CD4bs B-cell lineage

A PBMC sample from 107 weeks post-infection, when the CD4bs lineage was likely to be expanding, was selected for B-cell isolation. Single memory B-cells were isolated as $CD3^-$, $CD14^-$, $CD16^-$, IgD^-, RHPA-ADW^-, $CD19^+$, RHPA-RC^+ by flow cytometry (Figure 2A). At least one antibody heavy or light chain could be recovered from 65% of the 94 sorted cells, and DNA sequencing revealed that RHPA-RC selected for three antibody lineages. The first of these was a family of five IGHV4-59/61 heavy chains that were 16%-18% mutated from germline, and shared the same heavy chain family as the CD4bs antibody CH103 (Supplementary Figure 2A). However, the paired light chains for this antibody family could not be recovered. Similarly, a family of six unpaired IGKV1-NL1 light chains that were between 5%-16% mutated were also isolated but could not be functionally assessed without complementary heavy chain sequences (Supplementary Figure 2B). The third family was derived from IGHV3-33

heavy and IGLV3-10 light chains, and is referred to hereafter as the CAP257-RH lineage (Figure 2B and Supplementary Figure 2C). CAP257-RH heavy and light chain genes were 8-11% and 4-13% mutated respectively, and had relatively normal CDR-H3 and CDR-L3 lengths of eleven amino acids each (Kabat numbering). One of these antibodies, CAP257-RH1, bound well to the wild-type RHPA gp120 core by ELISA, and weakly to the positive sorting antigen RHPA-RC (similar to the bNAb HJ16), but did not bind to the negative sorting antigen RHPA-ADW (Figure 2C), confirming the specific selection of CAP257-RH lineage antibodies.

CAP257-RH1 displays strain-specific heterologous neutralization and gp120 binding

We have previously shown that escape from CAP257 CD4bs antibodies was due to the sequential appearance of the three mutations at positions 279, 276/278, and 456. The N279D immunotype switch appeared first, and preceded the acquisition of breadth. Mutations that deleted the glycosylation sequon at position N276 (e.g. T278A) appeared next, while the R456W substitution was the last major escape mutation (36). These CD4bs mutants were used to compare the neutralization of monoclonal antibody (mAb) CAP257-RH1 to contemporaneous plasma from 107 weeks post-infection (Figure 2D). The plasma from 107 weeks post-infection neutralized RHPA at ID_{50} titres exceeding 1:1,000, and by this time had already adapted to tolerate the early D279 escape mutation, but were still dependent on N276 and R456 for effective neutralization (Figure 2D – left panel). CAP257-RH1 potently neutralized RHPA with an IC_{50} of 0.11 µg/mL (Figure 2D – right panel). This neutralization was completely abrogated by N276Q and T278A mutations that removed the N276 glycan, confirming that CAP257-RH1 was a component of the CAP257 CD4bs plasma neutralizing response (Figure 2D). However, unlike CAP257 plasma, CAP257-RH1 neutralization was substantially reduced (100-fold) by the early N279D mutation, and unaffected by the late R456W change. These data suggest that CAP257-RH1 appeared very early in the CAP257 CD4bs neutralizing response, before the emergence of CD4bs-specific neutralization breadth.

The cross-reactivity and breadth of mAb CAP257-RH1 was further examined by ELISA and neutralization assays respectively (Figure 2E and 2F). CAP257-RH1 showed binding to RHPA gp120, but was unable to bind any of the 11 heterologous clade C gp120 monomers tested, all of which were bound by a pooled HIV+ immunoglobulin control (HIV-Ig) (Figure 2E). Similarly, CAP257-RH1 displayed strain-specific

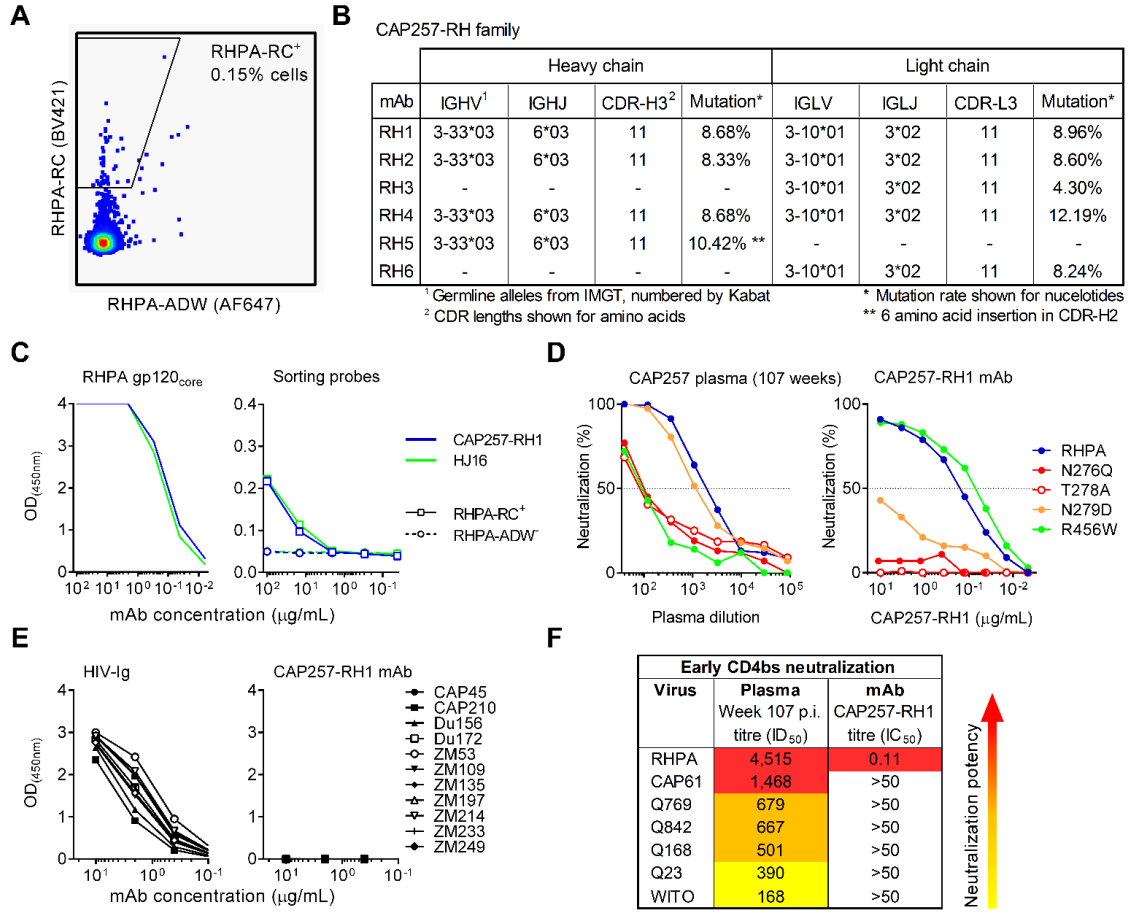

	Heavy chain				Light chain			
mAb	IGHV[1]	IGHJ	CDR-H3[2]	Mutation*	IGLV	IGLJ	CDR-L3	Mutation*
RH1	3-33*03	6*03	11	8.68%	3-10*01	3*02	11	8.96%
RH2	3-33*03	6*03	11	8.33%	3-10*01	3*02	11	8.60%
RH3	-	-	-	-	3-10*01	3*02	11	4.30%
RH4	3-33*03	6*03	11	8.68%	3-10*01	3*02	11	12.19%
RH5	3-33*03	6*03	11	10.42% **	-	-	-	-
RH6	-	-	-	-	3-10*01	3*02	11	8.24%

[1] Germline alleles from IMGT, numbered by Kabat
[2] CDR lengths shown for amino acids
* Mutation rate shown for nucelotides
** 6 amino acid insertion in CDR-H2

Early CD4bs neutralization		
Virus	**Plasma** Week 107 p.i. titre (ID_{50})	**mAb** CAP257-RH1 titre (IC_{50})
RHPA	4,515	0.11
CAP61	1,468	>50
Q769	679	>50
Q842	667	>50
Q168	501	>50
Q23	390	>50
WITO	168	>50

Figure 2: Isolation of an early N276 glycan-dependent CD4bs neutralizing antibody

A) Sort plot showing the percentage of memory B cells identified that were able to bind the RHPA-RC positive sorting antigen (fluorescence plotted on the y-axis) but not to the RHPA-ADW negative sorting antigen (fluorescence plotted on the x-axis). B) Properties of the CAP257-RH lineage members, defined by IMGT and numbered by Kabat. C) Comparison of the binding of CAP257-RH1 (blue) or HJ16 (green) to a wild type RHPA core gp120 (squares), as well as to the positive gp120 sorting antigen RHPA-RC (triangles) or the negative gp120 sorting antigen RHPA-ADW (circles and dashed lines) by ELISA. Absorbance is plotted on the y-axis versus antibody concentration on the x-axis. D) Neutralization of RHPA and select mutants with varied resistance to CAP257 CD4bs plasma antibodies, by either CAP257 plasma from 107 weeks post-infection, or the CAP257-RH1 monoclonal antibody isolated from the same time point. Percentage inhibition is plotted on the y-axis and dilution on the x-axis. E) ELISA binding of an anti-HIV immunoglobulin pool (positive control) or monoclonal antibody CAP257-RH1 to 11 clade C gp120 proteins. F) Neutralization of seven heterologous viruses sensitive to early CAP257 CD4bs antibodies, by either CAP257 plasma from 107 weeks post-infection, or the monoclonal antibody CAP257-RH1. Increasing potency is indicated by warmer colours.

heterologous neutralization of only RHPA among the 196 virus multi-clade panel tested, including other viruses neutralized by early CAP257 CD4bs neutralizing antibodies (Figure 2F and Supplementary Table 1). CAP257-RH1 did not display incomplete neutralization maxima, as seen with a number of recently isolated glycan-dependent HIV-1 bNAbs (45).

Structural classification of CAP257-RH1 as a CDR-H3-dominated class CD4bs antibody

A cocrystal structure of the CAP257-RH1 Fab region bound to the RHPA core gp120, was determined to 3.2Å resolution (Table 1 and Figure 3A). The structure included a NAG_2MAN_5 glycan at position N276 bound in the paratope (shown in light green), and confirmed the CD4bs as the target for CAP257-RH1 neutralization. The crystallization conditions included Endo H to facilitate slow, in-drop deglycosylation of gp120, since pre-incubation with Endo H disrupted the Fab-gp120 complexes, however the enzyme was at a very low concentration and did not contribute to the asymmetric unit. The CAP257-RH1 angle of approach was compatible with Env oligomerization, and did not clash with the V1V2 domain (Figure 3B) as has been seen for other narrowly neutralizing CD4bs antibodies (46, 47). The interface between CAP257-RH1 and $RHPA_{gp120}$ buries a total surface area of ~1,046 $Å^2$, to which the heavy chain contributes ~584 $Å^2$ and the light chain ~462 $Å^2$ respectively (Figure 3C and Supplementary Tables 2, 3, and 4). Unlike other CD4bs antibodies, CAP257-RH1 does not extend its CDRs deep into the cavity bound by CD4, but instead interacts with more peripheral regions of the CD4bs including loop D, V5, and the CD4 binding loop (Figure 3C, 3D, and Supplementary Figure 3). Accordingly protein-protein interactions with gp120 account for ~642 $Å^2$ of the total buried surface area. More than one third of the total interface (~404 $Å^2$) involves interactions with the N276 glycan, which fits snugly at the heavy-light chain interface where each chain contributes ~196 $Å^2$ and ~208 $Å^2$ of bound surface area respectively. This is similar to the 300 $Å^2$ to 400 $Å^2$ buried by N276 in the interfaces of some VRC01 relatives which are not glycan-dependent, but is only half as large as the interface with N276 made by 8ANC195 (48-50). The gp120 used for these crystallization experiments was grown in HEK293S GntI(-/-) cells to facilitate deglycosylation at pH 7. As a result, the cocrystal structure includes a low mannose glycan bound in the CAP257-RH1 paratope. Previously, the N276 glycan has been characterized on monomeric gp120 as mostly complex in composition (51-53), but a more recent analysis of native pre-fusion trimers suggests

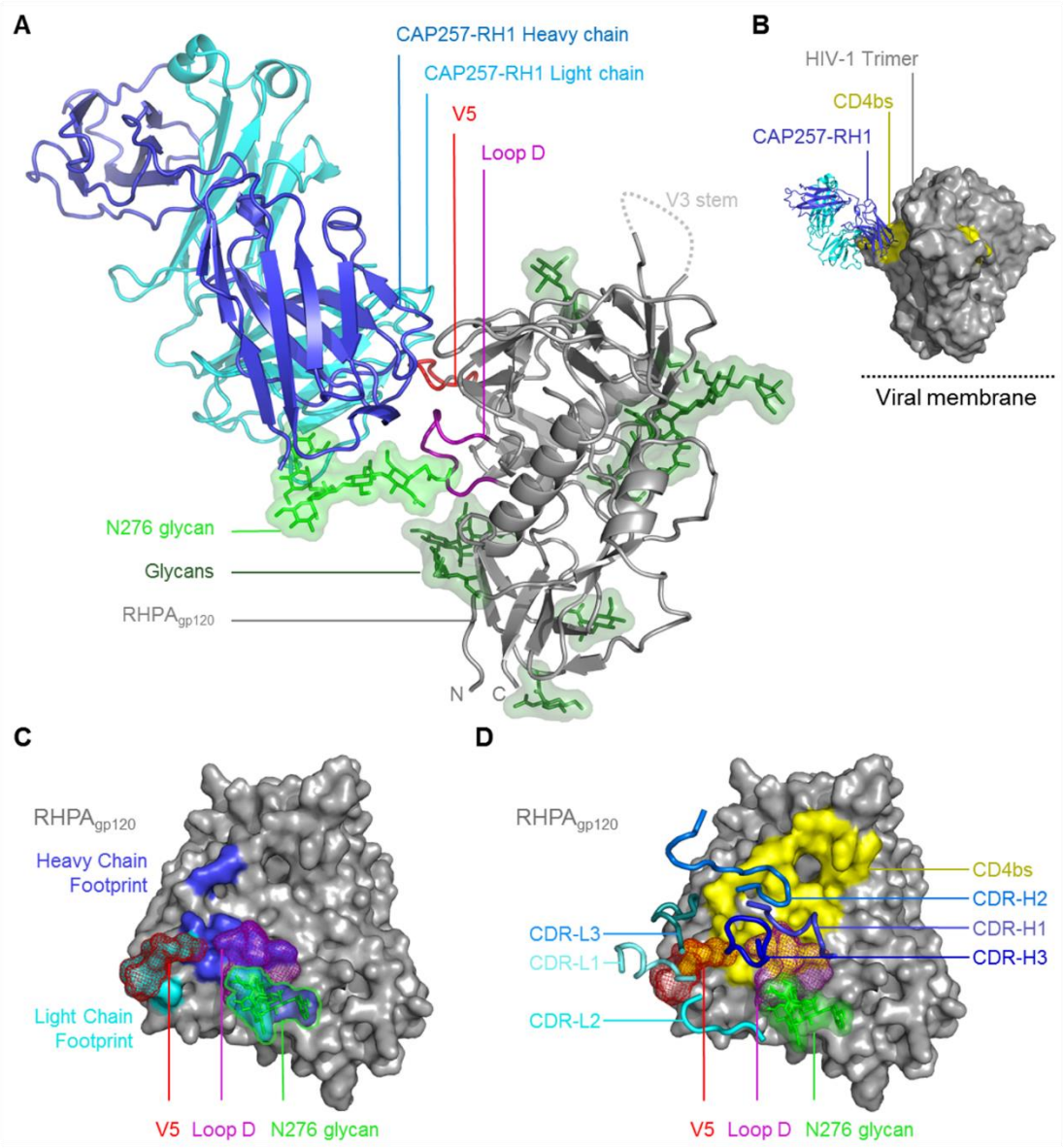

Figure 3: Crystal structure of CAP257-RH1 bound to the N276 glycan in RHPA gp120

A) An overview of the CAP257-RH1 Fab and RHPA core gp120 cocrystal structure shown in cartoon view. The CAP257-RH1 heavy and light chains are shown in dark and light blue respectively. RHPA gp120 is coloured grey, truncated N/C termini as well as the V3 loop stem are labelled, and loop D and V5 are shown in purple and red respectively. Glycans are shown in stick view, with green semi-transparent surfaces. The N276 glycan is indicated by its lighter shade. B) A surface view of the HIV-1 Env trimer (pdb 4TVP) is shown in grey, with the monoclonal antibody CAP257-RH1 shown in blue docked into its epitope (by superimposition). The CD4bs is coloured yellow, and the location of the viral membrane is indicated. C) Surface view of RHPA gp120 in grey, coloured in dark or light blue to show the CAP257-RH1 heavy and light chain footprints respectively. Loop D and V5 are indicated with purple or red mesh respectively, and the N276 glycan (shown in stick and surface view) is outlined in green. D) Surface view of RHPA gp120, with the CD4 binding footprint coloured yellow. Loop D, V5, and the N276 glycan are indicated as in C. The CAP257-RH1 CDRs are shown as thick cartoon loops.

Table 1: Data collection and refinement statistics (molecular replacement)

	CAP257-RH1 bound to RHPA gp120 core
Data collection	
Space group	$P2_12_12_1$
Cell dimensions	
a, *b*, *c* (Å)	68.176, 71.139, 190.596
α, β, γ (°)	90, 90, 90
Resolution (Å)	50-3.21 (3.36-3.27, 3.27-3.21)[a]
R_{merge}	5.9 (23.8, 27.1)[a]
$I / \sigma I$	10.72 (2.37, 2.12)[a]
Completeness (%)	81.99 (54.4, 33.1)[a]
Redundancy	3.5 (2.7, 2.3)[a]
Refinement	
Resolution (Å)	50-3.21
No. reflections	12,967
R_{work} / R_{free}	0.24 / 0.28
No. atoms (no H)	6,143
Protein	5,864
Glycan	271
Ligand	4
Water	2
B factors (no H)	101.36
Protein	99.54
Glycan	140.28
Water	65.05
Wilson B-factor (Å^2), all atoms	85.66
r.m.s deviations	
Bond lengths (Å)	0.003
Bond angles (°)	0.612
Ramachandran Favoured %	91 %
Ramachandran Allowed	99.7%
Ramachandran Outliers %	0.3 %
Molprobity clashscore	1.98
MolProbity overall score	1.48
C_1 carbohydrate geometry (%)	100
PDB ID	

[a]Values in parentheses are for highest-resolution shells.

that this glycan is mostly oligomannose in composition, and varies from Man_5 to Man_8 (54). Additional mannose residues could be modelled at the termini of each glycan arm in the CAP257-RH1 bound structure, suggesting that this antibodies binding was compatible with both NAG_2MAN_5 low and $NAG_2MAN_{8/9}$ high mannose glycans at position N276 (Figure 4A). In both CAP257-RH1 and 8ANC195 bound structures, the N276 glycan adopts a similar orientation that differs substantially from the reoriented glycan conformation bound by VRC01-like antibodies (Figure 4B). Similarly, the CAP257-RH1 bound orientation of the N276 glycan was compatible with an HJ16 bound gp120 (by superimposing the gp120 molecules from both structures) and packed closely against the HJ16 light chain in the model (Figure 4C), indicative of a common N276 glycan conformation bound by these neutralizing antibodies. Thus, this structure of the N276 glycan may represent a commonly occupied orientation of the N276 glycan when bound by bNAbs.

The CAP257-RH1 paratope is centred on its eleven amino acid long CDR-H3, which accounts for ~53% of the heavy chain interface (Figure 3D). The remaining heavy chain CDR loops were positioned to interact with the conserved CD4bs, while the light chain CDRs were more distal, in close proximity to V5. In concordance with plasma mapping, CAP257-RH1 does not interact productively with D368 in gp120, despite a CDR-H2 that extended toward the CD4 binding loop (similar to VRC01) where $H56_{HC}$ forms a hydrogen bond with the $S365_{gp120}$ backbone carbonyl oxygen (Figure 5A – 1st panel). The CDR-H1 and CDR-H3 loops are both in close proximity to gp120 loop D, where $E31_{HC}$ and $D100A_{HC}$ makes hydrogen bonds with $N279_{gp120}$ and $N280_{gp120}$ respectively (Figure 5A – 2nd panel). The interaction between $E31_{HC}$ and $N279_{gp120}$ explains the antibody's preference for an N279 immunotype, as a negatively charged aspartic acid immunotype at position 279 would clash electrostatically with the glutamic acid in the CDR-H1. The CDR-H3 also makes contact with the peptide backbone of loop D and V5 through $K99_{HC}$, and with the D2 arm of the N276 glycan through $D101_{HC}$, while $K32_{HC}$ in the CDR-H1 is positioned to make weak contact with the first NAG moiety. CAP257-RH1 also contacts the D1 arm of the N276 glycan via its heavy chain N terminal residue (Figure 5A 3rd panel). In addition to these heavy chain interactions, the CDR-L2 of the light chain also contributes to N276 glycan interactions by inserting $F55_{LC}$ in between the second NAG moiety and the D2 arm of the glycan, as well as a hydrogen bond with the backbone carbonyl of $S56_{LC}$ (Figure 5A 3rd panel).

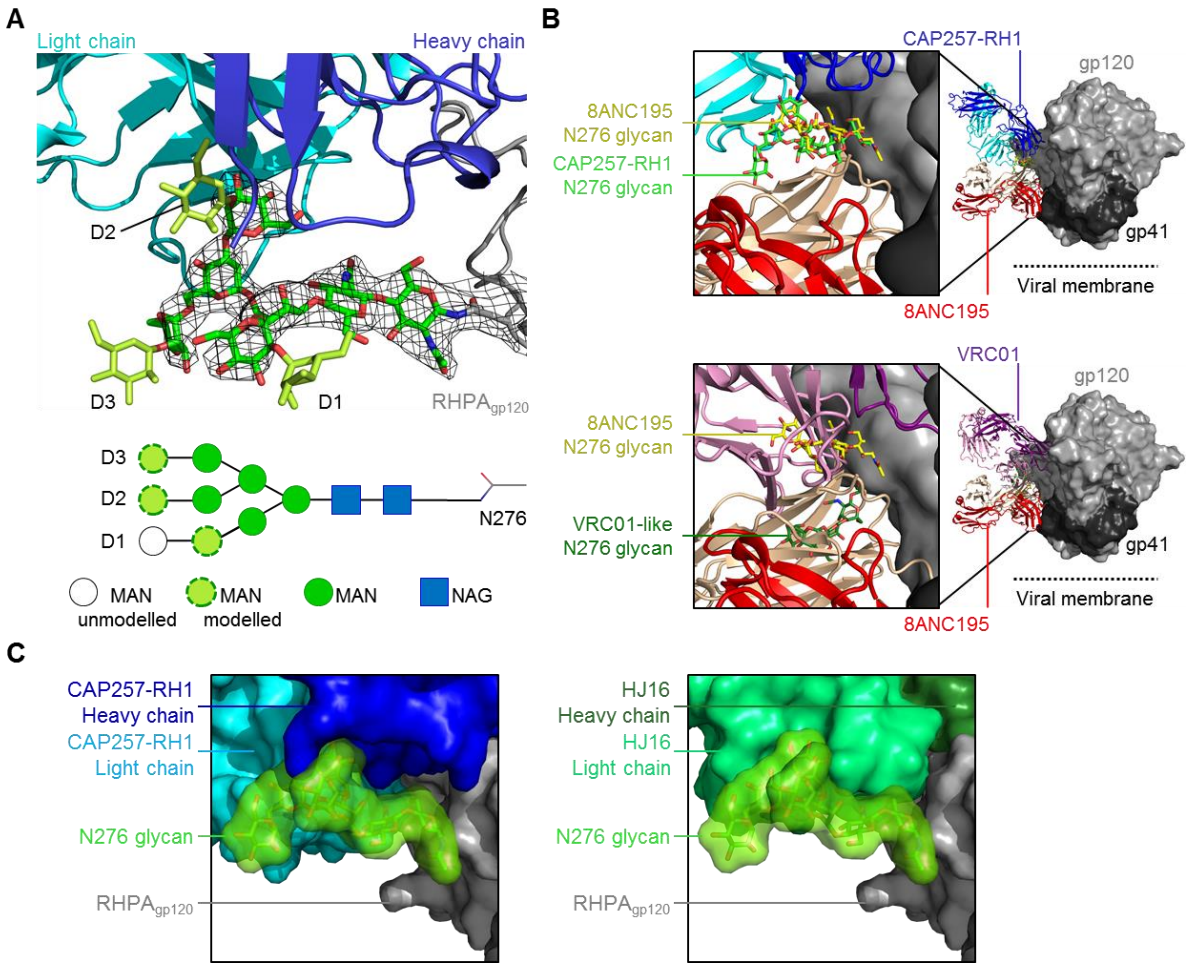

Figure 4: Analysis of the N276 glycan when bound by neutralizing antibodies
A) CAP257-RH1 is shown in cartoon view, coloured as in figure 3, interacting with the N276 glycan (shown with green sticks). The 2*Fo – Fc* electron density map (contoured at 1σ) of the N276 glycan is shown with black mesh. Additional mannose moieties added to the glycan termini are shown in lime green, and the glycan arms are labelled. A schematic of the glycan is also shown below, and sugars with either visible density or those modelled onto the structure, are labelled. B) A comparison of the N276 glycan orientations when bound by 8ANC195 (glycan shown in yellow, Fab heavy and light chains shown in peach and red respectively), CAP257-RH1 (glycan shown in light green, Fab heavy and light chain shown in blue and cyan respectively), or VRC01-like antibodies (glycan shown in dark green, Fab heavy and light chains shown in purple and pink respectively). The Fab bound glycan complexes (PDB codes 4P9H and 4JKP) were superimposed onto the HIV-1 Env trimer structure 4TVP shown in light (gp120) and dark (gp41) grey surface view. B) A surface view of the N276 glycan (green) bound by CAP257-RH1 (coloured as in A) is shown in the left panel. In the right panel, the HJ16 cocrystal structure (PDB code 4YE4) was superimposed onto the CAP257-RH1 bound gp120, showing compatibility with this N276 glycan orientation. HJ16 heavy and light chains are coloured light and dark green respectively.

To evaluate the relative contribution for each of the contacts identified above, alanine scanning mutants of the CAP257-RH1 paratope were made in the heavy chain (Figure 5B) or light chain (Figure 5C), and assessed for their ability to neutralize RHPA. Heavy chain mutations at positions $K32_{HC}$ in the CDR-H1 and $H56_{HC}$ in the CDR-H2 marginally affected CAP257-RH1 neutralization, while the $E31A_{HC}$ mutation had a much more substantial effect (Figure 5B). The reduction in potency of the $E31A_{HC}$ mutant against RHPA was equivalent to that of the wild type antibody against the $N279D_{gp120}$ mutant virus, consistent with the observed interaction between these two residues (Figure 2D compared to Figure 5B). In contrast to the CDR-H1/H2 contributions, all of the CDR-H3 mutants failed to neutralize RHPA, highlighting the important role of this region in mediating neutralization. These data support the classification of CAP257-RH1 as having a CDR-H3-dominated paratope, despite a CDR-H3 loop length much shorter than other HIV-1 CD4bs antibodies of this class.

The CDR-L2 $F55A_{LC}$ mutant, which disrupts interactions with the N276 glycan, was also unable to neutralize RHPA (Figure 5C). Two additional light chain contacts in the CDR-L1 at positions $K31_{LC}$ and $W32_{LC}$ also had a substantial contribution to CAP257-RH1 neutralization, but alanine mutations at these sites did not completely abrogate the antibody's activity (Figure 5C). While interactions with the conserved CD4bs (loop D and the CD4 binding loop) are mediated exclusively by the CAP257-RH1 heavy chain, the light chain is positioned close to V5, with its CDR-L1 binding perpendicularly over the V5 loop apex (Figure 5D). Light chain interactions with V5 account for ~259 $Å^2$ of buried surface area, and include extensive hydrogen bonding with the V5 peptide backbone, and notable van der Waals contributions by the $W32_{LC}$ side chain which inserts behind V5 to contact the backbone carbonyl of $D461_{gp120}$. This displaces the $D461_{gp120}$ side chain into the CAP257-RH1 paratope where it interacts with $K31_{LC}$ (Figure 5D). However, mutating $D461_{gp120}$ to alanine in the RHPA V5 loop affected IC_{50} but was not critical for neutralization, while mutating $V460_{gp120}$ actually enhanced CAP257-RH1 neutralization (Figure 5E). When taken altogether, both heavy and light chain interactions with the N276 glycan ($D101_{HC}$ and $F55_{LC}$, but not $K32_{HC}$), loop D ($E31_{HC}$ and $D100A_{HC}$), or the base of V5 ($K99_{HC}$) were critical to CAP257-RH1 neutralization, while specific contacts with the hypervariable V5 loop apex ($K31_{LC}$ and $W32_{LC}$) were not essential to neutralization and thus not the primary determinant of CAP257-RH1 strain-specificity.

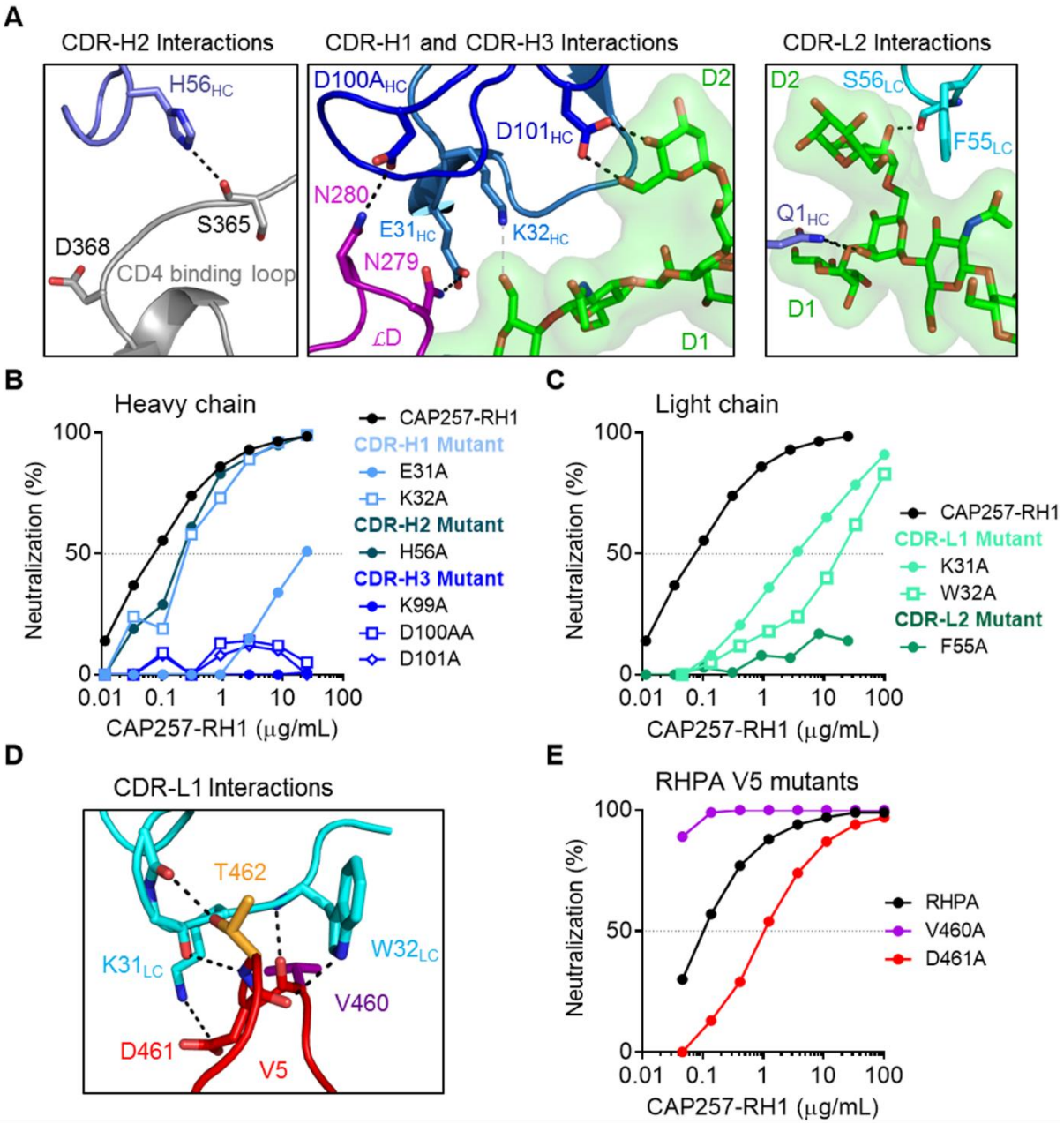

Figure 5: Atomic details of the CAP257-RH1 interaction with RHPA core gp120
A) Polar contacts between CAP257-RH1 the CD4bs/N276 glycan. The CAP257-RH1 CDRs are shown in various shades of blue, while the CD4b binding loop, loop D, and the N276 glycan are coloured grey, purple, and green respectively. Potential hydrogen bonds are shown with the black dotted lines. B) Paratope mapping of the CAP257-RH1 heavy chain by alanine scanning mutagenesis. Mutations are grouped by CDR loop using different shades of blue. Percentage inhibition is plotted on the y-axis and antibody concentration on the x-axis. C) Paratope mapping of the CAP257-RH1 light chain, labelled as in B. D) Atomic details of the interaction between the CAP257-RH1 CDR-L1 (cyan), and the V5 loop of RHPA (red). Polar interactions are indicated as in A. E) Neutralization of various RHPA alanine mutants, plotted as in B.

CAP257-RH1 neutralization was incompatible with glycosylated V5 loops

To better understand the strain specificity of CAP257-RH1, the cocrystal structures of other CD4bs antibodies were superimposed onto the cocrystal structure of CAP257-RH1 bound to RHPA gp120 (Figure 6). Both N276 glycan-dependent antibodies CAP257-RH1 and HJ16 infiltrated less substantially into the CD4bs when compared to the other CD4bs neutralizing antibodies (Figure 6A). The VH-gene-restricted bNAbs VRC01 and CH235.12 were predicted to clash significantly with the CAP257-RH1 bound orientation of the glycan at position N276, but the placement of this glycan was compatible with all of the CDR-H3-dominated class antibodies. These data are consistent with published observations that VH-gene-restricted bNAbs bind better to N276 glycan-deficient Env (31, 32, 55). Another striking difference between the CD4bs antibodies was their binding orientations relative to V5. While VH-gene-restricted CD4bs antibodies completely avoided the V5 loop apex, the binding of CDR-H3 dominated antibodies often placed their light chains in close proximity to V5 (Figure 6B). Overall, less penetration into the recessed CD4bs and greater overlap with the V5 loop apex correlated with reduced neutralization breadth. This was particularly prominent amongst the N276 glycan-dependent CD4bs antibodies HJ16 and CAP257-RH1, which both increased their interacting surfaces with V5 through a bulky tryptophan residue from the CDR-L3 or CDR-L1 loops respectively (shown in Figure 6B). The extent of this overlap suggested that the binding angles for these two antibodies were less tolerant of longer or more glycosylated V5 loops than other CD4bs antibodies such as VRC01.

The RHPA V5 loop is relatively short (five amino acids between position 460 and 464) and unusually glycan-free (Figure 6C). Indeed, glycan-free V5 loops make up only 6% of the ~5000 HIV-1 group M Env sequences in the LANL database. To test whether this lack of glycan contributed towards CAP257-RH1 strain-specificity, V5-glycosylated sequence variants of RHPA were made and tested for their sensitivity to CAP257-RH1, HJ16, and VRC01 (Figure 6D). These V5 mutants were all more resistant to the three CD4bs antibodies tested, though the effect varied depending on the location of the introduced glycosylation sequon. All the mutants were marginally less sensitive to neutralization by VRC01, and this effect was more pronounced for V5 N-terminal glycan substitutions. In contrast HJ16 neutralization was knocked out by a glycan site at position 460_{gp120} and substantially affected by a glycan site at position 462_{gp120}, while CAP257-RH1 neutralization was completely abrogated by introducing

Figure 6: CAP257-RH1 neutralization is constrained by V5 glycosylation

A) A comparison of the relative levels penetration into the recessed CD4bs for various CD4bs neutralizing antibodies when superimposed onto the RHPA crystal structure (grey) shown in surface view. The antibodies are grouped as CDR-H3-dominated or VH-gene-restricted, and ordered according to increasing neutralization breadth. N276 glycan-dependent antibodies are indicated. The N276 glycan is shown in green and the CD4bs is coloured yellow. For all antibodies, the light chains are coloured black, while the heavy chains are shown in varying colours. B) A comparison of the binding angles for the CD4bs antibodies shown in A, relative to the RHPA V5 (indicated with red mesh), with the CAP257-RH1 bound N276 glycan shown in green sticks and semi-transparent surface. All antibodies are shown in cartoon view, with the heavy chains coloured white and the light chains coloured according to the breadth in A. C) A zoomed view of the glycan-free RHPA V5 loop is shown in sticks with transparent surface, and amino acids 460 – 464 are labelled. D) Neutralization of RHPA and glycosylated V5 mutants by VRC01, HJ16, and CAP257-RH1. Percentage inhibition is plotted on the y-axis and antibody concentration on the x-axis.

glycosylation sequons at positions 460_{gp120}, 461_{gp120}, and 462_{gp120}, and significantly affected by a glycan site at position 464_{gp120}. A glycosylation sequon at position 463_{gp120} could not be tested because mutation of $E465_{gp120}$ resulted in non-functional virions. These data are consistent with the level of V5 overlap displayed by each of these antibodies, and supports the hypothesis that CAP257-RH1 neutralization breadth is substantially limited by V5 glycosylation.

A minority population of CAP257 autologous viruses lack glycans in V5

Donor CAP257 was infected with a clade C tier-2 virus, which from the earliest autologous V5 loop consensus (7 weeks post infection) was glycosylated at position 461_{gp120}, and consequently resistant to CAP257-RH1 neutralization (Supplementary Tables 1 and 5). To identify potential autologous glycan-free V5 loops, a panel of ~150 CAP257 Env sequences isolated by SGA from 16 time points throughout CAP257 infection were examined, but all were glycosylated making it unclear which virus stimulated the CAP257-RH lineage (Supplementary Figure 5). The autologous CAP257 viral sequences were further probed by deep sequencing of the V3 to V5 region of Env from 25 individual time points, between 7 weeks (study enrolment) and 202 weeks post-infection, resulting in 19,761 consensus V5 sequences (Figure 7A). The CAP257-RH lineage was isolated from 107 weeks post-infection, where the major viral population had two glycans per V5 loop. However, at time points between 7 weeks and 67 weeks post-infection, a minor population of CAP257 viruses were detected with completely glycan-free V5 loops that were dominated by a D461 immunotype (Figure 7A – red spheres). These sequences peaked in frequency (at 4.9% of total sequences) at 16 weeks post infection (Figure 7B), when the viral load was ~32,000 copies/mL (equating to ~1,568 RNA copies encoding glycan-free V5 Env sequences per mL of blood), but occurred less frequently after the detection of CAP257 CD4bs neutralizing plasma antibodies at 54 weeks post-infection (Figure 7C). A population of glycan-free V5 loops was consistently detectable at very low levels (<1% of total sequences) thereafter, alongside the evolving CAP257 CD4bs neutralizing antibody response, but appeared to be spontaneously generated and were unrelated to the initial glycan-free V5 loops detected prior to the development of CD4bs antibodies.

To evaluate the potential effect of these glycan-free V5 loops on the Env glycan shield, we modelled the surface coverage of NAG_2Man_9 glycans on the Env trimer. Accessibility to the underlying protein surface was evaluated using probe radii of either 1.4Å (the radius of a water molecule), or 10Å (the approximate radius of a single Fab

domain) (Figure 7D). This analysis revealed an unprotected region of the Env protein surface, showing how a glycan hole in V5 exposes epitopes for the induction of autologous neutralizing antibodies, such as CAP257-RH1.

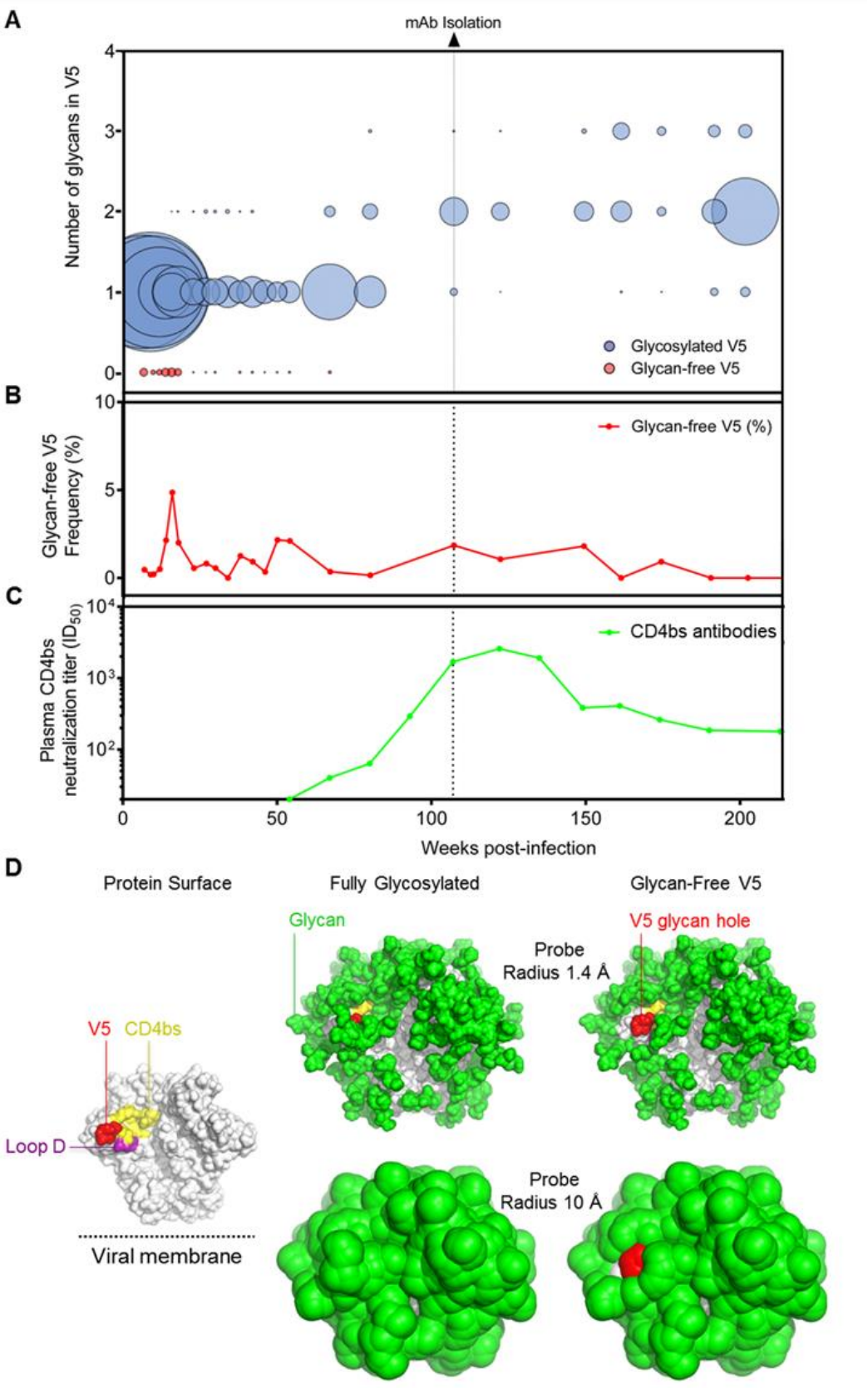

Figure 7: Rare glycan-free V5 sequences from CAP257 reveal a hole in the glycan shield
A) Deep sequencing of autologous V5 loop sequences in donor CAP257, with number of glycans on the y-axis and weeks post-infection on the x-axis. The relative frequencies for the number of glycans in V5 at a particular time point is represented by the size of the spheres, where larger spheres indicate a greater relative number of sequences at that particular time point that have the listed number of glycosylation sequons in V5. Populations of V5 sequences with one or more glycans are shown with blue spheres, while glycan-free V5 sequence populations are shown in red. A dotted vertical line is used to indicate the time point from which CAP257-RH1 was isolated. B) The relative number of glycan-free autologous V5 loops is plotted as a percentage of the total sequences (y-axis) over time (x-axis). C) The neutralization titres (plotted on the y-axis) of the second wave of broadly neutralizing antibodies from CAP257 plasma (as described in (36)), which target the CD4bs, are shown over time (x-axis). D) The HIV-1 Env trimer is shown as the solvent-accessible surface representation (grey), with Loop D, V5, and the CD4bs coloured purple, red, and yellow respectively. The location of the viral membrane is indicated. The glycan shield is modelled and displayed as the solvent-accessible surface of NAG_2Man_9 glycan coverage (green) based on two probe sizes of 1.4 Å (solvent radius, top) and 10.0 Å (the estimated steric footprint of an antibody combining region, bottom), using 4TVP with an additional glycosylation site modeled at residue 241. The solvent-accessible protein surface of V5 comprises a largely exposed region upon deletion of the commonly glycosylated site at residue at 462 (right).

Discussion

The CD4bs on the HIV-1 envelope is the most extensively studied site of vulnerability to antibody neutralization, but not much is known about how these antibodies arise in natural infection, or how they might be induced by vaccination. Here, we isolate and characterise a CD4bs antibody called CAP257-RH1, which recognizes an N276 glycan-dependent epitope targeted by early members of the CD4bs plasma bNAb response that developed in donor CAP257. A cocrystal structure that included the N276 glycan revealed extensive contacts between the CAP257-RH1 heavy chain and conserved elements of the CD4bs. Narrow neutralization breadth was attributed to a light chain binding angle that was incompatible with glycosylated V5 loops present in almost all HIV-1 strains. Rare autologous sequences from early in donor CAP257 infection were found to have glycan-free V5 loops that may have been responsible for engaging the naive B cell that produced this CD4bs antibody lineage. Thus, vaccine immunogens that lack glycans in V5 may provide better exposure for the epitopes targeted by N276 glycan-dependent CD4bs antibodies.

Although the CAP257-RH1 monoclonal antibody is strain-specific for the heterologous virus RHPA, it targets the same N276 glycan-dependent CD4bs epitope as CAP257

plasma bNAbs. In addition, CAP257-RH1 was very sensitive to the N279D mutation that in the plasma only affected the earliest of CAP257 CD4bs neutralizing antibodies, and coincided with the emergence of the later broadly neutralizing CD4bs response. Thus, CAP257-RH1 likely represents an early member of the neutralizing response to the CD4bs in this individual. Three studies detailing the ontogeny of bNAbs have shown that they arose from strain-specific precursors (17, 18, 20). While strain-specific neutralizing antibodies have long been known to target the hypervariable regions of Env (2, 3, 5-8), it has become apparent that the epitopes for strain-specific antibodies may also overlap substantially with the epitopes for bNAbs (56, 57). For instance, 2909 is strain-specific for the heterologous virus SF162, and targets an epitope in V2 (58), but the isolation of PG9 and PG16 showed that this epitope was also vulnerable to bNAbs (59). The limited neutralization breadth of 2909 could be explained by the requirement for a lysine at position 160 (normally glycosylated) creating a hole in the Env glycan shield (50, 57). CAP257-RH1 specificity was similarly constrained by the requirement for a glycan-free V5 loop and a slight preference for the D461 immunotype. However CAP257-RH1 still neutralized V5 alanine mutants of RHPA, and could conceivably mature to recognise more diverse V5 loop sequences. Alternatively, these antibodies may have helped drive viral diversity in the CD4bs, in turn promoting the development of plasma neutralization breadth, similar to the cooperative evolution of the CH103 and CH235 lineages in donor CH505 (21). It is not known whether the CAP257-RH lineage also went on to develop broadly neutralizing activity, and the isolation of CD4bs bNAbs from CAP257 would help to address this question.

CAP257-RH1, together with HJ16 and 179NC75, form a sub-class of the CDR-H3 dominated CD4bs antibodies (26, 28), that are critically dependent on the N276 glycan, but not D368 (28, 36, 60). CAP257-RH1 binds the N276 glycan in a recess created by the antibody heavy-light chain interface, and recognises the glycan with a similar orientation to bNAb 8ANC195 that targets the gp120-gp41 interface (49, 61). This glycan orientation could also be accommodated by glycan-dependent CD4bs antibody HJ16 in our modelling analysis, but not by the VH-gene-restricted antibodies which clash sterically with N276, consistent with published crystal structures showing relocation of this glycan by VRC01 and related antibodies (48, 50). The degree of similarity in N276 glycan recognition is comparable to the N332 glycan supersite, which is oriented in the same conformation by antibodies with very different epitopes

and angles of approach (62). Together with more recent insights into the structure of the glycan shield (50, 54), these data help to define the role of N276 in bNAb development. HJ16 and other CDR-H3-dominated class bNAbs increase interactions with the CD4 binding pocket through long CDR-H3 loops. CAP257-RH1 binds to the periphery of the CD4bs, but does not extend deep into the conformationally occluded CD4 binding pocket, and its deviation from the previously described CD4bs of vulnerability results in a narrow neutralization breadth profile.

CAP257-RH1 was unable to neutralize viruses with glycosylated V5 loops, including the CAP257 transmitted/founder virus. We speculate that the CAP257-RH lineage was elicited by low frequency autologous variants that had glycan-free V5 loops. These viruses never came to dominate the viral population, possibly due to selection pressures imposed by the CAP257-RH lineage. Alternatively, it is also possible that rare glycan skipping events in V5 (where glycosylation sequons are missed by oligosaccharyltransferase in the Golgi) stimulated the lineage. Interestingly, in another individual (CAP256) who developed broad and potent V2-reactive antibodies from a strain-specific precursor (17, 63), the bNAb-initiating Env was also found to be relatively rare compared to the dominantly circulating viral variant (64). Similar to the CAP257-RH1 epitope, several other studies have also identified strain-specific neutralizing antibody targets created by unusual holes in the glycan shield (22, 58, 65, 66). These include vaccine induced antibodies such as the strain-specific macaque antibody DH427, which targets a large glycan hole in both V5 and loop E, allowing an angle of approach that does not include the CD4bs, and therefore is unlikely to mature towards neutralization breadth (67). In donor 45, from which VRC01 was isolated, proviral sequences with a rare hole in the glycan shield at position N276 have been identified (68, 69), which may represent rare bNAb-initiating Envs that set off the VRC01-like lineages in this donor. Thus, glycan holes may elicit highly strain-specific responses unable to further mature towards neutralization breadth, but may also represent key features of HIV-1 immunogens that engage the appropriate precursors of HIV-1 bNAbs. While these holes may recruit the appropriate naïve B cells, driving the process towards breadth will likely require the addition of fully glycosylated native trimeric immunogens that select for mutations able to accommodate the Env glycan shield (34, 35).

Immunogens designed to activate VRC01-class VH-gene-restricted CD4bs bNAb precursors have so far shown promising results in animal studies. These antigens not

only lack the N276 glycan, but have also been modified to bind with higher affinity to the VH1-2 germline gene (31, 32). Germline gene knock-in mice immunized with these constructs produced antibodies with neutralization compatible mouse light chains (34, 35), and germline targeting antigens preferentially select for VH-gene-restricted precursors in healthy individuals (70). In addition to N276 mutants, Env immunogens that also lack glycans in V5 bind even better to the VH-gene-restricted CD4bs bNAb precursors (32). In this study, we show that viruses lacking glycans in V5 are also considerably better neutralized by N276 glycan-dependent antibodies. This sub-class of CD4bs antibodies would not be elicited by the N276-deficient Env immunogens designed to elicit VH-gene-restricted antibodies. Based on the CAP257-RH1 cocrystal structure, a glycan-free V5 may have been expressly required for activating the CAP257-RH lineage, and immunogens incorporating this feature may also improve binding to the precursors of other N276 glycan-dependent antibodies.

Altogether, these data provide insights into the N276 glycan as a target for HIV-1 neutralizing CD4bs antibodies, and the types of immunogens that might be required to activate their naïve B cell precursors. Further isolation and characterization of N276 glycan-dependent bNAbs will be important for understanding how CD4bs immunogens might better capture the entire repertoire of bNAb precursors by immunization. Future studies will aim at assessing the role of glycan holes in priming B cell responses that might mature to acquire broadly neutralizing activity.

Acknowledgements

We are grateful to participant CAP257 in the CAPRISA Acute Infection cohort and to the clinical/laboratory staff at CAPRISA for their continued commitment to the study, as well as to the staff at sector 22 (Southeast Region Collaborative Access Team) at the Advanced Photon Source, Argonne National Laboratory. We would like to thank Bronwen E Lambson, Jinal N Bhiman, and Nicole A Doria-Rose for useful discussions pertaining to monoclonal antibody isolation, and the Columbia University-Southern African Fogarty AIDS International Training and Research Program for providing the opportunity to learn protein x-ray crystallography at the Vaccine Research Center (C.K.W.).

References

1. Gray ES, Moore PL, Choge IA, Decker JM, Bibollet-Ruche F, Li H, Leseka N, Treurnicht F, Mlisana K, Shaw GM, Karim SS, Williamson C, Morris L. 2007. Neutralizing antibody responses in acute human immunodeficiency virus type 1 subtype C infection. J Virol 81:6187-6196.
2. Richman DD, Wrin T, Little SJ, Petropoulos CJ. 2003. Rapid evolution of the neutralizing antibody response to HIV type 1 infection. Proc Natl Acad Sci U S A 100:4144-4149.
3. Wei X, Decker JM, Wang S, Hui H, Kappes JC, Wu X, Salazar-Gonzalez JF, Salazar MG, Kilby JM, Saag MS, Komarova NL, Nowak MA, Hahn BH, Kwong PD, Shaw GM. 2003. Antibody neutralization and escape by HIV-1. Nature 422:307-312.
4. Tomaras GD, Yates NL, Liu P, Qin L, Fouda GG, Chavez LL, Decamp AC, Parks RJ, Ashley VC, Lucas JT, Cohen M, Eron J, Hicks CB, Liao HX, Self SG, Landucci G, Forthal DN, Weinhold KJ, Keele BF, Hahn BH, Greenberg ML, Morris L, Karim SS, Blattner WA, Montefiori DC, Shaw GM, Perelson AS, Haynes BF. 2008. Initial B-cell responses to transmitted human immunodeficiency virus type 1: virion-binding immunoglobulin M (IgM) and IgG antibodies followed by plasma anti-gp41 antibodies with ineffective control of initial viremia. J Virol 82:12449-12463.
5. Moore PL, Gray ES, Choge IA, Ranchobe N, Mlisana K, Abdool Karim SS, Williamson C, Morris L. 2008. The C3-V4 region is a major target of autologous neutralizing antibodies in human immunodeficiency virus type 1 subtype C infection. J Virol 82:1860-1869.
6. Moore PL, Ranchobe N, Lambson BE, Gray ES, Cave E, Abrahams MR, Bandawe G, Mlisana K, Abdool Karim SS, Williamson C, Morris L. 2009. Limited neutralizing antibody specificities drive neutralization escape in early HIV-1 subtype C infection. PLoS Pathog 5:e1000598.
7. Rong R, Bibollet-Ruche F, Mulenga J, Allen S, Blackwell JL, Derdeyn CA. 2007. Role of V1V2 and Other Human Immunodeficiency Virus Type 1 Envelope Domains in Resistance to Autologous Neutralization during Clade C Infection. J Virol 81:1350-1359.
8. Rong R, Gnanakaran S, Decker JM, Bibollet-Ruche F, Taylor J, Sfakianos JN, Mokili JL, Muldoon M, Mulenga J, Allen S, Hahn BH, Shaw GM, Blackwell JL, Korber BT, Hunter E, Derdeyn CA. 2007. Unique Mutational Patterns in the Envelope {alpha}2 Amphipathic Helix and Acquisition of Length in gp120 Hypervariable Domains Are Associated with Resistance to Autologous Neutralization of Subtype C Human Immunodeficiency Virus Type 1. J Virol 81:5658-5668.
9. Li Y, Svehla K, Louder MK, Wycuff D, Phogat S, Tang M, Migueles SA, Wu X, Phogat A, Shaw GM, Connors M, Hoxie J, Mascola JR, Wyatt R. 2009. Analysis of neutralization specificities in polyclonal sera derived from human immunodeficiency virus type 1-infected individuals. J Virol 83:1045-1059.
10. Sather DN, Armann J, Ching LK, Mavrantoni A, Sellhorn G, Caldwell Z, Yu X, Wood B, Self S, Kalams S, Stamatatos L. 2009. Factors associated with the development of cross-reactive neutralizing antibodies during human immunodeficiency virus type 1 infection. J Virol 83:757-769.
11. Simek MD, Rida W, Priddy FH, Pung P, Carrow E, Laufer DS, Lehrman JK, Boaz M, Tarragona-Fiol T, Miiro G, Birungi J, Pozniak A, McPhee DA, Manigart

O, Karita E, Inwoley A, Jaoko W, Dehovitz J, Bekker LG, Pitisuttithum P, Paris R, Walker LM, Poignard P, Wrin T, Fast PE, Burton DR, Koff WC. 2009. Human immunodeficiency virus type 1 elite neutralizers: individuals with broad and potent neutralizing activity identified by using a high-throughput neutralization assay together with an analytical selection algorithm. J Virol 83:7337-7348.

12. Gray ES, Madiga MC, Hermanus T, Moore PL, Wibmer CK, Tumba NL, Werner L, Mlisana K, Sibeko S, Williamson C, Abdool Karim SS, Morris L. 2011. The neutralization breadth of HIV-1 develops incrementally over four years and is associated with CD4+ T cell decline and high viral load during acute infection. J Virol 85:4828-4840.
13. Euler Z, van Gils MJ, Bunnik EM, Phung P, Schweighardt B, Wrin T, Schuitemaker H. 2010. Cross-reactive neutralizing humoral immunity does not protect from HIV type 1 disease progression. J Infect Dis 201:1045-1053.
14. Wibmer CK, Moore PL, Morris L. 2015. HIV broadly neutralizing antibody targets. Curr Opin HIV AIDS 10:135-143.
15. Moldt B, Rakasz EG, Schultz N, Chan-Hui PY, Swiderek K, Weisgrau KL, Piaskowski SM, Bergman Z, Watkins DI, Poignard P, Burton DR. 2012. Highly potent HIV-specific antibody neutralization in vitro translates into effective protection against mucosal SHIV challenge in vivo. Proc Natl Acad Sci U S A 109:18921-18925.
16. Pegu A, Yang ZY, Boyington JC, Wu L, Ko SY, Schmidt SD, McKee K, Kong WP, Shi W, Chen X, Todd JP, Letvin NL, Huang J, Nason MC, Hoxie JA, Kwong PD, Connors M, Rao SS, Mascola JR, Nabel GJ. 2014. Neutralizing antibodies to HIV-1 envelope protect more effectively in vivo than those to the CD4 receptor. Sci Transl Med 6:243ra288.
17. Doria-Rose NA, Schramm CA, Gorman J, Moore PL, Bhiman JN, DeKosky BJ, Ernandes MJ, Georgiev IS, Kim HJ, Pancera M, Staupe RP, Altae-Tran HR, Bailer RT, Crooks ET, Cupo A, Druz A, Garrett NJ, Hoi KH, Kong R, Louder MK, Longo NS, McKee K, Nonyane M, O'Dell S, Roark RS, Rudicell RS, Schmidt SD, Sheward DJ, Soto C, Wibmer CK, Yang Y, Zhang Z, Program NCS, Mullikin JC, Binley JM, Sanders RW, Wilson IA, Moore JP, Ward AB, Georgiou G, Williamson C, Abdool Karim SS, Morris L, Kwong PD, Shapiro L, Mascola JR. 2014. Developmental pathway for potent V1V2-directed HIV-neutralizing antibodies. Nature 509:55-62.
18. Liao HX, Lynch R, Zhou T, Gao F, Alam SM, Boyd SD, Fire AZ, Roskin KM, Schramm CA, Zhang Z, Zhu J, Shapiro L, Program NCS, Mullikin JC, Gnanakaran S, Hraber P, Wiehe K, Kelsoe G, Yang G, Xia SM, Montefiori DC, Parks R, Lloyd KE, Scearce RM, Soderberg KA, Cohen M, Kamanga G, Louder MK, Tran LM, Chen Y, Cai F, Chen S, Moquin S, Du X, Joyce MG, Srivatsan S, Zhang B, Zheng A, Shaw GM, Hahn BH, Kepler TB, Korber BT, Kwong PD, Mascola JR, Haynes BF. 2013. Co-evolution of a broadly neutralizing HIV-1 antibody and founder virus. Nature 496:469-476.
19. Moody MA, Gao F, Gurley TC, Amos JD, Kumar A, Hora B, Marshall DJ, Whitesides JF, Xia SM, Parks R, Lloyd KE, Hwang KK, Lu X, Bonsignori M, Finzi A, Vandergrift NA, Alam SM, Ferrari G, Shen X, Tomaras GD, Kamanga G, Cohen MS, Sam NE, Kapiga S, Gray ES, Tumba NL, Morris L, Zolla-Pazner S, Gorny MK, Mascola JR, Hahn BH, Shaw GM, Sodroski JG, Liao HX, Montefiori DC, Hraber PT, Korber BT, Haynes BF. 2015. Strain-Specific V3 and CD4 Binding Site Autologous HIV-1 Neutralizing Antibodies Select Neutralization-Resistant Viruses. Cell Host Microbe 18:354-362.

20. Bonsignori M, Zhou T, Sheng Z, Chen L, Gao F, Joyce MG, Ozorowski G, Chuang GY, Schramm CA, Wiehe K, Alam SM, Bradley T, Gladden MA, Hwang KK, Iyengar S, Kumar A, Lu X, Luo K, Mangiapani MC, Parks RJ, Song H, Acharya P, Bailer RT, Cao A, Druz A, Georgiev IS, Kwon YD, Louder MK, Zhang B, Zheng A, Hill BJ, Kong R, Soto C, Program NCS, Mullikin JC, Douek DC, Montefiori DC, Moody MA, Shaw GM, Hahn BH, Kelsoe G, Hraber PT, Korber BT, Boyd SD, Fire AZ, Kepler TB, Shapiro L, Ward AB, Mascola JR, Liao HX, et al. 2016. Maturation Pathway from Germline to Broad HIV-1 Neutralizer of a CD4-Mimic Antibody. Cell doi:10.1016/j.cell.2016.02.022.
21. Gao F, Bonsignori M, Liao HX, Kumar A, Xia SM, Lu X, Cai F, Hwang KK, Song H, Zhou T, Lynch RM, Alam SM, Moody MA, Ferrari G, Berrong M, Kelsoe G, Shaw GM, Hahn BH, Montefiori DC, Kamanga G, Cohen MS, Hraber P, Kwong PD, Korber BT, Mascola JR, Kepler TB, Haynes BF. 2014. Cooperation of B cell lineages in induction of HIV-1-broadly neutralizing antibodies. Cell 158:481-491.
22. Moore PL, Gray ES, Wibmer CK, Bhiman JN, Nonyane M, Sheward DJ, Hermanus T, Bajimaya S, Tumba NL, Abrahams MR, Lambson BE, Ranchobe N, Ping L, Ngandu N, Abdool Karim Q, Abdool Karim SS, Swanstrom RI, Seaman MS, Williamson C, Morris L. 2012. Evolution of an HIV glycan-dependent broadly neutralizing antibody epitope through immune escape. Nat Med 18:1688-1692.
23. Corti D, Langedijk JP, Hinz A, Seaman MS, Vanzetta F, Fernandez-Rodriguez BM, Silacci C, Pinna D, Jarrossay D, Balla-Jhagjhoorsingh S, Willems B, Zekveld MJ, Dreja H, O'Sullivan E, Pade C, Orkin C, Jeffs SA, Montefiori DC, Davis D, Weissenhorn W, McKnight A, Heeney JL, Sallusto F, Sattentau QJ, Weiss RA, Lanzavecchia A. 2010. Analysis of memory B cell responses and isolation of novel monoclonal antibodies with neutralizing breadth from HIV-1-infected individuals. PLoS One 5:e8805.
24. Wu X, Yang ZY, Li Y, Hogerkorp CM, Schief WR, Seaman MS, Zhou T, Schmidt SD, Wu L, Xu L, Longo NS, McKee K, O'Dell S, Louder MK, Wycuff DL, Feng Y, Nason M, Doria-Rose N, Connors M, Kwong PD, Roederer M, Wyatt RT, Nabel GJ, Mascola JR. 2010. Rational design of envelope identifies broadly neutralizing human monoclonal antibodies to HIV-1. Science 329:856-861.
25. Scheid JF, Mouquet H, Ueberheide B, Diskin R, Klein F, Oliveira TY, Pietzsch J, Fenyo D, Abadir A, Velinzon K, Hurley A, Myung S, Boulad F, Poignard P, Burton DR, Pereyra F, Ho DD, Walker BD, Seaman MS, Bjorkman PJ, Chait BT, Nussenzweig MC. 2011. Sequence and structural convergence of broad and potent HIV antibodies that mimic CD4 binding. Science 333:1633-1637.
26. Zhou T, Lynch RM, Chen L, Acharya P, Wu X, Doria-Rose NA, Joyce MG, Lingwood D, Soto C, Bailer RT, Ernandes MJ, Kong R, Longo NS, Louder MK, McKee K, O'Dell S, Schmidt SD, Tran L, Yang Z, Druz A, Luongo TS, Moquin S, Srivatsan S, Yang Y, Zhang B, Zheng A, Pancera M, Kirys T, Georgiev IS, Gindin T, Peng HP, Yang AS, Program NCS, Mullikin JC, Gray MD, Stamatatos L, Burton DR, Koff WC, Cohen MS, Haynes BF, Casazza JP, Connors M, Corti D, Lanzavecchia A, Sattentau QJ, Weiss RA, West AP, Jr., Bjorkman PJ, Scheid JF, Nussenzweig MC, et al. 2015. Structural Repertoire of HIV-1-Neutralizing Antibodies Targeting the CD4 Supersite in 14 Donors. Cell 161:1280-1292.
27. Bonsignori M, Montefiori DC, Wu X, Chen X, Hwang KK, Tsao CY, Kozink DM, Parks RJ, Tomaras GD, Crump JA, Kapiga SH, Sam NE, Kwong PD, Kepler

TB, Liao HX, Mascola JR, Haynes BF. 2012. Two distinct broadly neutralizing antibody specificities of different clonal lineages in a single HIV-1-infected donor: implications for vaccine design. J Virol 86:4688-4692.

28. Freund NT, Horwitz JA, Nogueira L, Sievers SA, Scharf L, Scheid JF, Gazumyan A, Liu C, Velinzon K, Goldenthal A, Sanders RW, Moore JP, Bjorkman PJ, Seaman MS, Walker BD, Klein F, Nussenzweig MC. 2015. A New Glycan-Dependent CD4-Binding Site Neutralizing Antibody Exerts Pressure on HIV-1 In Vivo. PLoS Pathog 11:e1005238.
29. Zhou T, Zhu J, Wu X, Moquin S, Zhang B, Acharya P, Georgiev IS, Altae-Tran HR, Chuang GY, Joyce MG, Do Kwon Y, Longo NS, Louder MK, Luongo T, McKee K, Schramm CA, Skinner J, Yang Y, Yang Z, Zhang Z, Zheng A, Bonsignori M, Haynes BF, Scheid JF, Nussenzweig MC, Simek M, Burton DR, Koff WC, Program NCS, Mullikin JC, Connors M, Shapiro L, Nabel GJ, Mascola JR, Kwong PD. 2013. Multidonor analysis reveals structural elements, genetic determinants, and maturation pathway for HIV-1 neutralization by VRC01-class antibodies. Immunity 39:245-258.
30. Zhou T, Georgiev I, Wu X, Yang ZY, Dai K, Finzi A, Do Kwon Y, Scheid JF, Shi W, Xu L, Yang Y, Zhu J, Nussenzweig MC, Sodroski J, Shapiro L, Nabel GJ, Mascola JR, Kwong PD. 2010. Structural basis for broad and potent neutralization of HIV-1 by antibody VRC01. Science 329:811-817.
31. Jardine J, Julien JP, Menis S, Ota T, Kalyuzhniy O, McGuire A, Sok D, Huang PS, Macpherson S, Jones M, Nieusma T, Mathison J, Baker D, Ward AB, Burton DR, Stamatatos L, Nemazee D, Wilson IA, Schief WR. 2013. Rational HIV Immunogen Design to Target Specific Germline B Cell Receptors. Science doi:10.1126/science.1234150.
32. McGuire AT, Hoot S, Dreyer AM, Lippy A, Stuart A, Cohen KW, Jardine J, Menis S, Scheid JF, West AP, Schief WR, Stamatatos L. 2013. Engineering HIV envelope protein to activate germline B cell receptors of broadly neutralizing anti-CD4 binding site antibodies. J Exp Med doi:10.1084/jem.20122824.
33. Balla-Jhagjhoorsingh SS, Corti D, Heyndrickx L, Willems E, Vereecken K, Davis D, Vanham G. 2013. The N276 glycosylation site is required for HIV-1 neutralization by the CD4 binding site specific HJ16 monoclonal antibody. PLoS One 8:e68863.
34. Dosenovic P, von Boehmer L, Escolano A, Jardine J, Freund NT, Gitlin AD, McGuire AT, Kulp DW, Oliveira T, Scharf L, Pietzsch J, Gray MD, Cupo A, van Gils MJ, Yao KH, Liu C, Gazumyan A, Seaman MS, Bjorkman PJ, Sanders RW, Moore JP, Stamatatos L, Schief WR, Nussenzweig MC. 2015. Immunization for HIV-1 Broadly Neutralizing Antibodies in Human Ig Knockin Mice. Cell 161:1505-1515.
35. Jardine JG, Ota T, Sok D, Pauthner M, Kulp DW, Kalyuzhniy O, Skog PD, Thinnes TC, Bhullar D, Briney B, Menis S, Jones M, Kubitz M, Spencer S, Adachi Y, Burton DR, Schief WR, Nemazee D. 2015. HIV-1 VACCINES. Priming a broadly neutralizing antibody response to HIV-1 using a germline-targeting immunogen. Science 349:156-161.
36. Wibmer CK, Bhiman JN, Gray ES, Tumba N, Abdool Karim SS, Williamson C, Morris L, Moore PL. 2013. Viral escape from HIV-1 neutralizing antibodies drives increased plasma neutralization breadth through sequential recognition of multiple epitopes and immunotypes. PLoS Pathog 9:e1003738.
37. Montefiori DC. 2004. Evaluating neutralizing antibodies againts HIV, SIV and SHIV in luciferase reporter gene assays. *In* Coligan JE, Kruisbeek AM,

Margulies DH, Shevach EM, Strober W, Coico R (ed), Current Protocols in Immunology. John Wiley & Sons.

38. Huang J, Ofek G, Laub L, Louder MK, Doria-Rose NA, Longo NS, Imamichi H, Bailer RT, Chakrabarti B, Sharma SK, Alam SM, Wang T, Yang Y, Zhang B, Migueles SA, Wyatt R, Haynes BF, Kwong PD, Mascola JR, Connors M. 2012. Broad and potent neutralization of HIV-1 by a gp41-specific human antibody. Nature 491:406-412.
39. Tiller T, Meffre E, Yurasov S, Tsuiji M, Nussenzweig MC, Wardemann H. 2008. Efficient generation of monoclonal antibodies from single human B cells by single cell RT-PCR and expression vector cloning. J Immunol Methods 329:112-124.
40. Jabara CB, Jones CD, Roach J, Anderson JA, Swanstrom R. 2011. Accurate sampling and deep sequencing of the HIV-1 protease gene using a Primer ID. Proc Natl Acad Sci U S A 108:20166-20171.
41. Bolger AM, Lohse M, Usadel B. 2014. Trimmomatic: a flexible trimmer for Illumina sequence data. Bioinformatics 30:2114-2120.
42. Zhang J, Kobert K, Flouri T, Stamatakis A. 2014. PEAR: a fast and accurate Illumina Paired-End reAd mergeR. Bioinformatics 30:614-620.
43. Katoh K, Standley DM. 2013. MAFFT multiple sequence alignment software version 7: improvements in performance and usability. Mol Biol Evol 30:772-780.
44. Zhou S, Jones C, Mieczkowski P, Swanstrom R. 2015. Primer ID Validates Template Sampling Depth and Greatly Reduces the Error Rate of Next-Generation Sequencing of HIV-1 Genomic RNA Populations. J Virol 89:8540-8555.
45. McCoy LE, Falkowska E, Doores KJ, Le K, Sok D, van Gils MJ, Euler Z, Burger JA, Seaman MS, Sanders RW, Schuitemaker H, Poignard P, Wrin T, Burton DR. 2015. Incomplete Neutralization and Deviation from Sigmoidal Neutralization Curves for HIV Broadly Neutralizing Monoclonal Antibodies. PLoS Pathog 11:e1005110.
46. Chen L, Kwon YD, Zhou T, Wu X, O'Dell S, Cavacini L, Hessell AJ, Pancera M, Tang M, Xu L, Yang ZY, Zhang MY, Arthos J, Burton DR, Dimitrov DS, Nabel GJ, Posner MR, Sodroski J, Wyatt R, Mascola JR, Kwong PD. 2009. Structural basis of immune evasion at the site of CD4 attachment on HIV-1 gp120. Science 326:1123-1127.
47. Guttman M, Cupo A, Julien JP, Sanders RW, Wilson IA, Moore JP, Lee KK. 2015. Antibody potency relates to the ability to recognize the closed, pre-fusion form of HIV Env. Nat Commun 6:6144.
48. Diskin R, Klein F, Horwitz JA, Halper-Stromberg A, Sather DN, Marcovecchio PM, Lee T, West AP, Jr., Gao H, Seaman MS, Stamatatos L, Nussenzweig MC, Bjorkman PJ. 2013. Restricting HIV-1 pathways for escape using rationally designed anti-HIV-1 antibodies. J Exp Med 210:1235-1249.
49. Scharf L, Scheid JF, Lee JH, West AP, Jr., Chen C, Gao H, Gnanapragasam PN, Mares R, Seaman MS, Ward AB, Nussenzweig MC, Bjorkman PJ. 2014. Antibody 8ANC195 reveals a site of broad vulnerability on the HIV-1 envelope spike. Cell Rep 7:785-795.
50. Stewart-Jones GB, Soto C, Lemmin T, Chuang GY, Druz A, Kong R, Thomas PV, Wagh K, Zhou T, Behrens AJ, Bylund T, Choi CW, Davison JR, Georgiev IS, Joyce MG, Kwon YD, Pancera M, Taft J, Yang Y, Zhang B, Shivatare SS, Shivatare VS, Lee CC, Wu CY, Bewley CA, Burton DR, Koff WC, Connors M,

Crispin M, Baxa U, Korber BT, Wong CH, Mascola JR, Kwong PD. 2016. Trimeric HIV-1-Env Structures Define Glycan Shields from Clades A, B, and G. Cell 165:813-826.

51. Leonard CK, Spellman MW, Riddle L, Harris RJ, Thomas JN, Gregory TJ. 1990. Assignment of intrachain disulfide bonds and characterization of potential glycosylation sites of the type 1 recombinant human immunodeficiency virus envelope glycoprotein (gp120) expressed in Chinese hamster ovary cells. J Biol Chem 265:10373-10382.
52. Zhu X, Borchers C, Bienstock RJ, Tomer KB. 2000. Mass spectrometric characterization of the glycosylation pattern of HIV-gp120 expressed in CHO cells. Biochemistry 39:11194-11204.
53. Go EP, Liao HX, Alam SM, Hua D, Haynes BF, Desaire H. 2013. Characterization of host-cell line specific glycosylation profiles of early transmitted/founder HIV-1 gp120 envelope proteins. J Proteome Res 12:1223-1234.
54. Behrens AJ, Vasiljevic S, Pritchard LK, Harvey DJ, Andev RS, Krumm SA, Struwe WB, Cupo A, Kumar A, Zitzmann N, Seabright GE, Kramer HB, Spencer DI, Royle L, Lee JH, Klasse PJ, Burton DR, Wilson IA, Ward AB, Sanders RW, Moore JP, Doores KJ, Crispin M. 2016. Composition and Antigenic Effects of Individual Glycan Sites of a Trimeric HIV-1 Envelope Glycoprotein. Cell Rep 14:2695-2706.
55. Li Y, O'Dell S, Walker LM, Wu X, Guenaga J, Feng Y, Schmidt SD, McKee K, Louder MK, Ledgerwood JE, Graham BS, Haynes BF, Burton DR, Wyatt RT, Mascola JR. 2011. Mechanism of neutralization by the broadly neutralizing HIV-1 monoclonal antibody VRC01. J Virol 85:8954-8967.
56. Tang H, Robinson JE, Gnanakaran S, Li M, Rosenberg ES, Perez LG, Haynes BF, Liao HX, Labranche CC, Korber BT, Montefiori DC. 2011. epitopes immediately below the base of the V3 loop of gp120 as targets for the initial autologous neutralizing antibody response in two HIV-1 subtype B-infected individuals. J Virol 85:9286-9299.
57. Wu X, Changela A, O'Dell S, Schmidt SD, Pancera M, Yang Y, Zhang B, Gorny MK, Phogat S, Robinson JE, Stamatatos L, Zolla-Pazner S, Kwong PD, Mascola JR. 2011. Immunotypes of a quaternary site of HIV-1 vulnerability and their recognition by antibodies. J Virol 85:4578-4585.
58. Gorny MK, Stamatatos L, Volsky B, Revesz K, Williams C, Wang XH, Cohen S, Staudinger R, Zolla-Pazner S. 2005. Identification of a new quaternary neutralizing epitope on human immunodeficiency virus type 1 virus particles. J Virol 79:5232-5237.
59. Walker LM, Phogat SK, Chan-Hui PY, Wagner D, Phung P, Goss JL, Wrin T, Simek MD, Fling S, Mitcham JL, Lehrman JK, Priddy FH, Olsen OA, Frey SM, Hammond PW, Kaminsky S, Zamb T, Moyle M, Koff WC, Poignard P, Burton DR. 2009. Broad and potent neutralizing antibodies from an African donor reveal a new HIV-1 vaccine target. Science 326:285-289.
60. Pietzsch J, Scheid JF, Mouquet H, Klein F, Seaman MS, Jankovic M, Corti D, Lanzavecchia A, Nussenzweig MC. 2010. Human anti-HIV-neutralizing antibodies frequently target a conserved epitope essential for viral fitness. J Exp Med 207:1995-2002.
61. West AP, Jr., Scharf L, Horwitz J, Klein F, Nussenzweig MC, Bjorkman PJ. 2013. Computational analysis of anti-HIV-1 antibody neutralization panel data to identify potential functional epitope residues. Proc Natl Acad Sci U S A

doi:10.1073/pnas.1309215110.
62. Kong L, Lee JH, Doores KJ, Murin CD, Julien JP, McBride R, Liu Y, Marozsan A, Cupo A, Klasse PJ, Hoffenberg S, Caulfield M, King CR, Hua Y, Le KM, Khayat R, Deller MC, Clayton T, Tien H, Feizi T, Sanders RW, Paulson JC, Moore JP, Stanfield RL, Burton DR, Ward AB, Wilson IA. 2013. Supersite of immune vulnerability on the glycosylated face of HIV-1 envelope glycoprotein gp120. Nat Struct Mol Biol 20:796-803.
63. Moore PL, Sheward D, Nonyane M, Ranchobe N, Hermanus T, Gray ES, Abdool Karim SS, Williamson C, Morris L. 2013. Multiple pathways of escape from HIV broadly cross-neutralizing V2-dependent antibodies. J Virol 87:4882-4894.
64. Bhiman JN, Anthony C, Doria-Rose NA, Karimanzira O, Schramm CA, Khoza T, Kitchin D, Botha G, Gorman J, Garrett NJ, Abdool Karim SS, Shapiro L, Williamson C, Kwong PD, Mascola JR, Morris L, Moore PL. 2015. Viral variants that initiate and drive maturation of V1V2-directed HIV-1 broadly neutralizing antibodies. Nat Med 21:1332-1336.
65. Crooks ET, Tong T, Chakrabarti B, Narayan K, Georgiev IS, Menis S, Huang X, Kulp D, Osawa K, Muranaka J, Stewart-Jones G, Destefano J, O'Dell S, LaBranche C, Robinson JE, Montefiori DC, McKee K, Du SX, Doria-Rose N, Kwong PD, Mascola JR, Zhu P, Schief WR, Wyatt RT, Whalen RG, Binley JM. 2015. Vaccine-Elicited Tier 2 HIV-1 Neutralizing Antibodies Bind to Quaternary Epitopes Involving Glycan-Deficient Patches Proximal to the CD4 Binding Site. PLoS Pathog 11:e1004932.
66. Gray ES, Moody MA, Wibmer CK, Chen X, Marshall D, Amos J, Moore PL, Foulger A, Yu JS, Lambson B, Abdool Karim S, Whitesides J, Tomaras GD, Haynes BF, Morris L, Liao HX. 2011. Isolation of a monoclonal antibody that targets the alpha-2 helix of gp120 and represents the initial autologous neutralizing-antibody response in an HIV-1 subtype C-infected individual. J Virol 85:7719-7729.
67. Bradley T, Fera D, Bhiman J, Eslamizar L, Lu X, Anasti K, Zhang R, Sutherland LL, Scearce RM, Bowman CM, Stolarchuk C, Lloyd KE, Parks R, Eaton A, Foulger A, Nie X, Karim SS, Barnett S, Kelsoe G, Kepler TB, Alam SM, Montefiori DC, Moody MA, Liao HX, Morris L, Santra S, Harrison SC, Haynes BF. 2016. Structural Constraints of Vaccine-Induced Tier-2 Autologous HIV Neutralizing Antibodies Targeting the Receptor-Binding Site. Cell Rep 14:43-54.
68. Lynch RM, Wong P, Tran L, O'Dell S, Nason MC, Li Y, Wu X, Mascola JR. 2015. HIV-1 fitness cost associated with escape from the VRC01 class of CD4 binding site neutralizing antibodies. J Virol 89:4201-4213.
69. Wu X, Wang C, O'Dell S, Li Y, Keele BF, Yang Z, Imamichi H, Doria-Rose N, Hoxie JA, Connors M, Shaw GM, Wyatt RT, Mascola JR. 2012. Selection pressure on HIV-1 envelope by broadly neutralizing antibodies to the conserved CD4-binding site. J Virol 86:5844-5856.
70. Jardine JG, Kulp DW, Havenar-Daughton C, Sarkar A, Briney B, Sok D, Sesterhenn F, Ereno-Orbea J, Kalyuzhniy O, Deresa I, Hu X, Spencer S, Jones M, Georgeson E, Adachi Y, Kubitz M, deCamp AC, Julien JP, Wilson IA, Burton DR, Crotty S, Schief WR. 2016. HIV-1 broadly neutralizing antibody precursor B cells revealed by germline-targeting immunogen. Science 351:1458-1463.

Supplement

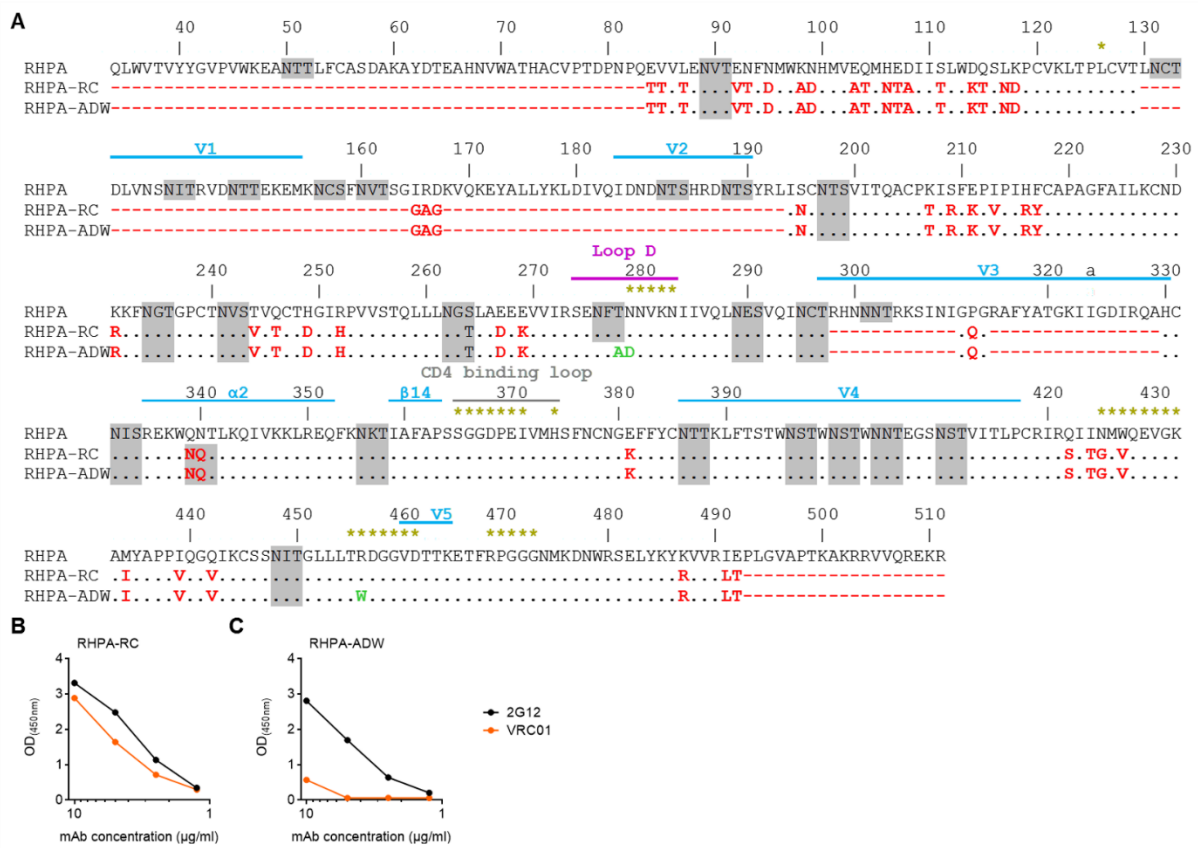

Supplementary Figure 1: Design of a resurfaced antigen based on RSC3 to isolate early CD4bs antibodies from donor CAP257

A) A sequence alignment of RHPA gp120, and the two newly designed sorting antigens RHPA-RC and RHPA-ADW. Truncations or resurfacing mutations are coloured red, potential N-linked glycosylation sequons are shaded grey, the hypervariable regions, loop D, and the CD4 binding loop are highlighted cyan, purple, and light grey respectively, and the CD4bs is indicated with yellow asterisks. The CAP257 escape mutations incorporated into the negative sorting antigen RHPA-ADW are coloured green. B) ELISA binding of VRC01 (orange) and 2G12 (black) to the RHPA-RC resurfaced gp120 positive sorting probe. Absorbance readings are plotted on the left y-axis, and monoclonal antibody concentration on the x-axis. C) ELISA binding of VRC01 and 2G12 to the RHPA-ADW resurfaced gp120 negative sorting probe, plotted as in B.

Supplementary Figure 2: Potentially related immunoglobulin clusters isolated from donor CAP257 at 107 weeks post-infection

Sequence alignments of the three potentially related immunoglobulin clusters isolated as RHPA-RC+, RHPA-ADW- by flow cytometry from CAP257 PBMC memory B cells, numbered according to Kabat. A) Heavy chain alignment of the IGHV4-59 genes. B) Kappa chain alignment of the IGKV1-NL1 genes. C) Heavy and light chain alignments of the IGHV3-33 and IGLV3-10 genes.

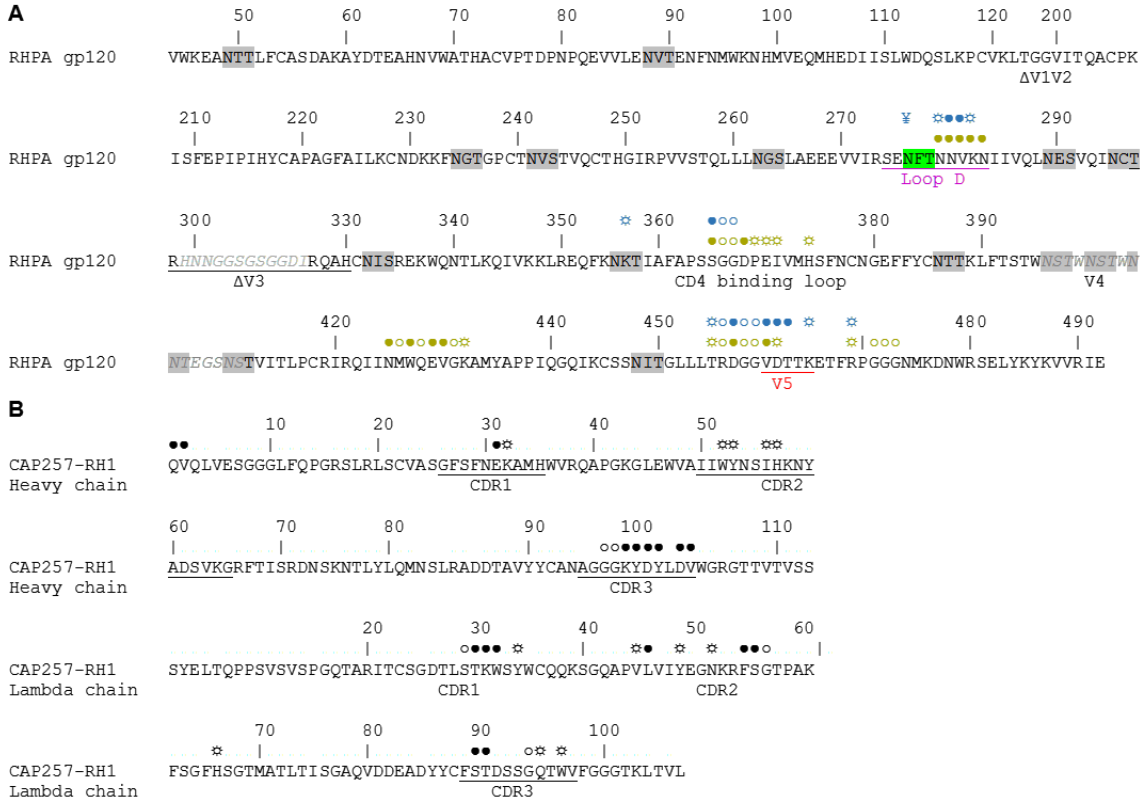

Supplementary Figure 3: Residue-by-residue contacts between RHPA gp120 and CAP257-RH1

A) The RHPA gp120 sequence is shown, and numbered according to the HxB2 convention. Potential N-linked glycosylation sequons are shaded grey, disordered regions are indicated in italics, and loop D or V5 are indicate with purple and red underlines respectively. Contacts for the cocrystal complex are shown in blue, while previously determined interactions between CD4 and gp120 are shown in gold. Open circles (○) indicate main chain contacts only, ray circles (☼) indicate side chain contacts only, closed circles (●) indicate both main chain and side chain contacts, and the ¥ symbol is used to specify glycan interactions. B) The heavy and light chain sequences for CAP257-RH1 are shown, the CDR loops are underlined, and contacts in the cocrystal complex are labelled as in A.

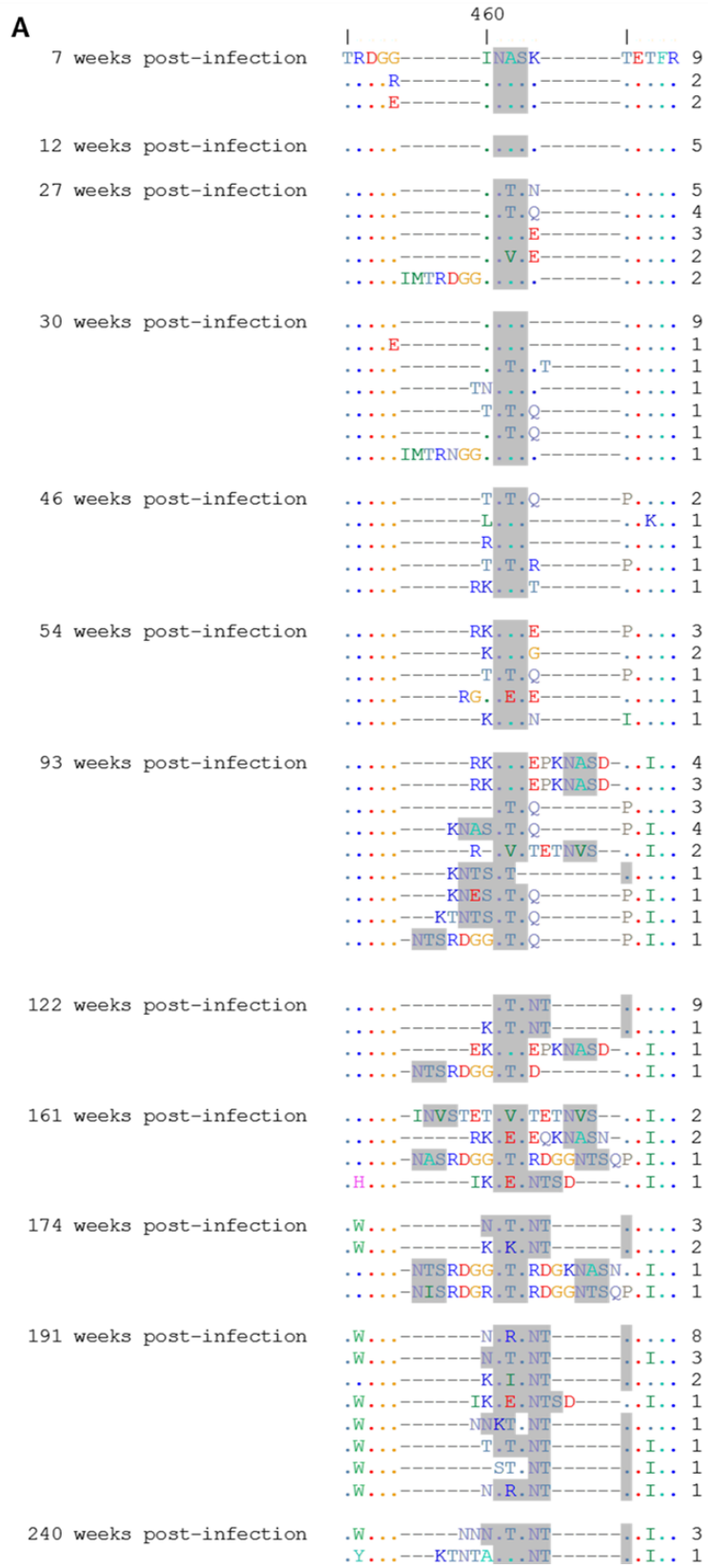

Supplementary Figure 5: Autologous CAP257 V5 sequences
A) An alignment of CAP257 Env V5 (and flanking regions) sequences identified by SGA from 7 weeks to 240 weeks post-infection. Potential N-linked glycosylation sequons are shaded grey, and the number of identical sequences are listed on the right of the figure.

Supplementary Table 1: Heterologous neutralization mediated by CAP257-RH1
Neutralization IC50 values of CAP257-RH1 tested on a multi-clade 196 virus panel. Titres <50 µg/mL are highlighted in red.

Virus	Clade	CAP257-RH1	Virus	Clade	CAP257-RH1	Virus	Clade	CAP257-RH1	Virus	Clade	CAP257-RH1
0260.v5.c36	A	>50	TH976.17	AE	>50	THRO.18	B	>50	CNE7	BC	>50
0330.v4.c3	A	>50	235-47	AG	>50	TRJO.58	B	>50	286.36	C	>50
0439.v5.c1	A	>50	242-14	AG	>50	TRO.11	B	>50	288.38	C	>50
3365.v2.c20	A	>50	263-8	AG	>50	WITO.33	B	>50	DU422.01	C	>50
3415.v1.c1	A	>50	269-12	AG	>50	X2278.C2.B1	B	>50	MW965.26	C	>50
3718.v3.c11	A	>50	271-11	AG	>50	YU2.DG	B	>50	SO18.18	C	>50
BB201.B42	A	>50	928-28	AG	>50	BJOX002000.03.2	BC	>50	TV1.29	C	>50
BI369.9A	A	>50	DJ263.8	AG	>50	CH038.12	BC	>50	TZA125.17	C	>50
BS208.B1	A	>50	T250-4	AG	>50	CH070.1	BC	>50	TZBD.02	C	>50
KER2008.12	A	>50	T251-18	AG	>50	CH117.4	BC	>50	ZA012.29	C	>50
KER2018.11	A	>50	T253-11	AG	>50	CH119.10	BC	>50	ZM106.9	C	>50
KNH1209.18	A	>50	T255-34	AG	>50	CH181.12	BC	>50	ZM109.4	C	>50
MB201.A1	A	>50	T257-31	AG	>50	CNE15	BC	>50	ZM135.10a	C	>50
MB539.2B7	A	>50	T266-60	AG	>50	CNE20	BC	>50	ZM176.66	C	>50
MI369.A5	A	>50	T278-50	AG	>50	CNE21	BC	>50	ZM197.7	C	>50
MS208.A1	A	>50	T280-5	AG	>50	CNE40	BC	>50	ZM214.15	C	>50
Q23.17	A	>50	T33-7	AG	>50	0013095-2.11	C	>50	ZM215.8	C	>50
Q259.17	A	>50	3988.25	B	>50	001428-2.42	C	>50	ZM233.6	C	>50
Q769.d22	A	>50	5768.04	B	>50	0077_V1.C16	C	>50	ZM249.1	C	>50
Q769.h5	A	>50	6101.10	B	>50	00836-2.5	C	>50	ZM53.12	C	>50
Q842.d12	A	>50	6535.3	B	>50	0921.V2.C14	C	>50	ZM55.28a	C	>50
QH209.14M.A2	A	>50	7165.18	B	>50	16055-2.3	C	>50	3326.V4.C3	CD	>50
RW020.2	A	>50	45_01dG5	B	>50	16845-2.22	C	>50	3337.V2.C6	CD	>50
UG037.8	A	>50	89.6.DG	B	>50	16936-2.21	C	>50	3817.v2.c59	CD	>50
246-F3.C10.2	AC	>50	AC10.29	B	>50	25710-2.43	C	>50	191821.E6.1	D	>50
3301.V1.C24	AC	>50	ADA.DG	B	>50	25711-2.4	C	>50	231965.c1	D	>50
3589.V1.C4	AC	>50	Bal.01	B	>50	25925-2.22	C	>50	247-23	D	>50
6540.v4.c1	AC	>50	BaL.26	B	>50	26191-2.48	C	>50	3016.v5.c45	D	>50
6545.V4.C1	AC	>50	BG1168.01	B	>50	3168.V4.C10	C	>50	57128.vrc15	D	>50
0815.V3.C3	ACD	>50	BL01.DG	B	>50	3637.V5.C3	C	>50	6405.v4.c34	D	>50
6095.V1.C10	ACD	>50	BR07.DG	B	>50	3873.V1.C24	C	>50	A03349M1.vrc4a	D	>50
3468.V1.C12	AD	>50	BX08.16	B	>50	6322.V4.C1	C	>50	NKU3006.ec1	D	>50
Q168.a2	AD	>50	CAAN.A2	B	>50	6471.V1.C16	C	>50	UG021.16	D	>50
Q461.e2	AD	>50	CNE10	B	>50	6631.V3.C10	C	>50	UG024.2	D	>50
620345.c1	AE	>50	CNE12	B	>50	6644.V2.C33	C	>50	P0402.c2.11	G	>50
BJOX009000.02.4	AE	>50	CNE14	B	>50	6785.V5.C14	C	>50	P1981.C5.3	G	>50
BJOX010000.06.2	AE	>50	CNE4	B	>50	6838.V1.C35	C	>50	X1193.c1	G	>50
BJOX025000.01.1	AE	>50	CNE57	B	>50	96ZM651.02	C	>50	X1254.c3	G	>50
BJOX028000.10.3	AE	>50	HO86.8	B	>50	BR025.9	C	>50	X1632.S2.B10	G	>50
C1080.c3	AE	>50	HT593.1	B	>50	CAP210.E8	C	>50	X2088.c9	G	>50
C2101.c1	AE	>50	HXB2.DG	B	>50	CAP244.D3	C	>50	SIVmac251.30.SG3	NA	>50
C4118.09	AE	>50	JRCSF.JB	B	>50	CAP45.G3	C	>50	SVA.MLV	NA	>50
CNE3	AE	>50	JRFL.JB	B	>50	Ce1176.A3	C	>50			
CNE5	AE	>50	MN.3	B	>50	CE703010217.B6	C	>50			
CNE55	AE	>50	PVO.04	B	>50	CNE30	C	>50			
CNE56	AE	>50	QH0515.01	B	>50	CNE31	C	>50			
CNE59	AE	>50	QH0692.42	B	>50	CNE53	C	>50			
CNE8	AE	>50	REJO.67	B	>50	CNE58	C	>50			
M02138	AE	>50	RHPA.7	B	0.056	DU123.06	C	>50			
R1166.c1	AE	>50	SC422.8	B	>50	DU151.02	C	>50			
R2184.c4	AE	>50	SF162.LS	B	>50	DU156.12	C	>50			
TH966.8	AE	>50	SS1196.01	B	>50	DU172.17	C	>50			

Supplementary Table 2: CAP257-RH1 interacting residues

	CDR/ FWR	Interfacial residue	Bond type*	Accessible Surface Area (Å^2)	Buried Surface Area (Å^2)	Buried Area (%)	Δ^iG
	FW1	Gln 1		192.96	98.79	51 |||||	-1.11
	FW1	Val 2		48.63	13.62	28 |||	0.20
	H1	Glu 31	S	113.78	66.67	59 |||||	-0.21
	H1	Lys 32		56.94	22.25	39 ||||	-0.78
	H2	Trp 52		32.72	15.31	47 |||||	0.24
	H2	Tyr 53		73.91	24.99	34 ||||	0.15
	H2	Ile 56		115.67	41.72	36 ||||	0.67
Heavy	H2	His 57		87.94	40.64	46 |||||	0.15
chain	H3	Gly 101		13.90	10.22	74 |||||||	0.16
	H3	Gly 102	H	14.19	14.19	100 |||||||||	-0.03
	H3	Lys 103	HS	113.24	99.92	88 ||||||||	-1.03
	H3	Tyr 104		121.41	26.24	22 |||	-0.08
	H3	Asp 105	H	48.06	33.46	70 ||||||	-0.33
	H3	Tyr 106		148.72	14.62	10 |	0.11
	H3	Asp 108	H	82.66	37.09	45 |||||	-0.50
	H3	Val 109		46.08	26.95	59 |||||	0.43
	L1	Ser 28		82.42	12.64	15 ||	-0.14
	L1	Thr 29		97.95	42.89	44 |||||	-0.19
	L1	Lys 30	HS	51.25	38.12	74 |||||||	-0.18
	L1	Trp 31	H	114.19	66.03	58 |||||	0.37
	L1	Tyr 33		42.19	20.91	50 |||||	-0.11
	FW2	Val 44		91.14	10.54	12 ||	0.17
	FW2	Leu 45		78.06	12.84	17 ||	0.17
	FW2	Tyr 48		45.42	0.98	2 |	-0.01
Light	L2	Glu 49		43.99	2.09	5 |	-0.04
chain	L2	Lys 53		93.58	9.92	11 ||	-0.37
	L2	Phe 54		127.23	80.58	63 ||||||	1.19
	L2	Ser 55		99.63	38.95	39 ||||	-0.42
	FW3	Gly 56		83.26	59.71	72 |||||||	-0.29
	FW3	His 65		41.11	4.51	11 ||	-0.05
	L3	Ser 89		1.12	0.95	85 ||||||||	-0.00
	L3	Thr 90		13.39	12.26	93 |||||||||	0.06
	L3	Gly 94		33.82	2.51	7 |	0.04
	L3	Gln 95		158.72	2.04	1 |	-0.02
	L3	Trp 97		146.90	13.81	9 |	0.22

FWR/CDR: Framework region or complementarity determining region of CAP257-RH1

*H = hydrogen bond, S = salt bridge.

Supplementary Table 3: RHPA gp120 interacting residues

gp120 region	Heavy chain interfacial residue	Bond type*	Accessible Surface Area (Å²)	Buried Surface Area (Å²)	Buried Area (%)	Δ^iG
	Asn 279		53.85	26.73	50 |||||	-0.38
Loop D	Asn 280	H	61.65	55.30	90 |||||||||	-0.48
	Val 281		108.51	89.11	82 |||||||||	1.30
	Lys 282	S	78.92	19.52	25 |||	0.17
CD4	Ser 365		76.81	31.57	41 |||||	-0.01
binding	Gly 366		42.88	16.80	39 ||||	0.26
loop	Gly 367		67.48	30.21	45 |||||	0.19
	Thr 455		36.44	10.58	29 |||	0.13
	Arg 456	H	29.80	4.66	16 ||	-0.05
β23	Asp 457	HS	45.32	19.96	44 |||||	-0.12
	Gly 458		19.75	4.23	21 |||	0.04
	Gly 459		70.96	41.97	59 ||||||	0.11
V5	Val 460		145.24	19.44	13 ||	0.31
β24	Arg 469		79.21	10.89	14 ||	-0.12
	NAG1276		357.39	14.70	04|	-0.28
	BMA1278		285.85	18.41	06|	-0.22
Glycans	MAN1279		287.39	46.01	16 ||	-0.56
	MAN1280		291.13	17.30	06|	0.28
	MAN1281	H	286.77	103.54	36 ||||	-1.12

gp120 region	Light chain interfacial residue	Bond type*	Accessible Surface Area (Å²)	Buried Surface Area (Å²)	Buried area (%)	Δ^iG
Loop E	Lys 357		62.41	3.01	5|	-0.11
	Gly 459		70.96	6.75	10|	-0.06
	Val 460	H	145.24	125.80	87 |||||||||	1.65
V5	Asp 461	HS	70.34	40.34	57 ||||||	-0.44
	Thr 462		126.91	99.54	78 |||||||	0.80
	Lys 465		127.60	11.97	9|	0.19
β24	Arg 469		79.21	2.04	3|	-0.08
	NAG1277		358.92	35.73	10|	-0.53
	BMA1278		285.85	18.13	06|	-0.50
Glycans	MAN1280		291.13	57.97	20 ||	-0.73
	MAN1281		286.77	60.50	21 |||	-0.19
	MAN1282		290.04	38.77	13 ||	-0.62

*H = hydrogen bond, S = salt bridge.

Supplementary Table 4: List of hydrogen bonds and salt bridges

Hydrogen bonds

gp120 residue	**Distance (Å)**	**Heavy chain residue**
ASN 280[HD21]	2.47	ASP 105[OD2]
ASN 280[OD1]	2.48	GLY 102[H]
ARG 456[O]	1.90	LYS 103[HZ2]
ASP 457[OD1]	2.21	LYS 103[HZ3]
MAN1281[O6]	2.40	ASP 108[OD2]
gp120 residue	**Distance (Å)**	**Light chain residue**
VAL 460[O]	2.07	TRP 31[H]
ASP 461[OD1]	2.35	LYS 30[HZ3]

Salt bridges

gp120 residue	**Distance (Å)**	**Heavy chain residue**
LYS 282[NZ]	3.71	GLU 31[OE2]
ASP 457[OD1]	2.78	LYS 103[NZ]
gp120 residue	**Distance (Å)**	**Light chain residue**
ASP 461[OD1]	3.24	LYS 30[NZ]

Supplementary Table 5: Frequency of glycosylation at position N276 and in the V5 loop of a multi-clade 196 virus panel

The V5 loop sequence motifs for the CAP257 transmitted/founder clone, and the 196 heterologous strain from supplementary table 1 are shown. Potential N-linked glycosylation sequons are highlighted in red. The presence or absence of the N276 glycan for each virus is indicated.

Virus	N276	V5 Sequence	Virus	N276	V5 Sequence	Virus	N276	V5 Sequence	Virus	N276	V5 Sequence
0260.v5.c36	Y	DNNTITT	TH976.17	Y	AANSAS	THRO.18	Y	SDGGSKNSSKNETGT	CNE7	N	INGTNNT
0330.v4.c3	Y	NNNNGANGN	235-47	Y	GNSSSAN	TRJO.58	Y	KTANNTT	286.36	Y	IINDT
0439.v5.c1	Y	NNATN	242-14	Y	FRNDTNETY	TRO.11	Y	NNNSSGP	288.38	Y	TNNTNNT
3365.v2.c20	Y	NNNNSSN	263-8	Y	IINNSTS	WITO.33	Y	SNSSQN	DU422.01	Y	ENSTE
3415.v1.c1	Y	ENNST	269-12	Y	LNDSSTN	X2278.C2.B1	Y	ENNGTT	MW965.26	Y	ENNRT
3718.v3.c11	Y	ENET	271-11	Y	NNNNNAT	YU2.DG	Y	KDTNGT	SO18.18	Y	HNSTN
BB201.B42	Y	NNNGTS	928-28	Y	NNGTNDT	BJOX002000.03.2	Y	PENDT	TV1.29	Y	FNITNNT
BI369.9A	Y	GNNNTN	DJ263.8	N	SNNSTN	CH038.12	Y	RSNETNDT	TZA125.17	Y	NNTNGT
BS208.B1	Y	YNNTN	T250-4	N	NSTQN	CH070.1	Y	NINRTN	TZBD.02	Y	GESNET
KER2008.12	Y	NSTVN	T251-18	Y	NNGSKAN	CH117.4	Y	RDINNT	ZA012.29	Y	EDNKTE
KER2018.11	Y	NTGNNSRTN	T253-11	Y	ANSSTN	CH119.10	Y	TESNNTETNNT	ZM109.9	Y	NGDTNDT
KNH1209.18	Y	NGNSTN	T255-34	Y	NNNSMN	CH181.12	Y	ETNQTNFT	ZM109.4	Y	NNNNSTE
MB201.A1	Y	NNNGTS	T257-31	Y	DSNDTNGN	CNE15	Y	NEDKNNT	ZM135.10a	Y	LNNKENGT
MB539.2B7	Y	NDNSTNEN	T266-60	Y	VANDTNTT	CNE20	Y	TESNDT	ZM176.66	Y	NDDNDT
MJ369.A5	Y	GNNNTN	T278-50	Y	GDEKAN	CNE21	Y	MTNETNKT	ZM197.7	Y	NKSAGI
MS208.A1	Y	PNTTN	T280-5	N	NNSGSN	CNE40	Y	KEANGT	ZM214.15	Y	NGNDTNDT
Q23.17	Y	KDNNVN	T33-7	Y	NNNAAT	CNE8	Y	NGNDTNKT	ZM215.8	Y	TNNTN
Q259.17	Y	KDSNIT	3988.25	Y	NNNNTNTT	001428-2.42	Y	KNNNT	ZM233.6	Y	ENSSSTT
Q769.d22	Y	IINSTE	5768.04	Y	GSNSSNTSE	0077_V1.C16	Y	ETNDGNTNETGTKTFKSNETET	ZM249.1	Y	SKNNTE
Q769.h5	Y	IINSTDTD	6101.1	Y	DNNNTI	00836-2.5	N	NHEEANTT	ZM53.12	Y	LTNFSK
Q842.d12	Y	NTNSTR	6535.3	Y	NETNVT	0921.V2.C14	Y	NGGADNST	ZM55.28a	Y	ENTTDNGT
QH209.14M.A2	Y	DDENNT	7165.18	Y	ENRTDNGT	16055-2.3	Y	VESNET	3328.V4.C3	Y	NSH
RW020.2	Y	NNSTN	45_01d05	N	SSTNGTT	16845-2.22	Y	NSNDTNEP	3337.V2.C6	Y	NTSE
UG037.8	Y	GNINES	89.6.DG	Y	NSTETET	16936-2.21	Y	PDNVT	3817.v2.c59	Y	LNTSNN
246-F3.C10.2	Y	NTNSTK	AC10.29	Y	RGNQTDNQT	25710-2.43	Y	TGSESNKT	191821.E6.1	Y	INSNTSSS
3301.V1.C24	Y	SDGNSTK	ADA.DG	Y	TNSSGS	25711-2.4	Y	RGEEVKNDT	231965.c1	Y	RDNSSSN
3589.V1.C4	Y	GNNSSEN	Bal.01	Y	PEDNKT	25925-2.22	Y	TGLNSST	247-23	N	SNNTNET
6540.v4.c1	N	NNNSDN	Bal.26	Y	PEDDKT	26191-2.48	Y	NSNSTE	3016.v5.c45	Y	NTSDDH
6545.V4.C1	N	NRSSDN	BG1168.01	Y	DTNNGT	3168.V4.C10	Y	KGNNET	57128.vrc15	Y	GADNNRQN
0815.V3.C3	Y	SNTNAS	BL01.DG	Y	KVGTEGT	3637.V5.C3	Y	ISNGTDNKN	6405.v4.c34	Y	ADNSSHN
6095.V1.C10	Y	VNNDSQS	BR07.DG	Y	NTSSEA	3873.V1.C24	Y	TGKNDTENAT	A03349M1.vrc4a	Y	GNESSQN
3468.V1.C12	Y	DTSSMN	BX08.16	Y	SDNSSSGK	6322.V4.C1	Y	KDNNMT	NKU3006.ec1	Y	NTNSTN
Q168.a2	Y	NNNSTN	CAAN.A2	Y	NDNETNGT	6471.V1.C16	N	KTSNDPDT	UG021.16	Y	VKNNSQN
Q461.e2	Y	GENDT	CNE10	Y	NESTTTET	6631.V3.C10	Y	PNSTN	UG024.2	Y	NTSQN
620345.c1	N	GGPTADN	CNE12	Y	KNESNTT	6644.V2.C33	Y	SINGSEDENNT	P0402.c2.11	Y	GNNTNET
BJOX009000.02.4	Y	DINASN	CNE14	Y	DNENTTT	6785.V5.C14	Y	SINGSEDNT	P1981.C5.3	Y	NTNGT
BJOX010000.06.2	N	NISATN	CNE4	Y	HNGNGSNET	6838.V1.C35	Y	NGTERN	X1193.c1	Y	KSNETNGT
BJOX025000.01.1	N	NNTNTS	CNE57	Y	NNTDKNT	96ZM651.02	Y	STNDSTNNNT	X1254.c3	Y	TNNNTN
BJOX028000.10.3	Y	DDNGT	HO86.8	Y	KNNKST	BR025.9	Y	TGMHDT	X1632.S2.B10	Y	TNKDTNEA
C1080.c3	Y	DANATNDT	HT593.1	Y	NNNKTNGT	CAP210.E8	Y	ENKTENNDT	X2088.c9	Y	NDTHDKEN
C2101.c1	Y	NNNTN	HXB2.DG	Y	NSNNES	CAP244.D3	Y	EANGTNNI	SIVmac251.30.SG3	N/A	-
C4118.09	Y	TNNTNSS	JRCSF.JB	Y	KNESEI	CAP45.G3	Y	KTDRNDT	SVA.MLV	N/A	-
CNE3	N	NNSNAN	JRFL.JB	Y	INENGT	Ce1176.A3	Y	INGTGE	Autologous T/F		
CNE5	Y	NNNSTGN	MN.3	Y	EDTDTNDT	CE703010217.B6	Y	NNKSTP	CAP257.2.00.Luc	Y	INASK
CNE55	Y	GNNRSN	PVO.04	Y	ANNTN	CNE30	Y	TTNNTNNT			
CNE56	Y	DNTTDS	QH0515.01	Y	TNGTNET	CNE31	Y	KTNKTE			
CNE59	Y	NNMTN	QH0692.42	Y	VNGTR	CNE53	Y	SQPNNT			
CNE8	Y	TNMSN	REJO.67	Y	NSSLSSP	CNE58	Y	TNNATT			
MD2138	Y	INRTYN	RHPA.7	Y	VDTTK	DU123.06	Y	NTSNSTP			
R1166.c1	Y	VNNSTN	SC422.8	Y	NNNSTT	DU151.02	Y	KNTTN			
R2184.c4	Y	TNTSKNN	SF162.LS	Y	KEISNTT	DU156.12	Y	GNVTENRT			
TH966.8	Y	ANNTSN	SS1196.01	Y	NNTTNGTQT	DU172.17	Y	KEKNDT			

UNIVERSITY OF THE WITWATERSRAND, JOHANNESBURG
Division of the Deputy Registrar (Research)

HUMAN RESEARCH ETHICS COMMITTEE (MEDICAL)
R14/49 Mr Constantinos K Wimber

CLEARANCE CERTIFICATE	**M120626**
PROJECT	Identification, Isolation and Characterisation of HIV-1 Neutralising Antibodies
INVESTIGATORS	Mr Constantinos K Wimber.
DEPARTMENT	School of Pathology/Virology
DATE CONSIDERED	29/06/2012
DECISION OF THE COMMITTEE*	Approved unconditionally

Unless otherwise specified this ethical clearance is valid for 5 years and may be renewed upon application.

DATE 29/06/2012 **CHAIRPERSON** .....
(Professor PE Cleaton-Jones)

*Guidelines for written 'informed consent' attached where applicable
cc: Supervisor : Professor Lynn Morris

DECLARATION OF INVESTIGATOR(S)
To be completed in duplicate and **ONE COPY** returned to the Secretary at Room 10004, 10th Floor, Senate House, University.
I/We fully understand the conditions under which I am/we are authorized to carry out the abovementioned research and I/we guarantee to ensure compliance with these conditions. Should any departure to be contemplated from the research procedure as approved I/we undertake to resubmit the protocol to the Committee. **I agree to a completion of a yearly progress report.**

PLEASE QUOTE THE PROTOCOL NUMBER IN ALL ENQUIRIES...